Non-Coaxial Rotations of a Porous Disk for Unsteady MHD Flows in Newtonian and Non-Newtonian Fluids

QUAID-I-AZAM UNIVERSITY
ISLAMABAD

By

TAHIRA HAROON

DEPARTMENT OF MATHEMATICS
QUAID-I-AZAM UNIVERSITY
ISLAMABAD, PAKISTAN
2001

Non-Coaxial Rotations of a Porous Disk for Unsteady MHD Flows in Newtonian and Non-Newtonian Fluids

By

Tahira Haroon

A thesis
submitted in partial fulfillment of
the requirement for the
degree of

Doctor of Philosophy
in Mathematics

DEPARTMENT OF MATHEMATICS
QUAID-I-AZAM UNIVERSITY
ISLAMABAD, PAKISTAN
2001

Certificate

Non-Coaxial Rotations of a Porous Disk for Unsteady MHD Flows in Newtonian and non-Newtonian fluids

BY
TAHIRA HAROON

A thesis submitted in the partial fulfillment
of the requirement for the degree of doctor of philosophy
in Mathematics

We accept this thesis as conforming to the required standard.

1. ____________________
(Chairman)
Prof. Dr. Qaiser Mushtaq

2. Saleem Asghar
(Supervisor)
Prof. Dr. Saleem Asghar

(External Examiners)

3. ____________________
Brig. Dr. Muhammad Rafique
NUST, Rawalpindi.

4. ____________________
Dr. Salahuddin, PSO,
PAEC, Islamabad.

DEPARTMENT OF MATHEMATICS
QUAID-I-AZAM UNIVERSITY
ISLAMABAD, PAKISTAN
2001

Acknowledgments

Primarily and foremost, all praise for ***Almighty Allah,*** the benevolent and merciful, the creator of the universe, who provided me the apt ability, strength and courage to complete the work presented here. I invoke peace for ***Hazrat Muhammad (peace be upon him),*** the last prophet of Allah who is forever a torch of guidance for humanity as a whole.

I want to express my heartiest gratitude to my eminent, affectionate, candid and devoted supervisor, ***Professor Saleem Asghar***, for his encouraging discussions, valuable guidance, loving care which enabled me in broadening and improving my capabilities. Without his generous encouragement and patient guidance, it was not possible for me to complete this work.

I can offer here only an inadequate acknowledgment of my appreciation to ***Dr. Tasawar Hayat***, for his effective guidance, cooperation and great care in preparing this thesis. I learned a lot from him and owe him deep thanks.

Thanks are also due to ***Dr. A. M. Siddique***, who played a major role in introducing this field of study in the Department of Mathematics, Quaid-i-Azam University. He has been the source of literature and guidance for the work presented in this thesis.

This thesis is the outgrowth of Dr. A. Q. Khan Research Laboratories, KRL. I thank Dr. A. Q. Khan and Dr. M. Alam for permitting me to do this work. I especially wish to thank Mr. Azmatullah Bhatti, Director STINFOD, KRL. for providing valuable help and the loan of books.

Thanks are due to COMSATS Institute of Information Technology and Dr. S. M. Junaid Zaidi, Rector CIIT, for providing me computational facilities to complete this work.

I would certainly not be where I stand today without the continuous support, help and – most of all – encouragement of my family. Especially my parents who have supported me tremendously during all these years.

I have no words to express my gratitude to ***Haroon***, who supported me in a thousand and one ways despite his busy schedule. It wouldn't be possible for me to even think about Ph. D. without his encouragement and interest.

I can not finish without expressing my feelings for my children ***Junaid*** and ***Ubaid***, who suffered a lot in their young age due to my involvement in Ph. D. work.

It is not possible for me to name all those people who have contributed towards completion of my work. I want to thank all my well-wishers for their sincere support.

TAHIRA HAROON

To *Haroon, Junaid* and *Ubaid*
for all their love and understanding

Preface

The study of motions in a conducting fluid in the presence of a magnetic field has greatly increased due to its extensive applications in the cosmical and geophysical fluid dynamics. Rotation plays an important role in the cosmical, astrophysical and large scale circulations in the atmosphere and thus the concept of motion of a body in a rotating fluid is of great significance. In spite of the importance of the effects of rotation and electromagnetic force on the hydromagnetic flow the simultaneous influence of these factors appear to have been investigated in only a few specific cases.

The effects of porosity on the hydromagnetic flow phenomena and the structures of the associated boundary layers, the initial value investigations of Newtonian and non-Newtonian problems in the presence of a magnetic field is of considerable interest in geophysical, astrophysical and cosmical fluid dynamics. The aim of this thesis is to contribute in this direction by studying some magnetohydrodynamic flow problems due to non-coaxial rotations of porous disk and a fluid at infinity.

Considerable attention has been given to the boundary layers due to Newtonian and non-Newtonian fluids. Shear flows of non-Newtonian fluids are of special interest in engineering science. An illustrated example is found in chemical engineering science, where in industrial technological processes the steady flows and unsteady shear flows of non-Newtonian fluids of second and third grade are involved. Recently, with increasing interest in the production of heavy crude and conventional oils paraffin contents, it has become essential for oil reservoir engineering to have an adequate understanding of the rheological effects of second and third grade fluids on shear flow through porous media. The following four problems are discussed in this direction:

1. The flow due to non-coaxial rotations of a porous disk and a fluid at infinity is considered in chapter 2. The velocity field for the case of Newtonian flow is presented and the effects of porosity and magnetic field are examined. It is found that boundary layer thickness decreases with the increase in magnetic field.

2. The magnetohydrodynamic (MHD) flow of second grade fluid due to non-coaxial rotations of a porous disk and a fluid at infinity is considered in chapter 3. Exact analytical solution is found using Laplace transform technique. It is found that the boundary layer thickness increases with the increase in material parameter of the second grade fluid. Exact value of the material parameter exhibiting the property of second grade fluid is determined.

3. Chapter 4 is devoted to the extended analysis of chapter 3 for third grade fluid. This analysis is important because a second grade fluid exhibits normal stresses but is not shear thinning; the shear viscosity is constant. The third order approximation of a simple fluid exhibits shear dependent viscosity. The governing partial differential equation is non-linear which is not amenable to an analytic solution and so numerical solution is constructed. It is observed that the boundary layer thickness increases much with the increase in material parameter of the third grade fluid.

4. The problem considered in chapter 4 is generalized to the case of oscillating porous disk and a numerical solution is given using modified Crank-Nicolson implicit method with forward time difference and central space difference ap-

proximations. Unlike the hydrodynamic situation for the resonant oscillations, the solution for magnetohydrodynamic fluid satisfies the boundary condition at infinity for all values of the frequency parameter and the associated boundary layers remain bounded for all values of the frequency including the resonant frequency.

Contents

List of Figures

0 Introduction **1**

1 Preliminaries **9**

1.1 Porous Medium 9

1.2 Constitutive Equation 9

1.3 Torsional Flows 10

1.4 Boundary Layer 10

1.5 Boundary Layer Separation 11

1.6 Physical behavior 13

1.7 Non-Newtonian Fluids 14

1.7.1 Time Independent (Visco-Inelastic) fluids 15

1.7.2 Time Dependent Fluids 17

1.7.3 Viscoelastic Fluids 18

1.8 MHD Equations 19

1.8.1 Maxwells Equations 19

1.8.2 Ohm's Law 20

1.8.3 Equation of Continuity 21

1.8.4 Equation of Motion for the Third Grade Fluid . . . 21

2 Unsteady MHD Flow Due to Non-Coaxial Rotations of a Porous Disk and a Fluid at Infinity 42
2.1 The Basic Equations and Boundary Conditions 42
2.2 The Solution of the Problem 45

3 Unsteady MHD Flow of a Second Grade Fluid Due to Eccentric Rotations of a Porous Disk and a Fluid at Infinity 54
3.1 Basic Equations 55
3.2 Solution of the problem for suction 59
3.2.1 System of Order Zero 60
3.2.2 System of Order One 60
3.2.3 Zeroth order Solution 60
3.2.4 First order Solution 60
3.3 Blowing solution 68
3.4 Discussion 72

4 MHD Flow of a Third Grade Fluid Due to Eccentric Rotations of a Porous Disk and a Fluid at Infinity 73
4.1 Basic Equations 73
4.2 Numerical Discussion 83

5 MHD Flow of a Third Grade Fluid Induced by Non-Coaxial Rotations of a Porous Disk Executing Non-Torsional Oscillations and a Fluid at Infinity 88
5.1 Governing Equations 89
5.2 Numerical Discussion 91
References

List of Figures

Figure 1. Flow geometry 95

Figure 2.1 The influence of porosity in the absence of magnetic field ($N = 0$) on f and g with ξ when $\tau = 12$. 96

Figure 2.2 The influence of suction ($\epsilon = 0.5$) in the presence of magnetic field ($N = 2$) on f and g with ξ for different values of τ. 96

Figure 2.3 The influence of blowing ($\epsilon = -0.5$) in the presence of magnetic field ($N = 2$) on f and g with ξ for different values of τ. 97

Figure 3.1 Variation in f and g with ξ for $\tau = 12$ without suction or magnetic field for different values of α. 97

Figure 3.2 Variation in f and g with ξ for $\tau = 12,\ \epsilon = 2,\ N = 0$ for different values of α. 98

Figure 3.3 Variation in f and g with ξ for $\tau = 12,\ \epsilon = -2,\ N = 0$ for different values of α. 98

Figure 3.4 Variation in f and g with ξ for $\tau = 12,\ N = 2$, and $\alpha = 1$ for different values of ϵ 99

Figure 4.1 Variation in f and g with ξ for different values of τ, when $\alpha = 0,\ \beta = 0,\ \epsilon = 0,\ N = 0$. 99

Figure 4.2 Variation in f and g with ξ for different values of τ, when $\alpha = 1,\ \beta = 0,\ \epsilon = 0,\ N = 0$. 100

Figure 4.3 Variation in f and g with ξ for different values of τ, when

$\alpha = 1,\ \beta = 1,\ \epsilon = 0,\ N = 0.$ 100
Figure 4.4 Variation in f and g with ξ for different values of τ, when
$\alpha = 0,\ \beta = 0,\ \epsilon = 2,\ N = 0.$ 101
Figure 4.5 Variation in f and g with ξ for different values of τ, when
$\alpha = 1,\ \beta = 0,\ \epsilon = 2,\ N = 0.$ 101
Figure 4.6 Variation in f and g with ξ for different values of τ, when
$\alpha = 1,\ \beta = 1,\ \epsilon = 2,\ N = 0.$ 102
Figure 4.7 Variation in f and g with ξ for different values of τ, when
$\alpha = 0,\ \beta = 0,\ \epsilon = 2,\ N = 2.$ 102
Figure 4.8 Variation in f and g with ξ for different values of τ, when
$\alpha = 1,\ \beta = 0,\ \epsilon = 2,\ N = 2.$ 103
Figure 4.9 Variation in f and g with ξ when $\tau = 100,\ \beta = 0,\ \epsilon = 0,$
$N = 0$ for different values of α. 103
Figure 4.10 Variation in f and g with ξ when $\tau, = 100,\ \beta = 0,\ \epsilon = 2,$
$N = 0$ for different values of α. 104
Figure 4.11 Variation in f and g with ξ when $\tau = 100,\ \beta = 0,\ \epsilon = 2,$
$N = 2$ for different values of α. 104
Figure 4.12 Variation in f and g with ξ when $\tau = 100,\ \beta = 0,\ \epsilon = 0,$
$N = 2$ for different values of α. 105
Figure 4.13 Variation in f and g with ξ when $\tau = 100,\ \alpha = 1,\ \epsilon = 0,$
$N = 0$ for different values of β. 105
Figure 4.14 Variation in f and g with ξ when $\tau = 100,\ \alpha = 1,\ \epsilon = 0,$
$N = 2$ for different values of β. 106
Figure 4.15 Variation in f and g with ξ when $\tau = 100,\ \alpha = 1,\ \epsilon = 2,$
$N = 0$ for different values of β. 106
Figure 4.16 Variation in f and g with ξ for different values of β when
$\tau = 100,\ \alpha = 1,\ \epsilon = 2,\ N = 2.$ 107

Figure 4.17 Variation in f and g with ξ for different values of β when $\tau = 100,\ \alpha = 1,\ \epsilon = -2,\ N = 2.$ 107
Figure 4.18 Variation in f and g with ξ for different values of β when $\tau = 100,\ \alpha = 1,\ \epsilon = -2,\ N = 0.$ 108
Figure 4.19 Variation in f and g with ξ for different values of α when $\tau = 100,\ \beta = 1,\ \epsilon = -2,\ N = 0.$ 108
Figure 5.1 Variation in f with ξ for different values of time for cosine oscillation at $\frac{U}{\Omega l} = 4,\ \frac{n}{\Omega} = .5,\ \epsilon = 2,\ \alpha = 2,\ \beta = 0,\ N = 0.$ . . . 109
Figure 5.2 Variation in f with ξ for different values of time for cosine oscillation at $\frac{U}{\Omega l} = 4,\ \frac{n}{\Omega} = .5,\ \epsilon = 2,\ \alpha = 2,\ \beta = 5,\ N = 0.$ . . . 109
Figure 5.3 Variation in g with ξ for different values of time for cosine oscillation at $\frac{U}{\Omega l} = 4,\ \frac{n}{\Omega} = .5,\ \epsilon = 2,\ \alpha = 2,\ \beta = 0,\ N = 0.$ . . . 110
Figure 5.4 Variation in g with ξ for different values of time for cosine oscillation at $\frac{U}{\Omega l} = 4,\ \frac{n}{\Omega} = .5,\ \epsilon = 2,\ \alpha = 2,\ \beta = 5,\ N = 0.$ . . . 110
Figure 5.5 Variation in f with ξ for different values of time for cosine oscillation at $\frac{U}{\Omega l} = 4,\ \frac{n}{\Omega} = 5,\ \epsilon = 2,\ \alpha = 2,\ \beta = 0,\ N = 0.$ . . . 111
Figure 5.6 Variation in f with ξ for different values of time for cosine oscillation at $\frac{U}{\Omega l} = 4,\ \frac{n}{\Omega} = 5,\ \epsilon = 2,\ \alpha = 2,\ \beta = 5,\ N = 0.$ . . . 111
Figure 5.7 Variation in g with ξ for different values of time for cosine oscillation at $\frac{U}{\Omega l} = 4,\ \frac{n}{\Omega} = 5,\ \epsilon = 2,\ \alpha = 2,\ \beta = 0,\ N = 0.$ . . . 112
Figure 5.8 Variation in g with ξ for different values of time for cosine oscillation at $\frac{U}{\Omega l} = 4,\ \frac{n}{\Omega} = 5,\ \epsilon = 2,\ \alpha = 2,\ \beta = 5,\ N = 0.$ . . . 112
Figure 5.9 Variation in f with ξ for different values of time for sine oscillation at $\frac{U}{\Omega l} = 4,\ \frac{n}{\Omega} = .5,\ \epsilon = 2,\ \alpha = 2,\ \beta = 0,\ N = 0.$ . . . 113
Figure 5.10 Variation in f with ξ for different values of time for sine oscillation at $\frac{U}{\Omega l} = 4,\ \frac{n}{\Omega} = .5,\ \epsilon = 2,\ \alpha = 2,\ \beta = 5,\ N = 0.$ . . . 113
Figure 5.11 Variation in g with ξ for different values of time for sine

oscillation at $\frac{U}{\Omega l} = 4$, $\frac{n}{\Omega} = .5$, $\epsilon = 2$, $\alpha = 2$, $\beta = 0$, $N = 0$. . . . 114

Figure 5.12 Variation in g with ξ for different values of time for sine oscillation at $\frac{U}{\Omega l} = 4$, $\frac{n}{\Omega} = .5$, $\epsilon = 2$, $\alpha = 2$, $\beta = 5$, $N = 0$. . . . 114

Figure 5.13 Variation in f with ξ for different values of time for sine oscillation at $\frac{U}{\Omega l} = 4$, $\frac{n}{\Omega} = 5$, $\epsilon = 2$, $\alpha = 2$, $\beta = 0$, $N = 0$. . . . 115

Figure 5.14 Variation in f with ξ for different values of time for sine oscillation at $\frac{U}{\Omega l} = 4$, $\frac{n}{\Omega} = 5$, $\epsilon = 2$, $\alpha = 2$, $\beta = 5$, $N = 0$. . . . 115

Figure 5.15 Variation in g with ξ for different values of time for sine oscillation at $\frac{U}{\Omega l} = 4$, $\frac{n}{\Omega} = 5$, $\epsilon = 2$, $\alpha = 2$, $\beta = 0$, $N = 0$. . . . 116

Figure 5.16 Variation in g with ξ for different values of time for sine oscillation at $\frac{U}{\Omega l} = 4$, $\frac{n}{\Omega} = 5$, $\epsilon = 2$, $\alpha = 2$, $\beta = 5$, $N = 0$. . . . 116

Figure 5.17 Variation in f with ξ for different values of time for cosine oscillation at $\frac{U}{\Omega l} = 4$, $\frac{n}{\Omega} = 1$, $\epsilon = -2$, $\alpha = 2$, $\beta = 5$, $N = 2$. . . 117

Figure 5.18 Variation in f with ξ for different values of time for sine oscillation at $\frac{U}{\Omega l} = 4$, $\frac{n}{\Omega} = 1$, $\epsilon = -2$, $\alpha = 2$, $\beta = 5$, $N = 2$. . . 117

Figure 5.19 Variation in g with ξ for different values of time for cosine oscillation at $\frac{U}{\Omega l} = 4$, $\frac{n}{\Omega} = 1$, $\epsilon = -2$, $\alpha = 2$, $\beta = 5$, $N = 2$. . . 118

Figure 5.20 Variation in g with ξ for different values of time for sine oscillation at $\frac{U}{\Omega l} = 4$, $\frac{n}{\Omega} = 1$, $\epsilon = -2$, $\alpha = 2$, $\beta = 5$, $N = 2$. . . 118

Chapter 0

Introduction

Rotation plays an important role in several important phenomena such as the cosmical, astrophysical, large-scale circulations in the atmosphere etc. The concept of motion of a body or object in an unbounded rotating fluid is appropriate in these cases. These phenomena thus motivate the search for exact solutions of fluid dynamics equations in the rotating fields. However, there are situations in which the limiting values of the physical parameters such as kinematic viscosity, time and length scale etc. need to be invoked making the final results to depend upon the ordering of the limits. In other words the problems of this type may not be generally well-posed. Flows generated entirely by rotary motion of solid boundaries have immediate technical applications (rotating machinery, lubrication, viscometry, heat and mass exchangers, biomechanics, oceanography), but quite apart from that they have intrinsic interest. Thus, the solution of many practical rotating flow problems in an unsteady flow created by a rotating fluid has been the subject of a large number of investigations which in turn depends upon the behavior of the unsteady boundary layers. The flow due to a single, infinite disk was first discussed by von Kármán [1] , and later by Batchelor [2]. Reference may also be made to the interesting work of Greenspan and Howard [3]. After the initiation of this work several researchers such as Holton [4], Walin [5], Siegmann [6] and Debnath [7] examined the spin-up mechanism in a rotating viscous fluid.

The flow between eccentric rotating disks has been examined by a number of investigators. Berker [8, 9] showed the existence of an infinite number of non-trivial solutions to the Navier-Stokes equations between two infinite parallel plates rotating about a common axis or about different axes. Erdogan [10] found an exact solution of the time-dependent flow between eccentric rotating disks for a Newtonian fluid. Rajagopal [11] has considered the flow of a simple fluid in an orthogonal rheometer. Abbot and Walters [12] obtained an exact solution for classical incompressible fluid, and visco-elastic fluid. Rajagopal [13] introduced the concept of suction or blowing and studied the flow of a Newtonian fluid between two infinite porous parallel plates rotating about the same axis.

The flow due to a single disk in a variety of situations has also been a subject of great importance. Berker [14] has considered the Newtonian flow due to non-coaxial rotations of a disk and a fluid at infinity with the same angular velocity and implied the possibility of an exact solution of the Navier-Stokes equations. After Berker, there have been many works on the flow due to non-coaxial rotations of a disk and a fluid at infinity. The unsteady flow due to non-coaxial rotations of a porous disk and a fluid at infinity rotating about different axes has been studied by Erdogan [15]. The flow due to a disk and a fluid at infinity which are rotating non-coaxially at slightly different angular velocities in an incompressible viscous fluid has been considered by Coirier [16]. Mention may also be made to the works of Gupta [17] and Erdogan [18, 19]. Gupta obtained an exact solution of the steady three-dimensional Navier-Stokes equations for the case of flow past a porous plate at zero incidence in a rotating frame of reference, subject to uniform suction. In [18, 19], Erdogan obtained exact solutions of the three dimensional Navier-Stokes equations for the flow due to non-coaxial rotations of a porous disk and a fluid at infinity. Erdogan found that for uniform suction and uniform blowing at the disk, asymptotic solutions exist for the velocity distributions.

The work of Berker [9] to unsteady case has been extended by Smith [20]. Kasiviswanathan and Rao [21] obtained an exact solution of the unsteady Navier-Stokes equations for the flow due to non-coaxial rotations of a porous disk, executing non-torsional oscillations in its own plane, and a fluid at infinity. The unsteady flow due to eccentric rotations of a disk and a fluid at infinity which are impulsively started is investigated by Pop [22]. He assumed that the flow is two-dimensional, and both the disk and the fluid at infinity are initially at rest and that they are impulsively started at time zero. However, under the assumed conditions by Pop [22], the flow does not become two-dimensional, it becomes three dimensional. Erdogan [15] suggested a change in the initial condition and proposed that the disk and the fluid are initially rotating about the $z'-$ axis and suddenly sets in motion; the disk rotating about $z-$ axis and fluid about $z'-$ axis. He showed that the problem is two-dimensional and presented an analytical solution for the velocity field.

An investigation of MHD boundary layers under the influence of viscous forces is of importance in understanding a variety of cosmical, geophysical, astrophysical and engineering phenomena. The MHD effect on the Ekman layer over an infinite horizontal plate at rest relative to an electrically conducting liquid which is rotating with uniform angular velocity about a vertical axes has been studied by Gupta [23]. Murthy and Ram [24] have derived an exact solution of the steady three-dimensional Navier-Stokes equations and energy equation for the case of flow due to non-coaxial rotations of a porous disk and a fluid at infinity in the presence of a uniform transverse magnetic field. Magnetohydrodynamic flow of a Newtonian, incompressible, conducting fluid between eccentric rotating insulated disks with the same angular velocity in the presence of a uniform transverse magnetic field was investigated by Mohanty [25]. Ekman [26] examined the same problem including the induced magnetic field.

There is yet another area in which the rotating flow has drawn special attention to the researchers. It is the fluid dynamics of the non-Newtonian fluids. The flow of non-Newtonian (viscoelastic) fluids has gained considerable importance because of its applications in various branches of science, engineering and technology, particularly in material processing, chemical and nuclear industries, geophysics, and bioengineering. Most industrial fluid processing includes non-Newtonian liquids. The study of non-Newtonian fluid flow through porous media is of significant interest in oil reservoir engineering. In view of both industrial and technological applications, considerable attention has been given to the flow of non-Newtonian fluids due to rotating plates and disks. These fluids can not be adequately explained on the basis of the classical, linearly viscous model. Several constitutive equations have been suggested to characterize such non-Newtonian behavior. Amongst there are fluids of the differential type of grade n (Truesdell and Noll [27]), such as second grade (second-order) fluid, third grade (third-order) fluid, Maxwell fluid, Oldroyd B fluid etc, the incompressible and homogeneous fluid of first grade being the linearly viscous fluid.

Srivastava [28] studied the flow of a Reiner-Rivlin fluid between rotating parallel plates. Bhatnagar [29] studied the flow between two disks of a Reiner-Rivlin fluid in which one disk is stationary and the other rotating. Erdogan [30] has studied the steady flow of a second grade fluid due to a disk and a fluid at infinity which are rotating non-coaxially at slightly different angular velocities. Later, Bhatnagar and Zago [31] studied the flow of a second grade fluid due to two rotating disks, about a common axis. The flows of Newtonian and non-Newtonian fluids between parallel disks rotating about a common axis has been reviewed by Rajagopal [32]. Maxwell and Chartoff [33] pointed out that it is possible to determine the complex dynamic viscosity of an elastico-viscous liquid by using the orthogonal rheometer. Blyler and

Kurtz [34] and Bird and Harris [35] established various studies to obtain the complex viscosity of the fluid. The inertia of the fluid was neglected in Refs. [33, 34, 35]. Abbott and Walters [12] both introduced an exact solution for a Newtonian fluid including inertia effects and examined the flow of a viscoelastic fluid. The same problem was investigated for a second grade fluid by Rajagopal [36]. The stability of a second grade fluid between two parallel plates rotating about non-coincident axes was investigated by Rajagopal and Gupta [37], for a BKZ (Bernstein, Kearsley, and Zapas) fluid by Rajagopal and Wineman [38], and for a K-BKZ (Kaye, Bernstein, Kearsley, and Zapas) fluid by Dai et al. [39]. Separately, Göğüs [40] obtained an exact solution for a mixture of two incompressible Newtonian fluids. Rao and Kasiviswanathan [41] extended work of Mohanty [25] by considering flow between eccentric rotating disks with the same angular velocity for micropolar fluid, in the presence of a uniform transverse magnetic field. Rajagopal [42] considered the flow of an Oldroyd-B fluid between two infinite parallel plates rotating about non-coincident axes. An exact solution for the magnetohydrodynamics flow of a conducting, incompressible Oldroyd-B fluid between two infinite parallel insulated disks rotating about non-coincident axes normal to the disks in the presence of a uniform transverse magnetic field was given by Ersoy [43]. Knight [44] investigated the inertia effects of the non-Newtonian flow between eccentric disks rotating at different speeds. Parter and Rajagopal [45] proved that when the disks rotate with different angular velocities about distinct axes or a common axis, there is a one parameter family of solutions. It has been shown by many authors that for some types of problems, in which the flow is sufficiently slow in the visco-elastic sense, the results given by the constitutive equations such as the Oldroyd type are not significantly different from those of second or third Rivlin-Erickson constitutive equation. Therefore, if this is the sense of solutions, to which the problems are interpreted, it is reasonable to use the second or third grade Rivlin-Erickson equation for the numerical calculations. This is partially so due to the fact, that the calculations will generally be simpler. A list of problems may be found in [46].

Keeping in view the importance of **unsteady flows, Newtonian and non-Newtonian fluids, MHD, suction/blowing, boundary layer thickness** due to non-coaxial rotations of a disk and a fluid at infinity under different conditions, we proceed to present our work as follows :-

In chapter 2 an exact solution for the **unsteady flow** of a **viscous fluid** in three-dimensions is derived for the case of non-coaxial rotations of a porous disk and a fluid at infinity in the presence of a uniform transverse magnetic field. It is found that the boundary layer thickness in the cases of suction/blowing decreases with the increase in magnetic parameter. This study helps us to know how the geophysically important suction/blowing velocity is effected by magnetic field and rotation. This work has been published in ***ACTA MECHANICA 151,127-134(2001)***

In chapter 3 an exact solution of the **unsteady flow** of a **second grade fluid** due to non-coaxial rotations of a porous disk and a fluid at infinity in the presence of a uniform transverse magnetic field is investigated. The effects of magnetic field, the material parameters of the second grade fluid, suction and blowing on the velocity distribution are studied. From the solution of a rigid disk, it is found that for dimensionless normal stress modulus $\alpha > .01$, a non-Newtonian effect is present in the velocity field and for $\alpha < .01$ the velocity field becomes a Newtonian one. These observations have been published in ***ACTA MECHANICA 147, 99-109(2001)***

The problem of magnetohydrodynamics (MHD) flow of a conducting, incompressible **third grade fluid** due to non-coaxial rotations of a porous disk and a fluid at infinity in the presence of a uniform transverse magnetic field is considered in chapter 4. An exact analysis is carried out to model the governing non-linear partial differential equation. Since the analytical solution for the equation of third grade fluid is difficult, a numerical solution of the non-linear partial differential equation has been obtained. Several graphs have been drawn to show the influence of porosity, magnetic parameter and material parameters on the velocity distribution. It is found that when normal stress moduli are zero, we get solution for the Newtonian fluid, and results matched with the analytical solution with very small relative error. Numerically, we found the behavior of velocity components at different positions for various time corresponding to three types of flows (Newtonian, second grade and third grade), with and without suction and magnetic parameter. We observed that; for the Newtonian case boundary layer thickness increases with the increase in time before reaching steady state. For the second grade fluid boundary layer thickness increases with the increase in material parameter. Time taken to reach steady-state is also increased. Also boundary layer thickness increases with the increase in time in third grade fluid during the transient period and then becomes stable. The large material parameter of the second grade fluid increases the boundary layer thickness and also the time to approach its steady state. In third grade fluid boundary layer thickness increases further as compared to the results of second grade fluid and also time to reach steady state is increased but these values are small in comparison with the case when suction was not present in the third grade fluid. Magnetic parameter is responsible for further reduction in boundary layer thickness as well as time to reach steady-state in all three cases. We also observe that the boundary layer thickness increases with the increase in material parameters. The magnitude of radial velocity component decreases near the disk while its value increases in a considerable amount at some distance away from the disk for the second grade fluid. These effects are enhanced further for the third grade fluid.

Suction and magnetic parameter are always responsible for the reduction in the boundary layer thickness and also reduce the magnitudes of radial and azimuthal velocity components. The effect of the magnetic parameter on the azimuthal velocity component is more prominent as compared to its effect on the radial velocity component.

For blowing, boundary layer thickness becomes very large and it approaches the free stream at a very large distance (solution exists), and for the second and third grade fluids it increases further but by introducing magnetic parameter, boundary layer thickness is reduced drastically. The contents of chapter 4 have been accepted for publication in ***INT. J. NON-LINEAR MECHANICS.***

In chapter 5, a numerical solution of the time-dependent non-linear partial differential equation for the magnetohydrodynamic incompressible flow due to non-coaxial rotations of a porous disk and a third grade fluid at infinity is given. Additionally, the disk is executing oscillations in its own plane. The solutions for three cases when the angular velocity is greater, smaller or equal to the frequency of oscillation are examined. The structure of the velocity distributions and the associated boundary layers are investigated including the case of blowing and resonant oscillations. Many known results are recovered as the special cases of the attempted problems. These observations are already submitted to ZAMM.

Chapter 1

Preliminaries

This chapter reviews the basic definitions and concepts used in the thesis.

1.1 Porous Medium

A porous medium is a continuous solid phase with intervening void or gas pockets. Natural porous media include soil, sand, mineral salts, sponge, wood and others. Synthetic porous media include paper, cloth filters, chemical reaction catalysts, and membranes.

1.2 Constitutive Equation

The constitutive equation is an equation of state under flow and deformation that differentiates the behavior of the rheologically different fluids, even when subjected to identical flow conditions. This is consistent with the physics of the liquids involved; not all fluids will behave similarly under the same flow conditions (geometry and pressure gradient etc). Some fluids, for example water, will flow easily even under infinitesimal pressure and stress gradients. But other liquids, for example ketchup, will require large such a gradient to flow. The equation that specifies how a given fluid flows or deforms when subject to force gradients (such as pressure difference, gravity, or shear difference) is called the constitutive equation. The constitutive equation relates all the stress components to the velocity and therefore permits solution to equation of motion. The constitutive equation is not a conservation equation. It is a relation between the stress and the velocity and its derivatives and is characteristic of the fluid alone.

1.3 Torsional Flows

Rotating solid boundaries in contact with liquids induces torsional flows. The liquid, due to the no-slip boundary conditions, has to follow the motion of the boundary, and therefore, a torsional flow is generated. These flows are important in mixing, agitation, and centrifugal separations. They are utilized by commercial viscometers, where viscosity can be deduced from the torque, $\mathbf{T}$, necessary to turn a rod with angular velocity $\mathbf{\Omega}$.

1.4 Boundary Layer

The influence of viscosity for the moving fluid is confined to a very thin layer in the immediate neighborhood of the disk, known as boundary layer. In this thin layer the velocity of the fluid increases from zero at the disk (no-slip) to its full value, which corresponds to external frictionless flow. The thickness of the boundary layer increases along the disk in the down stream direction continuously, as increasing quantities of fluid become effected. The thickness of the boundary layer decreases with decreasing viscosity. On the other hand, even with very small viscosities (large Reynolds numbers) the frictional shearing stresses $\tau = \mu \frac{\partial u}{\partial y}$ in the boundary layer are considerable because of large velocity gradient across the flow, whereas outside the boundary layer they are very small.

1.5 Boundary Layer Separation

The decelerated fluid particles in the boundary layer, a thin region near solid boundary where the viscous terms are important, do not, in all cases, remain in the thin layer, which adheres to the body along the whole wetted length of the wall. In some cases the boundary layer increases its thickness considerably in the down stream direction and the flow in the boundary layer becomes reversed. This causes the decelerated fluid particles to be forced outwards, which means the boundary layer is separated from the wall. Separation is an undesirable phenomenon because it entails large energy losses. The most obvious method of avoiding separation is to attempt to prevent the formation of a boundary layer. For this reason methods have been devised for the prevention of separation. These can be classified as follows: -

1. Motion of the solid wall
2. Acceleration of the boundary layer (blowing)
3. Suction
4. blowing of a different gas (binary boundary layer)
5. Prevention of transition to turbulent flow by the provision of suitable shapes (laminar aerofoils)
6. Cooling of the wall

The simplest method from the physical point of view is to move the wall with the stream in order to reduce the velocity difference between them, and hence to remove the cause of boundary layer formation, but this is very difficult to achieve in engineering practice. Another very effective method for the prevention of separation is boundary layer suction. The effect of suction consists in the removal of decelerated fluid particles from the boundary layer through a slit in the wall into the interior of the body before they are given a chance to cause separation. A new boundary layer that is again capable of overcoming a certain adverse pressure gradient is allowed to form in the region behind the slit. With a suitable arrangement of the slits and under favorable conditions separation can be prevented completely. Suction can also be applied to reduce friction. By the use of suitable arrangements of suction slits, it is possible to shift the point of transition in the boundary layer in the down stream direction, this causes the friction coefficient to decrease, because laminar friction is substantially smaller than turbulent friction. The effect of the delay in transition caused by suction is to reduce the boundary layer thickness, which then has a less tendency to turn turbulent. However, the velocity profiles in a boundary layer with suction, being fuller, have forms that are less likely to induce turbulent compared with those in laminar boundary layers without suction and of equal thickness.

Suction has effects in two ways. First, it reduces the boundary layer thickness and the thinner boundary layer has less tendency to become turbulent. Secondly, it creates a laminar velocity profile, which possesses a higher limit of stability (critical Reynold number) than a velocity profile with no suction. It is possible to obtain any desired reduction in boundary layer thickness and hence to keep the Reynolds number below the limit of stability, provided that enough fluid is sucked away. However, a large suction volume is uneconomical because a large proportion of the saving in power due to the reduction in friction is then used to derive the suction pump. It is therefore important to determine the minimum suction volume, which is required in order to maintain laminar flow. The saving in friction achieved through suction is greatest when this minimum value is used because any higher suction volume will lead to a thinner boundary layer and to an increase in shearing stress at the wall.

An alternative method of preventing separation consists in supplying additional energy to the fluid particles, which are being retarded in the boundary layer. This result can be achieved by discharging fluid from the interior of the body using slits. In this case additional energy is imparted to the fluid particles in the boundary layer near the wall. The boundary layer thickness in the downstream direction increases with the increase in blowing. Blowing also reduces friction.

1.6 Physical behavior

Consider a flow on an infinite disk, which rotates about an axis perpendicular to its plane with a uniform angular velocity in a fluid otherwise at rest. Due to friction, the fluid in the immediate neighborhood of the disk is carried by it and then forced outwards due to the action of centrifugal forces. The fluid which is forced outwards in a radial direction is replaced by a fluid stream in the axial direction towards the disk to be in turn carried and ejected centrifugally. Thus the velocity in the boundary layer has a radial and a tangential component, and the mass of fluid which is driven outwards by centrifugal forces, is replaced by an axial flow. Thus the case is seen to be one of fully three-dimensional flow i.e. there exist velocity components in all three directions, u in radial direction, v in circumferential direction and w in axial direction.

When the fluid rotates over the wall this is a similar effect but its sign is reversed (in the opposite direction). The particles, which rotate at a large distance from the wall, are in equilibrium under the influence of the centrifugal force, which is balanced by a radial pressure gradient. The peripheral velocity of the particles near the wall is reduced, thus decreasing materially the centrifugal force, whereas the radial pressure gradient directed towards the axis remain the same. This set of circumstances causes the particles near the wall to flow radially inwards, and for reasons of continuity that motion must be compensated by an axial flow upwards. A superimposed field of flow of this nature which occurs in the boundary layer and whose direction deviates from that in the external flow is quite generally referred to as a secondary flow.

The secondary flow which accompanies rotation near a solid wall can be clearly observed in a glass of water with some grains: after the rotation has been generated by vigorous stirring and after that the flow has been left to itself for a short while, the radial inward flow field near the bottom will be formed. Its existence can be conformed from the fact that grains settled in a little heap near the centre at the bottom.

1.7 Non-Newtonian Fluids

The theory of non-Newtonian fluids is a branch of fluid mechanics based on the continuum hypothesis that a fluid particle may be regarded as continuous in structure. Non-Newtonian fluids are classified on the basis of their behavior in shear. A fluid that exhibits a linear relationship between the shear stress and shear rate, giving rise to a constant viscosity, is always characterized to be a *Newtonian fluid.* The constitutive equation of an incompressible Newtonian fluid is given by

$$T_{ij} = -p\,\delta_{ij} + 2\mu D_{ij} \tag{1.1}$$

where

T_{ij}	=	stress tensor
p	=	arbitrary isotropic pressure
δ_{ij}	=	Kronecker delta
μ	=	viscosity coefficient that could vary with pressure and temperature
D_{ij}	=	rate of strain (deformation) tensor, defined in terms of

velocity vector v_i, as

$$D_{ij} = \frac{1}{2}\left(\frac{\partial v_i}{\partial x_j} + \frac{\partial v_j}{\partial x_i}\right).$$

There are many real fluids, e.g. water, air, alcohol, glycerin, fluids with low molecular weight, etc. that are faithfully described by equation (1.1)

But a constant viscosity relation is not always a Newtonian fluid relation because there are fluids like a second grade fluid, a convected Maxwell fluid and an Oldroyd fluid A and B that are certainly non-Newtonian, but also show a constant viscosity. A material under a given circumstances may fall in one category, yet the same material under different conditions may belong to a different category. Silly Putty, for example, will fracture like a solid under a sudden applied load, while it will flow freely like a liquid when subjected to a load of low magnitude.

A fluid that is not characterized by equation (1.1) will be defined as a non-Newtonian fluid, e.g., solutions and melts of high polymers, suspension of particles in liquids, plastic and synthetic fibers, rubber, petroleum, soap and detergents, pharmaceuticals and biological fluids, paper pulp and printing materials etc. Non-Newtonian fluids can best be classified in response to their non-linear relationship between shear stress and the rate of shear, i.e. flow curve, is non-linear, may be divided into three broad groups. Time Independent (Visco-Inelastic) fluids, Time Dependent Fluids and Viscoelastic Fluids.

1.7.1 Time Independent (Visco-Inelastic) fluids

These fluids are isotropic and homogeneous at rest. The rate of shear at any point of the fluid is solely dependent upon the instantaneous shear stress at that point. If $\dot{\gamma}$ is the shear rate and τ is the corresponding shear stress at a point then for such fluids:

$$\dot{\gamma} = f(\tau) \tag{1.2}$$

Non-Newtonian viscous fluids and generalized non-Newtonian fluids are other names given to such fluids because their constitutive equation is similar to Newton's law of viscosity; however the viscosity itself is a function of the shear rate. These liquids exhibit shear-thinning or shear-thickening viscosity, but no normal stresses in viscometric flows and no elasticity or memory.

Depending upon the nature of equation (1.2), these fluids are conveniently subdivided into three distinct types: Bingham plastics, Pseudoplastic fluids and dilatant fluids.

Bingham Plastics

A Bingham plastic flows only if subjected to a shear stress bigger than a characteristic stress, the yield stress. This is characterized by a flow curve that is a straight line having an intercept t_o on the shear stress axis. The yield stress τ_o, is the magnitude of the stress that must exceed by the shear stress before the flow starts. A physical explanation for such behavior is that a Bingham plastic at rest contains a three dimensional structure with sufficient rigidity to resist any stress less than the yield stress τ_o, which is characteristic of the material. Once this stress is exceeded, the structure disintegrates and the system behaves like a Newtonian fluid. If their yield stress falls below τ_o, these liquids behave like elastic solids. Paints, ketchup, mayonnaise, fiber suspensions are some examples of Bingham plastic.

Pseudoplastic Fluids

These fluids show no yield stress. A flow curve for these material shows that the ratio of shear stress to rate of shear falls progressively with the increase in the shear rate. At very low and at very high shear rates, the slopes are almost linear.

Dilatant Fluids

These fluids show an increase in viscosity with an increase in shear rate and thus exhibit a shear thickening behavior. In older literature, the term dilatancy described the property of volume expansion with shear. Though early usage of the term meant volume expansion, the current more widely accepted definition is: dilatancy is the isothermal reversible increase of viscosity with increasing shear rate with no measurable time dependence. The process may or may not be accompanied by detectable volume change.

1.7.2 Time Dependent Fluids

Some fluids in the presence of impressed steady rate of shear show an increase or decrease in viscosity as time passes. This is because the applied shear changes the whole sequence of structure of time dependent fluids. The fluids that show an increase in viscosity as time progresses are called rheopectic, i.e. shear thickening with time and the fluids that show a decrease in viscosity as time progresses are called thixotropic i.e. shear thinning with time. Rheopexy and thixotropy are time dependent effects not shear dependent effects. A detail study of such fluids requires molecular structure of the fluids. Because of this, the mathematical development of time dependent fluids becomes hopelessly complicated. The theoretical study of these fluids, therefore, is based on many simplifying assumptions. In a thixotropic material, if the flow curve is plotted in a single experiment in which the shear rate is steadily increased from zero to maximum value and then decreased steadily towards zero, a form of hysteresis loop is obtained. The criterion of reversibility is a necessary condition of this definition (the structure recovers upon setting), because an irreversible decrease in viscosity would imply shear degradation [47, 48].

Rheopexy is essentially the reverse of thixotropy. In this case, gradual formation of a structure is accompanied by shear. Polymeric melts and polymeric solutions are examples of shear thinning while the examples of shear thickening are suspensions and emulsions.

1.7.3 Viscoelastic Fluids

These are the non-Newtonian fluids that possess a certain degree of elasticity and memory in addition to the shear-thinning or shear-thickening viscosity. As a result, in a flow, a certain amount of energy is stored in the fluid as a strain energy in addition to various dissipation in the form of heat. In a viscoelastic fluid, we, therefore have to consider the strain no matter how small it may be. On the removal of the stress, strain is responsible for the fluid's partial recovery to its original state and the reverse flow that ensues. During the flow, the natural state of a viscoelastic fluid changes continuously. It tries to attain the instantaneous state of the deformed state, but it never completely succeeds. This lag is a measure of the elasticity of the fluid or the so-called memory of the fluid. All liquids of polymeric origin (melts, solutions, suspensions) are viscoelastic. For Newtonian liquids the deformation and the stress are in phase, for viscoelastic liquids they are out of phase, and therefore viscoelastic liquids may continue to be under stress even under zero deformation or shear rate. The viscous character of viscoelastic liquids is controlled by their ability to orient themselves differently under different flow conditions, which gives rise to shear thinning. The elastic character is controlled by the flexibility and ability of elastic macromolecules to respond to shear and extensional deformations. The simplest viscoelastic model is the Maxwell model, which is based on the assumption that a viscoelastic liquid exhibits both viscous resistance to flow, measured by its viscosity μ, and elastic resistance to deformation, measured by relaxation time.

1.8 MHD Equations

Magnetohydrodynamics (MHD) is the study of the motion of fluid in the presence of a magnetic field. The situation is essentially one of mutual interaction between the fluid velocity field and the electromagnetic field: electric currents induced in the fluid as a result of its motion modify the field; at the same time their flow in the magnetic field produces mechanical forces which modify the motion. Applications of MHD to natural events received a delayed motivation when astrophysicists came to realize how established throughout the universe are conducting, ionized gases (plasmas) and significantly strong magnetic fields. Geophysicists have considered the problem of explaining the earths field by motions of its postulated core of conducting fluid. MHD is important in astrophysics because the enormous scale of events makes up for the compactness of the conductivities and magnetic fields. MHD differs from ordinary hydrodynamics in that the fluid is electrically conducting. It is not magnetic; it effects a magnetic field not by its mere presence but only by virtue of electric currents flowing in it. The fluid conducts because it contains free charges that can move indefinitely. The full nonlinear equations of MHD (including thermal and diffusive effects) are so complex that they often need to be approximated drastically by focusing on the dominant physical mechanisms in any particular phenomena.

In the Magnetohydrodynamics approximation, the behavior of the continuous electrically conducting fluid is governed by a simplified form of Maxwells equations, together with Ohms law and equations of continuity and motion.

1.8.1 Maxwells Equations

We begin with Maxwells equations in m. k. s. units,

$$curl\,\mathbf{B} = \mu\,\mathbf{J} + \frac{1}{c^2}\frac{\partial \mathbf{E}}{\partial t}, \tag{1.3}$$

$$div\,\mathbf{B} = 0, \tag{1.4}$$

$$curl\,\mathbf{E} = -\frac{\partial \mathbf{B}}{\partial t}, \tag{1.5}$$

$$div\,\mathbf{E} = \frac{\rho^*}{\epsilon}, \tag{1.6}$$

where $\mathbf{B}$ is the total magnetic field, $\mathbf{E}$ is the electric field, ρ^* the charge density, $\mathbf{J}$ the current density, μ the magnetic permeability and ϵ the permittivity. The first Maxwell equation shows that either currents or time varying electric field may produce magnetic field, whereas the third and fourth equations imply that either electric charges or time varying magnetic field may give rise to electric fields. The second equation assumes that there are no magnetic poles and implies that a magnetic flux tube has a constant strength along its length. A fundamental supposition of magnetohydrodynamics is that the electromagnetic variations are non relativistic or quasi-steady. In other words,

$$\mathbf{V}_\circ << c, \tag{1.7}$$

where $\mathbf{V}_\circ$ is a characteristic electromagnetic (or electrically conducting fluid) speed, while c is the speed of light. Thus one consequence of equation (1.7) is that the term $\frac{1}{c^2}\frac{\partial \mathbf{E}}{\partial t}$ may be neglected in equation (1.3). Another is that the equation of charge continuity, which is obtained from the divergence of equation (1.3), becomes $\nabla.\mathbf{J} = \mathbf{0}$; this implies physically that local accumulations in time of charge are negligible and electric currents flow in closed circuits.

1.8.2 Ohm's Law

Electrically conducting fluid moving at a non-relativistic speed in the presence of a magnetic field is subject to an electric field $(\mathbf{V} \times \mathbf{B})$ in addition to the electric field (**E**) which would act on material at rest. Ohm's Law asserts that the current density is proportional to the total electric field (in a frame of reference moving with the electrically conducting fluid), and it may be written as

$$\mathbf{J} = \sigma(\mathbf{E} + \mathbf{V} \times \mathbf{B}), \tag{1.8}$$

where σ is the electric conductivity

1.8.3 Equation of Continuity

The equation of continuity expresses the fact that for a unit volume there is a balance between the masses entering and leaving per unit time and the change in density and is independent of the nature of fluid. In the case of unsteady flow of a compressible fluid this equation is given by

$$\frac{D\rho}{Dt} + \rho \, div\mathbf{V} = \frac{\partial \rho}{\partial t} + div(\rho \, \mathbf{V}) = 0, \tag{1.9}$$

whereas for an incompressible fluid, with $\rho =$ constant, the equation of continuity assumes the simplified form

$$div\mathbf{V} = 0. \tag{1.10}$$

The symbol $\frac{D\rho}{Dt}$ denotes here the substantive derivative which consists of the local contribution (in unsteady flow) $\frac{\partial \rho}{\partial t}$, and the convective contribution (due to translation), $\mathbf{V} \, . \, grad \, \rho$.

1.8.4 Equation of Motion for the Third Grade Fluid

In this thesis we have considered non-Newtonian fluids particularly second grade and third grade fluids. The momentum equation for the MHD third grade fluid in the vector form is:

$$\rho \frac{D\mathbf{V}}{Dt} = \mathbf{J} \times \mathbf{B} + \nabla.\mathbf{T} \tag{1.11}$$

with no gravity effects. The symbol $\frac{D\mathbf{V}}{Dt}$ denotes here the substantive acceleration which, like the substantive derivative of density, consists of the local contribution (in unsteady flow) $\frac{\partial \mathbf{V}}{\partial t}$, and the convective contribution (due to translation), $(\mathbf{V}\ .\ grad)\ \mathbf{V}$. The Cauchy stress tensor for an incompressible third grade fluid is

$$\begin{aligned} \mathbf{T} &= -p\mathbf{I} + \mu\mathbf{A}_1 + \alpha_1\mathbf{A}_2 + \alpha_2\mathbf{A}_1^2 \\ &+ \beta_1\mathbf{A}_3 + \beta_2(\mathbf{A}_1\mathbf{A}_2 + \mathbf{A}_2\mathbf{A}_1) + \beta_3(tr\mathbf{A}_1^2)\mathbf{A}_1, \end{aligned} \tag{1.12}$$

where $\alpha_1, \alpha_2, \beta_1, \beta_2$ and β_3 are material constants. Cauchy stresses for second grade and viscous fluids are obtained by putting $\beta_1 = \beta_2 = \beta_3 = 0$ and $\alpha_1 = \alpha_2 = \beta_1 = \beta_2 = \beta_3 = 0$ respectively, in equation (1.12).

The equations of motion are derived from Newton's Second Law, which states that the product of mass and acceleration is equal to the sum of the all forces acting on the body. In electrically conducting fluid motion it is necessary to consider the following three types of forces, the electromagnetic force $\mathbf{F}^{em}$, the mechanical force $\mathbf{F}^{m}$ and the external force $\mathbf{F}^{ex}$. Electromagnetic field induced the charge and current density at the same time which lead to the electric force $q\mathbf{E}$ and the magnetic force $\mathbf{J} \times \mathbf{B}$, respectively, which act on the substantial or moving element of the fluid. The electromagnetic force acting on a unit area is given by the equation

$$\mathbf{F}^{em} = q\mathbf{E} + \mathbf{J} \times \mathbf{B} \tag{1.13}$$

which is also known as Lorentz force and reduces to

$$\mathbf{F}^{em} = \mathbf{J} \times \mathbf{B}. \tag{1.14}$$

Since, by dimensional analysis, it is readily seen that the electric and magnetic parts of the body force $q\mathbf{E} + \mathbf{J} \times \mathbf{B}$ are in ratio equal to $\frac{\mathbf{V}_\circ^2}{c^2}$ which is very small so we neglect $q\mathbf{E}$.

The force acting on a unit area due to mechanical stress is given by the equation

$$\mathbf{F}^{m} = \nabla.\mathbf{T}, \tag{1.15}$$

where $\mathbf{T}$ is the sum of pressure and frictional forces. For viscous fluid

$$\mathbf{T} = -p\mathbf{I} + \mu\mathbf{A}_1, \tag{1.16}$$

where $p\mathbf{I}$ is the indeterminate part of the stress, μ is the coefficient of viscosity and $\mathbf{A}_1$ is a kinematical tensor defined by

$$\mathbf{A}_1 = (\mathbf{grad\ V}) + (\mathbf{grad\ V})^{\mathbf{T}}. \tag{1.17}$$

If $\mathbf{F}^{ex}$ is an ordinary gravitational force per unit volume, then

$$\mathbf{F}^{ex} = \rho\mathbf{g}, \tag{1.18}$$

where $\mathbf{g}$ is the acceleration vector due to gravity. External forces are usually neglected unless their effect is of special significance.

The equation of motion in the vector form

$$\rho\,\frac{D\mathbf{V}}{Dt} = \mathbf{F}^{em} + \mathbf{F}^{m} + \mathbf{F}^{ex} \tag{1.19}$$

In equation (1.11) $\mathbf{J} \times \mathbf{B}$ is directed across the magnetic field, so that any motion along field lines must be produced by other forces, such as gravity, pressure gradient or frictional forces. The Lorentz force has two effects. It acts both to shorten magnetic field lines through the tension force and also to compress electrically conducting fluid through the pressure term.

For the second grade fluid

$$\mathbf{T} = -p\mathbf{I} + \mu\mathbf{A}_1 + \alpha_1\mathbf{A}_2 + \alpha_2\mathbf{A}_1^2, \tag{1.20}$$

where α_1 and α_2 are the normal stress moduli satisfying $\alpha_1 > 0$, $\alpha_1 + \alpha_2 = 0$ [49], $\mathbf{A_1}$ is defined as equation (1.17) and $\mathbf{A_2}$ is defined by the equation

$$\mathbf{A}_2 = \frac{D\mathbf{A}_1}{Dt} + \mathbf{A}_1\,(\mathbf{grad\ V}) + (\mathbf{grad\ V})^{\mathbf{T}}\,\mathbf{A}_1. \tag{1.21}$$

The tensors $\mathbf{A}_3$ used in equation (1.12) is defined through [50]:

$$\mathbf{A}_3 = \frac{D\mathbf{A}_2}{Dt} + \mathbf{A}_2\,(\mathbf{grad\ V}) + (\mathbf{grad\ V})^{T}\,\mathbf{A}_2, \tag{1.22}$$

We shall not consider the model defined by equation (1.12) as an approximation to a simple fluid [51] in the sense of a retardation, but consider it to be an exact model in the sense described by Fosdick and Rajagopal in [52] (see also [53]). We require that the Clausius-Duhem inequality hold and that the specific Helmholtz free energy be a minimum when the fluid is locally at rest, which leads to the following restrictions on the material coefficients:

$$\begin{gathered}\mu \geq 0, \quad \alpha_1 \geq 0, \quad \beta_1 = \beta_2 = 0, \quad \beta_3 \geq 0, \\ -\sqrt{24\mu\beta_3} \ \leq \alpha_1 + \alpha_2 \ \leq \sqrt{24\mu\beta_3}.\end{gathered} \tag{1.23}$$

The model of equation (1.12) thus reduces to

$$\mathbf{T} = -p\mathbf{I} + \mu\mathbf{A}_1 + \alpha_1\mathbf{A}_2 + \alpha_2\mathbf{A}_1^2 + \beta_3(tr\mathbf{A}_1^2)\mathbf{A}_1. \tag{1.24}$$

Left hand side of equation (1.11) can be written as

$$(\rho\frac{D\mathbf{V}}{Dt})_x = \rho(\frac{\partial u}{\partial t} + u\frac{\partial u}{\partial x} + v\frac{\partial u}{\partial y} + w\frac{\partial u}{\partial z}), \tag{1.25}$$

$$(\rho\frac{D\mathbf{V}}{Dt})_y = \rho(\frac{\partial v}{\partial t} + u\frac{\partial v}{\partial x} + v\frac{\partial v}{\partial y} + w\frac{\partial v}{\partial z}), \tag{1.26}$$

$$(\rho\frac{D\mathbf{V}}{Dt})_z = \rho(\frac{\partial w}{\partial t} + u\frac{\partial w}{\partial x} + v\frac{\partial w}{\partial y} + w\frac{\partial w}{\partial z}), \tag{1.27}$$

where the subscripts denote the x, y and $z-$components. Also

$$\mathbf{J} \times \mathbf{B} = \sigma\left[(\mathbf{V} \times \mathbf{B}) \times \mathbf{B}\right] \tag{1.28}$$

We make the following assumptions:

1. The quantities ρ, ν, μ and σ are all constants throughout the flow field.

2. The magnetic field $\mathbf{B}$ is perpendicular to the velocity field $\mathbf{V}$ and the induced magnetic field is negligible compared with the imposed field so that the magnetic Reynolds number R_m is small [54].

3. The electric field is assumed to be zero.

4. The velocity vector $\mathbf{V}$ is a function of z and t alone with $w = -w_\circ$.

In view of these assumption, the electromagnetic body force involved in (1.28) can be written as [55]

$$\mathbf{J} \times \mathbf{B} = -\sigma \mathbf{B}_{\circ}^{2} \mathbf{V}, \tag{1.29}$$

where $(\sigma\ \mathbf{B}_{\circ}^{2})$ has the same dimension as $\rho\, \mathbf{\Omega}$.

$$-p\,\mathbf{I} \;=\; \begin{pmatrix} -p & 0 & 0 \\ 0 & -p & 0 \\ 0 & 0 & -p \end{pmatrix}, \tag{1.30}$$

$$\textbf{grad V} \;=\; \begin{pmatrix} \frac{\partial u}{\partial x} & \frac{\partial u}{\partial y} & \frac{\partial u}{\partial z} \\ \frac{\partial v}{\partial x} & \frac{\partial v}{\partial y} & \frac{\partial v}{\partial z} \\ \frac{\partial w}{\partial x} & \frac{\partial w}{\partial y} & \frac{\partial w}{\partial z} \end{pmatrix}, \tag{1.31}$$

$$(\textbf{grad V})^{T} \;=\; \begin{pmatrix} \frac{\partial u}{\partial x} & \frac{\partial v}{\partial x} & \frac{\partial w}{\partial x} \\ \frac{\partial u}{\partial y} & \frac{\partial v}{\partial y} & \frac{\partial w}{\partial y} \\ \frac{\partial u}{\partial z} & \frac{\partial v}{\partial z} & \frac{\partial w}{\partial z} \end{pmatrix}, \tag{1.32}$$

$$\mathbf{A}_1 \;=\; \begin{pmatrix} 2\frac{\partial u}{\partial x} & \frac{\partial u}{\partial y}+\frac{\partial v}{\partial x} & \frac{\partial u}{\partial z}+\frac{\partial w}{\partial x} \\ \frac{\partial v}{\partial x}+\frac{\partial u}{\partial y} & 2\frac{\partial v}{\partial y} & \frac{\partial v}{\partial z}+\frac{\partial w}{\partial y} \\ \frac{\partial w}{\partial x}+\frac{\partial u}{\partial z} & \frac{\partial w}{\partial y}+\frac{\partial v}{\partial z} & 2\frac{\partial w}{\partial z} \end{pmatrix}, \tag{1.33}$$

$$\frac{D\mathbf{A}_1}{Dt} = \frac{\partial \mathbf{A}_1}{\partial t} + (\mathbf{V}\,.\,\nabla)\,\mathbf{A}_1,$$

$$\left(\frac{D\mathbf{A}_1}{Dt}\right)_{xx} = 2\left(\frac{\partial^2 u}{\partial t \partial x} + u\,\frac{\partial^2 u}{\partial x^2} + v\,\frac{\partial^2 u}{\partial y \partial x} + w\,\frac{\partial^2 u}{\partial z \partial x}\right), \tag{1.34}$$

$$\left(\frac{D\mathbf{A}_1}{Dt}\right)_{xy} = \frac{\partial}{\partial t}\left(\frac{\partial u}{\partial y} + \frac{\partial v}{\partial x}\right) + u\,\frac{\partial}{\partial x}\left(\frac{\partial u}{\partial y} + \frac{\partial v}{\partial x}\right)$$

$$+\ v\,\frac{\partial}{\partial y}\left(\frac{\partial u}{\partial y} + \frac{\partial v}{\partial x}\right) + w\,\frac{\partial}{\partial z}\left(\frac{\partial u}{\partial y} + \frac{\partial v}{\partial x}\right), \tag{1.35}$$

$$\left(\frac{D\mathbf{A}_1}{Dt}\right)_{xz} = \frac{\partial}{\partial t}\left(\frac{\partial u}{\partial z} + \frac{\partial w}{\partial x}\right) + u\,\frac{\partial}{\partial x}\left(\frac{\partial u}{\partial z} + \frac{\partial w}{\partial x}\right)$$

$$+\ v\,\frac{\partial}{\partial y}\left(\frac{\partial u}{\partial z} + \frac{\partial w}{\partial x}\right) + w\,\frac{\partial}{\partial z}\left(\frac{\partial u}{\partial z} + \frac{\partial w}{\partial x}\right), \tag{1.36}$$

$$\left(\frac{D\mathbf{A}_1}{Dt}\right)_{yy} = 2\left(\frac{\partial^2 v}{\partial t \partial y} + u\,\frac{\partial^2 v}{\partial x \partial y} + v\,\frac{\partial^2 v}{\partial y^2} + w\,\frac{\partial^2 v}{\partial z \partial y}\right), \tag{1.37}$$

$$\left(\frac{D\mathbf{A}_1}{Dt}\right)_{yz} = \frac{\partial}{\partial t}\left(\frac{\partial v}{\partial z} + \frac{\partial w}{\partial y}\right) + u\,\frac{\partial}{\partial x}\left(\frac{\partial v}{\partial z} + \frac{\partial w}{\partial y}\right)$$

$$+\ v\,\frac{\partial}{\partial y}\left(\frac{\partial v}{\partial z} + \frac{\partial w}{\partial y}\right) + w\,\frac{\partial}{\partial z}\left(\frac{\partial v}{\partial z} + \frac{\partial w}{\partial y}\right), \tag{1.38}$$

$$\left(\frac{D\mathbf{A}_1}{Dt}\right)_{zz} = 2\left(\frac{\partial^2 w}{\partial t \partial z} + u\,\frac{\partial^2 w}{\partial x \partial z} + v\,\frac{\partial^2 w}{\partial y \partial z} + w\,\frac{\partial^2 w}{\partial z^2}\right), \tag{1.39}$$

$$\left(\frac{D\mathbf{A}_1}{Dt}\right)_{yx} = \left(\frac{D\mathbf{A}_1}{Dt}\right)_{xy}, \tag{1.40}$$

$$\left(\frac{D\mathbf{A}_1}{Dt}\right)_{zx} = \left(\frac{D\mathbf{A}_1}{Dt}\right)_{xz}, \tag{1.41}$$

$$\left(\frac{D\mathbf{A}_1}{Dt}\right)_{zy} = \left(\frac{D\mathbf{A}_1}{Dt}\right)_{yz}, \tag{1.42}$$

$$(\mathbf{A}_1\,(\mathbf{grad\ V}))_{xx} = 2\left(\frac{\partial u}{\partial x}\right)^2 + \frac{\partial v}{\partial x}\left(\frac{\partial u}{\partial y} + \frac{\partial v}{\partial x}\right) + \frac{\partial w}{\partial x}\left(\frac{\partial u}{\partial z} + \frac{\partial w}{\partial x}\right), \tag{1.43}$$

$$(\mathbf{A}_1\,(\mathbf{grad\ V}))_{xy} = 2\frac{\partial u}{\partial x}\frac{\partial u}{\partial y} + \frac{\partial v}{\partial y}\left(\frac{\partial u}{\partial y} + \frac{\partial v}{\partial x}\right) + \frac{\partial w}{\partial y}\left(\frac{\partial u}{\partial z} + \frac{\partial w}{\partial x}\right), \tag{1.44}$$

$$(\mathbf{A}_1\,(\mathbf{grad\ V}))_{xz} = 2\frac{\partial u}{\partial x}\frac{\partial u}{\partial z} + \frac{\partial v}{\partial z}\left(\frac{\partial u}{\partial y} + \frac{\partial v}{\partial x}\right) + \frac{\partial w}{\partial z}\left(\frac{\partial u}{\partial z} + \frac{\partial w}{\partial x}\right), \tag{1.45}$$

$$(\mathbf{A}_1\,(\mathbf{grad\ V}))_{yx} = \frac{\partial u}{\partial x}\left(\frac{\partial u}{\partial y} + \frac{\partial v}{\partial x}\right) + 2\frac{\partial v}{\partial x}\frac{\partial v}{\partial y} + \frac{\partial w}{\partial x}\left(\frac{\partial v}{\partial z} + \frac{\partial w}{\partial y}\right), \tag{1.46}$$

$$(\mathbf{A}_1\,(\mathbf{grad\ V}))_{yy} = \frac{\partial u}{\partial y}\left(\frac{\partial u}{\partial y} + \frac{\partial v}{\partial x}\right) + 2\left(\frac{\partial v}{\partial y}\right)^2 + \frac{\partial w}{\partial y}\left(\frac{\partial v}{\partial z} + \frac{\partial w}{\partial y}\right), \tag{1.47}$$

$$(\mathbf{A}_1\,(\mathbf{grad\ V}))_{yz} = \frac{\partial u}{\partial z}\left(\frac{\partial u}{\partial y} + \frac{\partial v}{\partial x}\right) + 2\frac{\partial v}{\partial z}\frac{\partial v}{\partial y} + \frac{\partial w}{\partial z}\left(\frac{\partial v}{\partial z} + \frac{\partial w}{\partial y}\right), \tag{1.48}$$

$$(\mathbf{A}_1\,(\mathbf{grad\ V}))_{zx} = \frac{\partial u}{\partial x}\left(\frac{\partial u}{\partial z} + \frac{\partial w}{\partial x}\right) + \frac{\partial v}{\partial x}\left(\frac{\partial v}{\partial z} + \frac{\partial w}{\partial y}\right) + 2\frac{\partial w}{\partial z}\frac{\partial w}{\partial x}, \tag{1.49}$$

$$(\mathbf{A}_1\,(\mathbf{grad\ V}))_{zy} = \frac{\partial u}{\partial y}\left(\frac{\partial u}{\partial z} + \frac{\partial w}{\partial x}\right) + \frac{\partial v}{\partial y}\left(\frac{\partial v}{\partial z} + \frac{\partial w}{\partial y}\right) + 2\frac{\partial w}{\partial z}\frac{\partial w}{\partial y}, \tag{1.50}$$

$$(\mathbf{A}_1\,(\mathbf{grad\ V}))_{zz} = \frac{\partial u}{\partial z}\left(\frac{\partial u}{\partial z} + \frac{\partial w}{\partial x}\right) + \frac{\partial v}{\partial z}\left(\frac{\partial v}{\partial z} + \frac{\partial w}{\partial y}\right) + 2\left(\frac{\partial w}{\partial z}\right)^2, \tag{1.51}$$

$$\left((\mathbf{grad\ V})^{\mathrm{T}}\,\mathbf{A}_1\right)_{xx} = 2\left(\frac{\partial u}{\partial x}\right)^2 + \frac{\partial v}{\partial x}\left(\frac{\partial u}{\partial y} + \frac{\partial v}{\partial x}\right) + \frac{\partial w}{\partial x}\left(\frac{\partial u}{\partial z} + \frac{\partial w}{\partial x}\right), \tag{1.52}$$

$$\left((\mathbf{grad\ V})^{\mathbf{T}}\ \mathbf{A}_1\right)_{xy} = \frac{\partial u}{\partial x}\left(\frac{\partial u}{\partial y}+\frac{\partial v}{\partial x}\right)+2\frac{\partial v}{\partial x}\frac{\partial v}{\partial y}+\frac{\partial w}{\partial x}\left(\frac{\partial v}{\partial z}+\frac{\partial w}{\partial y}\right), \quad (1.53)$$

$$\left((\mathbf{grad\ V})^{\mathbf{T}}\ \mathbf{A}_1\right)_{xz} = \frac{\partial u}{\partial x}\left(\frac{\partial u}{\partial z}+\frac{\partial w}{\partial x}\right)+\frac{\partial v}{\partial x}\left(\frac{\partial v}{\partial z}+\frac{\partial w}{\partial y}\right)+2\frac{\partial w}{\partial x}\frac{\partial w}{\partial z}, \quad (1.54)$$

$$\left((\mathbf{grad\ V})^{\mathbf{T}}\ \mathbf{A}_1\right)_{yx} = 2\frac{\partial u}{\partial y}\frac{\partial u}{\partial x}+\frac{\partial v}{\partial y}\left(\frac{\partial u}{\partial y}+\frac{\partial v}{\partial x}\right)+\frac{\partial w}{\partial y}\left(\frac{\partial u}{\partial z}+\frac{\partial w}{\partial x}\right), \quad (1.55)$$

$$\left((\mathbf{grad\ V})^{\mathbf{T}}\ \mathbf{A}_1\right)_{yy} = \frac{\partial u}{\partial y}\left(\frac{\partial u}{\partial y}+\frac{\partial v}{\partial x}\right)+2\left(\frac{\partial v}{\partial y}\right)^2+\frac{\partial w}{\partial y}\left(\frac{\partial v}{\partial z}+\frac{\partial w}{\partial y}\right), \quad (1.56)$$

$$\left((\mathbf{grad\ V})^{\mathbf{T}}\ \mathbf{A}_1\right)_{yz} = \frac{\partial u}{\partial y}\left(\frac{\partial u}{\partial z}+\frac{\partial w}{\partial x}\right)+\frac{\partial v}{\partial y}\left(\frac{\partial v}{\partial z}+\frac{\partial w}{\partial y}\right)+2\frac{\partial w}{\partial y}\frac{\partial w}{\partial z}, \quad (1.57)$$

$$\left((\mathbf{grad\ V})^{\mathbf{T}}\ \mathbf{A}_1\right)_{zx} = 2\frac{\partial u}{\partial z}\frac{\partial u}{\partial x}+\frac{\partial v}{\partial z}\left(\frac{\partial u}{\partial y}+\frac{\partial v}{\partial x}\right)+\frac{\partial w}{\partial z}\left(\frac{\partial u}{\partial z}+\frac{\partial w}{\partial x}\right), \quad (1.58)$$

$$\left((\mathbf{grad\ V})^{\mathbf{T}}\ \mathbf{A}_1\right)_{zy} = \frac{\partial u}{\partial z}\left(\frac{\partial u}{\partial y}+\frac{\partial v}{\partial x}\right)+2\frac{\partial v}{\partial z}\frac{\partial v}{\partial y}+\frac{\partial w}{\partial z}\left(\frac{\partial v}{\partial z}+\frac{\partial w}{\partial y}\right), \quad (1.59)$$

$$\left((\mathbf{grad\ V})^{\mathbf{T}}\ \mathbf{A}_1\right)_{zz} = \frac{\partial u}{\partial z}\left(\frac{\partial u}{\partial z}+\frac{\partial w}{\partial x}\right)+\frac{\partial v}{\partial z}\left(\frac{\partial v}{\partial z}+\frac{\partial w}{\partial y}\right)+2\left(\frac{\partial w}{\partial z}\right)^2, \quad (1.60)$$

$$\begin{aligned}(\mathbf{A}_2)_{xx} &= 2\left(\frac{\partial^2 u}{\partial t\partial x}+u\,\frac{\partial^2 u}{\partial x^2}+v\,\frac{\partial^2 u}{\partial y\partial x}+w\,\frac{\partial^2 u}{\partial z\partial x}\right)\\ &+ 4\left(\frac{\partial u}{\partial x}\right)^2+2\frac{\partial v}{\partial x}\left(\frac{\partial u}{\partial y}+\frac{\partial v}{\partial x}\right)+2\frac{\partial w}{\partial x}\left(\frac{\partial u}{\partial z}+\frac{\partial w}{\partial x}\right), \quad (1.61)\\ (\mathbf{A}_2)_{xy} &= \frac{\partial}{\partial t}\left(\frac{\partial u}{\partial y}+\frac{\partial v}{\partial x}\right)+u\,\frac{\partial}{\partial x}\left(\frac{\partial u}{\partial y}+\frac{\partial v}{\partial x}\right)+v\,\frac{\partial}{\partial y}\left(\frac{\partial u}{\partial y}+\frac{\partial v}{\partial x}\right)\end{aligned}$$

$$
\begin{aligned}
&+ \quad w\,\frac{\partial}{\partial z}\left(\frac{\partial u}{\partial y}+\frac{\partial v}{\partial x}\right)+3\frac{\partial u}{\partial x}\frac{\partial u}{\partial y}+\frac{\partial v}{\partial y}\frac{\partial u}{\partial y}+3\frac{\partial v}{\partial x}\frac{\partial v}{\partial y}\\
&+ \quad \frac{\partial w}{\partial y}\frac{\partial u}{\partial z}+2\frac{\partial w}{\partial x}\frac{\partial w}{\partial y}+\frac{\partial u}{\partial x}\frac{\partial v}{\partial x}+\frac{\partial v}{\partial z}\frac{\partial w}{\partial x},
\end{aligned}
\tag{1.62}
$$

$$
\begin{aligned}
(\mathbf{A}_2)_{xz} &= \frac{\partial}{\partial t}\left(\frac{\partial u}{\partial z}+\frac{\partial w}{\partial x}\right)+u\,\frac{\partial}{\partial x}\left(\frac{\partial u}{\partial z}+\frac{\partial w}{\partial x}\right)+v\,\frac{\partial}{\partial y}\left(\frac{\partial u}{\partial z}+\frac{\partial w}{\partial x}\right)\\
&+ \quad w\,\frac{\partial}{\partial z}\left(\frac{\partial u}{\partial z}+\frac{\partial w}{\partial x}\right)+3\frac{\partial u}{\partial x}\frac{\partial u}{\partial z}+\frac{\partial v}{\partial z}\frac{\partial u}{\partial y}+2\frac{\partial v}{\partial x}\frac{\partial v}{\partial z}\\
&+ \quad \frac{\partial w}{\partial z}\frac{\partial u}{\partial z}+3\frac{\partial w}{\partial x}\frac{\partial w}{\partial z}+\frac{\partial u}{\partial x}\frac{\partial w}{\partial x}+\frac{\partial v}{\partial x}\frac{\partial w}{\partial y},
\end{aligned}
\tag{1.63}
$$

$$
\begin{aligned}
(\mathbf{A}_2)_{yy} &= 2\left(\frac{\partial^2 v}{\partial t\partial y}+u\,\frac{\partial^2 v}{\partial x\partial y}+v\,\frac{\partial^2 v}{\partial y^2}+w\,\frac{\partial^2 v}{\partial z\partial y}\right)\\
&+ \quad 2\left(\frac{\partial u}{\partial y}\right)^2+2\frac{\partial u}{\partial y}\frac{\partial v}{\partial x}+4\left(\frac{\partial v}{\partial y}\right)^2+2\frac{\partial w}{\partial y}\frac{\partial v}{\partial z}+2\left(\frac{\partial w}{\partial y}\right)^2,
\end{aligned}
\tag{1.64}
$$

$$
\begin{aligned}
(\mathbf{A}_2)_{yz} &= \frac{\partial}{\partial t}\left(\frac{\partial v}{\partial z}+\frac{\partial w}{\partial y}\right)+u\,\frac{\partial}{\partial x}\left(\frac{\partial v}{\partial z}+\frac{\partial w}{\partial y}\right)+v\,\frac{\partial}{\partial y}\left(\frac{\partial v}{\partial z}+\frac{\partial w}{\partial y}\right)\\
&+ \quad w\,\frac{\partial}{\partial z}\left(\frac{\partial v}{\partial z}+\frac{\partial w}{\partial y}\right)+2\frac{\partial u}{\partial y}\frac{\partial u}{\partial z}+\frac{\partial u}{\partial z}\frac{\partial v}{\partial x}+3\frac{\partial v}{\partial y}\frac{\partial v}{\partial z}+\frac{\partial w}{\partial z}\frac{\partial v}{\partial z}\\
&+ \quad 3\frac{\partial w}{\partial y}\frac{\partial w}{\partial z}+\frac{\partial w}{\partial x}\frac{\partial u}{\partial y}+\frac{\partial v}{\partial y}\frac{\partial w}{\partial y},
\end{aligned}
\tag{1.65}
$$

$$
\begin{aligned}
(\mathbf{A}_2)_{zz} &= 2\left(\frac{\partial^2 w}{\partial t\partial z}+u\,\frac{\partial^2 w}{\partial x\partial z}+v\,\frac{\partial^2 w}{\partial y\partial z}+w\,\frac{\partial^2 w}{\partial z^2}\right)\\
&+ \quad 2\left(\frac{\partial u}{\partial z}\right)^2+2\frac{\partial u}{\partial z}\frac{\partial w}{\partial x}+2\left(\frac{\partial v}{\partial z}\right)^2+2\frac{\partial w}{\partial y}\frac{\partial v}{\partial z}+4\left(\frac{\partial w}{\partial z}\right)^2,
\end{aligned}
\tag{1.66}
$$

$$(\mathbf{A}_2)_{yx} = (\mathbf{A}_2)_{xy}, \tag{1.67}$$

$$(\mathbf{A}_2)_{zx} = (\mathbf{A}_2)_{xz}, \tag{1.68}$$

$$(\mathbf{A}_2)_{zy} = (\mathbf{A}_2)_{yz}, \tag{1.69}$$

$$\left(\mathbf{A}_1^2\right)_{xx} = \left(2\frac{\partial u}{\partial x}\right)^2 + \left(\frac{\partial u}{\partial y} + \frac{\partial v}{\partial x}\right)^2 + \left(\frac{\partial u}{\partial z} + \frac{\partial w}{\partial x}\right)^2, \tag{1.70}$$

$$\begin{aligned}\left(\mathbf{A}_1^2\right)_{xy} &= 2\frac{\partial u}{\partial x}\left(\frac{\partial u}{\partial y} + \frac{\partial v}{\partial x}\right) + 2\frac{\partial v}{\partial y}\left(\frac{\partial u}{\partial y} + \frac{\partial v}{\partial x}\right) \\ &+ \left(\frac{\partial u}{\partial z} + \frac{\partial w}{\partial x}\right)\left(\frac{\partial v}{\partial z} + \frac{\partial w}{\partial y}\right),\end{aligned} \tag{1.71}$$

$$\begin{aligned}\left(\mathbf{A}_1^2\right)_{xz} &= 2\frac{\partial u}{\partial x}\left(\frac{\partial u}{\partial z} + \frac{\partial w}{\partial x}\right) + \left(\frac{\partial v}{\partial z} + \frac{\partial w}{\partial y}\right)\left(\frac{\partial u}{\partial y} + \frac{\partial v}{\partial x}\right) \\ &+ 2\frac{\partial w}{\partial z}\left(\frac{\partial u}{\partial z} + \frac{\partial w}{\partial x}\right),\end{aligned} \tag{1.72}$$

$$\left(\mathbf{A}_1^2\right)_{yy} = \left(\frac{\partial u}{\partial y} + \frac{\partial v}{\partial x}\right)^2 + \left(2\frac{\partial v}{\partial y}\right)^2 + \left(\frac{\partial v}{\partial z} + \frac{\partial w}{\partial y}\right)^2, \tag{1.73}$$

$$\begin{aligned}\left(\mathbf{A}_1^2\right)_{yz} &= \left(\frac{\partial u}{\partial y} + \frac{\partial v}{\partial x}\right)\left(\frac{\partial u}{\partial z} + \frac{\partial w}{\partial x}\right) + 2\frac{\partial v}{\partial y}\left(\frac{\partial v}{\partial z} + \frac{\partial w}{\partial y}\right) \\ &+ 2\frac{\partial w}{\partial z}\left(\frac{\partial v}{\partial z} + \frac{\partial w}{\partial y}\right),\end{aligned} \tag{1.74}$$

$$\left(\mathbf{A}_1^2\right)_{zz} = \left(\frac{\partial u}{\partial z} + \frac{\partial w}{\partial x}\right)^2 + \left(\frac{\partial v}{\partial z} + \frac{\partial w}{\partial y}\right)^2 + \left(2\frac{\partial w}{\partial z}\right)^2, \tag{1.75}$$

$$\left(\mathbf{A}_1^2\right)_{yx} = \left(\mathbf{A}_1^2\right)_{xy}, \tag{1.76}$$

$$\left(\mathbf{A}_1^2\right)_{zx} = \left(\mathbf{A}_1^2\right)_{xz}, \tag{1.77}$$

$$\left(\mathbf{A}_1^2\right)_{zy} = \left(\mathbf{A}_1^2\right)_{yz}, \tag{1.78}$$

$$\begin{aligned}\left(tr\mathbf{A}_1^2\right) &= \left(2\frac{\partial u}{\partial x}\right)^2 + \left(2\frac{\partial v}{\partial y}\right)^2 + \left(2\frac{\partial w}{\partial z}\right)^2 + 2\left(\frac{\partial u}{\partial y} + \frac{\partial v}{\partial x}\right)^2 \\ &+ 2\left(\frac{\partial u}{\partial z} + \frac{\partial w}{\partial x}\right)^2 + 2\left(\frac{\partial v}{\partial z} + \frac{\partial w}{\partial y}\right)^2,\end{aligned} \tag{1.79}$$

$$\begin{aligned}\left[\left(tr\mathbf{A}_1^2\right)\mathbf{A}_1\right]_{xx} &= \left(2\frac{\partial u}{\partial x}\right)^3 + 8\frac{\partial u}{\partial x}\left(\frac{\partial v}{\partial y}\right)^2 + 8\frac{\partial u}{\partial x}\left(\frac{\partial w}{\partial z}\right)^2 \\ &+ 4\frac{\partial u}{\partial x}\left(\frac{\partial u}{\partial y} + \frac{\partial v}{\partial x}\right)^2 + 4\frac{\partial u}{\partial x}\left(\frac{\partial u}{\partial z} + \frac{\partial w}{\partial x}\right)^2 \\ &+ 4\frac{\partial u}{\partial x}\left(\frac{\partial v}{\partial z} + \frac{\partial w}{\partial y}\right)^2,\end{aligned} \tag{1.80}$$

$$\begin{aligned}\left[\left(tr\mathbf{A}_1^2\right)\mathbf{A}_1\right]_{xy} &= 4\left(\frac{\partial u}{\partial x}\right)^2\left(\frac{\partial u}{\partial y} + \frac{\partial v}{\partial x}\right) + 4\left(\frac{\partial v}{\partial y}\right)^2\left(\frac{\partial u}{\partial y} + \frac{\partial v}{\partial x}\right) \\ &+ 4\left(\frac{\partial w}{\partial z}\right)^2\left(\frac{\partial u}{\partial y} + \frac{\partial v}{\partial x}\right) + 4\left(\frac{\partial u}{\partial y} + \frac{\partial v}{\partial x}\right)^3 \\ &+ 2\left(\frac{\partial u}{\partial y} + \frac{\partial v}{\partial x}\right)\left(\frac{\partial u}{\partial z} + \frac{\partial w}{\partial x}\right)^2 + 2\left(\frac{\partial u}{\partial y} + \frac{\partial v}{\partial x}\right)\left(\frac{\partial v}{\partial z} + \frac{\partial w}{\partial y}\right)^2,\end{aligned} \tag{1.81}$$

$$\begin{aligned}\left[\left(tr\mathbf{A}_1^2\right)\mathbf{A}_1\right]_{xz} &= 4\left(\frac{\partial u}{\partial x}\right)^2\left(\frac{\partial u}{\partial z} + \frac{\partial w}{\partial x}\right) + 4\left(\frac{\partial v}{\partial y}\right)^2\left(\frac{\partial u}{\partial z} + \frac{\partial w}{\partial x}\right) \\ &+ 4\left(\frac{\partial w}{\partial z}\right)^2\left(\frac{\partial u}{\partial z} + \frac{\partial w}{\partial x}\right) + 2\left(\frac{\partial u}{\partial y} + \frac{\partial v}{\partial x}\right)^2\left(\frac{\partial u}{\partial z} + \frac{\partial w}{\partial x}\right)\end{aligned}$$

$$+ \quad 2\left(\frac{\partial u}{\partial z}+\frac{\partial w}{\partial x}\right)^3+2\left(\frac{\partial u}{\partial z}+\frac{\partial w}{\partial x}\right)\left(\frac{\partial v}{\partial z}+\frac{\partial w}{\partial y}\right)^2, \tag{1.82}$$

$$\begin{aligned}
\left[\left(tr\mathbf{A}_1^2\right)\mathbf{A}_1\right]_{yy} &= 8\frac{\partial v}{\partial y}\left(\frac{\partial u}{\partial x}\right)^2+8\left(\frac{\partial v}{\partial y}\right)^3+8\frac{\partial v}{\partial y}\left(\frac{\partial w}{\partial z}\right)^2 \\
&+ 4\frac{\partial v}{\partial y}\left(\frac{\partial u}{\partial y}+\frac{\partial v}{\partial x}\right)^2+4\frac{\partial v}{\partial y}\left(\frac{\partial u}{\partial z}+\frac{\partial w}{\partial x}\right)^2 \\
&+ 4\frac{\partial v}{\partial y}\left(\frac{\partial v}{\partial z}+\frac{\partial w}{\partial y}\right)^2,
\end{aligned} \tag{1.83}$$

$$\begin{aligned}
\left[\left(tr\mathbf{A}_1^2\right)\mathbf{A}_1\right]_{yz} &= 4\left(\frac{\partial u}{\partial x}\right)^2\left(\frac{\partial v}{\partial z}+\frac{\partial w}{\partial y}\right)+4\left(\frac{\partial v}{\partial y}\right)^2\left(\frac{\partial v}{\partial z}+\frac{\partial w}{\partial y}\right) \\
&+ 4\left(\frac{\partial w}{\partial z}\right)^2\left(\frac{\partial v}{\partial z}+\frac{\partial w}{\partial y}\right)+2\left(\frac{\partial u}{\partial y}+\frac{\partial v}{\partial x}\right)^2\left(\frac{\partial v}{\partial z}+\frac{\partial w}{\partial y}\right) \\
&+ 2\left(\frac{\partial u}{\partial z}+\frac{\partial w}{\partial x}\right)^2\left(\frac{\partial v}{\partial z}+\frac{\partial w}{\partial y}\right)+2\left(\frac{\partial v}{\partial z}+\frac{\partial w}{\partial y}\right)^3,
\end{aligned} \tag{1.84}$$

$$\begin{aligned}
\left[\left(tr\mathbf{A}_1^2\right)\mathbf{A}_1\right]_{zz} &= 8\frac{\partial w}{\partial z}\left(\frac{\partial u}{\partial x}\right)^2+8\frac{\partial w}{\partial z}\left(\frac{\partial v}{\partial y}\right)^2+8\left(\frac{\partial w}{\partial z}\right)^3 \\
&+ 4\frac{\partial w}{\partial z}\left(\frac{\partial u}{\partial y}+\frac{\partial v}{\partial x}\right)^2+4\frac{\partial w}{\partial z}\left(\frac{\partial u}{\partial z}+\frac{\partial w}{\partial x}\right)^2 \\
&+ 4\frac{\partial w}{\partial z}\left(\frac{\partial v}{\partial z}+\frac{\partial w}{\partial y}\right)^2,
\end{aligned} \tag{1.85}$$

$$\left[\left(tr\mathbf{A}_1^2\right)\mathbf{A}_1\right]_{yx} = \left[\left(tr\mathbf{A}_1^2\right)\mathbf{A}_1\right]_{xy}, \tag{1.86}$$

$$\left[\left(tr\mathbf{A}_1^2\right)\mathbf{A}_1\right]_{zx} = \left[\left(tr\mathbf{A}_1^2\right)\mathbf{A}_1\right]_{xz}, \tag{1.87}$$

$$\left[\left(tr\mathbf{A}_1^2\right)\mathbf{A}_1\right]_{zy} = \left[\left(tr\mathbf{A}_1^2\right)\mathbf{A}_1\right]_{yz}. \tag{1.88}$$

Substituting equations (1.30), (1.33), (1.61 - 1.78), (1.80- 1.88) into (1.24), we obtain

$$
\begin{aligned}
\mathbf{T}_{xx} &= \left(-p\,\mathbf{I} + \mu \mathbf{A}_1 + \alpha_1 \mathbf{A}_2 + \alpha_2 \mathbf{A}_1^2 + \beta_3 \left(tr\mathbf{A}_1^2\right)\mathbf{A}_1\right)_{xx} \\
&= -p + \mu\left(2\frac{\partial u}{\partial x}\right) + 2\alpha_1\left[\frac{\partial^2 u}{\partial t \partial x} + u\,\frac{\partial^2 u}{\partial x^2} + v\,\frac{\partial^2 u}{\partial y \partial x} + w\,\frac{\partial^2 u}{\partial z \partial x}\right. \\
&+ \left. 2\left(\frac{\partial u}{\partial x}\right)^2 + \frac{\partial v}{\partial x}\left(\frac{\partial u}{\partial y} + \frac{\partial v}{\partial x}\right) + \frac{\partial w}{\partial x}\left(\frac{\partial u}{\partial z} + \frac{\partial w}{\partial x}\right)\right] \\
&+ \alpha_2\left[\left(2\frac{\partial u}{\partial x}\right)^2 + \left(\frac{\partial u}{\partial y} + \frac{\partial v}{\partial x}\right)^2 + \left(\frac{\partial u}{\partial z} + \frac{\partial w}{\partial x}\right)^2\right] \\
&+ \beta_3\left[\left(2\frac{\partial u}{\partial x}\right)^3 + 8\frac{\partial u}{\partial x}\left(\frac{\partial v}{\partial y}\right)^2 + 8\frac{\partial u}{\partial x}\left(\frac{\partial w}{\partial z}\right)^2 + 4\frac{\partial u}{\partial x}\left(\frac{\partial u}{\partial y} + \frac{\partial v}{\partial x}\right)^2\right. \\
&+ \left. 4\frac{\partial u}{\partial x}\left(\frac{\partial u}{\partial z} + \frac{\partial w}{\partial x}\right)^2 + 4\frac{\partial u}{\partial x}\left(\frac{\partial v}{\partial z} + \frac{\partial w}{\partial y}\right)^2\right], \qquad (1.89)
\end{aligned}
$$

$$
\begin{aligned}
\mathbf{T}_{xy} &= \left(-p\,\mathbf{I} + \mu \mathbf{A}_1 + \alpha_1 \mathbf{A}_2 + \alpha_2 \mathbf{A}_1^2 + \beta_3 \left(tr\mathbf{A}_1^2\right)\mathbf{A}_1\right)_{xy} \\
&= \mu\left(\frac{\partial u}{\partial y} + \frac{\partial v}{\partial x}\right) + \alpha_1\left[\frac{\partial}{\partial t}\left(\frac{\partial u}{\partial y} + \frac{\partial v}{\partial x}\right) + u\,\frac{\partial}{\partial x}\left(\frac{\partial u}{\partial y} + \frac{\partial v}{\partial x}\right)\right. \\
&+ v\,\frac{\partial}{\partial y}\left(\frac{\partial u}{\partial y} + \frac{\partial v}{\partial x}\right) + w\,\frac{\partial}{\partial z}\left(\frac{\partial u}{\partial y} + \frac{\partial v}{\partial x}\right) + 3\frac{\partial u}{\partial x}\frac{\partial u}{\partial y} + \frac{\partial v}{\partial y}\frac{\partial u}{\partial y} \\
&+ \left. 3\frac{\partial v}{\partial x}\frac{\partial v}{\partial y} + \frac{\partial w}{\partial y}\frac{\partial u}{\partial z} + 2\frac{\partial w}{\partial x}\frac{\partial w}{\partial y} + \frac{\partial u}{\partial x}\frac{\partial v}{\partial x} + \frac{\partial v}{\partial z}\frac{\partial w}{\partial x}\right] \\
&+ \alpha_2\left[2\frac{\partial u}{\partial x}\left(\frac{\partial u}{\partial y} + \frac{\partial v}{\partial x}\right) + 2\frac{\partial v}{\partial y}\left(\frac{\partial u}{\partial y} + \frac{\partial v}{\partial x}\right) + \left(\frac{\partial u}{\partial z} + \frac{\partial w}{\partial x}\right)\left(\frac{\partial v}{\partial z} + \frac{\partial w}{\partial y}\right)\right]
\end{aligned}
$$

$$
\begin{aligned}
&+ \beta_3 \left[4 \left(\frac{\partial u}{\partial x} \right)^2 \left(\frac{\partial u}{\partial y} + \frac{\partial v}{\partial x} \right) + 4 \left(\frac{\partial v}{\partial y} \right)^2 \left(\frac{\partial u}{\partial y} + \frac{\partial v}{\partial x} \right) \right. \\
&+ 4 \left(\frac{\partial w}{\partial z} \right)^2 \left(\frac{\partial u}{\partial y} + \frac{\partial v}{\partial x} \right) + 4 \left(\frac{\partial u}{\partial y} + \frac{\partial v}{\partial x} \right)^3 + 2 \left(\frac{\partial u}{\partial y} + \frac{\partial v}{\partial x} \right) \left(\frac{\partial u}{\partial z} + \frac{\partial w}{\partial x} \right)^2 \\
&+ \left. 2 \left(\frac{\partial u}{\partial y} + \frac{\partial v}{\partial x} \right) \left(\frac{\partial v}{\partial z} + \frac{\partial w}{\partial y} \right)^2 \right], \qquad (1.90)
\end{aligned}
$$

$$
\begin{aligned}
\mathbf{T}_{xz} &= \left(-p\,\mathbf{I} + \mu \mathbf{A}_1 + \alpha_1 \mathbf{A}_2 + \alpha_2 \mathbf{A}_1^2 + \beta_3 \left(tr \mathbf{A}_1^2 \right) \mathbf{A}_1 \right)_{xz} \\
&= \mu \left(\frac{\partial u}{\partial z} + \frac{\partial w}{\partial x} \right) + \alpha_1 \left[\frac{\partial}{\partial t} \left(\frac{\partial u}{\partial z} + \frac{\partial w}{\partial x} \right) + u \frac{\partial}{\partial x} \left(\frac{\partial u}{\partial z} + \frac{\partial w}{\partial x} \right) \right. \\
&+ v \frac{\partial}{\partial y} \left(\frac{\partial u}{\partial z} + \frac{\partial w}{\partial x} \right) + w \frac{\partial}{\partial z} \left(\frac{\partial u}{\partial z} + \frac{\partial w}{\partial x} \right) + 3 \frac{\partial u}{\partial x} \frac{\partial u}{\partial z} \\
&+ \left. \frac{\partial v}{\partial z} \frac{\partial u}{\partial y} + 2 \frac{\partial v}{\partial x} \frac{\partial v}{\partial z} + \frac{\partial w}{\partial z} \frac{\partial u}{\partial z} + 3 \frac{\partial w}{\partial x} \frac{\partial w}{\partial z} + \frac{\partial u}{\partial x} \frac{\partial w}{\partial x} + \frac{\partial v}{\partial x} \frac{\partial w}{\partial y} \right] \\
&+ \alpha_2 \left[2 \frac{\partial u}{\partial x} \left(\frac{\partial u}{\partial z} + \frac{\partial w}{\partial x} \right) + \left(\frac{\partial v}{\partial z} + \frac{\partial w}{\partial y} \right) \left(\frac{\partial u}{\partial y} + \frac{\partial v}{\partial x} \right) \right. \\
&+ \left. 2 \frac{\partial w}{\partial z} \left(\frac{\partial u}{\partial z} + \frac{\partial w}{\partial x} \right) \right] + \beta_3 \left[4 \left(\frac{\partial u}{\partial x} \right)^2 \left(\frac{\partial u}{\partial z} + \frac{\partial w}{\partial x} \right) \right. \\
&+ 4 \left(\frac{\partial v}{\partial y} \right)^2 \left(\frac{\partial u}{\partial z} + \frac{\partial w}{\partial x} \right) + 4 \left(\frac{\partial w}{\partial z} \right)^2 \left(\frac{\partial u}{\partial z} + \frac{\partial w}{\partial x} \right) \\
&+ 2 \left(\frac{\partial u}{\partial y} + \frac{\partial v}{\partial x} \right)^2 \left(\frac{\partial u}{\partial z} + \frac{\partial w}{\partial x} \right) + 2 \left(\frac{\partial u}{\partial z} + \frac{\partial w}{\partial x} \right)^3 \\
&+ \left. 2 \left(\frac{\partial u}{\partial z} + \frac{\partial w}{\partial x} \right) \left(\frac{\partial v}{\partial z} + \frac{\partial w}{\partial y} \right)^2 \right], \qquad (1.91)
\end{aligned}
$$

$$
\begin{aligned}
\mathbf{T}_{yy} &= \left(-p\,\mathbf{I} + \mu\mathbf{A}_1 + \alpha_1\mathbf{A}_2 + \alpha_2\mathbf{A}_1^2 + \beta_3\left(tr\mathbf{A}_1^2\right)\mathbf{A}_1\right)_{yy} \\
&= -p + \mu\left(2\frac{\partial v}{\partial y}\right) + 2\alpha_1\left[\frac{\partial^2 v}{\partial t\partial y} + u\,\frac{\partial^2 v}{\partial x\partial y} + v\,\frac{\partial^2 v}{\partial y^2} + w\,\frac{\partial^2 v}{\partial z\partial y}\right. \\
&+ \left.\left(\frac{\partial u}{\partial y}\right)^2 + \frac{\partial u}{\partial y}\frac{\partial v}{\partial x} + 2\left(\frac{\partial v}{\partial y}\right)^2 + \frac{\partial w}{\partial y}\frac{\partial v}{\partial z} + \left(\frac{\partial w}{\partial y}\right)^2\right] \\
&+ \alpha_2\left[\left(\frac{\partial u}{\partial y} + \frac{\partial v}{\partial x}\right)^2 + \left(2\frac{\partial v}{\partial y}\right)^2 + \left(\frac{\partial v}{\partial z} + \frac{\partial w}{\partial y}\right)^2\right] \\
&+ \beta_3\left[8\frac{\partial v}{\partial y}\left(\frac{\partial u}{\partial x}\right)^2 + 8\left(\frac{\partial v}{\partial y}\right)^3 + 8\frac{\partial v}{\partial y}\left(\frac{\partial w}{\partial z}\right)^2\right. \\
&+ 4\frac{\partial v}{\partial y}\left(\frac{\partial u}{\partial y} + \frac{\partial v}{\partial x}\right)^2 + 4\frac{\partial v}{\partial y}\left(\frac{\partial u}{\partial z} + \frac{\partial w}{\partial x}\right)^2 \\
&+ \left.4\frac{\partial v}{\partial y}\left(\frac{\partial v}{\partial z} + \frac{\partial w}{\partial y}\right)^2\right], \qquad (1.92)
\end{aligned}
$$

$$
\begin{aligned}
\mathbf{T}_{yz} &= \left(-p\,\mathbf{I} + \mu\mathbf{A}_1 + \alpha_1\mathbf{A}_2 + \alpha_2\mathbf{A}_1^2 + \beta_3\left(tr\mathbf{A}_1^2\right)\mathbf{A}_1\right)_{yz} \\
&= \mu\left(\frac{\partial v}{\partial z} + \frac{\partial w}{\partial y}\right) + \alpha_1\left[\frac{\partial}{\partial t}\left(\frac{\partial v}{\partial z} + \frac{\partial w}{\partial y}\right) + u\,\frac{\partial}{\partial x}\left(\frac{\partial v}{\partial z} + \frac{\partial w}{\partial y}\right)\right. \\
&+ v\,\frac{\partial}{\partial y}\left(\frac{\partial v}{\partial z} + \frac{\partial w}{\partial y}\right) + w\,\frac{\partial}{\partial z}\left(\frac{\partial v}{\partial z} + \frac{\partial w}{\partial y}\right) + 2\frac{\partial u}{\partial y}\frac{\partial u}{\partial z} \\
&+ \left.\frac{\partial u}{\partial z}\frac{\partial v}{\partial x} + 3\frac{\partial v}{\partial y}\frac{\partial v}{\partial z} + \frac{\partial w}{\partial z}\frac{\partial v}{\partial z} + 3\frac{\partial w}{\partial y}\frac{\partial w}{\partial z} + \frac{\partial w}{\partial x}\frac{\partial u}{\partial y} + \frac{\partial v}{\partial y}\frac{\partial w}{\partial y}\right] \\
&+ \alpha_2\left[\left(\frac{\partial u}{\partial y} + \frac{\partial v}{\partial x}\right)\left(\frac{\partial u}{\partial z} + \frac{\partial w}{\partial x}\right) + 2\frac{\partial v}{\partial y}\left(\frac{\partial v}{\partial z} + \frac{\partial w}{\partial y}\right)\right.
\end{aligned}
$$

$$
\begin{aligned}
&+ \quad 2\frac{\partial w}{\partial z}\left(\frac{\partial v}{\partial z}+\frac{\partial w}{\partial y}\right)\Bigg] + \beta_3\left[4\left(\frac{\partial u}{\partial x}\right)^2\left(\frac{\partial v}{\partial z}+\frac{\partial w}{\partial y}\right)\right. \\
&+ \quad 4\left(\frac{\partial v}{\partial y}\right)^2\left(\frac{\partial v}{\partial z}+\frac{\partial w}{\partial y}\right)+4\left(\frac{\partial w}{\partial z}\right)^2\left(\frac{\partial v}{\partial z}+\frac{\partial w}{\partial y}\right) \\
&+ \quad 2\left(\frac{\partial u}{\partial y}+\frac{\partial v}{\partial x}\right)^2\left(\frac{\partial v}{\partial z}+\frac{\partial w}{\partial y}\right)+2\left(\frac{\partial u}{\partial z}+\frac{\partial w}{\partial x}\right)^2\left(\frac{\partial v}{\partial z}+\frac{\partial w}{\partial y}\right) \\
&+ \quad 2\left.\left(\frac{\partial v}{\partial z}+\frac{\partial w}{\partial y}\right)^3\right], \qquad (1.93)
\end{aligned}
$$

$$
\begin{aligned}
\mathbf{T}_{zz} &= \left(-p\,\mathbf{I}+\mu\mathbf{A}_1+\alpha_1\mathbf{A}_2+\alpha_2\mathbf{A}_1^2+\beta_3\left(tr\mathbf{A}_1^2\right)\mathbf{A}_1\right)_{zz} \\
&= -p+\mu\left(2\frac{\partial w}{\partial z}\right)+2\alpha_1\left[\frac{\partial^2 w}{\partial t\partial z}+u\,\frac{\partial^2 w}{\partial x\partial z}+v\,\frac{\partial^2 w}{\partial y\partial z}+w\,\frac{\partial^2 w}{\partial z^2}\right. \\
&+ \left.\left(\frac{\partial u}{\partial z}\right)^2+\frac{\partial u}{\partial z}\frac{\partial w}{\partial x}+\left(\frac{\partial v}{\partial z}\right)^2+\frac{\partial w}{\partial y}\frac{\partial v}{\partial z}+2\left(\frac{\partial w}{\partial z}\right)^2\right] \\
&+ \alpha_2\left[\left(\frac{\partial u}{\partial z}+\frac{\partial w}{\partial x}\right)^2+\left(\frac{\partial v}{\partial z}+\frac{\partial w}{\partial y}\right)^2+\left(2\frac{\partial w}{\partial z}\right)^2\right] \\
&+ 4\beta_3\left[2\frac{\partial w}{\partial z}\left(\frac{\partial u}{\partial x}\right)^2+2\frac{\partial w}{\partial z}\left(\frac{\partial v}{\partial y}\right)^2+2\left(\frac{\partial w}{\partial z}\right)^3\right. \\
&+ \left.\frac{\partial w}{\partial z}\left(\frac{\partial u}{\partial y}+\frac{\partial v}{\partial x}\right)^2+\frac{\partial w}{\partial z}\left(\frac{\partial u}{\partial z}+\frac{\partial w}{\partial x}\right)^2+\frac{\partial w}{\partial z}\left(\frac{\partial v}{\partial z}+\frac{\partial w}{\partial y}\right)^2\right], \qquad (1.94)
\end{aligned}
$$

$$
\mathbf{T}_{zx} = \mathbf{T}_{xz}, \qquad (1.95)
$$

$$
\mathbf{T}_{yx} = \mathbf{T}_{xy}, \qquad (1.96)
$$

$$
\mathbf{T}_{zy} = \mathbf{T}_{yz}. \qquad (1.97)
$$

Using equations (1.25 - 1.27), (1.29), (1.89 - 1.97) in equation (1.11), we get

$$
\begin{aligned}
\rho\left[\frac{\partial u}{\partial t}\right. &+ \left. u\frac{\partial u}{\partial x}+v\frac{\partial u}{\partial y}+w\frac{\partial u}{\partial z}\right] = -\sigma B_\circ^2 u - \frac{\partial p}{\partial x} + \mu\,\nabla^2 u \\
&+ \alpha_1\left[\left(\frac{\partial}{\partial t}+u\frac{\partial}{\partial x}+v\frac{\partial}{\partial y}+w\frac{\partial}{\partial z}\right)\nabla^2 u + \nabla^2 v\,\frac{\partial v}{\partial x} + \nabla^2 w\,\frac{\partial w}{\partial x}\right. \\
&+ \left. 2\frac{\partial w}{\partial z}\frac{\partial^2 w}{\partial x\partial z} + 2\frac{\partial v}{\partial y}\frac{\partial^2 v}{\partial x\partial y} + \frac{1}{2}\frac{\partial\psi_x^2}{\partial x}\right] + (3\alpha_1+2\alpha_2)\left[\nabla^2 u\frac{\partial u}{\partial x} + 2\frac{\partial u}{\partial x}\frac{\partial^2 u}{\partial x^2}\right] \\
&+ (\alpha_1+\alpha_2)\left[\nabla^2 w\psi_y + \nabla^2 v\psi_z + 2\left(\frac{\partial w}{\partial z}\frac{\partial\psi_y}{\partial z} + \frac{\partial v}{\partial y}\frac{\partial\psi_z}{\partial y}\right)\right. \\
&+ \left. 2\left(\psi_y\frac{\partial^2 u}{\partial x\partial z} + \psi_z\frac{\partial^2 u}{\partial x\partial y}\right) + \psi_x\left(\frac{\partial\psi_z}{\partial z} + \frac{\partial\psi_y}{\partial y}\right)\right] \\
&+ (\alpha_1+\frac{\alpha_2}{2})\left[\frac{\partial\psi_y^2}{\partial x} + \frac{\partial\psi_z^2}{\partial x}\right] + \beta_3\left[4\nabla^2 u\left((\frac{\partial u}{\partial x})^2 + (\frac{\partial v}{\partial y})^2 + (\frac{\partial w}{\partial z})^2\right)\right. \\
&+ 2\nabla^2 u\left(\psi_x^2+\psi_y^2+\psi_z^2\right) + 4\frac{\partial u}{\partial x}\left(\frac{\partial\psi_x^2}{\partial x} + \frac{\partial\psi_y^2}{\partial x} + \frac{\partial\psi_z^2}{\partial x}\right) \\
&+ 2\psi_z\left(\frac{\partial\psi_x^2}{\partial y} + \frac{\partial\psi_y^2}{\partial y} + \frac{\partial\psi_z^2}{\partial y}\right) + 2\psi_y\left(\frac{\partial\psi_x^2}{\partial z} + \frac{\partial\psi_y^2}{\partial z} + \frac{\partial\psi_z^2}{\partial z}\right) \\
&+ 16\frac{\partial u}{\partial x}\left(\frac{\partial u}{\partial x}\frac{\partial^2 u}{\partial x^2} + \frac{\partial v}{\partial y}\frac{\partial^2 v}{\partial y\partial x} + \frac{\partial w}{\partial z}\frac{\partial^2 w}{\partial z\partial x}\right) + 8\psi_z\left(\frac{\partial u}{\partial x}\frac{\partial^2 u}{\partial x\partial y}\right. \\
&+ \left.\left. \frac{\partial v}{\partial y}\frac{\partial^2 v}{\partial y^2} + \frac{\partial w}{\partial z}\frac{\partial^2 w}{\partial z\partial y}\right) + 8\psi_y\left(\frac{\partial u}{\partial x}\frac{\partial^2 u}{\partial z\partial x} + \frac{\partial v}{\partial y}\frac{\partial^2 v}{\partial y\partial z} + \frac{\partial w}{\partial z}\frac{\partial^2 w}{\partial z^2}\right)\right],
\end{aligned}
\tag{1.98}
$$

$$
\rho\left[\frac{\partial v}{\partial t} + u\frac{\partial v}{\partial x}+v\frac{\partial v}{\partial y}+w\frac{\partial v}{\partial z}\right] = -\sigma B_\circ^2 v - \frac{\partial p}{\partial y} + \mu\,\nabla^2 v
$$

$$
\begin{aligned}
&+ \alpha_1 \left[\left(\frac{\partial v}{\partial t} + u\frac{\partial v}{\partial x} + v\frac{\partial v}{\partial y} + w\frac{\partial v}{\partial z} \right) \nabla^2 v + \nabla^2 u \, \frac{\partial u}{\partial y} + \nabla^2 w \, \frac{\partial w}{\partial y} \right. \\
&+ \left. 2\frac{\partial w}{\partial z}\frac{\partial^2 w}{\partial y \partial z} + 2\frac{\partial u}{\partial x}\frac{\partial^2 u}{\partial x \partial y} + \frac{1}{2}\frac{\partial \psi_y^2}{\partial y} \right] + (3\alpha_1 + 2\alpha_2) \left[\nabla^2 v \frac{\partial v}{\partial y} \right. \\
&+ \left. 2\frac{\partial v}{\partial y}\frac{\partial^2 v}{\partial y^2} \right] + (\alpha_1 + \alpha_2) \left[\nabla^2 w \psi_x + \nabla^2 u \psi_z + 2\left(\frac{\partial w}{\partial z}\frac{\partial \psi_x}{\partial z} + \frac{\partial u}{\partial x}\frac{\partial \psi_z}{\partial x} \right) \right. \\
&+ \left. 2\left(\psi_x \frac{\partial^2 v}{\partial y \partial z} + \psi_z \frac{\partial^2 v}{\partial x \partial y} \right) + \psi_y \left(\frac{\partial \psi_z}{\partial z} + \frac{\partial \psi_x}{\partial x} \right) \right] \\
&+ (\alpha_1 + \frac{\alpha_2}{2}) \left[\frac{\partial \psi_x^2}{\partial y} + \frac{\partial \psi_z^2}{\partial y} \right] + \beta_3 \left[4\nabla^2 v \left((\frac{\partial u}{\partial x})^2 + (\frac{\partial v}{\partial y})^2 + (\frac{\partial w}{\partial z})^2 \right) \right. \\
&+ 2\nabla^2 v \left(\psi_x^2 + \psi_y^2 + \psi_z^2 \right) + 2\psi_z \left(\frac{\partial \psi_y^2}{\partial x} + \frac{\partial \psi_x^2}{\partial x} + \frac{\partial \psi_z^2}{\partial x} \right) \\
&+ 4\frac{\partial v}{\partial y}\left(\frac{\partial \psi_x^2}{\partial y} + \frac{\partial \psi_y^2}{\partial y} + \frac{\partial \psi_z^2}{\partial y} \right) + 2\psi_x \left(\frac{\partial \psi_x^2}{\partial z} + \frac{\partial \psi_y^2}{\partial z} + \frac{\partial \psi_z^2}{\partial z} \right) \\
&+ 8\psi_z \left(\frac{\partial u}{\partial x}\frac{\partial^2 u}{\partial x^2} + \frac{\partial v}{\partial y}\frac{\partial^2 v}{\partial y \partial x} + \frac{\partial w}{\partial z}\frac{\partial^2 w}{\partial z \partial x} \right) + 16\frac{\partial v}{\partial y}\left(\frac{\partial u}{\partial x}\frac{\partial^2 u}{\partial x \partial y} \right. \\
&+ \left. \left. \frac{\partial v}{\partial y}\frac{\partial^2 v}{\partial y^2} + \frac{\partial w}{\partial z}\frac{\partial^2 w}{\partial z \partial y} \right) + 8\psi_x \left(\frac{\partial u}{\partial x}\frac{\partial^2 u}{\partial z \partial x} + \frac{\partial v}{\partial y}\frac{\partial^2 v}{\partial y \partial z} + \frac{\partial w}{\partial z}\frac{\partial^2 w}{\partial z^2} \right) \right],
\end{aligned}
\tag{1.99}
$$

$$
\begin{aligned}
\rho \left[\frac{\partial w}{\partial t} \right. &+ \left. u\frac{\partial w}{\partial x} + v\frac{\partial w}{\partial y} + w\frac{\partial w}{\partial z} \right] = -\sigma B_\circ^2 w - \frac{\partial p}{\partial z} + \mu \, \nabla^2 w \\
&+ \alpha_1 \left[\left(\frac{\partial w}{\partial t} + u\frac{\partial w}{\partial x} + v\frac{\partial w}{\partial y} + w\frac{\partial w}{\partial z} \right) \nabla^2 w + \nabla^2 v \, \frac{\partial v}{\partial z} + \nabla^2 u \, \frac{\partial u}{\partial z} \right. \\
&+ \left. 2\frac{\partial u}{\partial x}\frac{\partial^2 u}{\partial x \partial z} + 2\frac{\partial v}{\partial y}\frac{\partial^2 v}{\partial z \partial y} + \frac{1}{2}\frac{\partial \psi_z^2}{\partial z} \right] + (3\alpha_1 + 2\alpha_2) \left[\nabla^2 w \frac{\partial w}{\partial z} \right.
\end{aligned}
$$

$$
\begin{aligned}
&+ \quad 2\frac{\partial w}{\partial z}\frac{\partial^2 w}{\partial z^2}\Bigg] + (\alpha_1+\alpha_2)\left[\nabla^2 u\psi_y + \nabla^2 v\psi_x + 2\left(\frac{\partial u}{\partial x}\frac{\partial \psi_y}{\partial x} + \frac{\partial v}{\partial y}\frac{\partial \psi_x}{\partial y}\right)\right.\\
&+ \quad 2\left(\psi_y\frac{\partial^2 w}{\partial x\partial z} + \psi_x\frac{\partial^2 w}{\partial z\partial y}\right) + \psi_z\left(\frac{\partial \psi_x}{\partial x} + \frac{\partial \psi_y}{\partial y}\right)\Bigg]\\
&+ \quad (\alpha_1+\frac{\alpha_2}{2})\left[\frac{\partial \psi_y^2}{\partial z} + \frac{\partial \psi_x^2}{\partial z}\right] + \beta_3\left[4\nabla^2 w\left((\frac{\partial u}{\partial x})^2 + (\frac{\partial v}{\partial y})^2 + (\frac{\partial w}{\partial z})^2\right)\right.\\
&+ \quad 2\nabla^2 w\left(\psi_x^2+\psi_y^2+\psi_z^2\right) + 2\psi_y\left(\frac{\partial \psi_x^2}{\partial x} + \frac{\partial \psi_y^2}{\partial x} + \frac{\partial \psi_z^2}{\partial x}\right)\\
&+ \quad 2\psi_x\left(\frac{\partial \psi_x^2}{\partial y} + \frac{\partial \psi_y^2}{\partial y} + \frac{\partial \psi_z^2}{\partial y}\right) + 4\frac{\partial w}{\partial z}\left(\frac{\partial \psi_x^2}{\partial z} + \frac{\partial \psi_y^2}{\partial z} + \frac{\partial \psi_z^2}{\partial z}\right)\\
&+ \quad 8\psi_y\left(\frac{\partial u}{\partial x}\frac{\partial^2 u}{\partial x^2} + \frac{\partial v}{\partial y}\frac{\partial^2 v}{\partial y\partial x} + \frac{\partial w}{\partial z}\frac{\partial^2 w}{\partial z\partial x}\right) + 8\psi_x\left(\frac{\partial u}{\partial x}\frac{\partial^2 u}{\partial x\partial y}\right.\\
&+ \quad \left.\frac{\partial v}{\partial y}\frac{\partial^2 v}{\partial y^2} + \frac{\partial w}{\partial z}\frac{\partial^2 w}{\partial z\partial y}\right) + 16\frac{\partial w}{\partial z}\left(\frac{\partial u}{\partial x}\frac{\partial^2 u}{\partial z\partial x} + \frac{\partial v}{\partial y}\frac{\partial^2 v}{\partial y\partial z} + \frac{\partial w}{\partial z}\frac{\partial^2 w}{\partial z^2}\right)\Bigg],
\end{aligned} \tag{1.100}
$$

where

$$
\begin{aligned}
\nabla^2 &= \frac{\partial^2}{\partial x^2} + \frac{\partial^2}{\partial y^2} + \frac{\partial^2}{\partial z^2},\\
\psi_x &= \left(\frac{\partial v}{\partial z} + \frac{\partial w}{\partial y}\right),\\
\psi_y &= \left(\frac{\partial u}{\partial z} + \frac{\partial w}{\partial x}\right),\\
\psi_z &= \left(\frac{\partial u}{\partial y} + \frac{\partial v}{\partial x}\right).
\end{aligned}
$$

Equations (1.98), (1.99) and (1.100) are the components form of the momentum equation for the third grade fluid.

Chapter 2

Unsteady MHD Flow Due to Non-Coaxial Rotations of a Porous Disk and a Fluid at Infinity

In this chapter an exact solution of the unsteady three-dimensional Navier-Stokes equations is derived for the case of flow due to non-coaxial rotations of a porous disk and a fluid at infinity in the presence of a uniform transverse magnetic field. An analytical solution of the problem is established by the method of Laplace transform and the graphs are sketched. The boundary layer thickness is found to decrease with the increase in magnetic parameter for both suction and blowing .

2.1 The Basic Equations and Boundary Conditions

We consider a semi-infinite expanse of homogeneous, incompressible, electrically conducting viscous fluid which occupies the space $z > 0$ and is bounded by an infinite non-conducting porous disk at $z = 0$. The axes of rotation, of both the disk and the fluid, are assumed to be in the plane $x = 0$, with the distance between the axes being l. The disk and the fluid at infinity are initially rotating about the z' -axis with the same angular velocity Ω and at time $t = 0$ the disk starts to rotate suddenly about the z-axis with the same angular velocity Ω and the fluid at infinity continues to rotate about the z'-axis with the same angular velocity as shown in figure 1. The fluid is electrically conducting and assumed to be permeated by a magnetic field $B_\circ$ having no components in the x and y directions. The boundary and initial conditions are

$$\begin{aligned} u &= -\Omega y, & v &= \Omega x, & &\text{at } z = 0, & &t > 0, \\ u &= -\Omega(y - l), & v &= \Omega x, & &\text{as } z \to \infty & &\text{for all } t, \\ u &= -\Omega(y - l), & v &= \Omega x, & &\text{at } t = 0, & &z > 0, \end{aligned} \tag{2.1}$$

where u, v and w are the components of the velocity.

The boundary and initial conditions show that the motion is a summation of the helical and translatory motion with the velocity profiles being [15]

$$u = -\Omega y + f(z,t), \qquad v = \Omega x + g(z,t). \tag{2.2}$$

The unsteady motion of the conducting viscous fluid is governed by the conservation laws of mass and momentum which are obtained from equations (1.10) and (1.11)

$$div\,\mathbf{V} = 0, \tag{2.3}$$

$$\frac{\partial \mathbf{V}}{\partial t} + (\mathbf{V}.\nabla)\mathbf{V} = -\frac{1}{\rho}\nabla\mathbf{p} + \nu\nabla^2\mathbf{V} + \frac{1}{\rho}\mathbf{J}\times\mathbf{B}, \tag{2.4}$$

In above equations, $\mathbf{V}$ is the velocity vector, p is the pressure, ρ is the density, $\mathbf{J}$ is the electric current density, $\mathbf{B}$ is the total magnetic field so that $\mathbf{B} = \mathbf{B}_\circ + \mathbf{b}$, $\mathbf{b}$ is the induced magnetic field and $\nu = \dfrac{\mu}{\rho}$ is the kinematic viscosity.

The condition of incompressibility along with equation (2.2) yields $w = -w_\circ$. Clearly $w_\circ > 0$ is the suction velocity and $w_\circ < 0$ is the blowing velocity. With the help of equations (1.98 – 1.100), equation (2.4) can be written in component form as

$$\frac{\partial u}{\partial t} + u\frac{\partial u}{\partial x} + v\frac{\partial u}{\partial y} + w\frac{\partial u}{\partial z} = -\frac{1}{\rho}\frac{\partial p}{\partial x} + \nu\left(\frac{\partial^2 u}{\partial x^2} + \frac{\partial^2 u}{\partial y^2} + \frac{\partial^2 u}{\partial z^2}\right) - \frac{\sigma}{\rho}B_\circ^2 u, \tag{2.5}$$

$$\frac{\partial v}{\partial t} + u\frac{\partial v}{\partial x} + v\frac{\partial v}{\partial y} + w\frac{\partial v}{\partial z} = -\frac{1}{\rho}\frac{\partial p}{\partial y} + \nu\left(\frac{\partial^2 v}{\partial x^2} + \frac{\partial^2 v}{\partial y^2} + \frac{\partial^2 v}{\partial z^2}\right) - \frac{\sigma}{\rho}B_\circ^2 v, \tag{2.6}$$

$$\frac{\partial w}{\partial t} + u\frac{\partial w}{\partial x} + v\frac{\partial w}{\partial y} + w\frac{\partial w}{\partial z} = -\frac{1}{\rho}\frac{\partial p}{\partial z} + \nu\left(\frac{\partial^2 w}{\partial x^2} + \frac{\partial^2 w}{\partial y^2} + \frac{\partial^2 w}{\partial z^2}\right) - \frac{\sigma}{\rho}B_\circ^2 w. \tag{2.7}$$

Substitution of (2.2) in above equations yields

$$\frac{1}{\rho}\frac{\partial p}{\partial x} = \Omega^2 x + \Omega g + w_\circ\frac{\partial f}{\partial z} - \frac{\partial f}{\partial t} + \nu\frac{\partial^2 f}{\partial z^2} - \frac{\sigma}{\rho}B_\circ^2(f - \Omega y), \tag{2.8}$$

$$\frac{1}{\rho}\frac{\partial p}{\partial y} = \Omega^2 y - \Omega f + w_\circ\frac{\partial g}{\partial z} - \frac{\partial g}{\partial t} + \nu\frac{\partial^2 g}{\partial z^2} - \frac{\sigma}{\rho}B_\circ^2(g + \Omega x), \tag{2.9}$$

$$\frac{1}{\rho}\frac{\partial p}{\partial z} = \frac{\sigma}{\rho}B_\circ^2 w_\circ. \tag{2.10}$$

Differentiating (2.10) with respect to x and y respectively, we get

$$\frac{1}{\rho}\frac{\partial^2 p}{\partial x \partial z} = 0 = \frac{1}{\rho}\frac{\partial^2 p}{\partial y \partial z}. \tag{2.11}$$

Now differentiating (2.8) and (2.9) with respect to z and using (2.11) we have

$$\frac{\partial^2 f}{\partial z \partial t} - \Omega \frac{\partial g}{\partial z} - w_\circ \frac{\partial^2 f}{\partial z^2} = \nu \frac{\partial^3 f}{\partial z^3} - \frac{\sigma}{\rho} B_\circ^2 \frac{\partial f}{\partial z}, \tag{2.12}$$

$$\frac{\partial^2 g}{\partial z \partial t} + \Omega \frac{\partial f}{\partial z} - w_\circ \frac{\partial^2 g}{\partial z^2} = \nu \frac{\partial^3 g}{\partial z^3} - \frac{\sigma}{\rho} B_\circ^2 \frac{\partial g}{\partial z}. \tag{2.13}$$

Substituting (2.1) into (2.2), the initial and boundary conditions take the following form

$$\begin{aligned} f(0,t) &= 0, & g(0,t) &= 0, & &\text{for } t > 0, \\ f(z,t) &= \Omega l, & g(z,t) &= 0, & &\text{as } z \to \infty \text{ for all } t, \\ f(z,0) &= \Omega l, & g(z,0) &= 0, & &\text{for } z > 0. \end{aligned} \tag{2.14}$$

Defining

$$F^* = f + ig \tag{2.15}$$

equations (2.12 – 2.14) give

$$\nu \frac{\partial^3 F^*}{\partial z^3} + w_\circ \frac{\partial^2 F^*}{\partial z^2} - \frac{\partial^2 F^*}{\partial t \partial z} - (i\Omega + \frac{\sigma}{\rho} B_\circ^2) \frac{\partial F^*}{\partial z} = 0, \tag{2.16}$$

$$F^*(0,t) = 0, \quad F^*(\infty,t) = \Omega l, \quad F^*(z,0) = \Omega l, \tag{2.17}$$

2.2 The Solution of the Problem

The problem [(2.16) and (2.17)] can directly be solved by the use of the Laplace transform pair [56]

$$\psi(z,s) = \int_0^\infty F^*(z,t)e^{-st}dt, \tag{2.18}$$

$$F^*(z,t) = \frac{1}{2\pi i}\int_{\lambda-i\infty}^{\lambda+i\infty} \psi(z,s)e^{st}ds, \quad \lambda > 0. \tag{2.19}$$

Multiplying equation (2.16) throughout with e^{-st}, integrating from 0 to ∞ with respect to t, and using definition (2.18) we have

$$\nu\psi'''(z,s) + w_\circ\psi''(z,s) - (s + i\Omega + \frac{\sigma}{\rho}B_\circ^2)\psi'(z,s) = 0 \tag{2.20}$$

with conditions

$$\psi(0,s) = 0, \qquad \psi(\infty,s) = \frac{\Omega l}{s}, \tag{2.21}$$

where primes denote differentiation with respect to z.

The solution of the differential system (2.20) is of the form

$$\begin{aligned}\psi(z,s) &= A + B\, exp\left\{-\left(\frac{w_\circ}{2\nu} + \sqrt{(\frac{w_\circ}{2\nu})^2 + \left(\frac{s}{\nu} + \frac{i\Omega}{\nu} + \frac{\sigma B_\circ^2}{\rho\nu}\right)}\right)z\right\} \\ &+ C\, exp\left\{-\left(\frac{w_\circ}{2\nu} - \sqrt{(\frac{w_\circ}{2\nu})^2 + \left(\frac{s}{\nu} + \frac{i\Omega}{\nu} + \frac{\sigma B_\circ^2}{\rho\nu}\right)}\right)z\right\},\end{aligned} \tag{2.22}$$

where A, B and C are arbitrary constants. Using conditions (2.21), we obtain

$$A = \frac{\Omega l}{s}, \quad B = -\frac{\Omega l}{s}, \quad C = 0.$$

Making use of the values of A, B and C, equation (2.22) takes the following form

$$\psi(z,s)=\frac{\Omega l}{s}\left[1-exp\left\{-\left(\frac{w_\circ}{2\nu}+\sqrt{(\frac{w_\circ}{2\nu})^2+\left(\frac{s}{\nu}+\frac{i\Omega}{\nu}+\frac{\sigma B_\circ^2}{\rho\nu}\right)}\right)z\right\}\right]. \tag{2.23}$$

Laplace inversion of (2.23) yields

$$\begin{aligned} F^*(z,t) &= \frac{\Omega l}{2\pi i}\int_{\lambda-i\infty}^{\lambda+i\infty}\frac{e^{st}}{s}ds \\ &- \frac{\Omega l}{2\pi i}\int_{\lambda-i\infty}^{\lambda+i\infty}\frac{1}{s}\,exp\left\{-\left(\frac{w_\circ}{2\nu}+\sqrt{(\frac{w_\circ}{2\nu})^2+\left(\frac{s}{\nu}+\frac{i\Omega}{\nu}+\frac{\sigma B_\circ^2}{\rho\nu}\right)}\right)z+st\right\}ds. \end{aligned}$$

Using the results

$$\begin{aligned} \frac{1}{2\pi i}\int_{\lambda-i\infty}^{\lambda+i\infty}\frac{e^{\eta t}}{\eta}d\eta &= 1, \\ \frac{e^{-a^2t}}{2\pi i}\int_{\lambda-i\infty}^{\lambda+i\infty}\frac{e^{\eta^2t-b\eta}}{\eta^2-a^2}\eta d\eta &= \frac{1}{2}\left\{e^{ab}erfc\left(\frac{b+2at}{2\sqrt{t}}\right)+e^{-ab}erfc\left(\frac{b-2at}{2\sqrt{t}}\right)\right\} \end{aligned}$$

in the above equation we arrive at

$$\begin{aligned} \frac{f}{\Omega l} &+ i\frac{g}{\Omega l}=1-\frac{e^{-\frac{w_\circ}{2\nu}z}}{2} \\ &\times \left[e^{-z\sqrt{\frac{w_\circ^2}{4\nu^2}+\frac{i\Omega}{\nu}+\frac{\sigma B_\circ^2}{\rho\nu}}}erfc\left(\frac{z}{2\sqrt{\nu t}}-\sqrt{\left(\frac{w_\circ^2}{4\nu}+i\Omega+\frac{\sigma B_\circ^2}{\rho}\right)t}\right)\right. \\ &+ \left. e^{z\sqrt{\frac{w_\circ^2}{4\nu^2}+\frac{i\Omega}{\nu}+\frac{\sigma B_\circ^2}{\rho\nu}}}erfc\left(\frac{z}{2\sqrt{\nu t}}+\sqrt{\left(\frac{w_\circ^2}{4\nu}+i\Omega+\frac{\sigma B_\circ^2}{\rho}\right)t}\right)\right], \end{aligned} \tag{2.24}$$

where $erfc(x)$ is the complementary error function defined by

$$erfc(x) = 1 - erf(x) = \int_x^{\infty} e^{-y_1^2} dy_1. \tag{2.25}$$

We note from (2.24) that $w_\circ = 0$ gives the impermeable case while $w_\circ = 0 = B_\circ$ gives Erdogan's problem [15]. The real part gives $\frac{f}{\Omega l}$ and the imaginary part gives $\frac{g}{\Omega l}$. Equation (2.24) can also be rewritten as

$$\begin{aligned}
\frac{f}{\Omega l} &+ i\frac{g}{\Omega l} = 1 - \frac{e^{-\frac{w_\circ}{2\nu}z}}{2} \\
&\times \left[e^{-\frac{\alpha z}{\sqrt{\nu}}} \left(\cos\frac{\beta z}{\sqrt{\nu}} - i \sin\frac{\beta z}{\sqrt{\nu}} \right) erfc\left(\frac{z}{2\sqrt{\nu t}} - (\alpha + i\beta)\sqrt{t} \right) \right. \\
&+ \left. e^{\frac{\alpha z}{\sqrt{\nu}}} \left(\cos\frac{\beta z}{\sqrt{\nu}} + i \sin\frac{\beta z}{\sqrt{\nu}} \right) erfc\left(\frac{z}{2\sqrt{\nu t}} + (\alpha + i\beta)\sqrt{t} \right) \right],
\end{aligned} \tag{2.26}$$

where

$$\begin{aligned}
\alpha &= \left[\frac{1}{2} \left\{ \sqrt{\left(\frac{w_\circ^2}{4\nu} + \frac{\sigma B_\circ^2}{\rho} \right)^2 + \Omega^2} + \left(\frac{w_\circ^2}{4\nu} + \frac{\sigma B_\circ^2}{\rho} \right) \right\} \right]^{\frac{1}{2}}, \\
\beta &= \left[\frac{1}{2} \left\{ \sqrt{\left(\frac{w_\circ^2}{4\nu} + \frac{\sigma B_\circ^2}{\rho} \right)^2 + \Omega^2} - \left(\frac{w_\circ^2}{4\nu} + \frac{\sigma B_\circ^2}{\rho} \right) \right\} \right]^{\frac{1}{2}}
\end{aligned}$$

and $erfc(x + i\,y)$ can be calculated in terms of the tabulated functions [57]. The tables given in [57] do not give $erfc(x + i\,y)$ directly but an auxiliary function $H(x + iy)$ which is defined as

$$erfc(x + i\,y) = e^{-(x+iy)^2} H(-y + ix), \tag{2.27}$$

where

$$H(-x+iy) = \overline{H(x+iy)},$$

$$H(x-iy) = 2e^{-(x+iy)^2} - \overline{H(x+iy)},$$

and $\overline{H(x+iy)}$ is the complex conjugate of $H(x+iy)$. For large times, we can write (2.26) as

$$\begin{aligned}
\frac{f}{\Omega l} + i\frac{g}{\Omega l} &= \left[1 - e^{-\frac{w_\circ}{2\nu}z - \frac{\alpha z}{\sqrt{\nu}}}\left(\cos\frac{\beta z}{\sqrt{\nu}} - i\sin\frac{\beta z}{\sqrt{\nu}}\right)\right] + \frac{e^{-\frac{w_\circ}{2\nu}z}}{2} \\
&\times \left[e^{-\frac{\alpha z}{\sqrt{\nu}}}\left(\cos\frac{\beta z}{\sqrt{\nu}} - i\sin\frac{\beta z}{\sqrt{\nu}}\right) erfc\left((\alpha+i\beta)\sqrt{t} - \frac{z}{2\sqrt{\nu t}}\right)\right. \\
&- \left. e^{\frac{\alpha z}{\sqrt{\nu}}}\left(\cos\frac{\beta z}{\sqrt{\nu}} + i\sin\frac{\beta z}{\sqrt{\nu}}\right) erfc\left((\alpha+i\beta)\sqrt{t} + \frac{z}{2\sqrt{\nu t}}\right)\right],
\end{aligned} \tag{2.28}$$

where the first term of the right-hand side corresponds to the steady state and the second one denotes the deviation from it.

For $z << 2\sqrt{\nu t}$ and $t >> 1$ the velocity field (2.28) has the approximate form

$$\begin{aligned}
\frac{f}{\Omega l} &= 1 - e^{-\frac{w_\circ}{2\nu}z - \frac{\alpha z}{\sqrt{\nu}}}\cos\frac{\beta z}{\sqrt{\nu}} - \frac{e^{-\frac{w_\circ}{2\nu}z + (\beta^2-\alpha^2)t}}{\sqrt{\pi t}(\alpha^2+\beta^2)} \\
&\times \left[(\alpha\cos 2\alpha\beta t - \beta\sin 2\alpha\beta t)\sinh\frac{\alpha z}{\sqrt{\nu}}\cos\frac{\beta z}{\sqrt{\nu}}\right.
\end{aligned}$$

$$+ \quad (\beta\cos 2\alpha\beta t + \alpha\sin 2\alpha\beta t)\cosh\frac{\alpha z}{\sqrt{\nu}}\sin\frac{\beta z}{\sqrt{\nu}}\Bigg], \tag{2.29}$$

$$\frac{g}{\Omega l} = e^{-\frac{w_\circ}{2\nu}z - \frac{\alpha z}{\sqrt{\nu}}}\sin\frac{\beta z}{\sqrt{\nu}} - \frac{e^{-\frac{w_\circ}{2\nu}z + (\beta^2-\alpha^2)t}}{\sqrt{\pi t}(\alpha^2+\beta^2)}$$

$$\times \quad \Bigg[(\alpha\cos 2\alpha\beta t - \beta\sin 2\alpha\beta t)\cosh\frac{\alpha z}{\sqrt{\nu}}\sin\frac{\beta z}{\sqrt{\nu}}$$

$$- \quad (\beta\cos 2\alpha\beta t + \alpha\sin 2\alpha\beta t)\sinh\frac{\alpha z}{\sqrt{\nu}}\cos\frac{\beta z}{\sqrt{\nu}}\Bigg]. \tag{2.30}$$

Blowing:- Here $w_\circ < 0$, say $w_\circ = -\tilde{w}_\circ$. The solution in this case is given by

$$\frac{f}{\Omega l} = 1 - e^{-\frac{\tilde{w}_\circ}{2\nu}z - \frac{\tilde{\alpha} z}{\sqrt{\nu}}}\cos\frac{\tilde{\beta} z}{\sqrt{\nu}} - \frac{e^{-\frac{\tilde{w}_\circ}{2\nu}z + (\tilde{\beta}^2-\tilde{\alpha}^2)t}}{\sqrt{\pi t}(\tilde{\alpha}^2+\tilde{\beta}^2)}$$

$$\times \quad \Bigg[\left(\tilde{\alpha}\cos 2\tilde{\alpha}\tilde{\beta} t - \tilde{\beta}\sin 2\tilde{\alpha}\tilde{\beta} t\right)\sinh\frac{\tilde{\alpha} z}{\sqrt{\nu}}\cos\frac{\tilde{\beta} z}{\sqrt{\nu}}$$

$$+ \quad \left(\tilde{\beta}\cos 2\tilde{\alpha}\tilde{\beta} t + \tilde{\alpha}\sin 2\tilde{\alpha}\tilde{\beta} t\right)\cosh\frac{\tilde{\alpha} z}{\sqrt{\nu}}\sin\frac{\tilde{\beta} z}{\sqrt{\nu}}\Bigg], \tag{2.31}$$

$$\frac{g}{\Omega l} = e^{-\frac{\tilde{w}_\circ}{2\nu}z - \frac{\tilde{\alpha} z}{\sqrt{\nu}}}\sin\frac{\tilde{\beta} z}{\sqrt{\nu}} - \frac{e^{-\frac{\tilde{w}_\circ}{2\nu}z + (\tilde{\beta}^2-\tilde{\alpha}^2)t}}{\sqrt{\pi t}(\tilde{\alpha}^2+\tilde{\beta}^2)}$$

$$\Bigg[\left(\tilde{\alpha}\cos 2\tilde{\alpha}\tilde{\beta} t - \tilde{\beta}\sin 2\tilde{\alpha}\tilde{\beta} t\right)\cosh\frac{\tilde{\alpha} z}{\sqrt{\nu}}\sin\frac{\tilde{\beta} z}{\sqrt{\nu}}$$

$$- \quad \left(\tilde{\beta}\cos 2\tilde{\alpha}\tilde{\beta} t + \tilde{\alpha}\sin 2\tilde{\alpha}\tilde{\beta} t\right)\sinh\frac{\tilde{\alpha} z}{\sqrt{\nu}}\cos\frac{\tilde{\beta} z}{\sqrt{\nu}}\Bigg], \tag{2.32}$$

where

$$\tilde{\alpha} = \left[\frac{1}{2}\left\{\sqrt{\left(\frac{\tilde{w}_\circ^2}{4\nu} + \frac{\sigma B_\circ^2}{\rho}\right)^2 + \Omega^2} + \left(\frac{\tilde{w}_\circ^2}{4\nu} + \frac{\sigma B_\circ^2}{\rho}\right)\right\}\right]^{\frac{1}{2}}, \tag{2.33}$$

$$\tilde{\beta} = \left[\frac{1}{2}\left\{\sqrt{\left(\frac{\tilde{w}_\circ^2}{4\nu} + \frac{\sigma B_\circ^2}{\rho}\right)^2 + \Omega^2} - \left(\frac{\tilde{w}_\circ^2}{4\nu} + \frac{\sigma B_\circ^2}{\rho}\right)\right\}\right]^{\frac{1}{2}}. \tag{2.34}$$

It is found that an asymptotic solution exists for the velocity distribution unlike the case of a porous disk subjected to uniform blowing in the case of non-rotating frame. The existence of asymptotic solution is due to the fact that the vorticity layer thickness decreases with increase in rotation. It is interesting to note that the velocity boundary layer has thickness of order $\left(\frac{w_\circ}{2\nu} + \frac{\alpha}{\sqrt{\nu}}\right)^{-1}$ in the case of suction and of order $\left(\frac{\tilde{w}_\circ}{2\nu} + \frac{\tilde{\alpha}}{\sqrt{\nu}}\right)^{-1}$ in the case of blowing. It is clear that the layer of thickness of order $\left(\frac{w_\circ}{2\nu} + \frac{\alpha}{\sqrt{\nu}}\right)^{-1}$ decreases with increase in $w_\circ$ and $B_\circ$ and the layer thickness of order $\left(\frac{\tilde{w}_\circ}{2\nu} + \frac{\tilde{\alpha}}{\sqrt{\nu}}\right)^{-1}$ decreases with increase in $\tilde{w}_\circ$ and $B_\circ$. The solution with zero magnetic field and a nonporous disk obtained by Erdogan [15] can be recovered directly from (2.29) and (2.30) with $w_\circ = B_\circ = 0$.

Introducing the non-dimensional quantities

$$\xi = \sqrt{\frac{\Omega}{2\nu}}z, \quad \tau = \Omega t, \quad \hat{f}(\xi,\tau) = \frac{f}{\Omega l}, \quad \hat{g}(\xi,\tau) = \frac{g}{\Omega l},$$

$$\epsilon = \frac{w_\circ}{\sqrt{2\nu\Omega}}, \quad N = \frac{\sigma}{\rho\Omega}B_\circ^2, \quad \hat{\alpha} = \sqrt{\frac{2}{\Omega}}\alpha \quad \hat{\beta} = \sqrt{\frac{2}{\Omega}}\beta$$

$$\breve{\epsilon} = \frac{\tilde{w}_\circ}{\sqrt{2\nu\Omega}}, \quad \breve{\alpha} = \sqrt{\frac{2}{\Omega}}\tilde{\alpha} \quad \breve{\beta} = \sqrt{\frac{2}{\Omega}}\tilde{\beta} \tag{2.35}$$

expressions (2.29 – 2.30) for suction become

$$
\begin{aligned}
\hat{f} &= 1 - e^{-(\epsilon + \hat{\alpha})\xi} \cos \hat{\beta}\xi - \sqrt{\frac{2}{\pi\tau}}\, \frac{e^{-\epsilon\xi + (\hat{\beta}^2 - \hat{\alpha}^2)\frac{\tau}{2}}}{(\hat{\alpha}^2 + \hat{\beta}^2)} \\
&\times \Big[\Big(\hat{\alpha} \cos \hat{\alpha}\hat{\beta}\tau - \hat{\beta} \sin \hat{\alpha}\hat{\beta}\tau\Big) \sinh \hat{\alpha}\xi \cos \hat{\beta}\xi \\
&+ \Big(\hat{\beta} \cos \hat{\alpha}\hat{\beta}\tau + \hat{\alpha} \sin \hat{\alpha}\hat{\beta}\tau\Big) \cosh \hat{\alpha}\xi \sin \hat{\beta}\xi\Big], \qquad (2.36)
\end{aligned}
$$

$$
\begin{aligned}
\hat{g} &= e^{-(\epsilon + \hat{\alpha})\xi} \sin \hat{\beta}\xi - \sqrt{\frac{2}{\pi\tau}}\, \frac{e^{-\epsilon\xi + (\hat{\beta}^2 - \hat{\alpha}^2)\frac{\tau}{2}}}{(\hat{\alpha}^2 + \hat{\beta}^2)} \\
&\times \Big[\Big(\hat{\alpha} \cos \hat{\alpha}\hat{\beta}\tau - \hat{\beta} \sin \hat{\alpha}\hat{\beta}\tau\Big) \cosh \hat{\alpha}\xi \sin \hat{\beta}\xi \\
&- \Big(\hat{\beta} \cos \hat{\alpha}\hat{\beta}\tau + \hat{\alpha} \sin \hat{\alpha}\hat{\beta}\tau\Big) \sinh \hat{\alpha}\xi \cos \hat{\beta}\xi\Big], \qquad (2.37)
\end{aligned}
$$

and for blowing yield

$$
\begin{aligned}
\hat{f} &= 1 - e^{-(\breve{\epsilon} + \breve{\alpha})\xi} \cos \breve{\beta}\xi - \sqrt{\frac{2}{\pi\tau}}\, \frac{e^{-\breve{\epsilon}\xi + (\breve{\beta}^2 - \breve{\alpha}^2)\frac{\tau}{2}}}{(\breve{\alpha}^2 + \breve{\beta}^2)} \\
&\times \Big[\Big(\breve{\alpha} \cos \breve{\alpha}\breve{\beta}\tau - \breve{\beta} \sin \breve{\alpha}\breve{\beta}\tau\Big) \sinh \breve{\alpha}\xi \cos \breve{\beta}\xi \\
&+ \Big(\breve{\beta} \cos \breve{\alpha}\breve{\beta}\tau + \breve{\alpha} \sin \breve{\alpha}\breve{\beta}\tau\Big) \cosh \breve{\alpha}\xi \sin \breve{\beta}\xi\Big], \qquad (2.38)
\end{aligned}
$$

$$\hat{g} = e^{-(\breve{\epsilon} + \breve{\alpha})\xi} \sin \breve{\beta}\xi - \sqrt{\frac{2}{\pi\tau}} \frac{e^{-\breve{\epsilon}\xi + (\breve{\beta}^2 - \breve{\alpha}^2)\frac{\tau}{2}}}{(\breve{\alpha}^2 + \breve{\beta}^2)}$$

$$\times \left[\left(\breve{\alpha} \cos \breve{\alpha}\breve{\beta}\tau - \breve{\beta} \sin \breve{\alpha}\breve{\beta}\tau\right) \cosh \breve{\alpha}\xi \sin \breve{\beta}\xi\right.$$

$$- \left.\left(\breve{\beta} \cos \breve{\alpha}\breve{\beta}\tau + \breve{\alpha} \sin \breve{\alpha}\breve{\beta}\tau\right) \sinh \breve{\alpha}\xi \cos \breve{\beta}\xi\right]. \quad (2.39)$$

The effect of suction, blowing, and zero porosity without magnetic field at time $\tau = 12$ is presented in figure 2.1. Figures 2.2 and 2.3 show the variations of $\hat{f}$ and $\hat{g}$ for $N = 2$ for different values of time. We observe that the boundary layer thickness steadily increases and takes a steady state after some time. In absence of porosity and magnetic field, steady state is achieved at $\tau = 8$. In the presence of a magnetic field and no porosity we get steady state rather quickly at $\tau = .5$. In case of suction and no magnetic field, it is at $\tau = 2$. Also the boundary layer decreases with increase in the suction parameter. This is in line with the fact that suction causes reduction in boundary layer thickness. In case of blowing and no magnetic field, steady state is obtained after $\tau = 10$. Further, it is seen that the influence of the magnetic parameter for both the suction and blowing is to decrease the velocity. However the effect is more marked in blowing than suction.

Chapter 3

Unsteady MHD Flow of a Second Grade Fluid Due to Eccentric Rotations of a Porous Disk and a Fluid at Infinity

In this chapter, we extended the analysis of chapter 2 for the case of non-Newtonian fluid. The fluid considered is second grade. An exact solution of the unsteady flow due to non-coaxial rotations of a porous disk and a fluid at infinity in the presence of a uniform transverse magnetic field is investigated. The main purpose of the analysis is three fold. Firstly, to discuss the flow of a second grade fluid produced by a disk which rotates non-coaxially with the fluid at infinity. It is shown that equations of motion have an exact solution. Secondly, to examine the influence of an externally applied magnetic field on the velocity distribution. Thirdly, to include the effects of porosity by taking into account the porous disk. It is observed that in the case of a rigid disk, non-Newtonian effect can be observed in the velocity field when material parameter of second grade fluid α is greater than .01. However, for

$\alpha < .01$ the velocity field becomes a Newtonian one.

3.1 Basic Equations

We introduce a Cartesian coordinate system with the $z-$ axis normal to the porous disk, which lies in the plane $z = 0$. The axes of rotation, of both the disk and the fluid, are assumed to be in the plane $x = 0$, with the distance between the axes being l. The common angular velocity of the disk and the fluid is taken as $\mathbf{\Omega}$. The fluid is electrically conducting and assumed to be permeated by a magnetic field B_o having no components in the x and y directions. For the problem under consideration, we seek a velocity field of the form (2.2), subject to the conditions (2.1).

The unsteady motion of the electrically conducting, incompressible second grade fluid is governed by the conservation laws of mass and momentum. For the convenience of the readers we can write from (1.10) and (1.11) as

$$\nabla . \mathbf{V} = 0, \tag{3.1}$$

$$\rho \frac{D\mathbf{V}}{Dt} = \nabla . \mathbf{T} + \mathbf{J} \times \mathbf{B}, \tag{3.2}$$

The Cauchy stress $\mathbf{T}$ in an incompressible fluid of second grade is given by equation (1.20)

$$\mathbf{T} = -p\mathbf{I} + \mu\mathbf{A}_1 + \alpha_1\mathbf{A}_2 + \alpha_2\mathbf{A}_1^2, \tag{3.3}$$

where $\mathbf{A}_1$ and $\mathbf{A}_2$ are the kinematical tensors given by

$$\mathbf{A}_1 = (\mathbf{grad\ V}) + (\mathbf{grad\ V})^{\mathbf{T}},$$

$$A_2 = \frac{DA_1}{Dt} + A_1\,(\mathbf{grad}\ \mathbf{V}) + (\mathbf{grad}\ \mathbf{V})^{\mathrm{T}}\ \mathbf{A_1}. \tag{3.4}$$

If an incompressible fluid of second grade is to have motions which are compatible with thermodynamics in the sense of the Clausius-Duhem inequality and the condition that the Helmholtz free energy be a minimum when the fluid is at rest, then the following conditions must be satisfied

$$\mu \geq 0, \quad \alpha_1 \geq 0, \quad \alpha_1 + \alpha_2 = 0.$$

Using equation (2.2), equations (1.98 – 1.100) for the case of second grade fluid becomes

$$\rho\left[\frac{\partial f}{\partial t} - \Omega^2 x - \Omega g - w_\circ \frac{\partial f}{\partial z}\right] = -\frac{\partial P}{\partial x} + \mu\frac{\partial^2 f}{\partial z^2} - \sigma B_\circ^2 (f - \Omega y)$$

$$+ \alpha_1 \left[\frac{\partial^3 f}{\partial t \partial z^2} - w_\circ \frac{\partial^3 f}{\partial z^3} + \Omega \frac{\partial^2 g}{\partial z^2}\right], \tag{3.5}$$

$$\rho\left[\frac{\partial g}{\partial t} - \Omega^2 y + \Omega f - w_\circ \frac{\partial g}{\partial z}\right] = -\frac{\partial P}{\partial y} + \mu\frac{\partial^2 g}{\partial z^2} - \sigma B_\circ^2 (g + \Omega x)$$

$$+ \alpha_1 \left[\frac{\partial^3 g}{\partial t \partial z^2} - w_\circ \frac{\partial^3 g}{\partial z^3} - \Omega \frac{\partial^2 f}{\partial z^2}\right], \tag{3.6}$$

$$\sigma B_\circ^2 w_\circ = \frac{\partial P}{\partial z}, \tag{3.7}$$

where

$$P = p - (2\alpha_1 + \alpha_2)\left\{\left(\frac{\partial f}{\partial z}\right)^2 + \left(\frac{\partial g}{\partial z}\right)^2\right\} \tag{3.8}$$

subject to the boundary and initial conditions (2.14).

Differentiating equations (3.5) and (3.6) with respect to z and then using (3.7) in the resulting expressions we get

$$\rho\left[\frac{\partial^2 f}{\partial z\partial t} - \Omega\frac{\partial g}{\partial z} - w_\circ\frac{\partial^2 f}{\partial z^2}\right] = \mu\frac{\partial^3 f}{\partial z^3} - \sigma B_\circ^2\frac{\partial f}{\partial z} + \alpha_1\left[\frac{\partial^4 f}{\partial t\partial z^3} - w_\circ\frac{\partial^4 f}{\partial z^4} + \Omega\frac{\partial^3 g}{\partial z^3}\right],$$

$$\rho\left[\frac{\partial^2 g}{\partial z\partial t} + \Omega\frac{\partial f}{\partial z} - w_\circ\frac{\partial^2 g}{\partial z^2}\right] = \mu\frac{\partial^3 g}{\partial z^3} - \sigma B_\circ^2\frac{\partial g}{\partial z} + \alpha_1\left[\frac{\partial^4 g}{\partial t\partial z^3} - w_\circ\frac{\partial^4 g}{\partial z^4} - \Omega\frac{\partial^3 f}{\partial z^3}\right].$$

Integrating above equations and then using the boundary condition (2.14), we obtain

$$\rho\left[\frac{\partial f}{\partial t} - \Omega g - w_\circ\frac{\partial f}{\partial z}\right] = \mu\frac{\partial^2 f}{\partial z^2} - \sigma B_\circ^2 f + \sigma B_\circ^2\Omega l + \alpha_1\left[\frac{\partial^3 f}{\partial t\partial z^2} - w_\circ\frac{\partial^3 f}{\partial z^3} + \Omega\frac{\partial^2 g}{\partial z^2}\right], \tag{3.9}$$

$$\rho\left[\frac{\partial g}{\partial t} + \Omega f - w_\circ\frac{\partial g}{\partial z}\right] = \mu\frac{\partial^2 g}{\partial z^2} - \sigma B_\circ^2 g + \rho\,\Omega^2 l + \alpha_1\left[\frac{\partial^3 g}{\partial t\partial z^2} - w_\circ\frac{\partial^3 g}{\partial z^3} - \Omega\frac{\partial^2 f}{\partial z^2}\right]. \tag{3.10}$$

With the help of equation (2.15), equations (3.9) and (3.10) can be combined into the following partial differential equation

$$
\frac{\alpha_1}{\rho}\frac{\partial^3 F^*}{\partial t \partial z^2} - \frac{\alpha_1 w_\circ}{\rho}\frac{\partial^3 F^*}{\partial z^3} + (\nu - i\frac{\alpha_1 \Omega}{\rho})\frac{\partial^2 F^*}{\partial z^2} + w_\circ \frac{\partial F^*}{\partial z}
$$

$$
- \frac{\partial F^*}{\partial t} - \Omega(i + \frac{\sigma B_\circ^2}{\rho \Omega})F^* = -\Omega^2 l(i + \frac{\sigma B_\circ^2}{\rho \Omega}) \tag{3.11}
$$

with the initial and boundary conditions (2.17).

Defining dimensionless parameters

$$
\xi = \sqrt{\frac{\Omega}{2\nu}}z, \quad \tau = \Omega t, \quad \alpha = \frac{\Omega \alpha_1}{\nu \rho}, \quad \epsilon = \frac{w_\circ}{\sqrt{2\nu\Omega}},
$$

$$
N = \frac{\sigma B_\circ^2}{\rho \Omega}, \quad F(\xi, \tau) = \frac{F^*}{\Omega l} - 1 \tag{3.12}
$$

equation (3.11) takes the following form

$$
\alpha \frac{\partial^3 F}{\partial \tau \partial \xi^2} - \alpha\, \epsilon \frac{\partial^3 F}{\partial \xi^3} + (1 - i\alpha)\frac{\partial^2 F}{\partial \xi^2}
$$

$$
+ 2\epsilon \frac{\partial F}{\partial \xi} - 2\frac{\partial F}{\partial \tau} - 2(i + N)F = 0. \tag{3.13}
$$

Introducing

$$
H(\xi, \tau) = F(\xi, \tau)\, e^{i\tau} \tag{3.14}
$$

equation (3.13) and conditions (2.17) become

$$
\alpha \frac{\partial^3 H}{\partial \tau \partial \xi^2} - \alpha\epsilon \frac{\partial^3 H}{\partial \xi^3} + (1 - 2i\alpha)\frac{\partial^2 H}{\partial \xi^2} + 2\epsilon \frac{\partial H}{\partial \xi} - 2\frac{\partial H}{\partial \tau} - 2NH = 0, \tag{3.15}
$$

$$
H(0, \tau) = -e^{i\tau}, \quad H(\infty, \tau) = 0, \quad H(\xi, 0) = 0. \tag{3.16}
$$

3.2 Solution of the problem for suction

Let us suppose that $H(\xi,\tau)$ is an arbitrary function that has a Laplace transform in the variable τ. That is,

$$\bar{H}(\xi,s)=\int_0^\infty H(\xi,\tau)e^{-s\tau}d\tau. \tag{3.17}$$

The initial-boundary value problem in the transformed $s-$plane can be rewritten as

$$\alpha\epsilon\bar{H}'''-(1-2i\alpha+\alpha s)\bar{H}''-2\epsilon\bar{H}'+2(s+N)\bar{H}=0, \tag{3.18}$$

$$\bar{H}(0,s)=-\frac{1}{s-i},\qquad \bar{H}(\infty,s)=0, \tag{3.19}$$

where primes denote differentiation with respect to ξ.

Before proceeding with the solution of the above problem it would be interesting to remark here that although in the classical viscous case ($\alpha=0$), we encounter differential equation of order two [15]. The presence of material parameters of second grade fluid increases the order to three. It would, therefore, seem that an additional boundary condition must be imposed in order to get a unique solution. The difficulty, in the present case, is however, removed by seeking a solution of the form [58]

$$\bar{H}=\bar{H}_1+\alpha\bar{H}_2+O(\alpha^2) \tag{3.20}$$

which is valid for small values of α only .

Substituting expression (3.20) into equation (3.18) and boundary conditions (3.19) and then collecting terms of like powers of α, one obtains the following systems of differential equations along with the appropriate boundary conditions:

3.2.1 System of Order Zero

$$\bar{H}_1'' + 2\epsilon \bar{H}_1' - 2(s+N)\bar{H}_1 = 0, \tag{3.21}$$

$$\bar{H}_1(0,s) = -\frac{1}{s-i}, \qquad \bar{H}_1(\infty,s) = 0. \tag{3.22}$$

3.2.2 System of Order One

$$\epsilon \bar{H}_1''' - \bar{H}_2'' - (s-2i)\bar{H}_1'' - 2\epsilon \bar{H}_2' + 2(s+N)\bar{H}_2 = 0, \tag{3.23}$$

$$\bar{H}_2(0,s) = 0, \qquad \bar{H}_2(\infty,s) = 0. \tag{3.24}$$

3.2.3 Zeroth order Solution

The solution of equation (3.21) is

$$\bar{H}_1 = Ae^{-m\xi} + Be^{-n\xi}, \tag{3.25}$$

where

$$m = \epsilon + \sqrt{\epsilon^2 + 2(s+N)},$$
$$n = \epsilon - \sqrt{\epsilon^2 + 2(s+N)}. \tag{3.26}$$

Making use of boundary conditions (3.22), we can write

$$\bar{H}_1 = -\frac{1}{s-i}e^{-m\xi} \tag{3.27}$$

3.2.4 First order Solution

With the help of (3.27), equation (3.23) takes the form

$$\bar{H}_2'' + 2\epsilon\bar{H}_2' - 2(s+N)\bar{H}_2 = (\frac{\epsilon\, m^3}{s-i} + \frac{(s-2i)\, m^2}{s-i})e^{-m\xi}. \tag{3.28}$$

The solution of equation (3.28) satisfying the boundary conditions (3.24) is given by

$$\bar{H}_2 = \frac{X}{Y}\xi e^{-m\xi}, \tag{3.29}$$

where

$$X = \frac{\epsilon\, m^3}{s-i} + \frac{(s-2i)\, m^2}{s-i},$$

$$Y = m^2\xi - 2m - 2\epsilon m\xi + 2\epsilon - 2(s+N)\xi.$$

Using value of m in the solution (3.29) we have

$$\begin{aligned}\bar{H}_2 &= -\frac{\xi e^{-(\epsilon + \sqrt{\epsilon^2 + 2(s+N)})\xi}}{(s-i)\sqrt{\epsilon^2 + 2(s+N)}}\left[2\epsilon^4 + 3\epsilon^2(s+N) + (\epsilon^2 + s + N)(s-2i)\right.\\ &+ \left.\epsilon(2\epsilon^2 + 2s + N - 2i)\sqrt{\epsilon^2 + 2(s+N)}\right]. \end{aligned} \tag{3.30}$$

Substitution of equations (3.27) and (3.30) in (3.20) yields

$$\begin{aligned}\bar{H}(\xi, s) &= -\frac{1}{s-i}e^{-(\epsilon + \sqrt{\epsilon^2 + 2(s+N)})\xi}\\ &- \frac{\alpha\xi e^{-(\epsilon + \sqrt{\epsilon^2 + 2(s+N)})\xi}}{(s-i)\sqrt{\epsilon^2 + 2(s+N)}}\left[2\epsilon^4 + 3\epsilon^2(s+N)\right.\end{aligned}$$

$$+ \quad (\epsilon^2 + s + N)(s - 2i)$$

$$+ \quad \epsilon(2\epsilon^2 + 2s + N - 2i)\sqrt{\epsilon^2 + 2(s+N)}\Big] . \qquad (3.31)$$

Note that the first term in equation (3.31) corresponds to zeroth-order solution while all the other terms correspond to first order solution. The inverse of $\bar{H}$ is given by

$$\begin{aligned}
H(\xi,\tau) &= \frac{1}{2\pi i}\int_{\lambda-i\infty}^{\lambda+i\infty} \bar{H}(\xi,s)e^{s\tau}ds, \qquad \lambda > 0. \\
&= -\frac{1}{2\pi i}\int_{\lambda-i\infty}^{\lambda+i\infty} \frac{e^{-(\epsilon+\sqrt{\epsilon^2+2(s+N)})\xi + s\tau}}{s-i}ds \\
&- \frac{\alpha\xi(2\epsilon^4 + 3\epsilon^2 N - 2i(\epsilon^2+N))}{2\pi i}\int_{\lambda-i\infty}^{\lambda+i\infty} \frac{e^{-(\epsilon+\sqrt{\epsilon^2+2(s+N)})\xi + s\tau}}{(s-i)\sqrt{\epsilon^2+2(s+N)}}ds \\
&- \frac{\alpha\xi(4\epsilon^2 + N - 2i)}{2\pi i}\int_{\lambda-i\infty}^{\lambda+i\infty} \frac{s\, e^{-(\epsilon+\sqrt{\epsilon^2+2(s+N)})\xi + s\tau}}{(s-i)\sqrt{\epsilon^2+2(s+N)}}ds \\
&- \frac{\alpha\xi}{2\pi i}\int_{\lambda-i\infty}^{\lambda+i\infty} \frac{s^2\, e^{-(\epsilon+\sqrt{\epsilon^2+2(s+N)})\xi + s\tau}}{(s-i)\sqrt{\epsilon^2+2(s+N)}}ds \\
&- \frac{\alpha\xi(2\epsilon^3 + \epsilon(N-2i))}{2\pi i}\int_{\lambda-i\infty}^{\lambda+i\infty} \frac{e^{-(\epsilon+\sqrt{\epsilon^2+2(s+N)})\xi + s\tau}}{s-i}ds \\
&- \frac{2\alpha\xi\epsilon}{2\pi i}\int_{\lambda-i\infty}^{\lambda+i\infty} \frac{s\, e^{-(\epsilon+\sqrt{\epsilon^2+2(s+N)})\xi + s\tau}}{s-i}ds, \qquad \lambda > 0. \qquad (3.32)
\end{aligned}$$

With the help of [59], we have

$$\frac{1}{2\pi i}\int_{\lambda-i\infty}^{\lambda+i\infty}\frac{e^{-(\epsilon+Y)\xi+s\tau}}{s-i}ds$$

$$=\frac{e^{-\epsilon\xi+i\tau}}{2}\left[e^{-Y\xi}erfc(\frac{\xi}{\sqrt{2\tau}}-Y\sqrt{\frac{\tau}{2}})+e^{Y\xi}erfc(\frac{\xi}{\sqrt{2\tau}}+Y\sqrt{\frac{\tau}{2}})\right], \quad (3.33)$$

$$\frac{1}{2\pi i}\int_{\lambda-i\infty}^{\lambda+i\infty}\frac{s\,e^{-(\epsilon+Y)\xi+s\tau}}{s-i}ds$$

$$=\frac{i\,e^{-\epsilon\xi+i\tau}}{2}\left[e^{-Y\xi}erfc(\frac{\xi}{\sqrt{2\tau}}-Y\sqrt{\frac{\tau}{2}})+e^{Y\xi}erfc(\frac{\xi}{\sqrt{2\tau}}+Y\sqrt{\frac{\tau}{2}})\right]$$

$$+\frac{\xi\,e^{-\epsilon\xi-\frac{\xi^2}{2\tau}-(\epsilon^2+2N)\frac{\tau}{2}}}{\sqrt{2\pi\tau^3}}, \quad (3.34)$$

$$\frac{1}{2\pi i}\int_{\lambda-i\infty}^{\lambda+i\infty}\frac{e^{-(\epsilon+Y)\xi+s\tau}}{(s-i)Y}ds$$

$$=\frac{e^{-\epsilon\xi+i\tau}}{4Y}\left[e^{-Y\xi}erfc(\frac{\xi}{\sqrt{2\tau}}-Y\sqrt{\frac{\tau}{2}})-e^{Y\xi}erfc(\frac{\xi}{\sqrt{2\tau}}+Y\sqrt{\frac{\tau}{2}})\right], \quad (3.35)$$

$$\frac{1}{2\pi i}\int_{\lambda-i\infty}^{\lambda+i\infty}\frac{s\,e^{-(\epsilon+Y)\xi+s\tau}}{(s-i)Y}ds$$

$$=\frac{i\,e^{-\epsilon\xi+i\tau}}{2Y}\left[e^{-Y\xi}erfc(\frac{\xi}{\sqrt{2\tau}}-Y\sqrt{\frac{\tau}{2}})-e^{Y\xi}erfc(\frac{\xi}{\sqrt{2\tau}}+Y\sqrt{\frac{\tau}{2}})\right]$$

$$+\frac{e^{-\epsilon\xi-\frac{\xi^2}{2\tau}-(\epsilon^2+2N)\frac{\tau}{2}}}{\sqrt{2\pi\tau}}, \quad (3.36)$$

$$\frac{1}{2\pi i}\int_{\lambda-i\infty}^{\lambda+i\infty}\frac{s^2\, e^{-(\epsilon+Y)\xi+s\tau}}{(s-i)Y}ds$$

$$=-\frac{e^{-\epsilon\xi+i\tau}}{2Y}\left[e^{-Y\xi}erfc(\frac{\xi}{\sqrt{2\tau}}-Y\sqrt{\frac{\tau}{2}})-e^{Y\xi}erfc(\frac{\xi}{\sqrt{2\tau}}+Y\sqrt{\frac{\tau}{2}})\right]$$

$$-\frac{(\epsilon^2-2(i-N))e^{-\epsilon\xi-\frac{\xi^2}{2\tau}-(\epsilon^2+2N)\frac{\tau}{2}}}{2\sqrt{2\pi\tau}},\qquad(3.37)$$

where

$$Y=\sqrt{\epsilon^2+2(i+N)}.\qquad(3.38)$$

Substitution of equations (3.33 - 3.37) into equation (3.32) give

$$\begin{aligned}H(\xi,\tau)\ &=\ e^{-(\epsilon+Y)\xi+i\tau}erfc(\frac{\xi}{\sqrt{2\tau}}-Y\sqrt{\frac{\tau}{2}})\left[-\frac{1}{2}(1+\xi\alpha(2\epsilon^3+\epsilon(N-2i)))\right.\\
&-\ \frac{\xi\alpha}{4Y}(2\epsilon^4+3\epsilon^2N-2i(\epsilon^2+N))-\frac{i\xi\alpha}{2Y}(4\epsilon^2+N-2i)\\
&+\ \left.\frac{\xi\alpha}{2Y}-i\xi\alpha\epsilon\right]+e^{-(\epsilon-Y)\xi+i\tau}erfc(\frac{\xi}{\sqrt{2\tau}}+Y\sqrt{\frac{\tau}{2}})\left[-\frac{1}{2}(1\right.\\
&+\ \xi\alpha(2\epsilon^3+\epsilon(N-2i)))+\frac{\xi\alpha}{4Y}(2\epsilon^4+3\epsilon^2N-2i(\epsilon^2+N))\\
&+\ \left.\frac{i\xi\alpha}{2Y}(4\epsilon^2+N-2i)-\frac{\xi\alpha}{2Y}-i\xi\alpha\epsilon\right]\\
&-\ \frac{\xi\alpha}{\sqrt{2\pi\tau}}(4\epsilon^2+N-2i)e^{-\epsilon\xi-\frac{\xi^2}{2\tau}-(\epsilon^2+2N)\frac{\tau}{2}}\end{aligned}$$

$$
\begin{aligned}
&+ \quad \frac{\xi\alpha}{2\sqrt{2\pi\tau}}(\epsilon^2+2N-2i)e^{-\epsilon\xi-\frac{\xi^2}{2\tau}-(\epsilon^2+2N)\frac{\tau}{2}} \\
&- \quad \frac{2\epsilon\xi^2\alpha}{\sqrt{2\pi\tau^3}}e^{-\epsilon\xi-\frac{\xi^2}{2\tau}-(\epsilon^2+2N)\frac{\tau}{2}}. \qquad (3.39)
\end{aligned}
$$

Using equation (3.14) and $F = \frac{f+ig}{\Omega l} - 1$, we obtain

$$
\begin{aligned}
\frac{f}{\Omega l} + i\frac{g}{\Omega l} &= 1 + e^{-z_1\xi}\,(\cos b\xi - i\sin b\xi)\; erfc\,(\frac{\xi}{\sqrt{2\tau}} - (a+ib)\,\sqrt{\frac{\tau}{2}}\,) \\
&\left[-\frac{1}{2} - \xi\alpha\left\{\epsilon^3 + \frac{\epsilon N}{2} + \frac{(a-ib)}{2(a^2+b^2)}\left(\epsilon^4 + \frac{3}{2}\epsilon^2 N + 3i\epsilon^2 + 1\right)\right\}\right] \\
&+ \quad e^{-z_2\xi}\,(\cos b\xi + i\sin b\xi)\; erfc\,(\frac{\xi}{\sqrt{2\tau}} + (a+ib)\,\sqrt{\frac{\tau}{2}}\,) \\
&\left[-\frac{1}{2} - \xi\alpha\left\{\epsilon^3 + \frac{\epsilon N}{2} - \frac{(a-ib)}{2(a^2+b^2)}\left(\epsilon^4 + \frac{3}{2}\epsilon^2 N + 3i\epsilon^2 + 1\right)\right\}\right] \\
&+ \quad \frac{e^{-\epsilon\xi-\frac{\xi^2}{2\tau}-(\epsilon^2+2N)\frac{\tau}{2}}}{\sqrt{2\pi\tau}}\xi\alpha(\cos\tau - i\sin\tau)\left[-\frac{7\epsilon^2}{2} + i - \frac{2\xi\epsilon}{\tau}\right],
\end{aligned}
$$

(3.40)

where

$$
z_1 = \epsilon + a, \qquad z_2 = \epsilon - a,
$$

$$
a = \left(\frac{\sqrt{(\epsilon^2+2N)^2+4} + (\epsilon^2+2N)}{2}\right)^{\frac{1}{2}},
$$

$$b = \left(\frac{\sqrt{(\epsilon^2 + 2N)^2 + 4} - (\epsilon^2 + 2N)}{2} \right)^{\frac{1}{2}}.$$

For large time solution (3.40) become

$$\begin{aligned}
\frac{f}{\Omega l} + i\frac{g}{\Omega l} &= \Big[1 - e^{-z_1\xi}(\cos b\xi - i\sin b\xi)\Big\{1 + \xi\alpha\Big(2\epsilon^3 + \epsilon N \\
&+ \frac{(a-ib)}{(a^2+b^2)}(2\epsilon^4 + 3\epsilon^2 N + 1 - i(N - 2\epsilon^2))\Big)\Big\}\Big] \\
&+ \Big[e^{-z_1\xi}\,(\cos b\xi - i\sin b\xi)\; erfc\,(\frac{\xi}{\sqrt{2\tau}} - (a+ib)\sqrt{\frac{\tau}{2}}\,) \\
&\Big\{-\frac{1}{2} - \xi\alpha\Big(\epsilon^3 + \frac{\epsilon N}{2} + \frac{(a-ib)}{2(a^2+b^2)}(\epsilon^4 + \frac{3}{2}\epsilon^2 N + 3i\epsilon^2 + 1)\Big)\Big\} \\
&+ e^{-z_2\xi}\,(\cos b\xi + i\sin b\xi)\; erfc\,(\frac{\xi}{\sqrt{2\tau}} + (a+ib)\sqrt{\frac{\tau}{2}}\,) \\
&\Big\{-\frac{1}{2} - \xi\alpha\Big(\epsilon^3 + \frac{\epsilon N}{2} - \frac{(a-ib)}{2(a^2+b^2)}(\epsilon^4 + \frac{3}{2}\epsilon^2 N + 3i\epsilon^2 + 1)\Big)\Big\} \\
&+ \frac{e^{-\epsilon\xi - \frac{\xi^2}{2\tau} - (\epsilon^2+2N)\frac{\tau}{2}}}{\sqrt{2\pi\tau}}\xi\alpha(\cos\tau - i\sin\tau)\Big\{-\frac{7\epsilon^2}{2} + i - \frac{2\xi\epsilon}{\tau}\Big\}\Big],
\end{aligned} \tag{3.41}$$

where the first term in bracket [.] on the right-hand side corresponds to the steady state and the second denotes the deviation from it.

For $\xi << \sqrt{2\tau}$ and $\tau >> 1$ we get the approximate form as

$$
\begin{aligned}
\frac{f}{\Omega l} &= 1 - e^{-z_1\xi}\cos b\xi - e^{-z_1\xi}\frac{\xi\alpha}{(a^2+b^2)}\Big[\{a(2\epsilon^4 + 3\epsilon^2 N + 1) \\
&- b(N - 2\epsilon^2)\}\cos b\xi - \{b(2\epsilon^4 + 3\epsilon^2 N + 1) + a(N - 2\epsilon^2)\}\sin b\xi\Big] \\
&- \xi\alpha e^{-z_1\xi}(2\epsilon^3 + \epsilon N)\cos b\xi + \frac{e^{-z_1\xi - (a^2-b^2)\frac{\tau}{2}}}{\sqrt{\frac{\pi\tau}{2}}(a^2+b^2)}\Big[\Big(\frac{a}{2} + a\xi\alpha(\epsilon^3 + \frac{\epsilon N}{2}) \\
&+ \frac{(a^2-b^2)}{2(a^2+b^2)}\xi\alpha(\epsilon^4 + \frac{3}{2}\epsilon^2 N + 1) + \frac{3ab\xi\alpha\epsilon^2}{(a^2+b^2)}\Big)\cos(b\xi + ab\tau) \\
&- \Big(\frac{b}{2} + b\xi\alpha(\epsilon^3 + \frac{\epsilon N}{2}) + \frac{ab\xi\alpha}{(a^2+b^2)}(\epsilon^4 + \frac{3}{2}\epsilon^2 N + 1) \\
&- \frac{3(a^2-b^2)}{2(a^2+b^2)}\xi\alpha\epsilon^2\Big)\sin(b\xi + ab\tau)\Big] - \frac{e^{-z_2\xi - (a^2-b^2)\frac{\tau}{2}}}{\sqrt{\frac{\pi\tau}{2}}(a^2+b^2)}\Big[\Big(\frac{a}{2} + a\xi\alpha(\epsilon^3 + \frac{\epsilon N}{2}) \\
&- \frac{(a^2-b^2)}{2(a^2+b^2)}\xi\alpha(\epsilon^4 + \frac{3}{2}\epsilon^2 N + 1) - \frac{3ab\xi\alpha\epsilon^2}{(a^2+b^2)}\Big)\cos(b\xi - ab\tau) \\
&+ \Big(\frac{b}{2} + b\xi\alpha(\epsilon^3 + \frac{\epsilon N}{2}) - \frac{ab\xi\alpha}{(a^2+b^2)}(\epsilon^4 + \frac{3}{2}\epsilon^2 N + 1) \\
&+ \frac{3(a^2-b^2)}{2(a^2+b^2)}\xi\alpha\epsilon^2\Big)\sin(b\xi - ab\tau)\Big], \qquad (3.42)
\end{aligned}
$$

$$
\begin{aligned}
\frac{g}{\Omega l} &= e^{-z_1\xi}\sin b\xi + e^{-z_1\xi}\frac{\xi\alpha}{(a^2+b^2)}\Big[\{a(2\epsilon^4 + 3\epsilon^2 N + 1) \\
&- b(N - 2\epsilon^2)\}\sin b\xi + \{b(2\epsilon^4 + 3\epsilon^2 N + 1) + a(N - 2\epsilon^2)\}\cos b\xi\Big]
\end{aligned}
$$

$$
\begin{aligned}
&+ \quad \xi\alpha e^{-z_1\xi}(2\epsilon^3+\epsilon N)\sin b\xi - \frac{e^{-z_1\xi-(a^2-b^2)\frac{\tau}{2}}}{\sqrt{\frac{\pi\tau}{2}}(a^2+b^2)}\left[\left(\frac{a}{2}+a\xi\alpha(\epsilon^3+\frac{\epsilon N}{2})\right.\right. \\
&+ \quad \left.\frac{(a^2-b^2)}{2(a^2+b^2)}\xi\alpha(\epsilon^4+\frac{3}{2}\epsilon^2N+1)+\frac{3ab\xi\alpha\epsilon^2}{(a^2+b^2)}\right)\sin(b\xi+ab\tau) \\
&+ \quad \left(\frac{b}{2}+b\xi\alpha(\epsilon^3+\frac{\epsilon N}{2})+\frac{ab\xi\alpha}{(a^2+b^2)}(\epsilon^4+\frac{3}{2}\epsilon^2N+1)\right. \\
&- \quad \left.\frac{3(a^2-b^2)}{2(a^2+b^2)}\xi\alpha\epsilon^2\right)\cos(b\xi+ab\tau) \\
&- \quad \left(\frac{b}{2}+b\xi\alpha(\epsilon^3+\frac{\epsilon N}{2})-\frac{ab\xi\alpha}{(a^2+b^2)}(\epsilon^4+\frac{3}{2}\epsilon^2N+1)\right. \\
&+ \quad \left.\frac{3\xi\alpha\epsilon^2(a^2-b^2)}{2(a^2+b^2)}\right)\cos(b\xi-ab\tau)+\left(\frac{a}{2}+a\xi\alpha(\epsilon^3+\frac{\epsilon N}{2})\right. \\
&- \quad \left.\left.\frac{(a^2-b^2)}{2(a^2+b^2)}\xi\alpha(\epsilon^4+\frac{3}{2}\epsilon^2N+1)-\frac{3ab\xi\alpha\epsilon^2}{(a^2+b^2)}\right)\sin(b\xi-ab\tau)\right]. \qquad (3.43)
\end{aligned}
$$

3.3 Blowing solution

In the case of blowing $\epsilon < 0$ and we take $\epsilon = -\delta$ so that $\delta > 0$. The asymptotic solution is given by

$$
\begin{aligned}
\frac{f}{\Omega l}+\iota\frac{g}{\Omega l} &= 1+e^{-x_1\xi}(\cos d\xi - i\sin d\xi)\ erfc(\frac{\xi}{\sqrt{2\tau}}-(c+id)\sqrt{\frac{\tau}{2}}) \\
&\quad \left[-\frac{1}{2}+\xi\alpha\left\{\delta^3+\frac{\delta N}{2}-\frac{(c-id)}{2(c^2+d^2)}\left(\delta^4+\frac{3\delta^2N}{2}+3i\delta^2+1\right)\right\}\right] \\
&+ \quad e^{x_2\xi}(\cos d\xi + i\sin d\xi)\ erfc(\frac{\xi}{\sqrt{2\tau}}+(c+id)\sqrt{\frac{\tau}{2}})
\end{aligned}
$$

$$\left[-\frac{1}{2}+\xi\alpha\left\{\delta^3+\frac{\delta N}{2}+\frac{(c-id)}{2(c^2+d^2)}\left(\delta^4+\frac{3\delta^2 N}{2}+3i\delta^2+1\right)\right\}\right]$$

$$+\quad\frac{e^{\delta\xi-\frac{\xi^2}{2\tau}-(\delta^2+2N)\frac{\tau}{2}}}{\sqrt{2\pi\tau}}\xi\alpha(\cos\tau-i\sin\tau)\left[-\frac{7\delta^2}{2}+i+\frac{2\xi\delta}{\tau}\right],$$

$$(3.44)$$

where

$$\begin{aligned}
x_1 &= c-\delta, \qquad\qquad x_2=c+\delta,\\
c &= \left\{\frac{\sqrt{(\delta^2+2N)^2+4}+(\delta^2+2N)}{2}\right\}^{\frac{1}{2}},\\
d &= \left\{\frac{\sqrt{(\delta^2+2N)^2+4}-(\delta^2+2N)}{2}\right\}^{\frac{1}{2}}.
\end{aligned}$$

For large times, equation (3.44) can be written in the following form

$$\begin{aligned}
\frac{f}{\Omega l}+i\frac{g}{\Omega l} &= \Big[1-e^{-x_1\xi}(\cos d\xi-i\sin d\xi)\Big\{1-\xi\alpha\Big(2\delta^3+\delta N\\
&- \frac{(c-id)}{(c^2+d^2)}(2\delta^4+3\delta^2 N+1-i(N-2\delta^2))\Big)\Big\}\Big]\\
&+ \Big[e^{-x_1\xi}(\cos d\xi-i\sin d\xi)\ erfc\,(\frac{\xi}{\sqrt{2\tau}}-(c-id)\sqrt{\frac{\tau}{2}})\\
&\quad\Big\{-\frac{1}{2}+\xi\alpha\Big(\delta^3+\frac{\delta N}{2}-\frac{(c-id)}{(c^2+d^2)}\{\delta^4+\frac{3\delta^2 N}{2}+3i\delta^2+1\}\Big)\Big\}
\end{aligned}$$

$$+ \quad e^{x_2\xi}(\cos d\xi + i\sin d\xi)\, erfc\,(\frac{\xi}{\sqrt{2\tau}} + (c+id)\sqrt{\frac{\tau}{2}})$$

$$\left\{-\frac{1}{2} + \xi\alpha\left(\delta^3 + \frac{\delta N}{2} + \frac{(c-id)}{(c^2+d^2)}\{\delta^4 + \frac{3\delta^2 N}{2} + 3i\delta^2 + 1\}\right)\right\}$$

$$\left. + \quad \frac{e^{\delta\xi - \frac{\xi^2}{2\tau} - (\delta^2+2N)\frac{\tau}{2}}}{\sqrt{2\pi\tau}}\xi\alpha(\cos\tau - i\sin\tau)\left\{-\frac{7\delta^2}{2} + i + \frac{2\xi\delta}{\tau}\right\}\right] . \tag{3.45}$$

The approximate form of the solution for $\xi << \sqrt{2\tau}$ and $\tau >> 1$ is

$$\frac{f}{\Omega l} = 1 - e^{-x_1\xi}\cos d\xi - e^{-x_1\xi}\frac{\xi\alpha}{(c^2+d^2)}\left[\{c(2\delta^4 + 3\delta^2 N + 1)\right.$$

$$- \quad d(N - 2\delta^2)\}\cos d\xi - \{d(2\delta^4 + 3\delta^2 N + 1) + c(N - 2\delta^2)\}\sin d\xi\Big]$$

$$+ \quad \xi\alpha e^{-x_1\xi}(2\delta^3 + \delta N)\cos d\xi + \frac{e^{-x_1\xi - (c^2-d^2)\frac{\tau}{2}}}{\sqrt{\frac{\pi\tau}{2}}(c^2+d^2)}\left[\left(\frac{c}{2} - c\xi\alpha(\delta^3 + \frac{\delta N}{2})\right.\right.$$

$$+ \quad \left.\frac{(c^2-d^2)}{2(c^2+d^2)}\xi\alpha(\delta^4 + \frac{3}{2}\delta^2 N + 1) + \frac{3cd\xi\alpha\delta^2}{(c^2+d^2)}\right)\cos(c\xi + cd\tau)$$

$$- \quad \left(\frac{d}{2} - d\xi\alpha(\delta^3 + \frac{\delta N}{2}) + \frac{cd\xi\alpha}{(c^2+d^2)}(\delta^4 + \frac{3}{2}\delta^2 N + 1)\right.$$

$$- \quad \left.\left.\frac{3(c^2-d^2)}{2(c^2+d^2)}\xi\alpha\delta^2\right)\sin(d\xi + cd\tau)\right] - \frac{e^{x_2\xi - (c^2-d^2)\frac{\tau}{2}}}{\sqrt{\frac{\pi\tau}{2}}(c^2+d^2)}\left[\left(\frac{c}{2} - c\xi\alpha(\delta^3 + \frac{\delta N}{2})\right.\right.$$

$$- \quad \left.\frac{(c^2-d^2)}{2(c^2+d^2)}\xi\alpha(\delta^4 + \frac{3}{2}\delta^2 N + 1) - \frac{3cd\xi\alpha\delta^2}{(c^2+d^2)}\right)\cos(d\xi - cd\tau)$$

$$
\begin{aligned}
&+ \left(\frac{d}{2} - d\xi\alpha(\delta^3 + \frac{\delta N}{2}) - \frac{cd\xi\alpha}{(c^2+d^2)}(\delta^4 + \frac{3}{2}\delta^2 N + 1)\right. \\
&+ \left.\frac{3(c^2-d^2)}{2(c^2+d^2)}\xi\alpha\delta^2\right)\sin(d\xi - cd\tau)\Bigg], \qquad (3.46)
\end{aligned}
$$

$$
\begin{aligned}
\frac{g}{\Omega l} &= e^{-x_1\xi}\sin d\xi + e^{-x_1\xi}\frac{\xi\alpha}{(c^2+d^2)}\left[\{c(2\delta^4 + 3\delta^2 N + 1)\right. \\
&- \left. d(N - 2\delta^2)\}\sin d\xi + \{d(2\delta^4 + 3\delta^2 N + 1) + c(N - 2\delta^2)\}\cos d\xi\right] \\
&- \xi\alpha e^{-x_1\xi}(2\delta^3 + \delta N)\sin d\xi - \frac{e^{-x_1\xi - (c^2-d^2)\frac{\tau}{2}}}{\sqrt{\frac{\pi\tau}{2}}(c^2+d^2)}\left[\left(\frac{c}{2} - c\xi\alpha(\delta^3 + \frac{\delta N}{2})\right.\right. \\
&+ \left.\frac{(c^2-d^2)}{2(c^2+d^2)}\xi\alpha(\delta^4 + \frac{3}{2}\delta^2 N + 1) + \frac{3cd\xi\alpha\delta^2}{(c^2+d^2)}\right)\sin(d\xi + cd\tau) \\
&+ \left(\frac{d}{2} - d\xi\alpha(\delta^3 + \frac{\delta N}{2}) + \frac{cd\xi\alpha}{(c^2+d^2)}(\delta^4 + \frac{3}{2}\delta^2 N + 1)\right. \\
&- \left.\frac{3(c^2-d^2)}{2(c^2+d^2)}\xi\alpha\delta^2\right)\cos(d\xi + cd\tau) \\
&- \left(\frac{d}{2} - d\xi\alpha(\delta^3 + \frac{\delta N}{2}) - \frac{cd\xi\alpha}{(c^2+d^2)}(\delta^4 + \frac{3}{2}\delta^2 N + 1)\right. \\
&+ \left.\frac{3\xi\alpha\delta^2(c^2-d^2)}{2(c^2+d^2)}\right)\cos(d\xi - cd\tau) + \left(\frac{c}{2} - c\xi\alpha(\delta^3 + \frac{\delta N}{2})\right. \\
&- \left.\left.\frac{(c^2-d^2)}{2(c^2+d^2)}\xi\alpha(\delta^4 + \frac{3}{2}\delta^2 N + 1) - \frac{3cd\xi\alpha\delta^2}{(c^2+d^2)}\right)\sin(d\xi - cd\tau)\right]. \qquad (3.47)
\end{aligned}
$$

3.4 Discussion

In order to get the nature of the velocity distribution near the disk the expressions for $\frac{f}{\Omega l}$ and $\frac{g}{\Omega l}$ are plotted.

When suction and magnetic field are absent i. e., $\epsilon = 0, N = 0$ in equations (3.42) and (3.43), the effect of material constant α is shown in figure 3.1. We note that for small values of α we get the same velocity profile and fluid behaves like Newtonian fluid which is in agreement with [60]. However, α starts influencing the flow field for its values near .01. We further observe that the boundary layer thickness increases with the increase in α.

Figure 3.2 shows the effect of α in the presence of suction $\epsilon = 2$ without magnetic field ($N = 0$). We found that boundary layer thickness is controlled by the suction parameter i. e., it decreases with an increase in suction parameter.

In case of blowing $\delta = 2$ and $N = 0$ the boundary layer thickness becomes very large as is expected physically and is shown in figure 3.3.

Figure 3.4 gives the variation in $\frac{f}{\Omega}$ and $\frac{g}{\Omega l}$ for the cases when $\alpha = 1,\ N = 2$.

Comparing figures 3.3 and 3.4, we observe that boundary layer thickness is drastically decreased by introducing magnetic field. Magnetic field thus controls the boundary layer structure of a fluid which is enhanced by introducing suction parameter.

Chapter 4

MHD Flow of a Third Grade Fluid Due to Eccentric Rotations of a Porous Disk and a Fluid at Infinity

In this chapter, the analysis of second grade fluid is extended to the case of third grade fluid. We consider the magnetohydrodynamic (MHD) flow of a conducting, incompressible third grade fluid, due to non-coaxial rotations of a porous disk and a fluid at infinity in the presence of a uniform transverse magnetic field. An exact analysis is carried out to model the governing non-linear partial differential equation. Numerical solution of the third order non-linear partial differential equation has been obtained. Several graphs have been drawn to show the influence of porosity, magnetic parameter and material parameters on the velocity distribution.

4.1 Basic Equations

An incompressible third grade fluid filling the semi-infinite space $z > 0$ in contact with an infinite porous disk at $z = 0$ is considered. The disk and fluid at infinity are initially rotating about the z'-axis with the same angular velocity $\mathbf{\Omega}$, and at time $t = 0$, the disk starts to rotate impulsively about the z-axis with the angular velocity $\mathbf{\Omega}$ and the fluid at infinity continues to rotate about the z'-axis with the same angular velocity. The axes of rotations of the disk and that of fluid at infinity are assumed to be in the plane $x = 0$ and distance between the axes is l as shown in figure 1. The fluid is electrically conducting and assumed to be permeated by a magnetic field $\mathbf{B}_\circ$ having no components in the x and y directions. The boundary and initial conditions are of the form (2.1), leading toward the solution of the form (2.2).

The incompressible, homogeneous and thermodynamic fluid of third grade is a simple fluid of the differential type whose Cauchy stress tensor $\mathbf{T}$ is represented by equation (1.24).

Using equation (2.2) into equations (1.98 - 1.100), we obtain

$$\begin{aligned}
\rho\left[\frac{\partial f}{\partial t} - \Omega^2 x - \Omega g - w_\circ \frac{\partial f}{\partial z}\right] &= -\frac{\partial P}{\partial x} + \mu \frac{\partial^2 f}{\partial z^2} - \sigma B_\circ^2 (f - \Omega y) \\
&+ \alpha_1 \left[\frac{\partial^3 f}{\partial t \partial z^2} - w_\circ \frac{\partial^3 f}{\partial z^3} + \Omega \frac{\partial^2 g}{\partial z^2}\right] \\
&+ 2\beta_3 \frac{\partial}{\partial z}\left[\frac{\partial f}{\partial z}\left\{\left(\frac{\partial f}{\partial z}\right)^2 + \left(\frac{\partial g}{\partial z}\right)^2\right\}\right], \qquad (4.1)
\end{aligned}$$

$$\begin{aligned}
\rho\left[\frac{\partial g}{\partial t} - \Omega^2 y + \Omega f - w_\circ \frac{\partial g}{\partial z}\right] &= -\frac{\partial P}{\partial y} + \mu \frac{\partial^2 g}{\partial z^2} - \sigma B_\circ^2 (g + \Omega x) \\
&+ \alpha_1 \left[\frac{\partial^3 g}{\partial t \partial z^2} - w_\circ \frac{\partial^3 g}{\partial z^3} - \Omega \frac{\partial^2 f}{\partial z^2}\right] \\
&+ 2\beta_3 \frac{\partial}{\partial z}\left[\frac{\partial g}{\partial z}\left\{\left(\frac{\partial f}{\partial z}\right)^2 + \left(\frac{\partial g}{\partial z}\right)^2\right\}\right], \qquad (4.2)
\end{aligned}$$

$$\sigma B_\circ^2 w_\circ = \frac{\partial P}{\partial z}, \tag{4.3}$$

where P is defined by equation (3.8). Elimination of P from equations (4.1 - 4.3) yields

$$\begin{aligned} \rho\left[\frac{\partial f}{\partial t} - \Omega g - w_\circ \frac{\partial f}{\partial z}\right] &= \mu \frac{\partial^2 f}{\partial z^2} - \sigma B_\circ^2 f \\ &+ \alpha_1 \left[\frac{\partial^3 f}{\partial t \partial z^2} - w_\circ \frac{\partial^3 f}{\partial z^3} + \Omega \frac{\partial^2 g}{\partial z^2}\right] \\ &+ 2\beta_3 \frac{\partial}{\partial z}\left[\frac{\partial f}{\partial z}\left\{\left(\frac{\partial f}{\partial z}\right)^2 + \left(\frac{\partial g}{\partial z}\right)^2\right\}\right] + \sigma B_\circ^2 \Omega l, \quad (4.4) \\ \rho\left[\frac{\partial g}{\partial t} + \Omega f - w_\circ \frac{\partial g}{\partial z}\right] &= \mu \frac{\partial^2 g}{\partial z^2} - \sigma B_\circ^2 g \\ &+ \alpha_1 \left[\frac{\partial^3 g}{\partial t \partial z^2} - w_\circ \frac{\partial^3 g}{\partial z^3} - \Omega \frac{\partial^2 f}{\partial z^2}\right] \\ &+ 2\beta_3 \frac{\partial}{\partial z}\left[\frac{\partial g}{\partial z}\left\{\left(\frac{\partial f}{\partial z}\right)^2 + \left(\frac{\partial g}{\partial z}\right)^2\right\}\right] + \rho\, \Omega^2 l. \quad (4.5) \end{aligned}$$

With the help of equation (2.15), equations (4.4) and (4.5) can be combined in the following form

$$\begin{aligned} \left[\frac{\partial F^*}{\partial t} + i\,\Omega F^* - w_\circ \frac{\partial F^*}{\partial z}\right] &= \nu \frac{\partial^2 F^*}{\partial z^2} - \frac{\sigma}{\rho} B_\circ^2 (F^* - \Omega l) + i\,\Omega^2 l \\ &+ \frac{\alpha_1}{\rho}\left[\frac{\partial^3 F^*}{\partial t \partial z^2} - w_\circ \frac{\partial^3 F^*}{\partial z^3} - i\,\Omega \frac{\partial^2 F^*}{\partial z^2}\right] \\ &+ 2\frac{\beta_3}{\rho}\frac{\partial}{\partial z}\left[\left(\frac{\partial F^*}{\partial z}\right)^2 \frac{\partial \bar{F}^*}{\partial z}\right], \quad (4.6) \end{aligned}$$

where $\bar{F^*}$ is the complex conjugate of F^* and the initial and boundary conditions are given by (2.17).

We note that for $\alpha_1 = \mathbf{B}_\circ = w_\circ = \beta_3 = 0$, equation (4.6) corresponds to the differential equations for classical viscous fluid and $\mathbf{B}_\circ = w_\circ = \beta_3 = 0$, for second grade fluids, respectively.

Introducing dimensionless parameters

$$\xi = \sqrt{\frac{\Omega}{2\nu}}z, \quad \tau = \Omega t, \quad \alpha = \frac{\Omega\alpha_1}{\rho\nu}, \quad \epsilon = \frac{w_\circ}{\sqrt{2\nu\Omega}}, \quad N = \frac{\sigma}{\rho\Omega}B_\circ^2,$$

$$\beta = \frac{\Omega^3 l^2 \beta_3}{\rho\nu^2}, \quad F(\xi,\tau) = \frac{F^*}{\Omega l} - 1, \quad \bar{F}(\xi,\tau) = \frac{\bar{F^*}}{\Omega l} - 1 \tag{4.7}$$

equation (4.6) and conditions (2.17) can be rewritten as

$$\begin{aligned} \alpha\frac{\partial^3 F}{\partial\tau\partial\xi^2} &- \alpha\epsilon\frac{\partial^3 F}{\partial\xi^3} + (1-i\alpha)\frac{\partial^2 F}{\partial\xi^2} + 2\epsilon\frac{\partial F}{\partial\xi} \\ &- 2\frac{\partial F}{\partial\tau} - 2(i+N)F + \beta\frac{\partial}{\partial\xi}\left[\left(\frac{\partial F}{\partial\xi}\right)^2\frac{\partial\bar{F}}{\partial\xi}\right] = 0, \end{aligned} \tag{4.8}$$

$$F(0,\tau) = -1, \quad F(\infty,\tau) = 0, \quad F(\xi,0) = 0. \tag{4.9}$$

We note that the equation (4.8) is a third order partial differential equation. Moreover, this equation is highly non-linear as compared to case of second grade and Newtonian flow equations. As a result, it seems to be impossible to obtain the general solution in closed form for arbitrary values of all parameters arising in this non-linear equation. Further, the choice of an appropriate numerical technique is closely related to the mathematical behavior of the partial differential equation (4.8). The equation (4.8) is parabolic with respect to time which allows a time marching solution to the equation. Dealing with parabolic equation, there is only one characteristic direction. The information at one point influences the entire region on one side of the vertical characteristic and contained within the two boundaries. Therefore, lend itself to marching solution. Starting with the initial data, the solution between the two boundaries is obtained by marching in the τ direction. The above equation is non-linear. The non-linearity must be suppressed in applying the Von Neumann stability analysis. This is done by treating solution-dependent coefficients multiplying derivatives as being temporarily frozen. The modified equation approach to analyzing non-linear computational algorithm is applicable [61] but the appearance of products of higher-order derivatives makes the construction of more accurate schemes less precise than the case of linear equations.

As this problem is time dependent and has mixed derivative with respect to time and space coordinates so we are forced to use an implicit scheme. Applying implicit scheme to nonlinear equation (4.8) is not as straight forward as for linear equations. To convert partial differential equation (4.8) to a system of algebraic equations a number of choices are available. If this parabolic partial differential equation is discretized in space first, it becomes an initial value problem of coupled ordinary differential equations. Therefore, numerical methods for a parabolic partial differential equation include both

1) a boundary value problem and
2) an initial value problem.

For these reasons, numerical methods for a parabolic partial differential equation can be developed by combining a numerical method for the initial value problems of ordinary differential equations and a numerical method for the boundary value problems. Most of the numerical methods for initial value problems may result in very complicated or, at least, inefficient methods e. g. higher order Runge-Kutta methods or predictor-corrector methods. This limitation leads us to the consideration of the simplest group of numerical methods for initial value problems. A modified Crank-Nicolson implicit formulation with forward time and central finite difference space approximation is commonly used to solve problems governed by parabolic equations, so equation (4.8) is transformed into algebraic equation of the form

$$\begin{aligned}
& \frac{\alpha}{\Delta\tau h^2}\left[(F_{j+1}^{n+1} - 2F_j^{n+1} + F_{j-1}^{n+1}) - (F_{j+1}^{n} - 2F_j^{n} + F_{j-1}^{n})\right] \\
+ \; & \frac{(1-i\alpha)}{2h^2}\left[(F_{j+1}^{n+1} - 2F_j^{n+1} + F_{j-1}^{n+1}) + (F_{j+1}^{n} - 2F_j^{n} + F_{j-1}^{n})\right] \\
- \; & \frac{\epsilon\alpha}{2h^3}(F_{j+2}^{n} - 2F_{j+1}^{n} + 2F_{j-1}^{n} - F_{j-2}^{n}) - 2(i+N)F_j^n \\
+ \; & \frac{\epsilon}{h}(F_{j+1}^{n} - F_{j-1}^{n}) - \frac{2}{\Delta\tau}(F_j^{n+1} - F_j^n) \\
+ \; & \frac{\beta}{4h^4}\left[(F_{j+1}^{n} - F_{j-1}^{n})^2(\bar{F}_{j+1}^{n} - 2\bar{F}_j^{n} + \bar{F}_{j-1}^{n})\right. \\
+ \; & \left. 2(F_{j+1}^{n} - F_{j-1}^{n})(F_{j+1}^{n} - 2F_j^{n} + F_{j-1}^{n})(\bar{F}_{j+1}^{n} - \bar{F}_{j-1}^{n})\right] = 0 \qquad (4.10)
\end{aligned}$$

Consider equation (4.10), the unknown F_j^{n+1} is not only expressed in terms of the known quantities at time level n, namely, $F_{j+2}^n, F_{j+1}^n, F_j^n, F_{j-1}^n$, and F_{j-2}^n, but also in terms of other unknown quantities at time level $n+1$, namely, F_{j+1}^{n+1} and F_{j-1}^{n+1}. In other words, equation (4.10) represents one equation with three unknowns, namely, F_{j+1}^{n+1}, F_j^{n+1}, and F_{j-1}^{n+1}. Hence, equation (4.10) applied at a given grid point i does not stand alone; it cannot by itself result in a solution for F_j^{n+1}. Rather equation (4.10) must be written at all interior grid points, resulting in a system of algebraic equations from which the unknowns F_j^{n+1} for all i can be solved simultaneously (an implicit approach). Because of this need to solve large systems of simultaneous algebraic equations, implicit methods are usually involved with the manipulations of large matrices. The implicit methods are unconditionally stable unless non-linear effects cause instability, which is controlled by suitable choice of $\Delta\tau$ and h. Equation (4.10) can be rearranged as

$$a_j^n F_{j-1}^{n+1} + b_j^n F_j^{n+1} + c_j^n F_{j+1}^{n+1} = d_j^n, \tag{4.11}$$

where

$$\begin{aligned}
a_j^n &= -\left(\frac{\alpha}{h^2} + \frac{(1-i\alpha)\Delta\tau}{2h^2}\right), \\
b_j^n &= 2\left(\frac{\alpha}{h^2} + \frac{(1-i\alpha)\Delta\tau}{2h^2} + 1\right), \\
c_j^n &= -\left(\frac{\alpha}{h^2} + \frac{(1-i\alpha)\Delta\tau}{2h^2}\right), \\
d_j^n &= -\left(\frac{\alpha}{h^2} + \frac{(1-i\alpha)\Delta\tau}{2h^2}\right)(F_{j+1}^n - 2F_j^n + F_{j-1}^n) \\
&- \frac{\epsilon\alpha\Delta\tau}{2h^3}(F_{j+2}^n - 2F_{j+1}^n + 2F_{j-1}^n - F_{j-2}^n) \qquad (4.12)\\
&+ \frac{\epsilon\Delta\tau}{h}(F_{j+1}^n - F_{j-1}^n) + 2(1-\Delta\tau(i+N))F_j^n \\
&+ \frac{\beta\Delta\tau}{4h^4}((F_{j+1}^n - F_{j-1}^n)^2(\bar{F}_{j+1}^n - 2\bar{F}_j^n + \bar{F}_{j-1}^n) \\
&+ 2(F_{j+1}^n - F_{j-1}^n)(F_{j+1}^n - 2F_j^n + F_{j-1}^n)(\bar{F}_{j+1}^n - \bar{F}_{j-1}^n)).
\end{aligned}$$

with initial-boundary conditions

$$F_1^{n+1} = -1, \quad F_M^{n+1} = 0, \quad F_j^1 = 0, \qquad j = 1, 2, 3, \cdots, M. \tag{4.13}$$

Here discrete domain is considered instead of continuous one. Only two conditions are needed on two boundaries ($z = 0$, and $z = \infty$) contrary to the case of an analytical solution of continuous function [62].

The right hand side of this equation (4.11), d_j^n, is considered in some fashion as known, say from the previous time step and left hand side as the dependent variable in a computational solution of an unsteady flow problem. The steady state approached asymptotically at large times.

Here $\xi = [\xi_j]_{j=1}^{j=M}$ is taken as strictly increasing sequence of discrete points such that $0 = \xi_1 < \xi_2 < \xi_3 < \cdots < \xi_M$ and $h = \xi_i - \xi_{i-1} = \frac{\xi_M - \xi_1}{M-1}$, where M is the number of grid points in space coordinates and $\Delta\tau = \tau^{n+1} - \tau^n$is time interval. The equation (4.11) must be written at all interior grid points resulting in a system of algebraic equations of order M from which the unknowns F_j^{n+1} for all j can be solved simultaneously.

Now apply equation (4.11) sequentially to grid points 2 through $M - 1$. At grid point 2:

$$a_2^n F_1^{n+1} + b_2^n F_2^{n+1} + c_2^n F_3^{n+1} = d_2^n, \tag{4.14}$$

Here, F_1^{n+1}, F_2^{n+1} and F_3^{n+1} represent three values at time level $n + 1$, and d_2^n is a known value. Moreover, boundary condition at grid point ξ_1 is known, so is F_1^{n+1}. Hence, in equation (4.14) the term involving the known F_1^{n+1} can be transferred to the right-hand side, resulting in

$$b_2^n F_2^{n+1} + c_2^n F_3^{n+1} = d_2^n - a_2^n F_1^{n+1} \tag{4.15}$$

Denoting $d_2^n - a_2^n F_1^{n+1}$ by $d_2^{n'}$, where $d_2^{n'}$ is a known value, equation (4.15) is written as

$$b_2^n F_2^{n+1} + c_2^n F_3^{n+1} = d_2^{n'}, \tag{4.16}$$

At grid point 3:

$$a_3^n F_2^{n+1} + b_3^n F_3^{n+1} + c_3^n F_4^{n+1} = d_3^n, \tag{4.17}$$

At grid point 4:

$$a_4^n F_3^{n+1} + b_4^n F_4^{n+1} + c_4^n F_5^{n+1} = d_4^n \tag{4.18}$$

and so on

At grid point $M-2$:

$$a_{M-2}^n F_{M-3}^{n+1} + b_{M-2}^n F_{M-2}^{n+1} + c_{M-2}^n F_{M-1}^{n+1} = d_{M-2}^n, \tag{4.19}$$

and at grid point $M-1$:

$$a_{M-1}^n F_{M-2}^{n+1} + b_{M-1}^n F_{M-1}^{n+1} + c_{M-1}^n F_M^{n+1} = d_{M-1}^n. \tag{4.20}$$

Here again boundary condition at grid point ξ_M is known, so is F_M^{n+1}. Hence, in equation (4.20) the term involving the known F_M^{n+1} can be transferred to the right-hand side, resulting in

$$a_{M-1}^n F_{M-2}^{n+1} + b_{M-1}^n F_{M-1}^{n+1} = d_{M-1}^n - c_{M-1}^n F_M^{n+1}, \tag{4.21}$$

or

$$a^n_{M-1}F^{n+1}_{M-2} + b^n_{M-1}F^{n+1}_{M-1} = d^{n'}_{M-1}, \tag{4.22}$$

where $d^{n'}_{M-1}$ is a known value.

Equation (4.16) to (4.19) and equation (4.22) are $M-2$ equations for $M-2$ unknowns $F^{n+1}_2, F^{n+1}_3, F^{n+1}_4, \cdots, F^{n+1}_{M-1}$. This system of equations can be written in matrix form as follows

$$\begin{pmatrix} b_2 & c_2 & & & & & & \\ a_3 & b_3 & c_3 & & & & & \\ & a_4 & b_4 & c_4 & & & & \\ & & \cdot & \cdot & \cdot & & & \\ & & & a_j & b_j & c_j & & \\ & & & & \cdot & \cdot & \cdot & \\ & & & & & a_{M-2} & b_{M-2} & c_{M-2} \\ & & & & & & a_{M-1} & b_{M-1} \end{pmatrix} \begin{bmatrix} F_2 \\ F_3 \\ F_4 \\ \cdot \\ F_j \\ \cdot \\ F_{M-2} \\ F_{M-1} \end{bmatrix} = \begin{bmatrix} d'_2 \\ d_3 \\ d_4 \\ \cdot \\ d_j \\ \cdot \\ d_{M-2} \\ d'_{M-1} \end{bmatrix}$$

Here, we have dropped the superscript for convenience. a_j, b_j, c_j and d_j are given by equation (4.11), non-zero values of d_j are associated with source terms or for d_1 and d_M with boundary conditions. All terms in $\mathbf{A}$ other than those shown are zero or we can write

$$\mathbf{A}\,\mathbf{F} = \mathbf{B}, \tag{4.23}$$

which can be solved by using the generalized Thomas algorithm.

The matrix $\mathbf{A}$ is typically sparse and the non-zero terms are close to the diagonal. As in our case $\mathbf{A}$ does not depend on $\mathbf{F}$, so only one step of outer iteration is required.

When the non-zero elements lie close to the main diagonal it is useful to consider variants of Gauss elimination that take advantage of the banded nature of $\mathbf{A}$.

The Thomas algorithm for solving above matrix consists of two parts:

First, the a_j coefficients have been eliminated and b_j coefficients normalized to unity. The equations are modified in a forward sweep.

The second stage consists of a backward-substitution (backward sweep).

The Thomas algorithm is particularly economical; it requires only 5M-4 operations (multiplications and divisions). But to prevent ill-conditioning it is necessary that $|b_j| > |a_j| + |c_j|$.

4.2 Numerical Discussion

Equation (4.11) has been solved by using a modified Crank Nicolson implicit formulation with forward time and central difference space approximation using 100 grid points ($\xi = 10$) for sufficient accuracy when the case of suction or no porosity is considered but for the case of blowing 1000 grid points ($\xi = 100$) are used. For all computations we have taken $h = .1$. For the case $\alpha = 0, \beta = 0$ we get solution for the Newtonian fluid, and results match with the analytical solution with very small relative error.

Figures (4.1 - 4.8) show $\frac{f}{\Omega l}$ and $\frac{g}{\Omega l}$ at different values of ξ for varying time corresponding to three types of flows (Newtonian, second grade and third grade), with and without suction and magnetic parameter. Results described below report solutions up to $\xi = 6$, where free stream velocities have not yet been reached in most cases. We observed that; initially fluid moves with the disk, so the magnitude of $\frac{f}{\Omega l}$ is large near the disk. With time the magnitude of $\frac{f}{\Omega l}$ decreases and then increases to become stable that can be observed in figure (4.1), which shows the effect of time on Newtonian fluid. At time $\tau = .5$ the magnitude of $\frac{f}{\Omega l}$ is relatively large and the magnitude of $\frac{g}{\Omega l}$ is small. After that $\frac{f}{\Omega l}$ decreases in its magnitude with time and then increases to become stable after $\tau = 10$, while $\frac{g}{\Omega l}$ keeps on increasing and then becomes stable. Boundary layer thickness increases with time and steady state approaches after $\tau = 10$.

Figure (4.2) illustrates the effect of time on $\frac{f}{\Omega l}$ and $\frac{g}{\Omega l}$ and boundary layer thickness due to second grade fluid i. e. when $\alpha \neq 0$. By introducing $\alpha = 1$ at the begining i. e. at $\tau = .5$, fluid adjacent to disk moves with the disk and $\frac{f}{\Omega l}$ and $\frac{g}{\Omega l}$ are very high. With time the values of $\frac{f}{\Omega l}$ decreases while the values of $\frac{g}{\Omega l}$ increases and then approaches its steady state condition. For the steady state case the values of $\frac{f}{\Omega l}$ near the disk are small as compared to figure (4.1) in which $\alpha = 0$, while the values of $\frac{f}{\Omega l}$ are large and they keep on increasing with time untill steady state condition is achieved. Boundary layer thickness increases with α. Time taken to reach steady state is larger as compared to its time for Newtonian fluid.

Figure (4.3) shows the effect of time on $\frac{f}{\Omega l}$ and $\frac{g}{\Omega l}$ for the third grade fluid i. e. $\alpha \neq 0$, $\beta \neq 0$ and $\alpha = 1, \beta = 1$. We observe that with β the values of $\frac{f}{\Omega l}$ and $\frac{g}{\Omega l}$ near the disk decrease with the increase in time. The values of $\frac{f}{\Omega l}$ decrease near the disk but increase at small distance away from the disk and then decrease to become free stream. Time τ also increases to approach its steady state condition. Boundary layer thickness increases with the increase in time in third grade fluid.

By introducing suction in Newtonian fluid there is a considerable decrease in boundary layer thickness and steady state is achieved quickly i. e. after $\tau = .5$, which can be observed from figure (4.4).

The effect of suction on second grade fluid is shown in figure (4.5). Boundary layer thickness decreases due to suction but in comparison with the Newtonian fluid its value is high and steady state is achieved after $\tau = 2$. It means that α increases the boundary layer thickness and also time to approach its steady state.

In third grade fluid i. e., for $\alpha = 1, \beta = 1$, boundary layer thickness increases a little as compared to the results of second grade fluid. Its steady state approaches after $\tau = 2$. This shows that the effect of suction is prominent here and inclusion of β doesn't have much effect on values of $\frac{f}{\Omega l}$ and $\frac{g}{\Omega l}$ as shown in figure (4.6).

Figure (4.7) represents the effect of suction and magnetic parameter on viscous fluid. Boundary layer thickness decreases further as compared to figure (4.4) and steady state is achieved before $\tau = .5$

The effect of suction and magnetic parameter on the second grade fluid is shown in figure (4.8). Boundary layer thickness decreases while comparing with the case of second grade fluid when only suction is present (figure (4.5)) or the case where suction or magnetic parameter, both are absent (figure (4.2)) and becomes steady state very quickly i. e. at $\tau = .5$

When we proceed from Newtonian fluid to non-Newtonian fluid the effect of α and β can be observed in figures (4.9 – 4.19). In figure (4.9) the effect of α in steady state condition is presented. We observe that the boundary layer thickness increases with the increase in α. Also the magnitudes of $\frac{f}{\Omega l}$ and $\frac{g}{\Omega l}$ increase with the increase in α.

Boundary layer thickness increases further in the presence of β. By increasing β boundary layer thickness increases. The values of $\frac{f}{\Omega l}$ and $\frac{g}{\Omega l}$ near the disk become smaller due to β and their magnitude decreases with the increase in β which is shown in figure (4.13).

In the presence of suction parameter boundary layer thickness decreases and the magnitudes of $\frac{f}{\Omega l}$ and $\frac{g}{\Omega l}$ also decrease in a considerable amount but with the increase in α, boundary layer thickness increases and the value of $\frac{f}{\Omega l}$ is decreased further while $\frac{g}{\Omega l}$ increases with the increase in α, which can be depicted in figure (4.10). In the presence of suction and magnetic parameter boundary layer thickness decreases further. The effect of N on $\frac{g}{\Omega l}$ is more prominent as compared to its effect on $\dfrac{f}{\Omega l}$ as shown in figure (4.11).

Figure (4.12) depicts the effect of α in the presence of magnetic field only. Magnetic field reduces boundary layer thickness and the magnitudes of $\dfrac{f}{\Omega l}$ and $\dfrac{g}{\Omega l}$ in a considerable amount when compared with figure (4.9) (the non-magnetic case). With the increase in α boundary layer thickness increases. Also α effects the magnitudes of $\dfrac{f}{\Omega l}$ and $\dfrac{g}{\Omega l}$.

Figure (4.13) shows the effect of β on the boundary layer thickness and the magnitudes of $\dfrac{f}{\Omega l}$ and $\dfrac{g}{\Omega l}$. Boundary layer thickness is increased with the increase in β and magnitudes of $\dfrac{f}{\Omega l}$ and $\dfrac{g}{\Omega l}$ decrease.

The effect of β in the presence of magnetic parameter on boundary layer thickness and on $\dfrac{f}{\Omega l}$ and $\dfrac{g}{\Omega l}$ is shown in figure (4.14).

The effect of β in the presence of suction velocity on boundary layer thickness and on $\dfrac{f}{\Omega l}$ and $\dfrac{g}{\Omega l}$ is shown in figure (4.15). Boundary layer thickness and magnitudes of $\dfrac{f}{\Omega l}$ and $\dfrac{g}{\Omega l}$ increased with β but considerably reduced as compared to the case when suction is absent (figure (4.13)).

The effect of β in the presence of suction and magnetic field is shown in figure (4.16). Boundary layer thickness and the magnitudes of $\dfrac{f}{\Omega l}$ and $\dfrac{g}{\Omega l}$ reduced due to suction velocity and magnetic parameter but boundary layer thickness is increased due to β and $\dfrac{f}{\Omega l}$ and $\dfrac{g}{\Omega l}$ decreased due to the increase in β.

When magnetic parameter is induced boundary layer thickness is reduced drastically. Figure (4.17) shows the effect of β. Magnetic effect is so dominant that blowing and variation in β is negligible.

Figure (4.18) represents the effect of β in the presence of blowing. Boundary layer thickness increases drastically when compared to suction (see figure (4.15)), without suction (see figure (4.13)) and approaches free stream at a very large distance from the disk.

Keeping $\beta = 1$, the effect on boundary layer thickness for different α's in the presence of blowing is shown in figure (4.19).

Chapter 5

MHD Flow of a Third Grade Fluid Induced by Non-Coaxial Rotations of a Porous Disk Executing Non-Torsional Oscillations and a Fluid at Infinity

In this chapter, the analysis of chapter 4 is extended to the case of oscillating disk. The oscillatory flow plays an important role in many engineering applications. The study on the flow of a semi-infinite incompressible fluid caused by the oscillation of a disk is not only of fundamental theoretical interest but it also occurs in many contexts of applied problems such as in acoustic streaming around an oscillating body. Another example is boundary layer with an imposed fluctuation in the free stream velocity. Since the flow is incompressible, it is immaterial whether the plate oscillates or the fluid oscillates. Unsteady problem of this type has practical importance in shock-tube applications. One of the fundamental solutions of such unsteady flow was presented by Stokes [63]; it is concerned with the flow of a Newtonian fluid near an oscillating plate. Lighthill [64] studied the effects of free stream oscillations on the boundary layer flow of a viscous, incompressible fluid past an infinite plate. Turbatu et al. [65] generalized the fluid flow problem of an oscillating plate in two directions. They discussed first the oscillating porous plate with superimposed blowing or suction. The second generalization is concerned with increasing or decreasing velocity amplitude of the oscillating plate. More recently, Erdogan [66] discussed the flow of a viscous fluid produced by a plane boundary oscillating with a sinusoidal variation in its own plane. In another paper Erdogan [67] considered non-coaxial rotations of a porous disk executing sinusoidal oscillation and a fluid at infinity.

In this chapter, numerical solution of the time-dependent non-linear partial differential equation for the magnetohydrodynamic incompressible flow due to non-coaxial rotations of a porous disk and a third grade fluid at infinity is given. Additionally, the disk is executing oscillations in its own plane. The solutions for three cases when the angular velocity is greater than the frequency of oscillation or it is smaller than the frequency or it is equal to the frequency are examined. The structure of the velocity distributions and the associated boundary layers are investigated including the case of blowing and resonant oscillations. Many known results are recovered as the special cases of the attempted problems.

5.1 Governing Equations

In this section, the geometry of the problem is the same as in previous chapter except that now the disk is performing oscillations. Therefore, the governing partial differential is (4.6) with the following initial and boundary conditions

$$
\left.\begin{array}{ll}
u = & \begin{array}{c} -\Omega y + U cosmt \\ \text{or} \\ -\Omega y + U sinmt \end{array}
\end{array}\right\}, \quad v = \Omega x, \qquad \text{at} \quad z = 0, \qquad t > 0,
$$

$$
\begin{array}{llll}
u = -\Omega(y - l), & v = \Omega x, & \text{as} \quad z \to \infty, & \text{for all } t, \\
u = -\Omega(y - l), & v = \Omega x, & \text{at} \quad t = 0, & \text{for} \quad z > 0,
\end{array}
\tag{5.1}
$$

where m is the frequency of the non-torsional oscillations and U the reference velocity.

In terms of F, the governing initial-boundary value problem can be written as

$$
\begin{aligned}
\alpha \frac{\partial^3 F}{\partial \tau \partial \xi^2} &- \alpha\epsilon \frac{\partial^3 F}{\partial \xi^3} + (1 - i\alpha) \frac{\partial^2 F}{\partial \xi^2} + 2\epsilon \frac{\partial F}{\partial \xi} \\
&- 2\frac{\partial F}{\partial \tau} - 2(i + N)F + \beta \frac{\partial}{\partial \xi} \left[\left(\frac{\partial F}{\partial \xi} \right)^2 \frac{\partial \bar{F}}{\partial \xi} \right] = 0,
\end{aligned}
\tag{5.2}
$$

$$
\begin{aligned}
F(0, \tau) &= U_\circ \cos mt - 1, \qquad \text{or} \qquad F(0, \tau) = U_\circ \sin mt - 1, \\
F(\infty, \tau) &= 0, \qquad\qquad\qquad\qquad\qquad F(\xi, 0) = 0.
\end{aligned}
\tag{5.3}
$$

We are now interested to solve the above initial-boundary value problem. For that we follow the same numerical techniques as in the chapter 4. In order to avoid repetition, the details of the numerical method is omitted and the governing initial-boundary value problem consist of equation (4.11) with coefficients defined as (4.12) with initial-boundary conditions

$$F_1^{n+1} = U_\circ \cos m^*\tau - 1, \quad \text{or} \quad F_1^{n+1} = U_\circ \sin m^*\tau - 1,$$

$$F_M^{n+1} = 0, \qquad F_j^1 = 0, \quad j = 1, 2, 3, \cdots, M \quad (5.4)$$

where $m^* = \dfrac{m}{\Omega}$

5.2 Numerical Discussion

Equation(5.2) with boundary and initial conditions (5.3) has been solved by using a modified Crank Nicolson implicit formulation with forward time and central difference space approximation using 100 grid points ($\xi = 10$) for sufficient accuracy. For all computations we have taken $h = .1$ and $\Delta\tau = .001$. For the case $\alpha = 0, \beta = 0$ we get solution for the Newtonian fluid, and results matched with the analytical solution [67]. Numerical solutions confirm that for large times the starting solutions tend to the steady-state solutions. For some times after the initiation of motion, the velocity field contain transients then these transients disappear and steady state is achieved.

The time required to attain steady flow for the cosine and sine oscillations is obtained for $m > \Omega$, $m = \Omega$ and $m < \Omega$. The value of this time for cosine oscillation is shorter than that for sine oscillation and it depends on the ratio of the frequency of oscillation to the angular velocity of the disk $\dfrac{m}{\Omega}$ and the ratio $\dfrac{U}{\Omega l}$.

In the case of $m > \Omega$, the oscillation of the disk dominates, then the time required to attain steady flow both for the cosine and sine oscillations becomes very short. However, in the case of $m < \Omega$ the time required to attain steady flow for the sine oscillation become large.

Numerically, we have computed the magnitudes of $\dfrac{f}{\Omega l}$ and $\dfrac{g}{\Omega l}$ with the distance from the disk for cosine and sine oscillations keeping amplitude constant $\dfrac{U}{\Omega l} = 4$ at

$\frac{m}{\Omega} = .5, 1, 2, 5$ with varying time corresponding to three types of flows (Newtonian, second grade and third grade), with and without suction. The full lines denote starting velocities and dotted lines show steady-state velocities. Results described below report solutions up to $\xi = 2$, where free stream velocities have not yet been reached in most cases.

For Newtonian fluids, we observed that without oscillations steady state is achieved after $\tau = 10$. When cosine or sine oscillations are introduced, time to reach steady state is reduced.

With the cosine oscillations, when suction ($\epsilon = 2$) is introduced, its value is reduced further and boundary layer thickness is also reduced due to suction. Magnitudes of $\frac{f}{\Omega l}$ also reduced but the magnitudes of $\frac{g}{\Omega l}$ near the disk are increased due to suction.

When only disk is rotating then time to reach its steady state is $\tau = 10$. Introducing cosine oscillation $\frac{m}{\Omega} = .5 < 1$ this time is reduced to $\tau = 5$, and for sine oscillation its values is 7. For $\frac{m}{\Omega} = 2 > 1$ due to cosine oscillation the value of τ when we get steady-state is 4.5 while for the sine oscillation its value is 5.5. For $\frac{m}{\Omega} = 5 > 1$ system with cosine oscillation approaches to its steady-state at $\tau = 2$ and for system with sine oscillation the value is $\tau = 3$ (By introducing oscillations time to reach steady-state is reduced. This time is shorter for cosine oscillations as compared to sine oscillations). No oscillatory behavior can be observed for the Newtonian fluids with and without suction.

For the second grade fluid ($\alpha \neq 0$) time to reach steady-state is increased and also oscillatory behavior become visible in fluid velocities ($\frac{f}{\Omega l}$ and $\frac{g}{\Omega l}$). Near the disk the magnitudes of the velocities ($\frac{f}{\Omega l}$ and $\frac{g}{\Omega l}$) is also increased. Boundary layer thickness is also increased due to α.

By introducing suction ($\epsilon = 2$) in the second grade fluid, time to reach steady-state is decreased but oscillatory behavior becomes very prominent, boundary layer thickness is increased. That is to say, that the oscillatory behavior is due to both non-Newtonian fluids and suction (become visible for non-Newtonian fluid and enhanced by suction, in our case). By increasing the value of α time to reach steady state is also increased. Boundary layer thickness is also increased due to non-Newtonian nature of the fluid and oscillatory behavior.

For the third grade fluid ($\alpha \neq 0, \beta \neq 0$) time to reach steady state is delayed further but oscillatory behavior diminish when β is introduced. Inclusion of suction increases oscillatory behavior. By increasing oscillation of the disk steady state is achieved much earlier. Increasing oscillations reduces boundary layer thickness. For the third grade fluid ($\alpha \neq 0, \beta \neq 0$) time to reach steady state is increased further but due to oscillations its value is reduced. When $\frac{m}{\Omega} = .5$ steady-state is achieved at $\tau = 3$, for $\frac{m}{\Omega} = 2$ we get $\tau > .5$ and when $\frac{m}{\Omega} = 5$ its value becomes $= .3$. The time to reach steady state for the third grade fluid in the presence of cosine oscillations is reduced. In the presence of suction ($\epsilon = 2$) time to reach steady state is increased in considerable amount. When $\frac{m}{\Omega} = .5$ its value is $\tau = 5$, for $\frac{m}{\Omega} = 2$, τ becomes 4 and for $\frac{m}{\Omega} = 5$, $\tau = 1$. i. e. time to reach steady state is further delayed in the third grade fluid (when suction is applied, perhaps this is due to oscillatory behavior).

When we consider the sine oscillations then we note that the time to reach steady-state is again reduced and with the increase in oscillations the time to reach steady-state is decreased further. By introducing suction ($\epsilon = 2$) time to reach steady-state is reduced in a considerable amount. Boundary layer thickness is also reduced. The magnitude of $\frac{f}{\Omega l}$ is reduced by suction while the magnitude of $\frac{g}{\Omega l}$ are increased near the disk.

For the second grade fluid the time to reach steady-state is increased. Oscillatory behavior can be seen near the disk. The magnitude of $\frac{f}{\Omega l}$ and $\frac{g}{\Omega l}$ near the disk is increased. Boundary layer thickness is also increased for the second grade fluid.

When suction is applied to the second grade fluid oscillatory behavior becomes prominent and can be seen up to considerable distance from the disk. Boundary layer thickness is increased due to this oscillatory behavior. Time to reach steady-state is reduced. For $m > \Omega$ boundary layer thickness is also reduced but oscillatory behavior is prominent and with the increase in frequency the value of boundary layer thickness is reduced further.

For $\frac{m}{\Omega} = 1$ (resonant case) boundary conditions at infinity for the steady case are not met when fluid is Newtonian or non-Newtonian. When suction is applied then condition at infinity is fulfilled but for blowing, the condition at infinity is not satisfied. If we consider electrically conducting fluid then boundary condition at infinity is also satisfied for blowing and resonance. It is likely that the magnetic field provides some mechanism to control the growth of the boundary layer thickness at the resonant frequency.

Concluding Remarks

From the graphs we observe that suction and blowing have opposite effects on the boundary layer flows. Indeed, the suction prevents the imposed nontorsional oscillations from spreading far away from the disk by viscous diffusion for all values of the frequency parameter m. On the contrary, the blowing promotes the spreading of the oscillations far away from the disk. In the case of blowing and resonance, the oscillatory boundary layer flows are no longer possible. The most distinctive feature is that unlike the hydrodynamic situation for the case of the resonant oscillations, the solution satisfies the boundary condition at infinity for all values of the frequency parameter m, and the associated boundary layers remain bounded for all values of the frequency including the resonant frequency. The physical implication of this conclusion is that for the case of resonance and blowing, the unbounded spreading of the oscillations away from the disk is controlled by the external magnetic field.

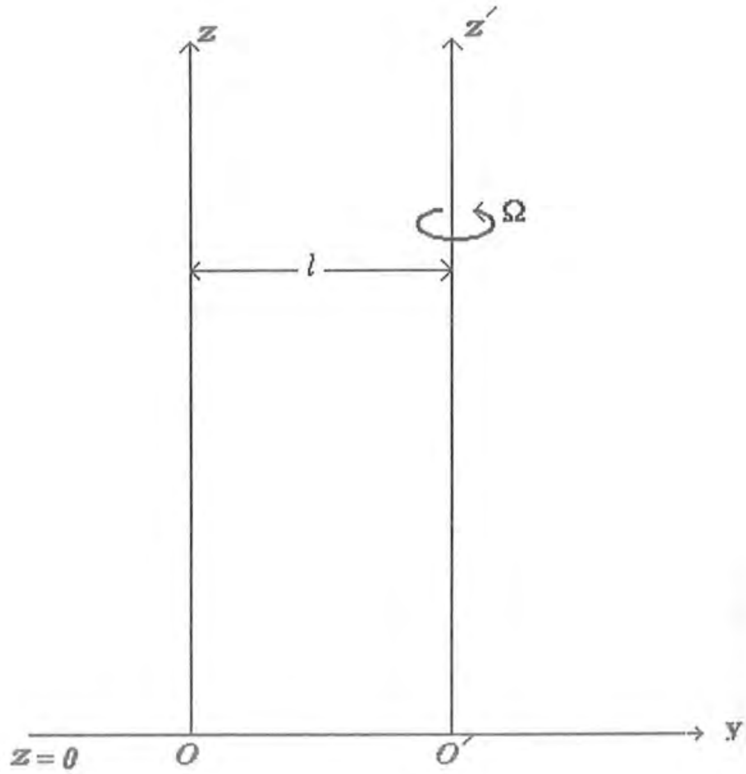

Figure 1. Flow geometry

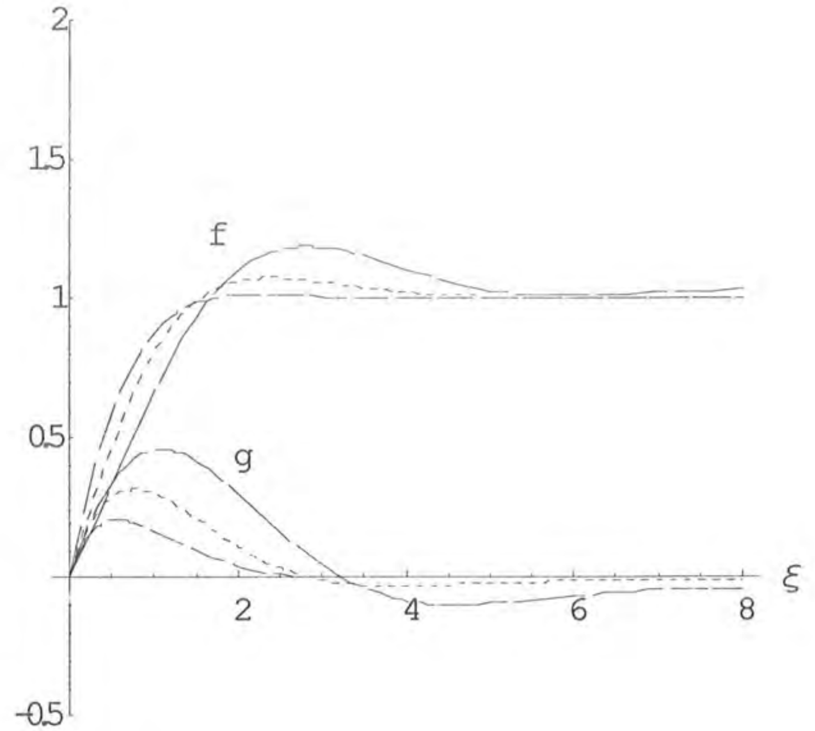

Figure 2.1 The influence of porosity in the absence of magnetic field (N=0) on f and g with ξ when τ =12, ε = -0.5 —— —— ——, ε = 0.5 — — — —, ε = 0.0 - - - - - - - -.

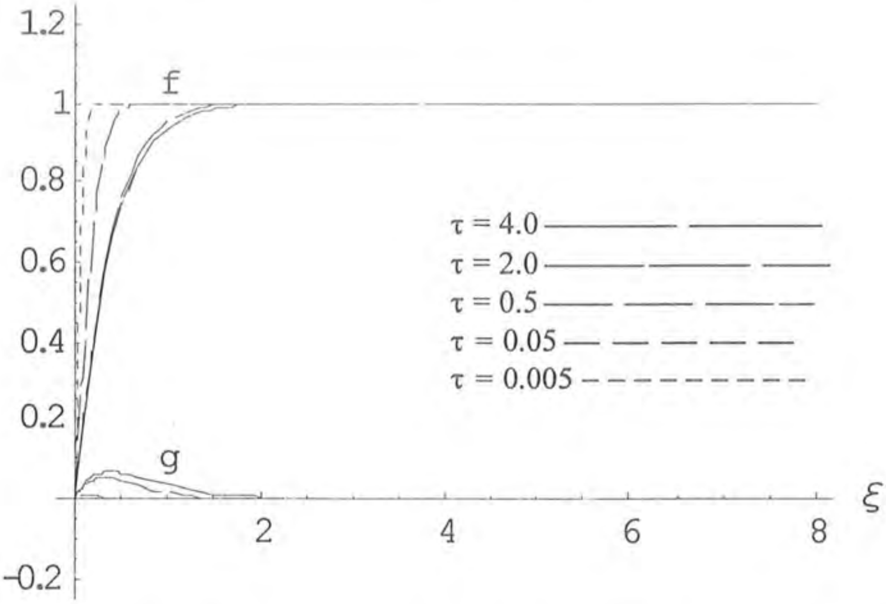

Figure 2.2 The influence of suction (ε=0.5) in the presence of magnetic field (N=2) on f and g with ξ for different values of τ

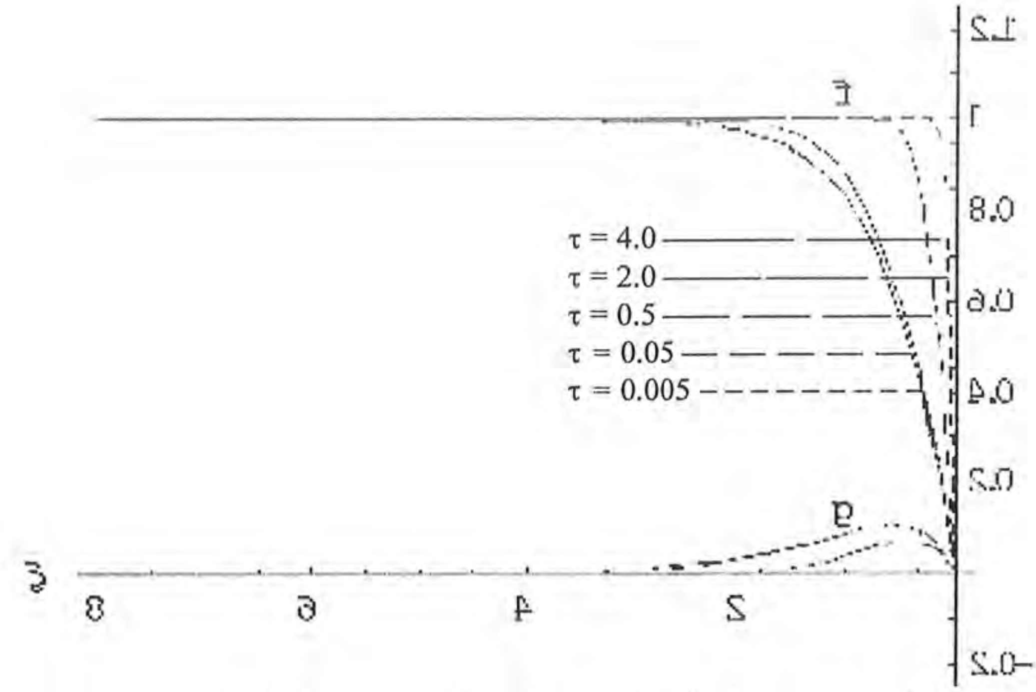

Figure 2.3 The influence of blowing (ε=-0.5) in the presence of magnetic field (N=2) on f and g with ξ for different values of τ

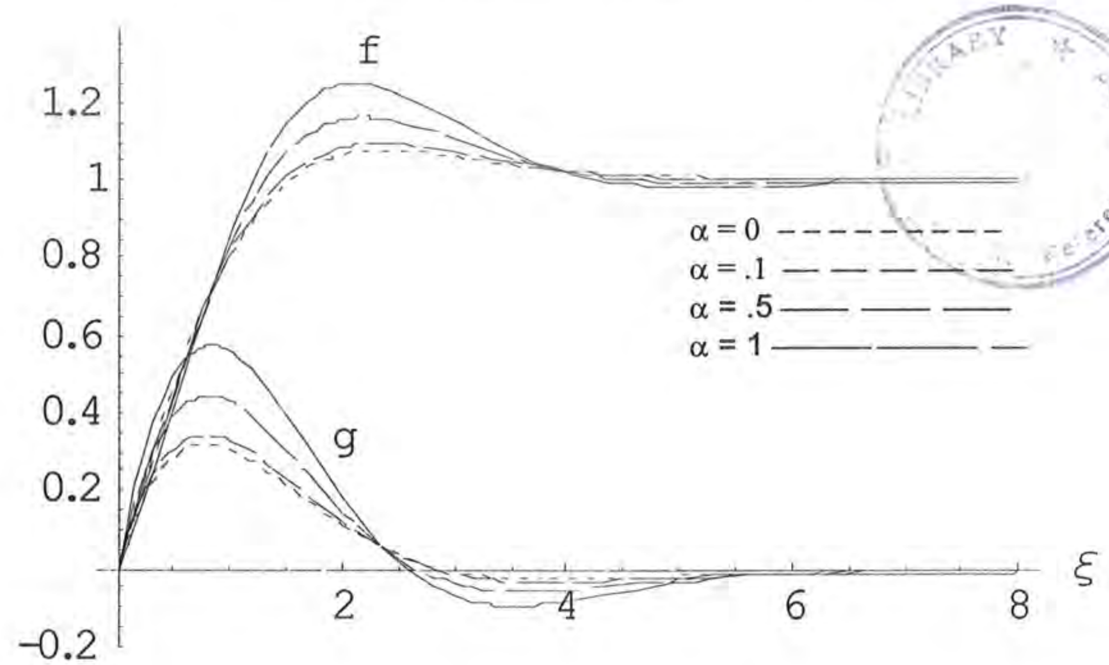

Figure 3.1 Variation in f and g with ξ for τ = 12 without suction or magnetic field for different values of α

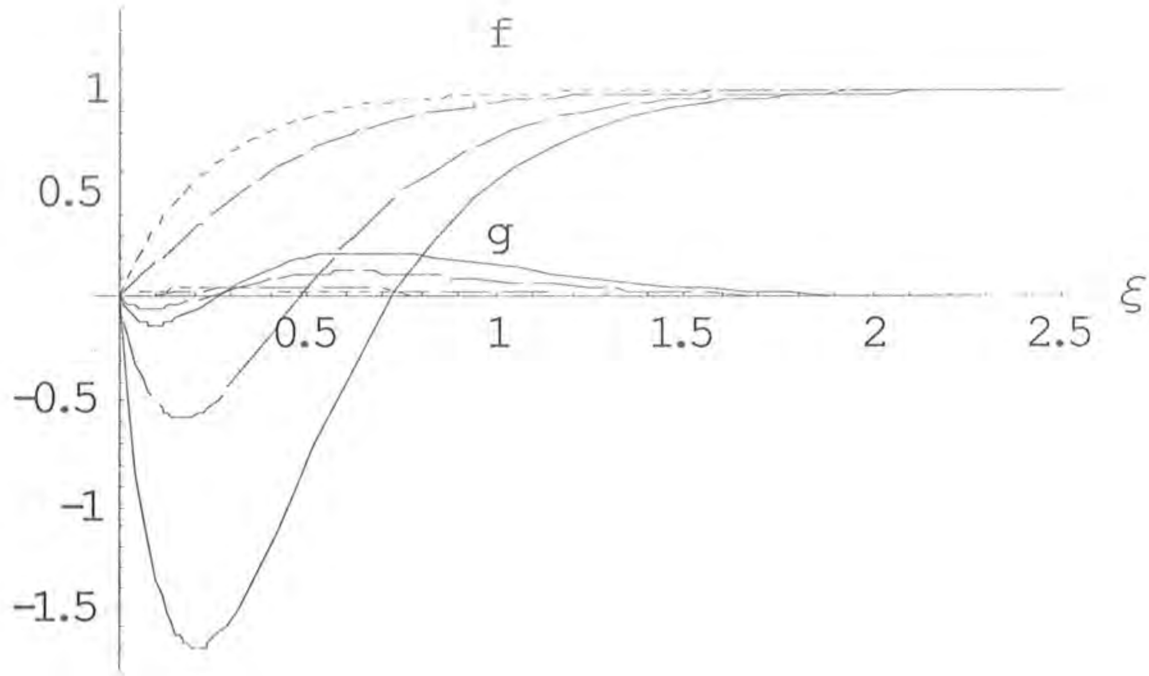

Figure 3.2 Variation in f and g with ξ for $\tau = 12$, $\varepsilon = 2$, $N = 0$ for different values of α, _ _ _ _ _ $\alpha = 0$, __ __ __ __ $\alpha = .1$, ___ ___ ___ ___ $\alpha = .5$, ___________ $\alpha = 1$

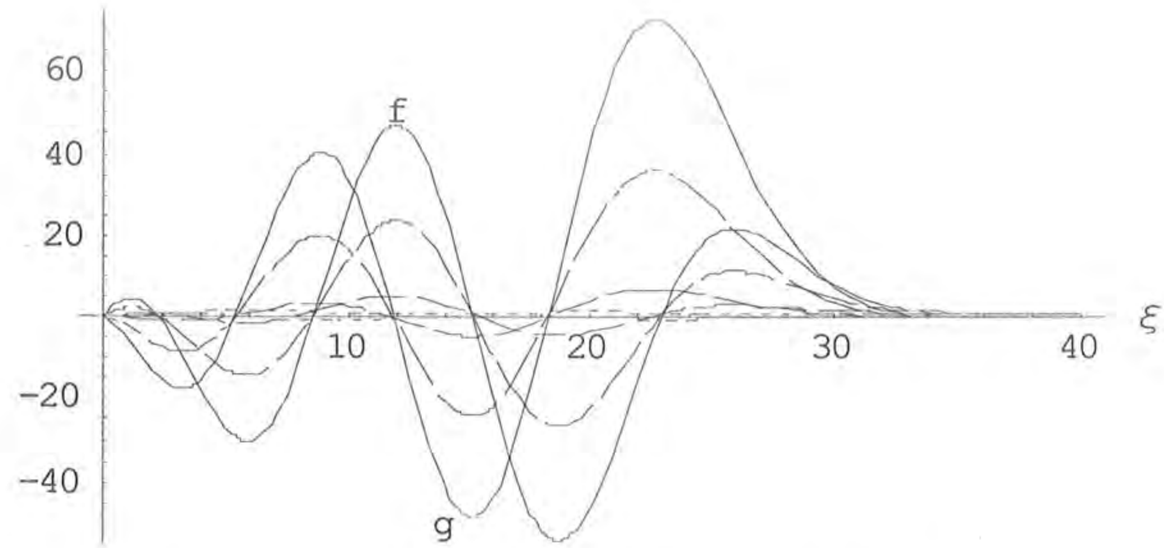

Figure 3.3 Variation in f and g with ξ for $\tau = 12$, $\varepsilon = -2$, $N = 0$ for different values of α, _ _ _ _ _ $\alpha = 0$, __ __ __ __ $\alpha = .1$, ___ ___ ___ ___ $\alpha = .5$, ___________ $\alpha = 1$.

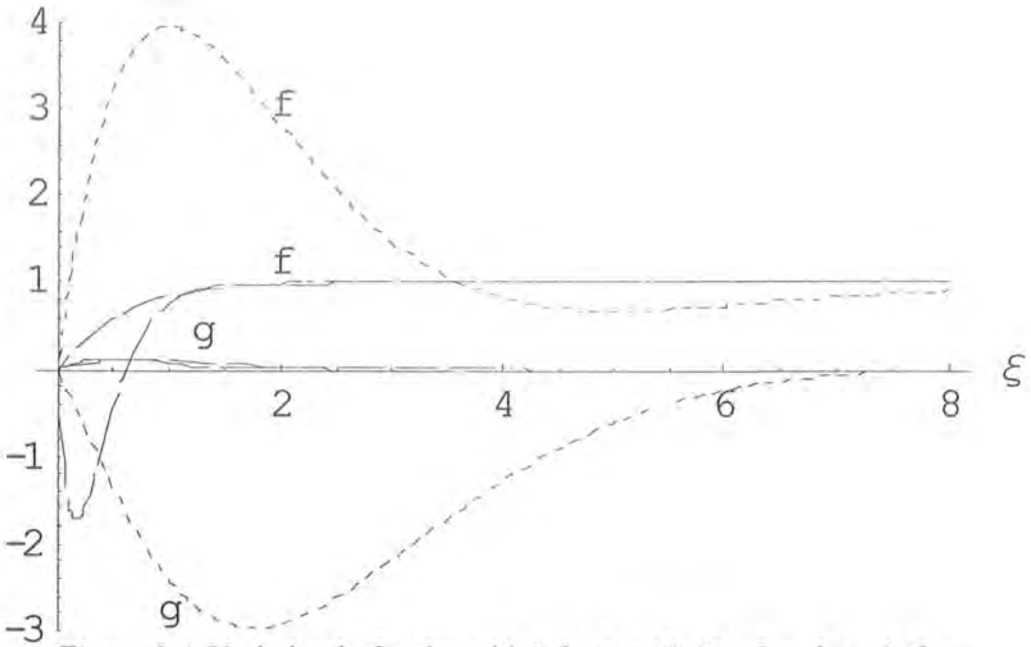

Figure 3.4 Variation in f and g with ξ for τ = 12, N = 2 and α =1 for different values of ε , _ _ _ _ _ ε = -2, ___ ___ ___ ___ ε = 0, ____________ ε = 2.

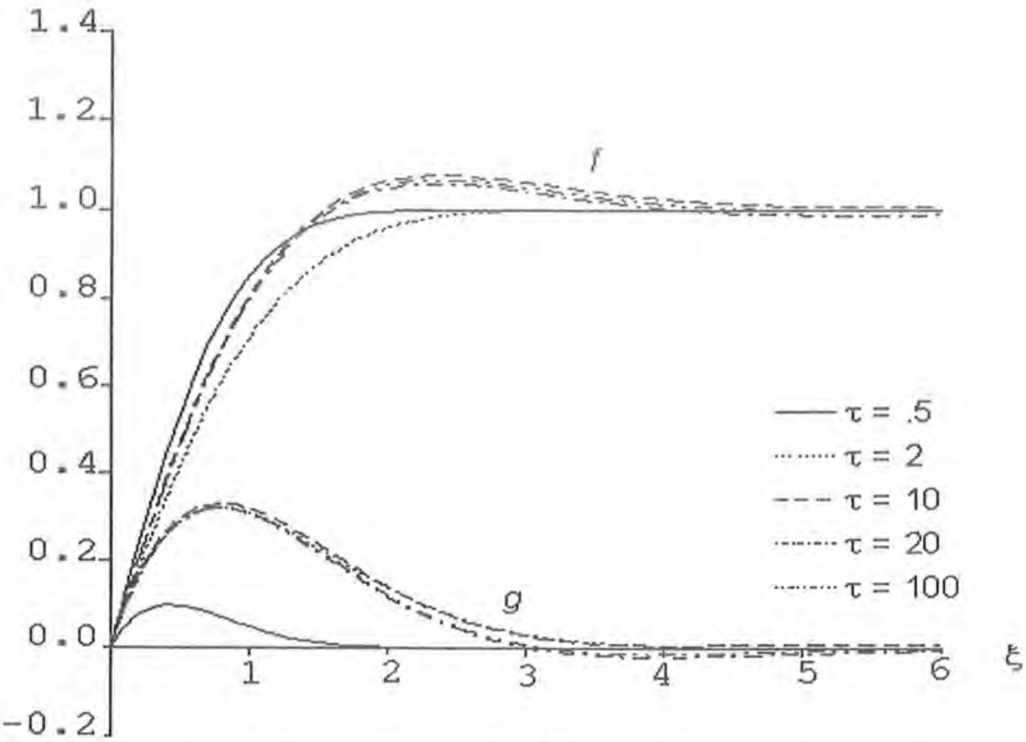

Figure 4.1 Variation in f and g with ξ for different values of τ, when α =0, β =0, ε = 0, N = 0.

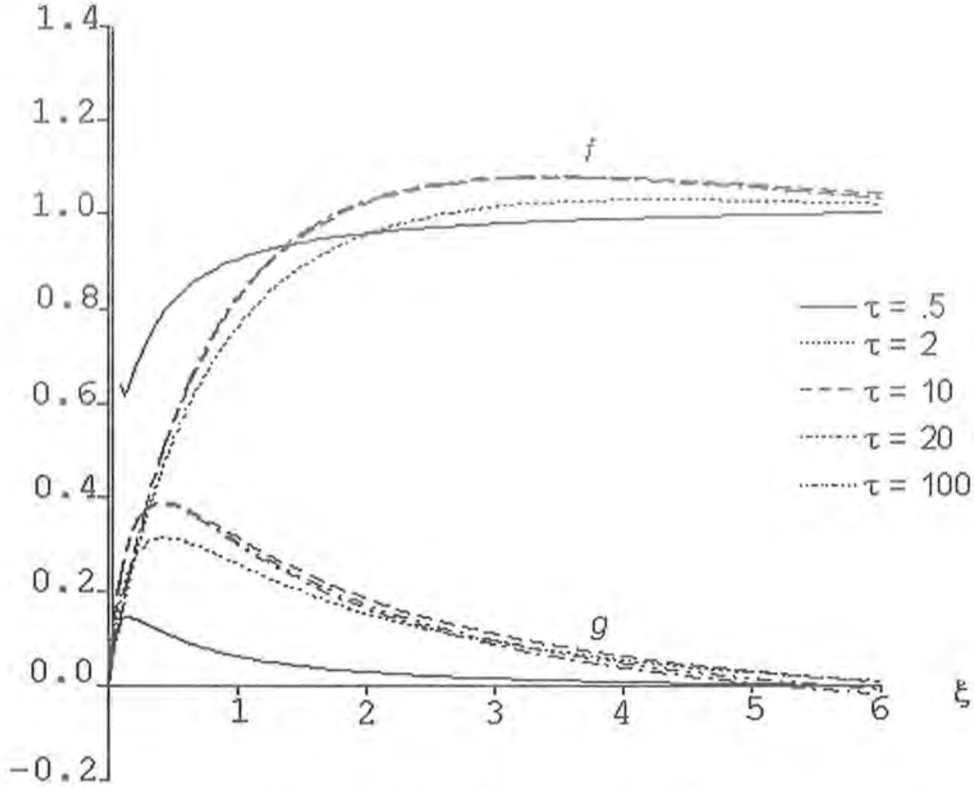

Figure 4.2 Variation in f and g with ξ for different values of τ, when $\alpha = 1$, $\beta = 0$, $\varepsilon = 0$, $N = 0$.

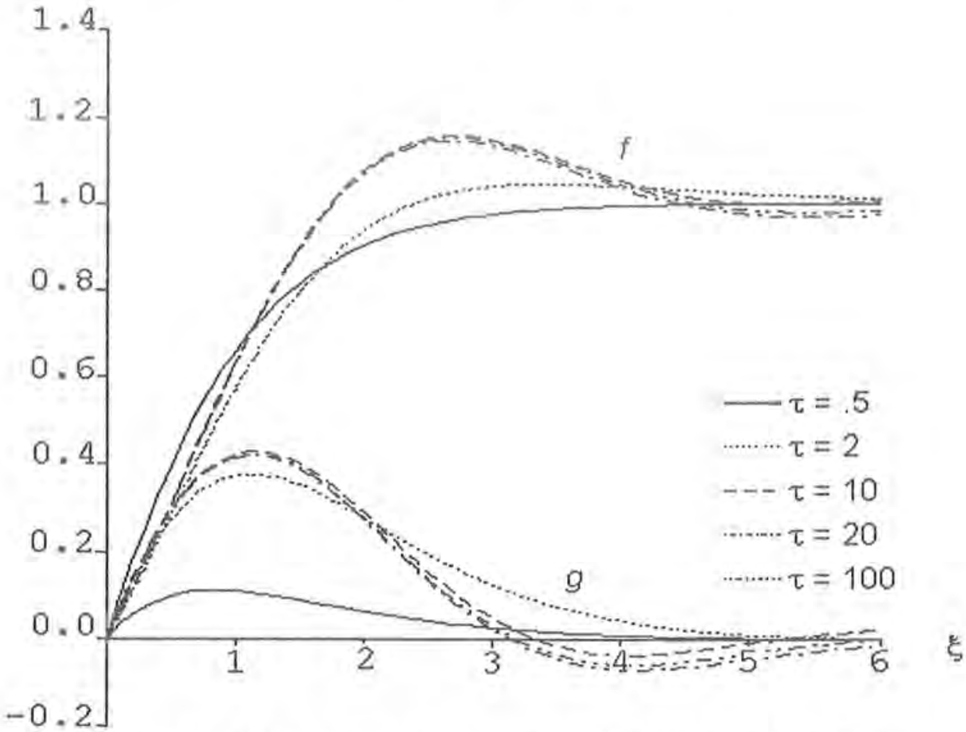

Figure 4.3 Variation in f and g with ξ for different values of τ, when $\alpha = 1$, $\beta = 1$, $\varepsilon = 0$, $N = 0$.

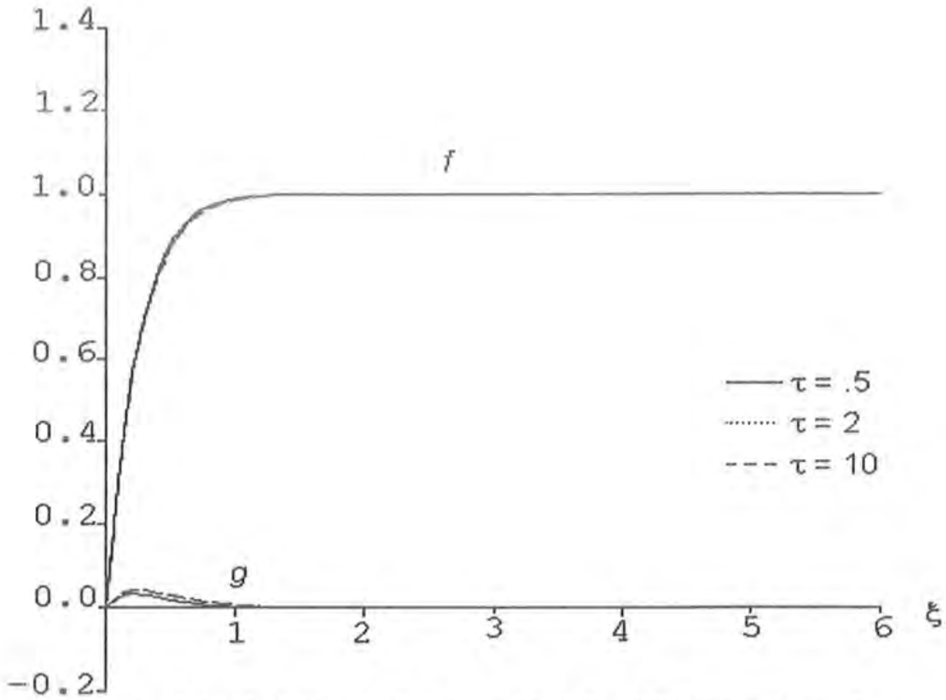

Figure 4.4 Variation in f and g with ξ for different values of τ, when $\alpha = 0$, $\beta = 0$, $\varepsilon = 2$, $N = 0$.

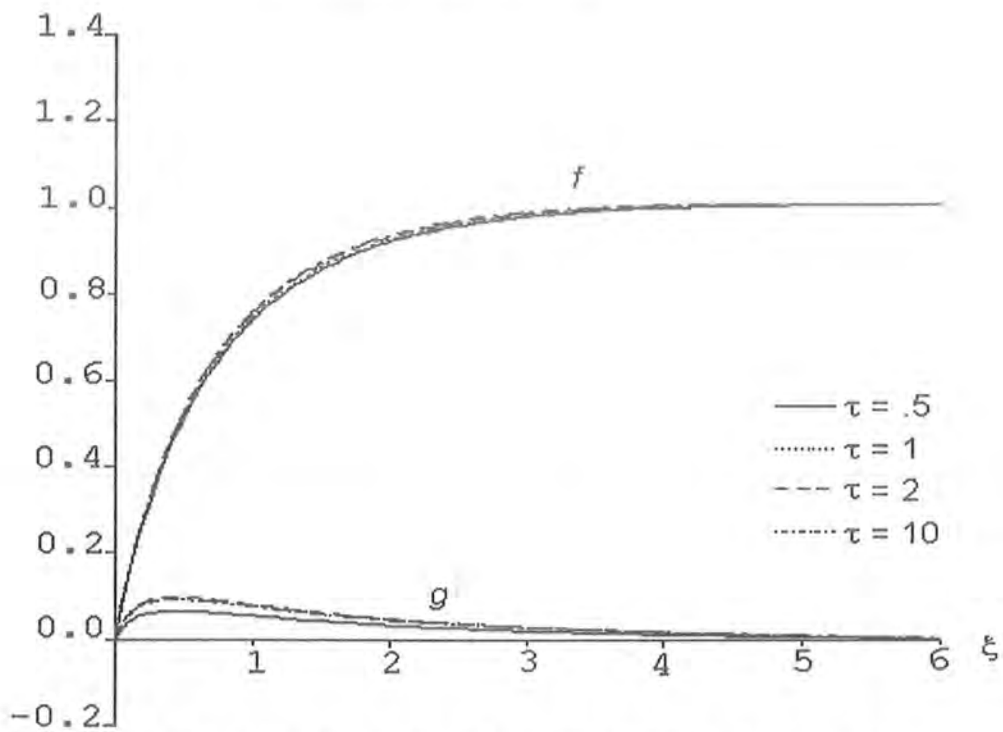

Figure 4.5 Variation in f and g with ξ for different values of τ, when $\alpha = 1$, $\beta = 0$, $\varepsilon = 2$, $N = 0$.

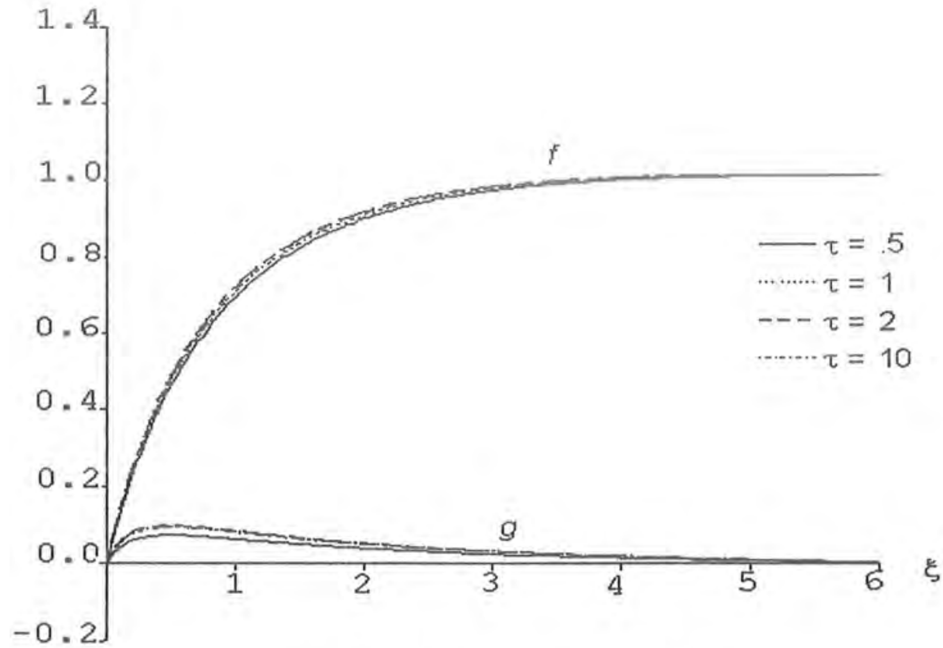

Figure 4.6 Variation in f and g with ξ for different values of τ, when $\alpha = 1$, $\beta = 1$, $\varepsilon = 2$, $N = 0$.

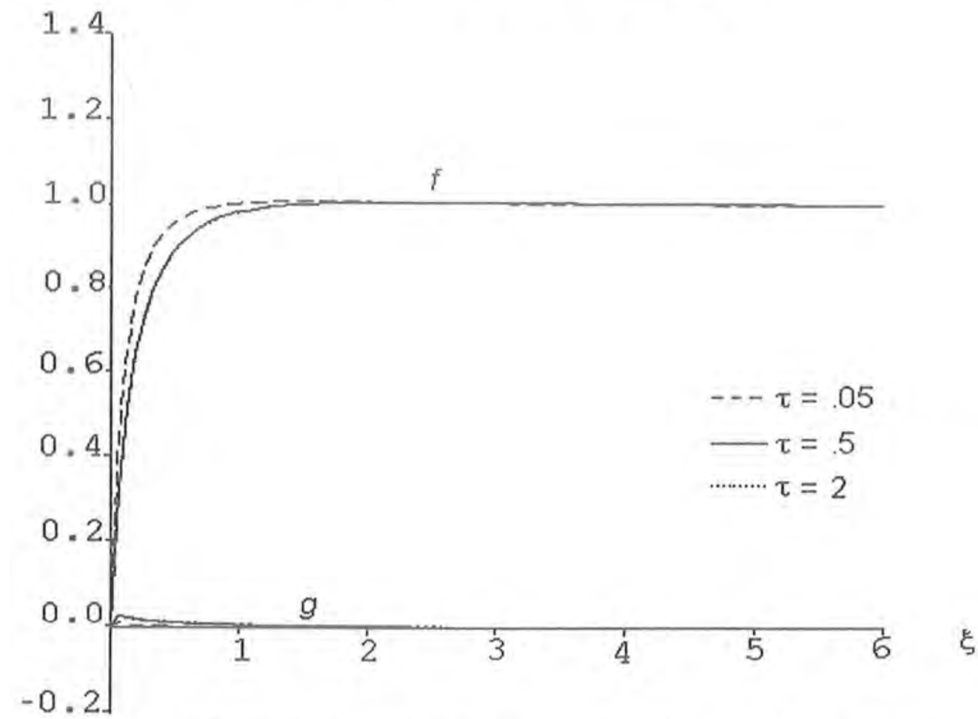

Figure 4.7 Variation in f and g with ξ for different values of τ, when $\alpha = 0$, $\beta = 0$, $\varepsilon = 2$, $N = 2$.

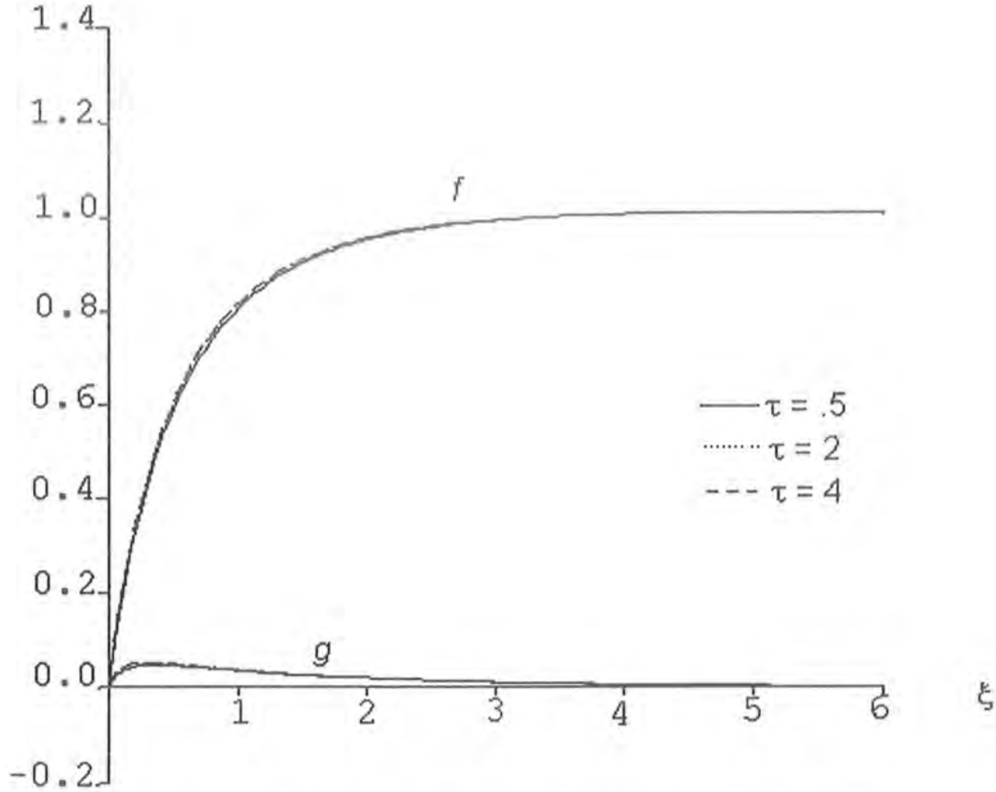

Figure 4.8 Variation in f and g with ξ for different values of τ, when $\alpha = 1$, $\beta = 0$, $\varepsilon = 2$, $N = 2$.

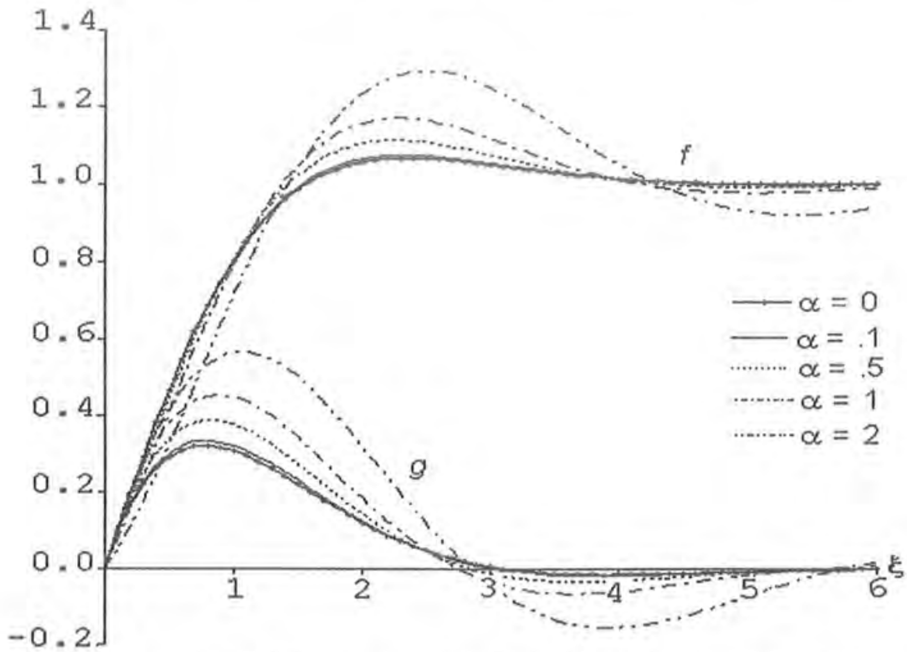

Figure 4.9 Variation in f and g with ξ when $\tau = 100$, $\beta = 0$, $\varepsilon = 0$, $N = 0$ for different values of α

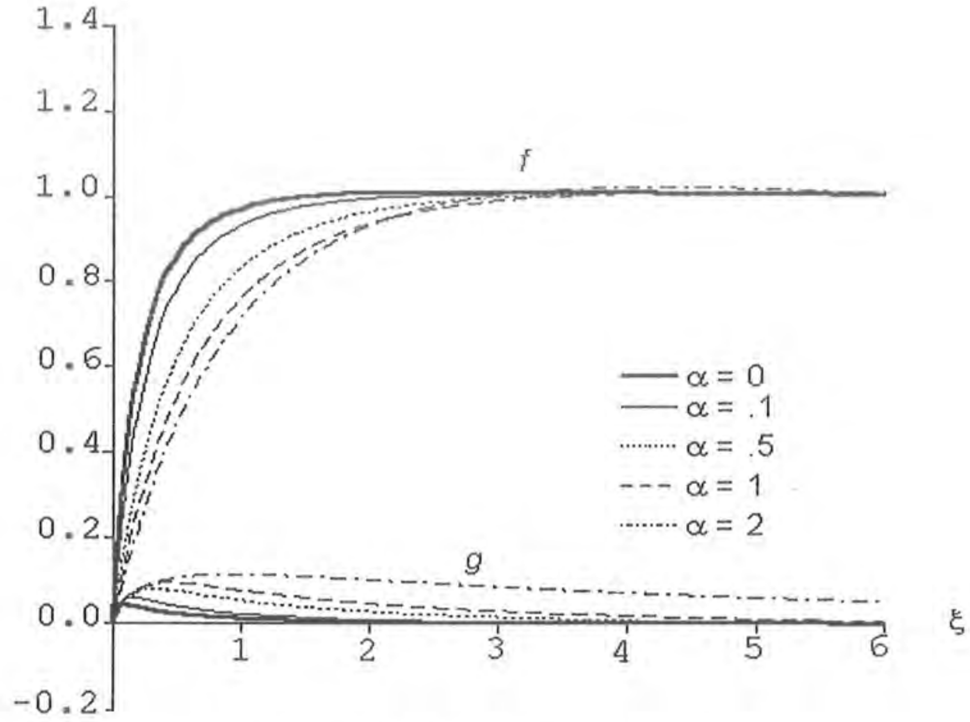

Figure 4.10 Variation in f and g with ξ when $\tau = 100$, $\beta = 0$, $\varepsilon = 2$, $N = 0$ for different values of α

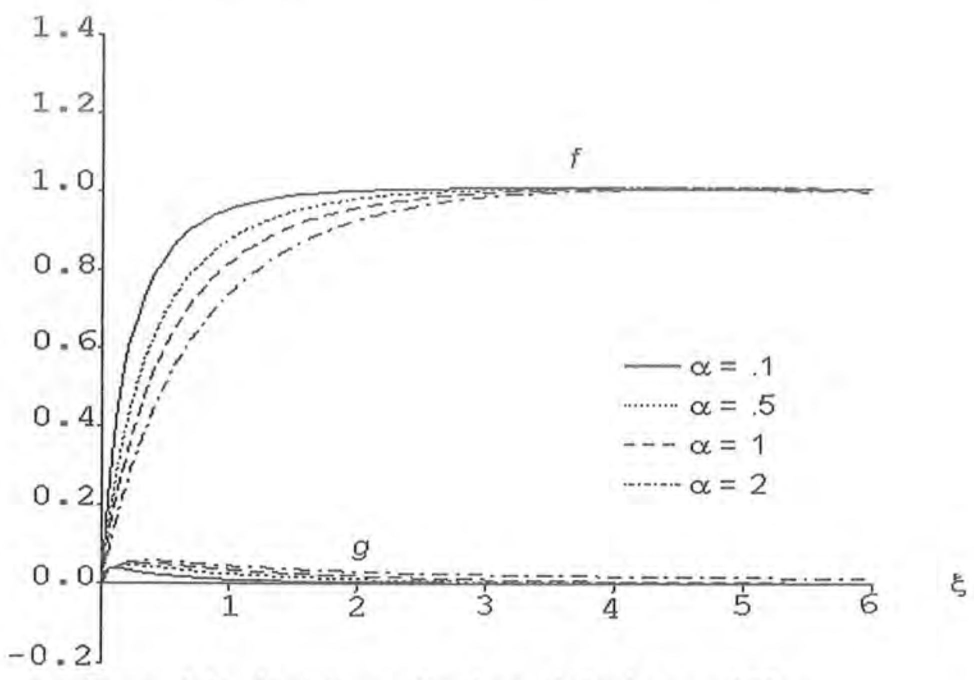

Figure 4.11 Variation in f and g with ξ when $\tau = 100$, $\beta = 0$, $\varepsilon = 2$, $N = 2$ for different values of α

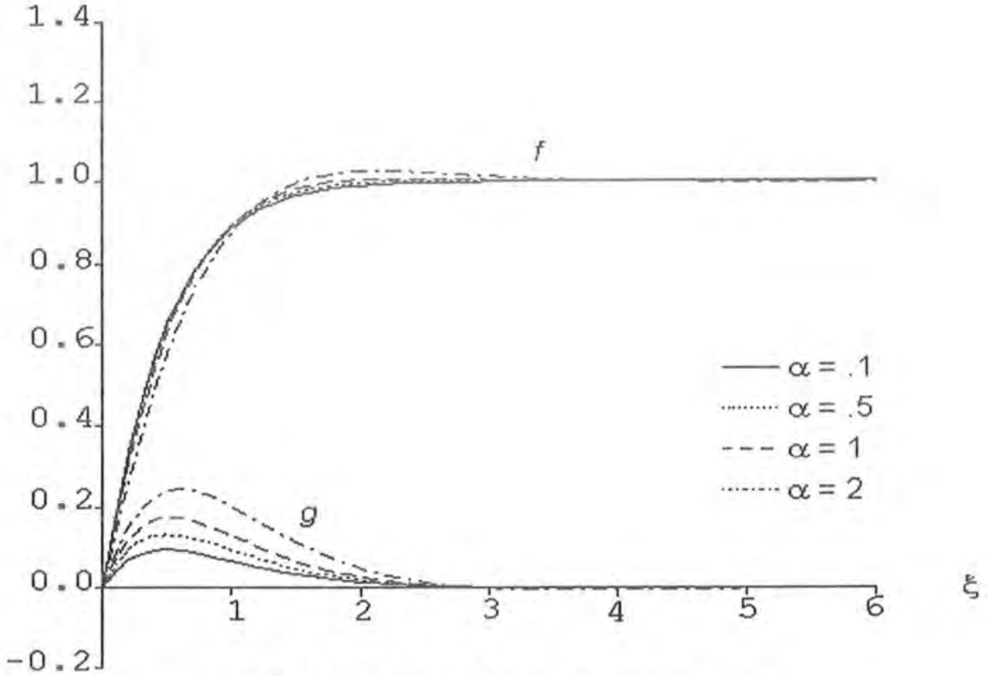

Figure 4.12 Variation in f and g with ξ when $\tau = 100$, $\beta = 0$, $\varepsilon = 0$, $N = 2$ for different values of α

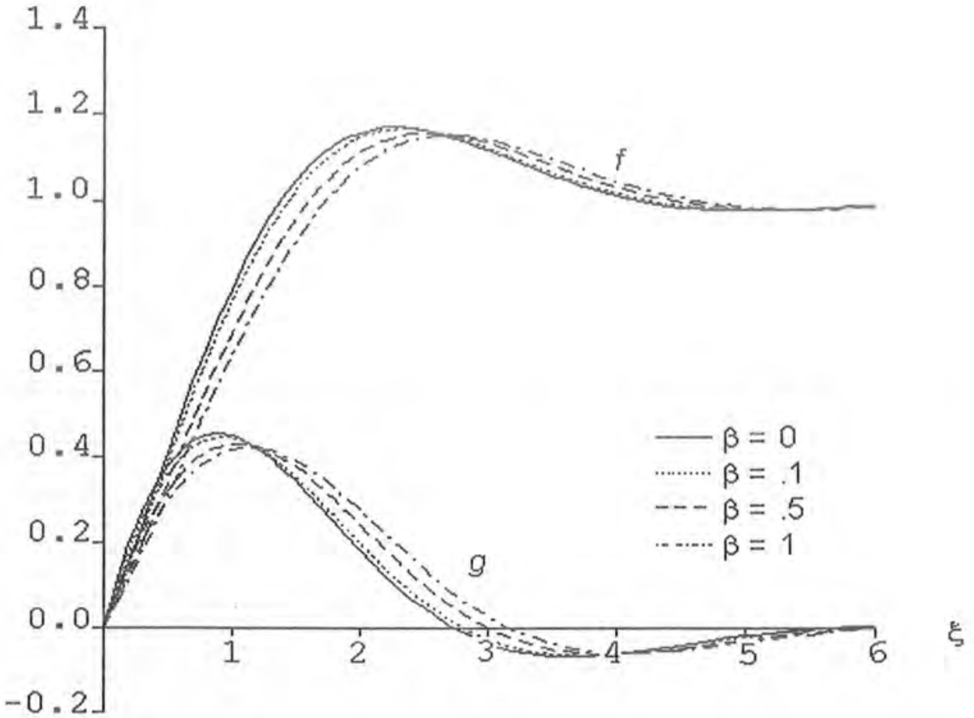

Figure 4.13 Variation in f and g with ξ when $\tau = 100$, $\alpha = 1$, $\varepsilon = 0$, $N = 0$ for different values of β

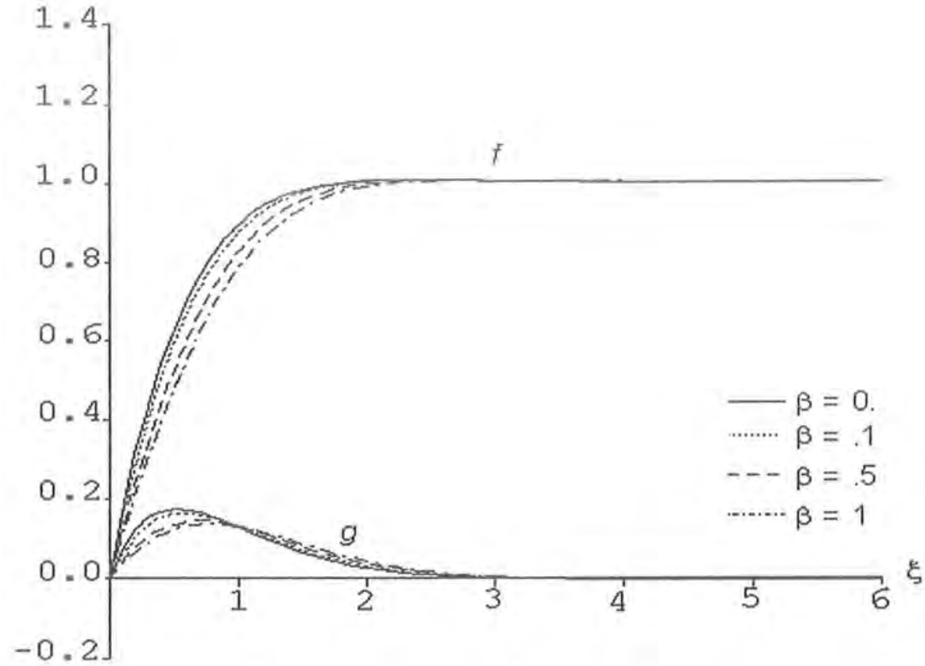

Figure 4.14 Variation in f and g with ξ when $\tau = 100$, $\alpha = 1$, $\varepsilon = 0$, $N = 2$ for different values of β

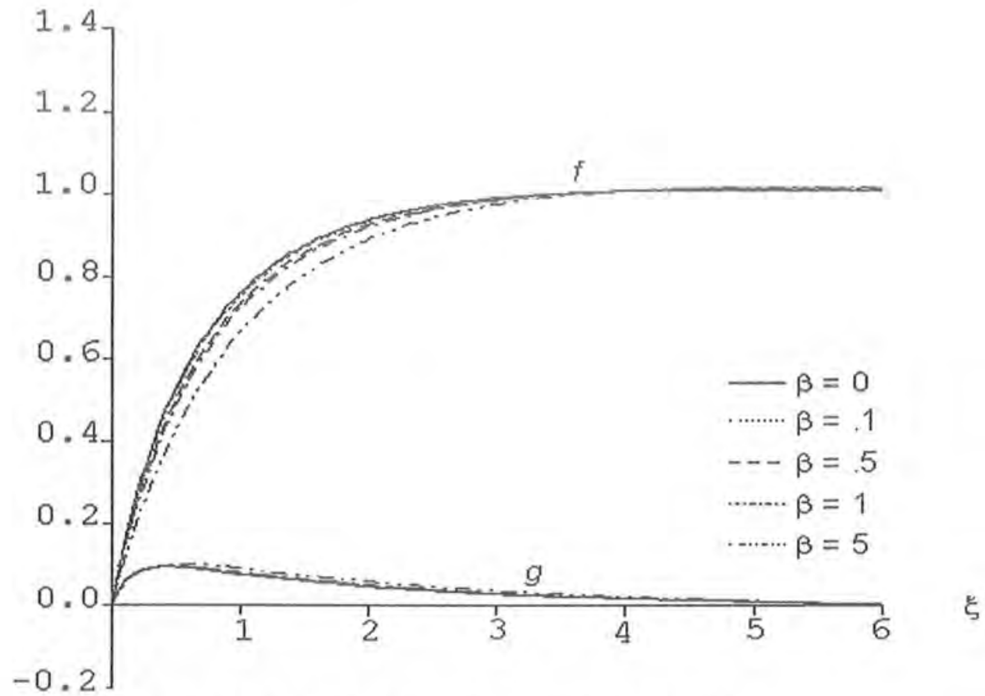

Figure 4.15 Variation in f and g with ξ when $\tau = 100$, $\alpha = 1$, $\varepsilon = 2$, $N = 0$ for different values of β

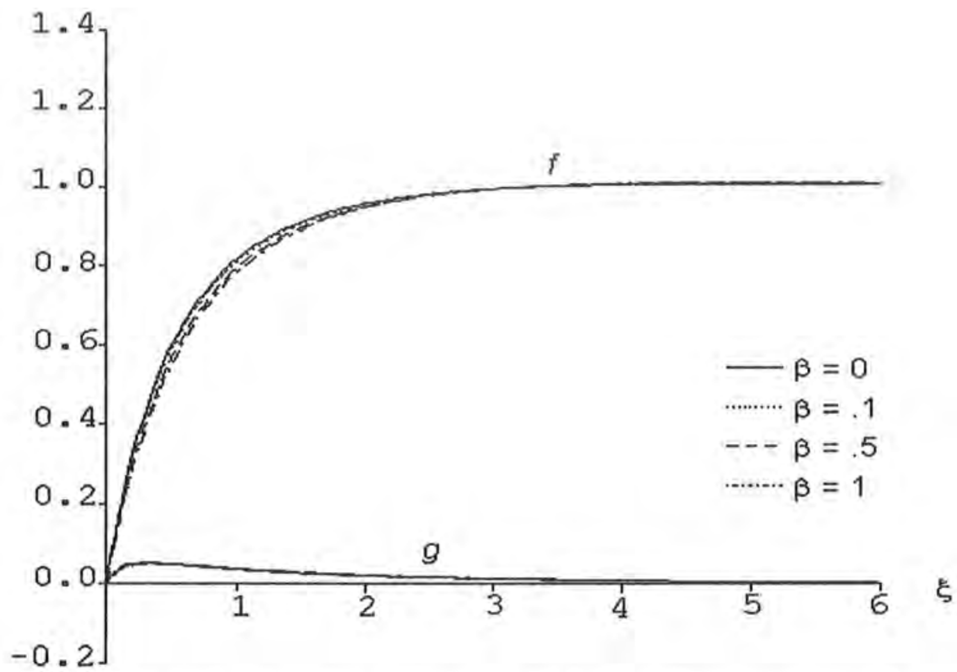

Figure 4.16 Variation in f and g with ξ for different values of β, when $\tau = 100$, $\alpha = 1$, $\varepsilon = 2$, $N = 2$

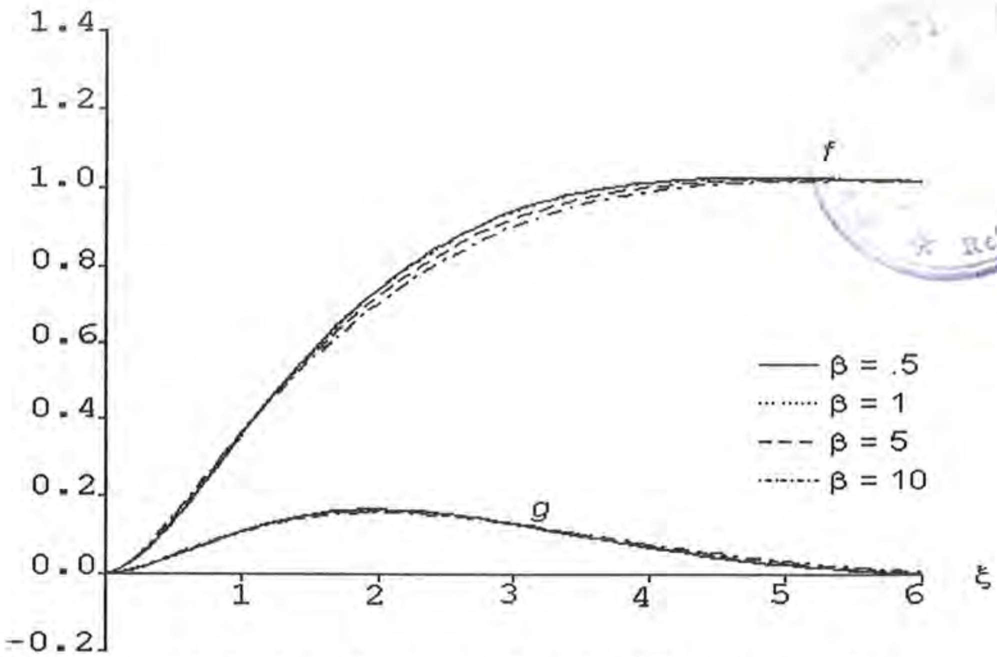

Figure 4.17 Variation in f and g with ξ for different values of β, when $\tau = 100$, $\alpha = 1$, $\varepsilon = -2$, $N = 2$

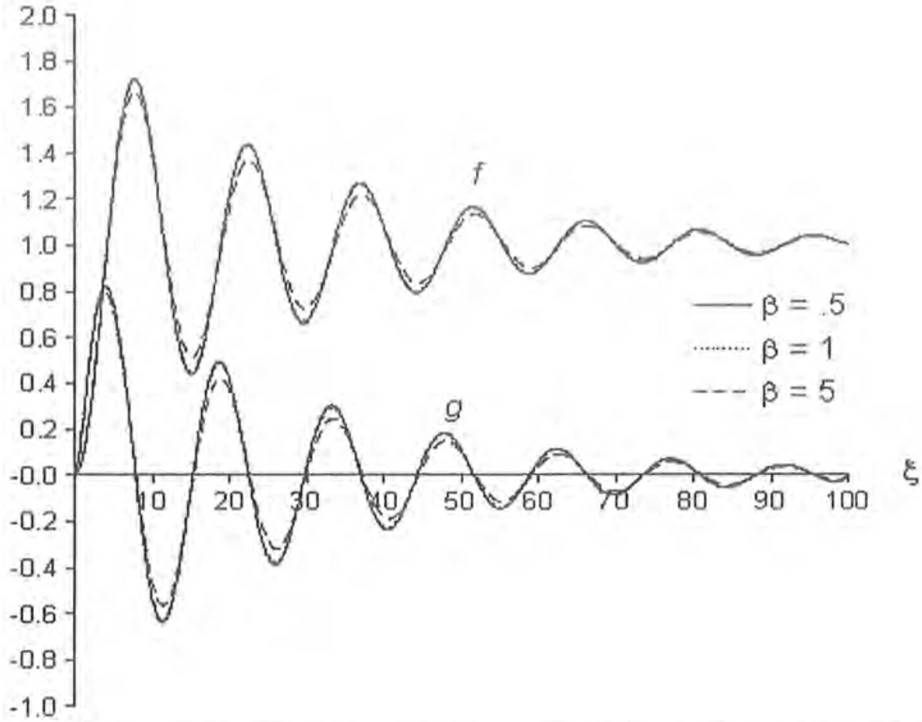

Figure 4.18 Variation in f and g with ξ for different values of β, when τ = 100, α = 1, ε = -2, N = 0

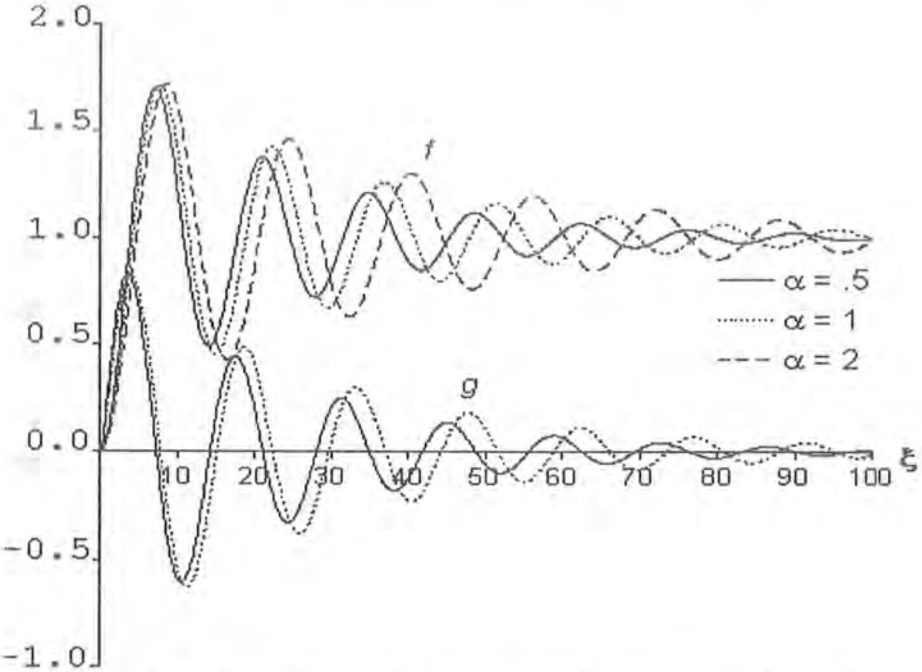

Figure 4.19 Variation in f and g with ξ for different values of α, when τ = 100, β = 1, ε = -2, N = 0

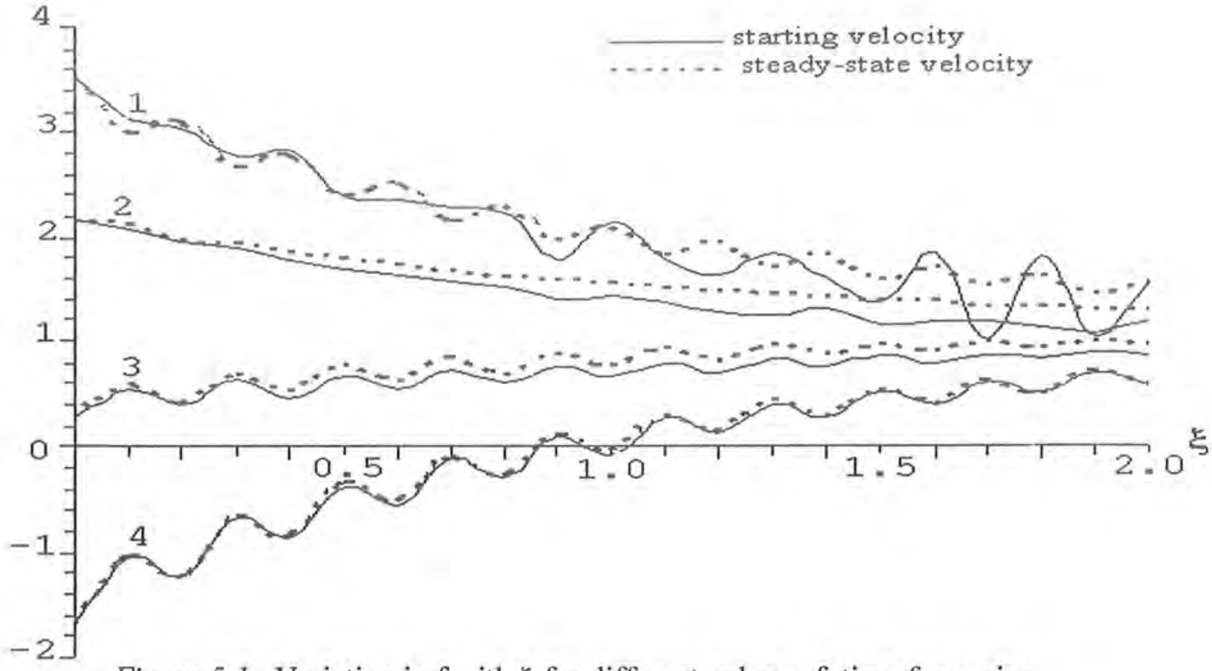

Figure 5.1 Variation in f with ξ for different values of time for cosine oscillation at $U/\Omega l = 4$, $n/\Omega = .5$, $\varepsilon = 2$, $\alpha = 2$, $\beta = 0$, $N = 0$

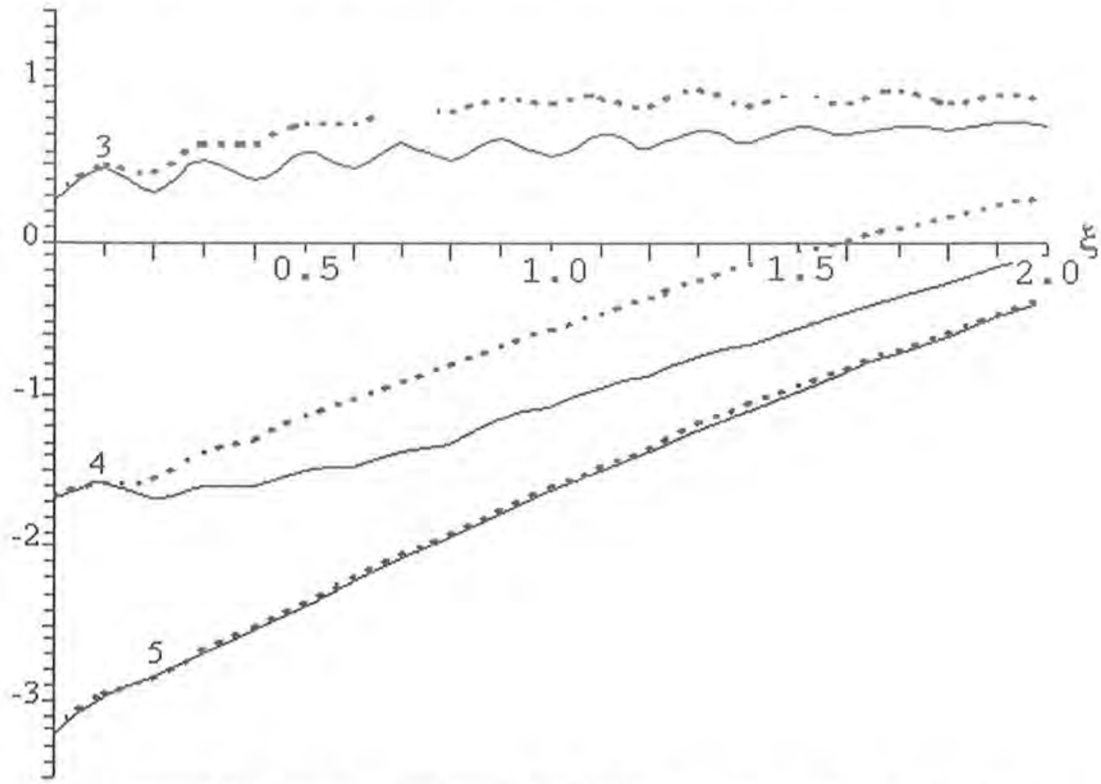

Figure 5.2 Variation in f with ξ for different values of time for cosine oscillation at $U/\Omega l = 4$, $n/\Omega = .5$, $\varepsilon = 2$, $\alpha = 2$, $\beta = 5$, $N = 0$

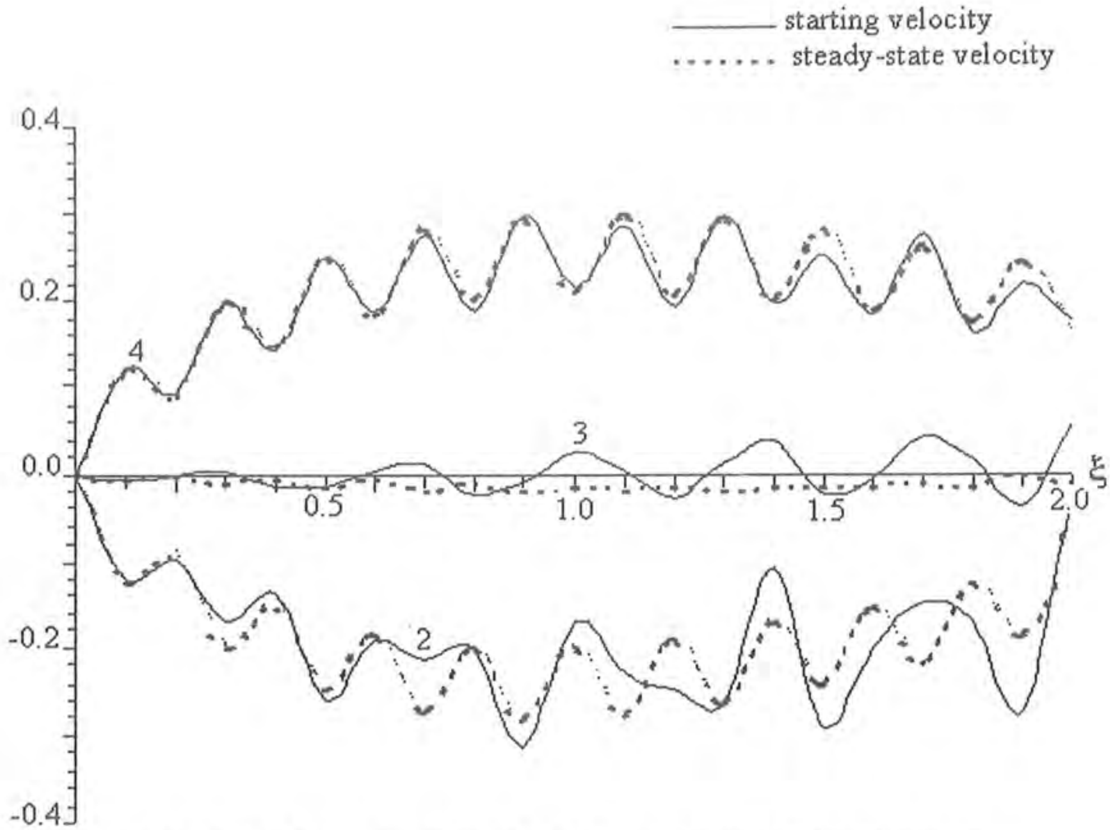

Figure 5.3 Variation in g with ξ for different values of time for cosine oscillation at $U/\Omega l = 4$, $n/\Omega = .5$, $\varepsilon = 2$, $\alpha = 2$, $\beta = 0$, $N = 0$

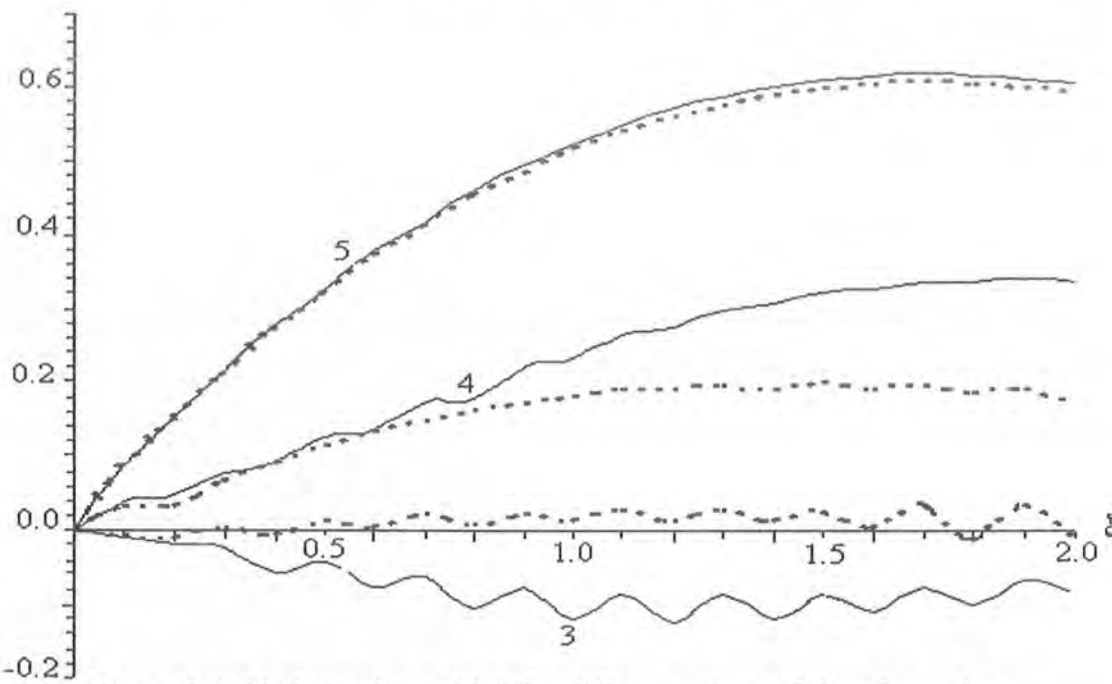

Figure 5.4 Variation in g with ξ for different values of time for cosine oscillation at $U/\Omega l = 4$, $n/\Omega = .5$, $\varepsilon = 2$, $\alpha = 2$, $\beta = 5$, $N = 0$

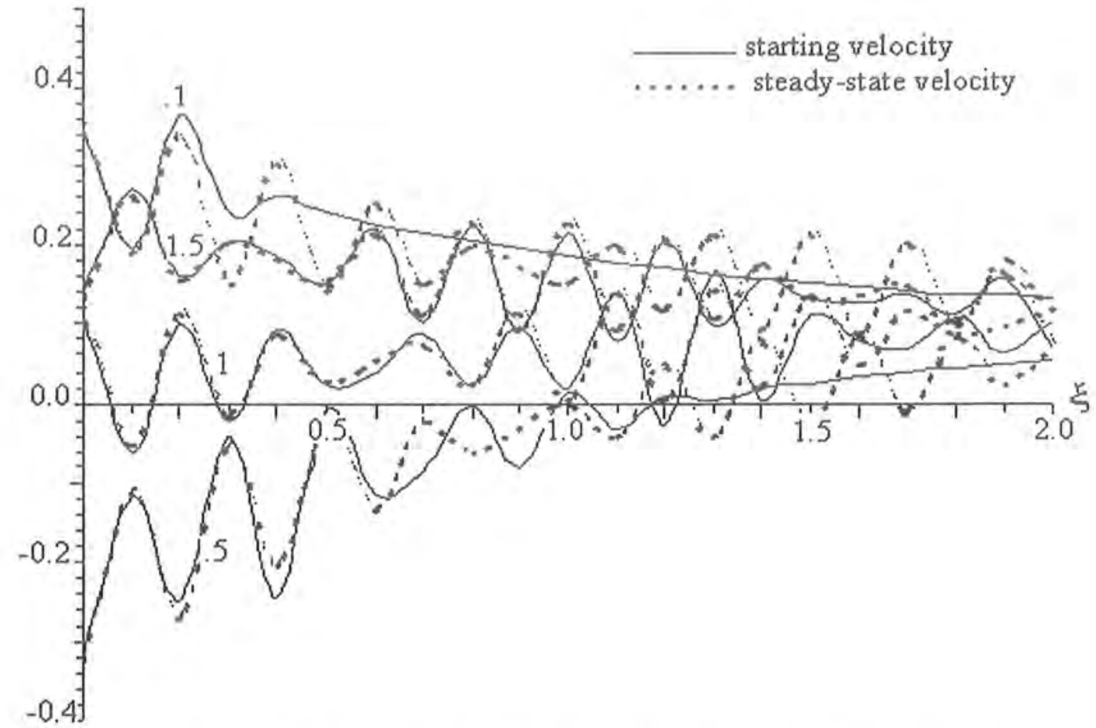

Figure 5.5 Variation in f with ξ for different values of time for cosine oscillation at $U/\Omega l = 4$, $n/\Omega = 5$, $\varepsilon = 2$, $\alpha = 2$, $\beta = 0$, $N = 0$

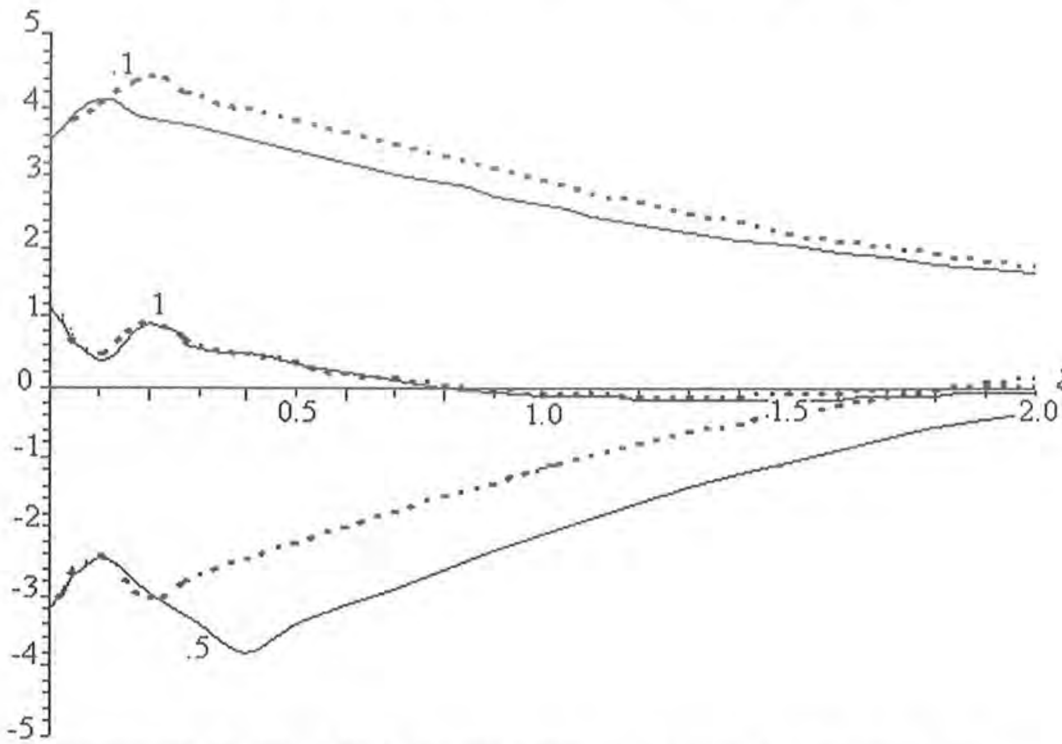

Figure 5.6 Variation in f with ξ for different values of time for cosine oscillation at $U/\Omega l = 4$, $n/\Omega = 5$, $\varepsilon = 2$, $\alpha = 2$, $\beta = 5$, $N = 0$

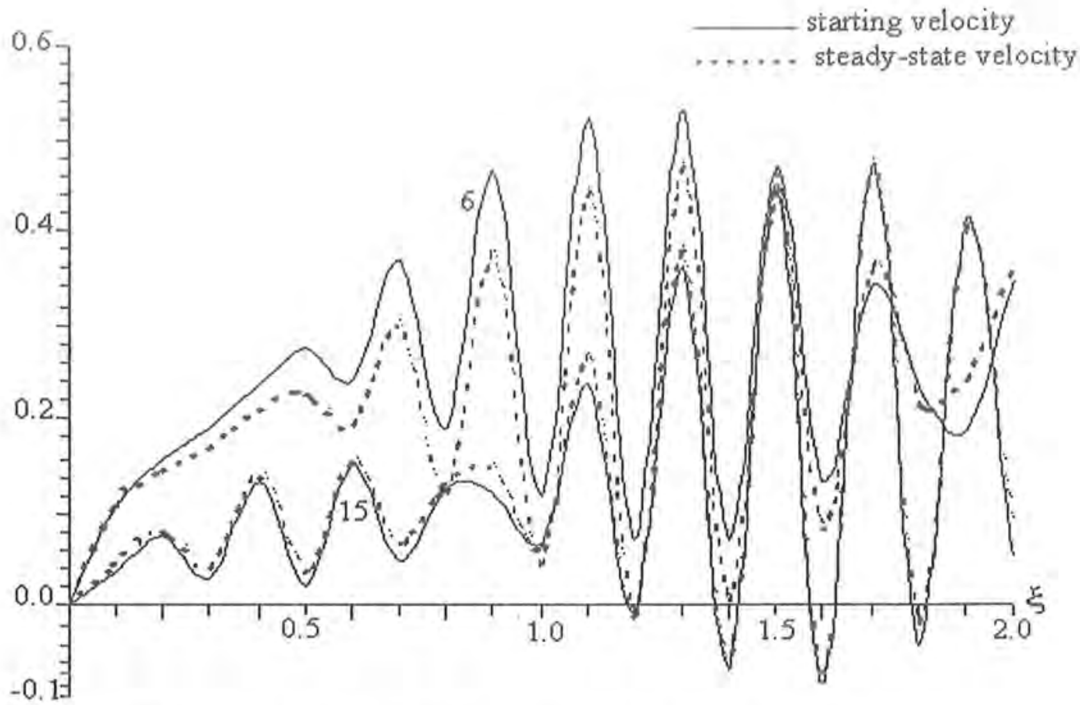

Figure 5.7 Variation in g with ξ for different values of time for cosine oscillation at U/Ωl = 4, n/Ω = 5, ε = 2, α = 2, β = 0, N = 0

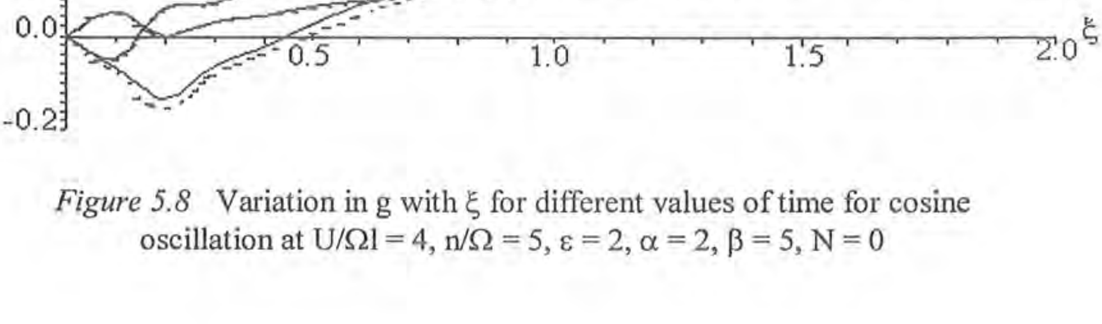

Figure 5.8 Variation in g with ξ for different values of time for cosine oscillation at U/Ωl = 4, n/Ω = 5, ε = 2, α = 2, β = 5, N = 0

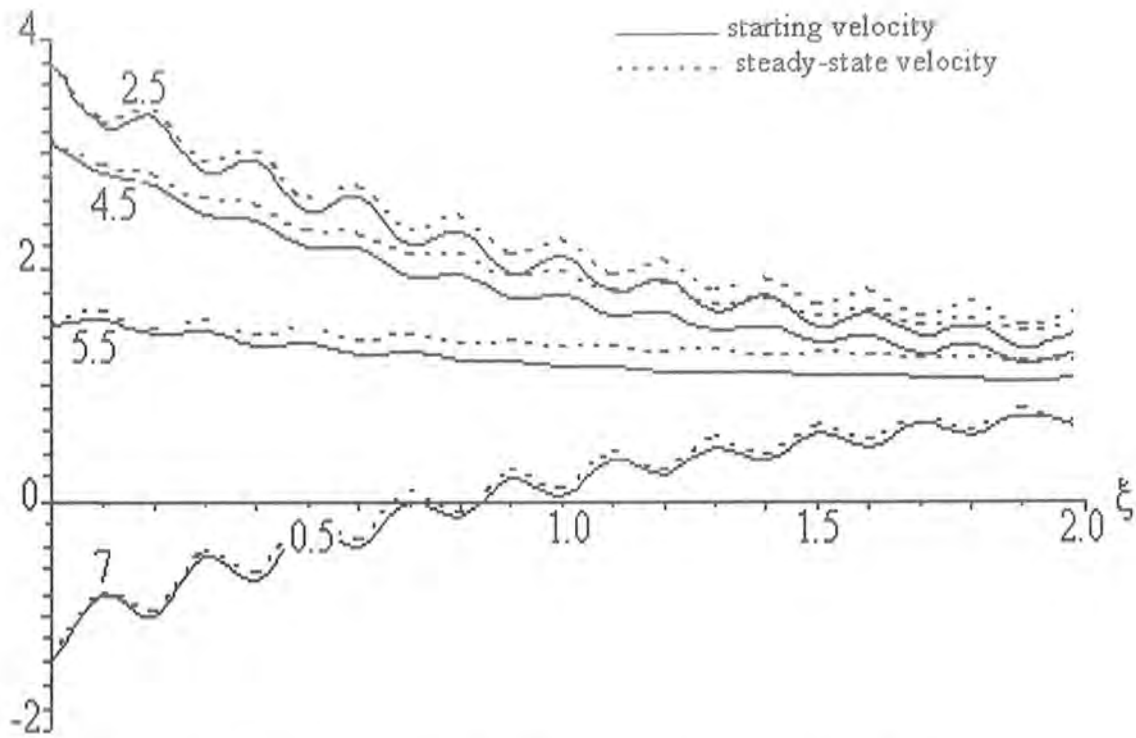

Figure 5.9 Variation in f with ξ for different values of time for sine oscillation at U/Ωl = 4, n/Ω = .5, ε = 2, α = 2, β = 0, N = 0

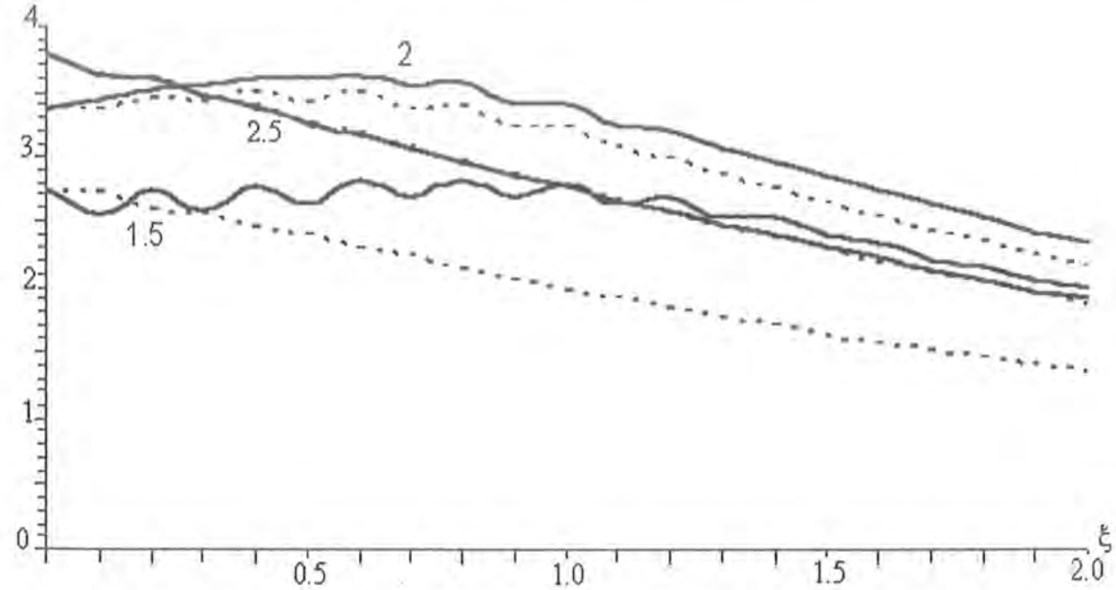

Figure 5.10 Variation in f with ξ for different values of time for sine oscillation at U/Ωl = 4, n/Ω = .5, ε = 2, α = 2, β = 5, N = 0

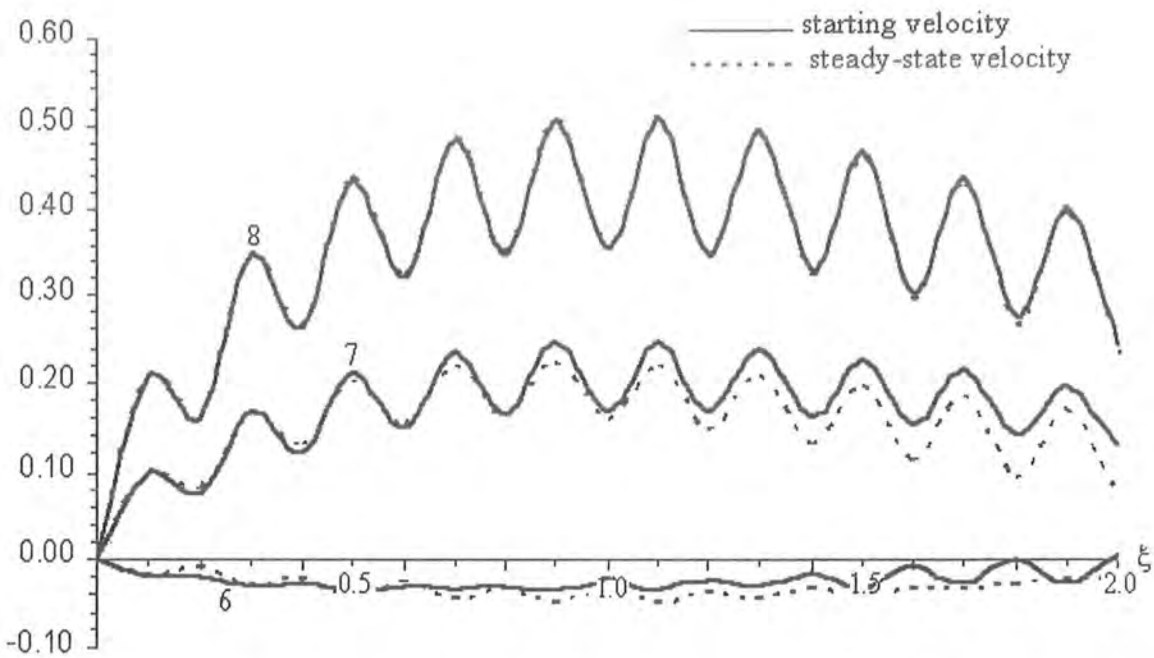

Figure 5.11 Variation in g with ξ for different values of time for sine oscillation at U/Ωl = 4, n/Ω = .5, ε = 2, α = 2, β = 0, N = 0

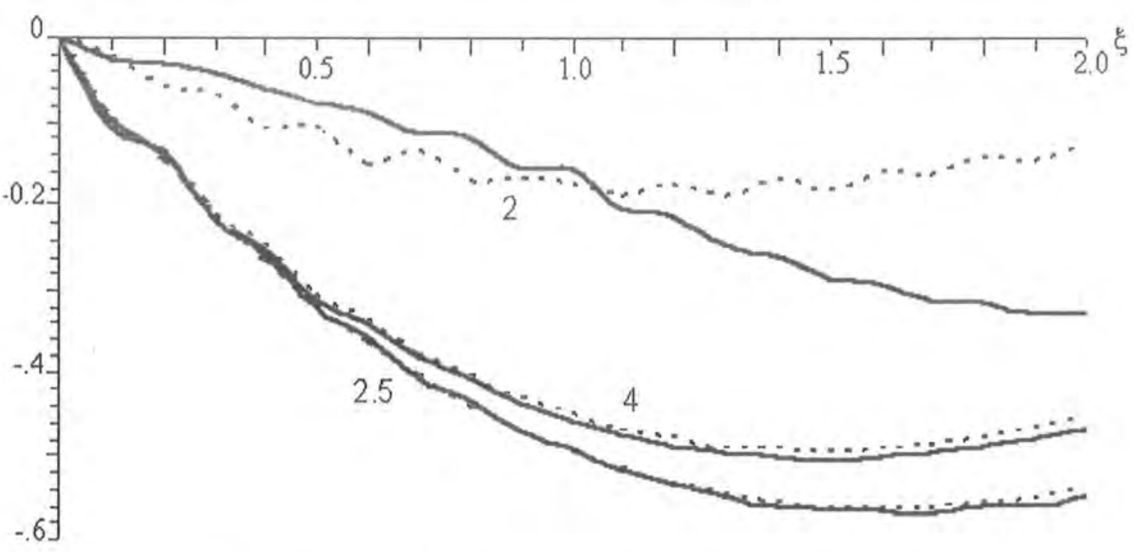

Figure 5.12 Variation in g with ξ for different values of time for sine oscillation at U/Ωl = 4, n/Ω = .5, ε = 2, α = 2, β = 5, N = 0

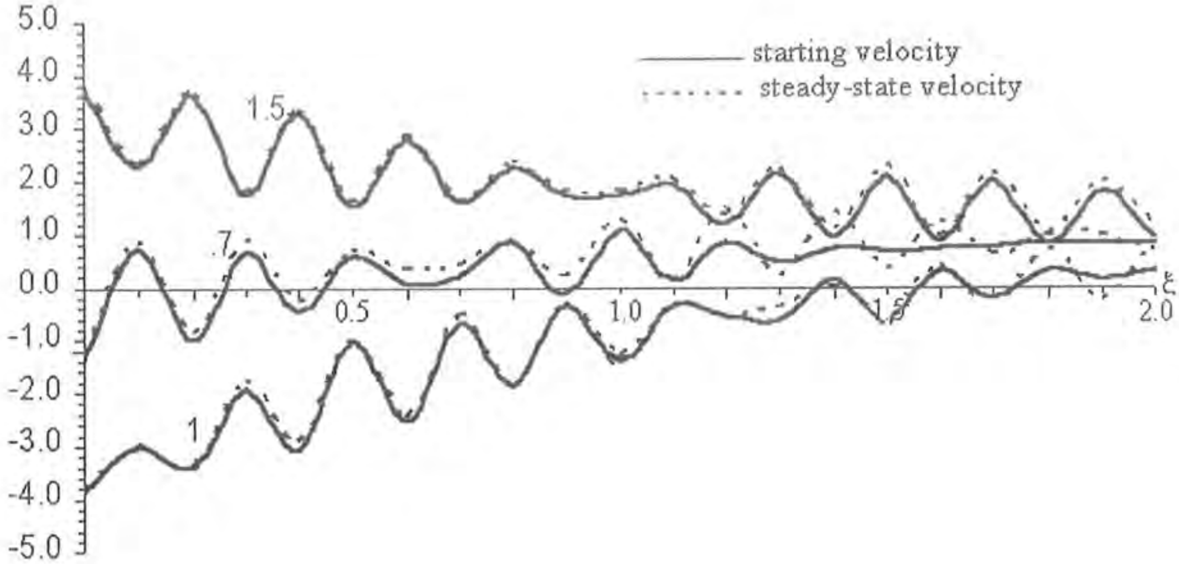

Figure 5.13 Variation in f with ξ for different values of time for sine oscillation at U/Ωl = 4, n/Ω = 5, ε = 2, α = 2, β = 0, N = 0

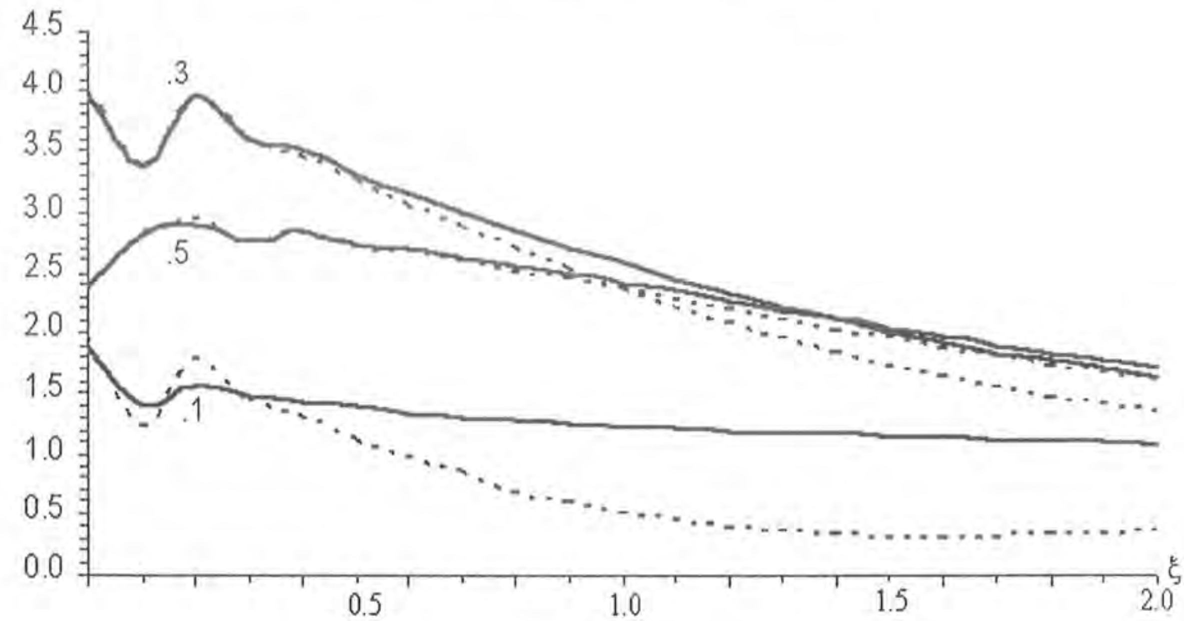

Figure 5.14 Variation in f with ξ for different values of time for sine oscillation at U/Ωl = 4, n/Ω = 5, ε = 2, α = 2, β = 5, N = 0

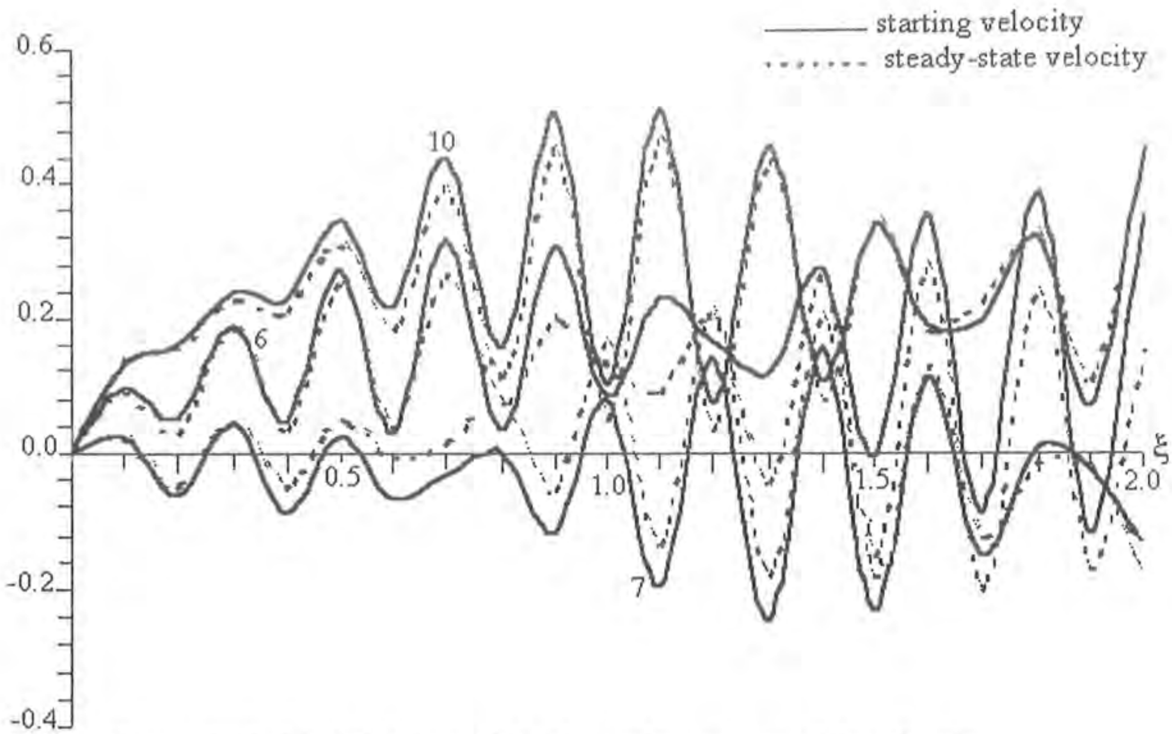

Figure 5.15 Variation in g with ξ for various values of time for sine oscillation at U/Ωl = 4, n/Ω = 5, ε = 2, α = 2, β = 0,N = 0

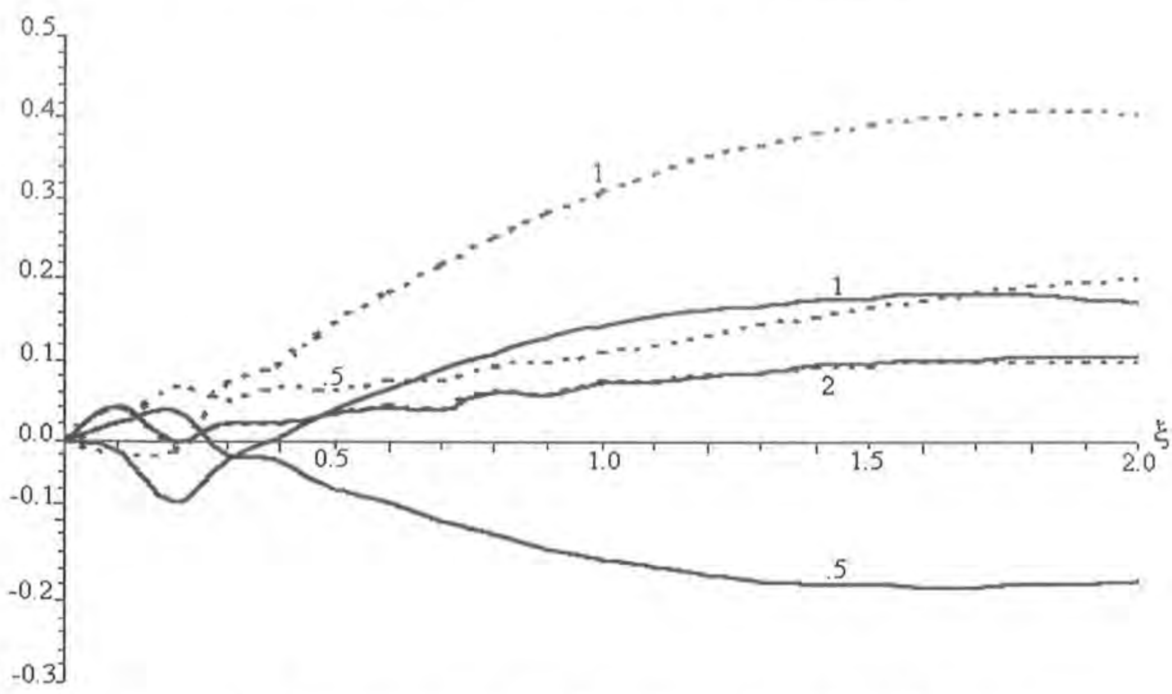

Figure 5.16 Variation in g with ξ for various values of time for sine oscillation at U/Ωl = 4, n/Ω = 5, ε = 2, α = 2, β = 5, N = 0

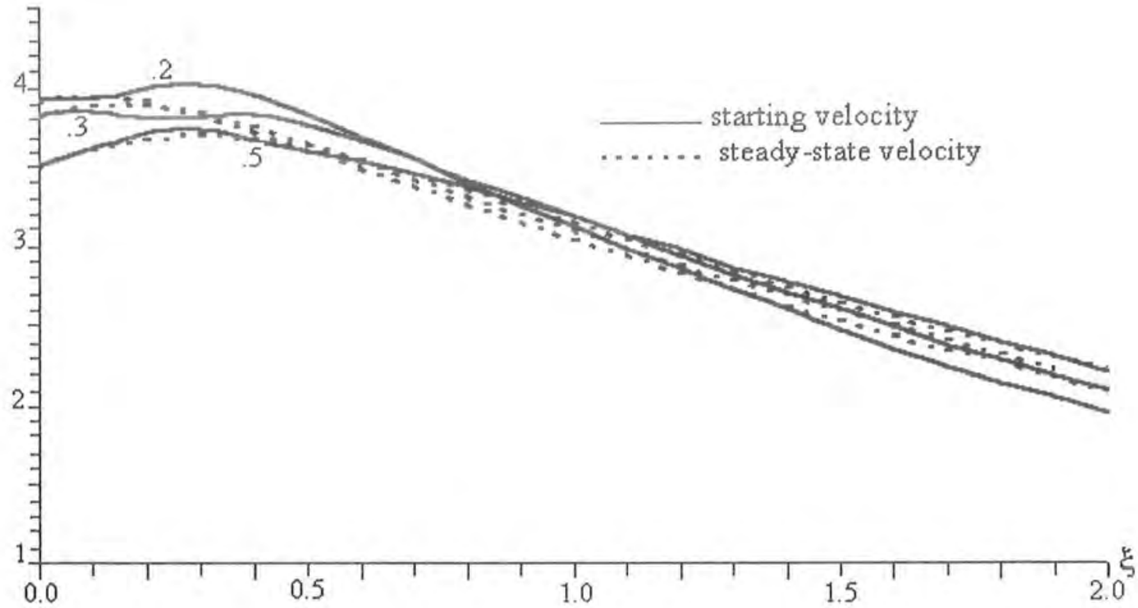

Figure 5.17 Variation in f with ξ for various values of time for cosine oscillation at $U/\Omega l = 4$, $n/\Omega = 1$, $\varepsilon = -2$, $\alpha = 2$, $\beta = 5$, $N = 2$

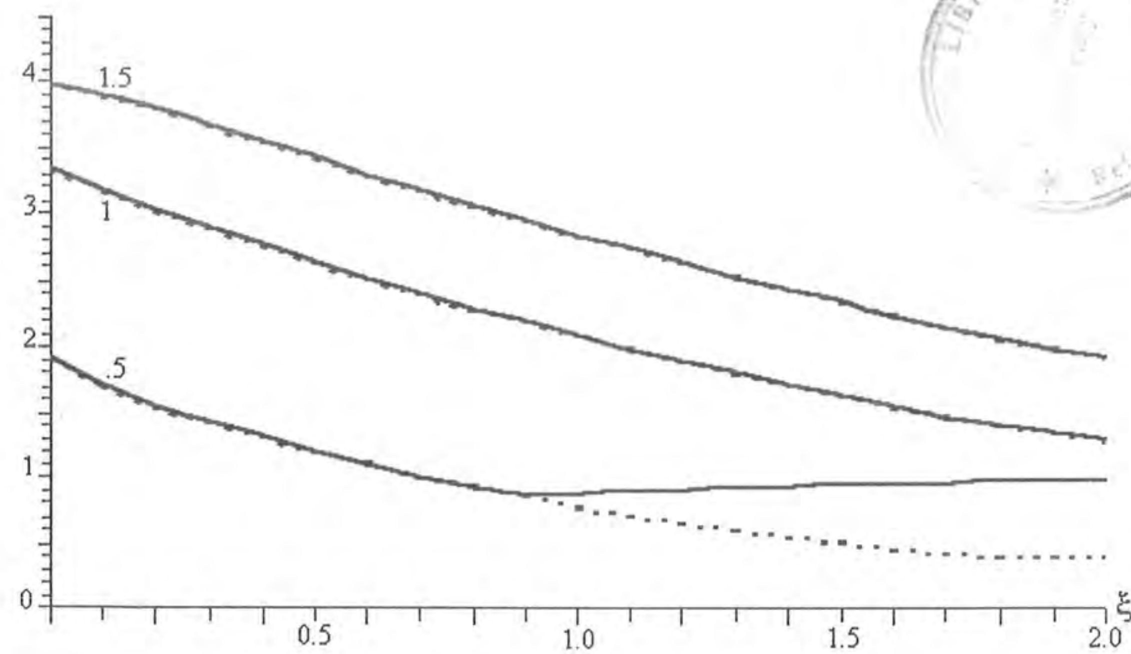

Figure 5.18 Variation in f with ξ for various values of time for sine oscillation at $U/\Omega l = 4$, $n/\Omega = 1$, $\varepsilon = -2$, $\alpha = 2$, $\beta = 5$, $N = 2$

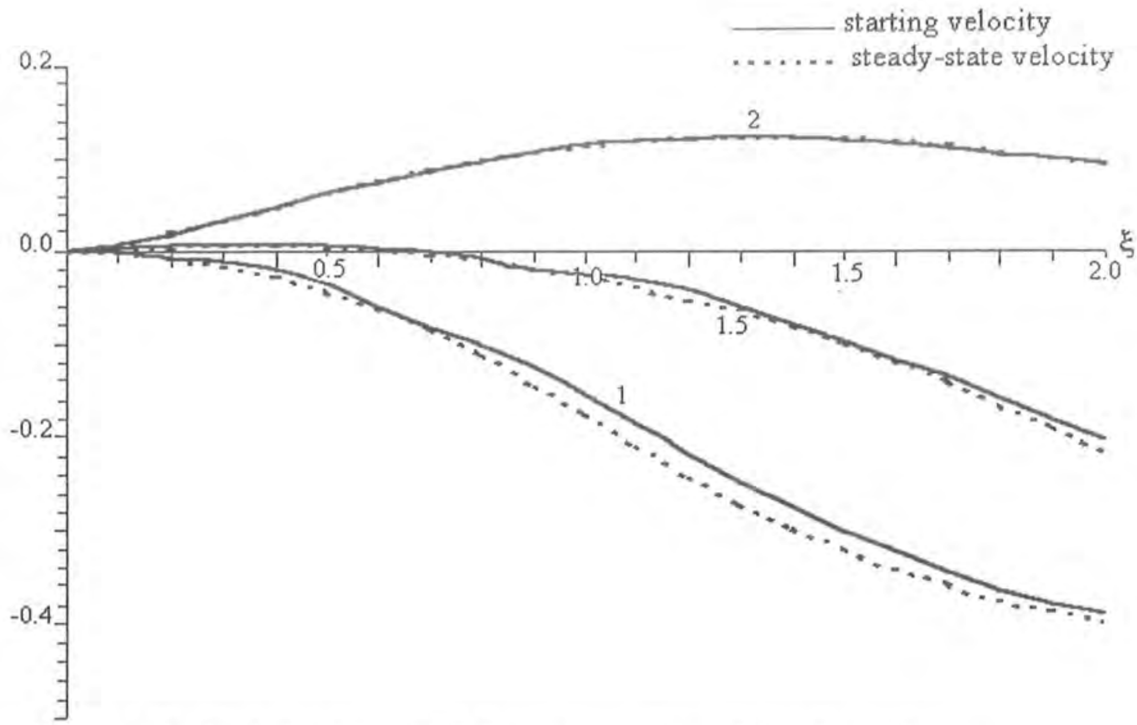

Figure 5.19 Variation in g with ξ for various values of time for cosine oscillation at U/Ωl = 4, n/Ω = 1, ε = -2, α = 2, β = 5, N = 2

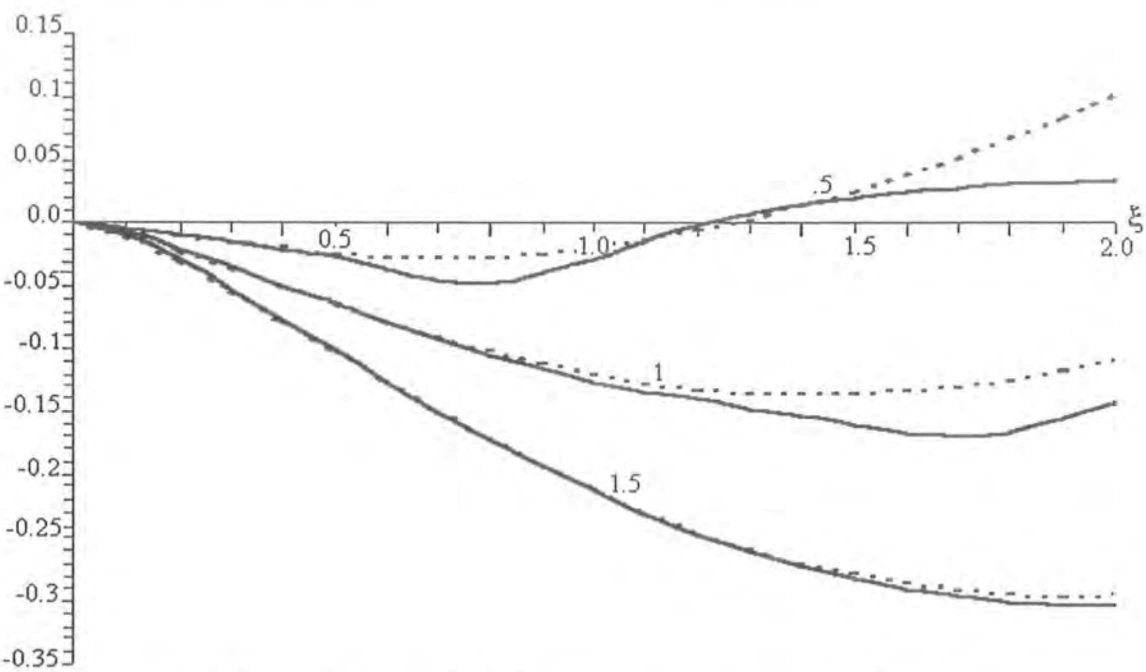

Figure 5.20 Variation in g with ξ for different values of time for sine oscillation at U/Ωl = 4, n/Ω = 1, ε = -2, α = 2, β = 5, N = 2

Bibliography

[1] T. von Kármán. Laminar und turbulente Reibung. *Z. angew. Math. Mech.*, **1**:233, (1921).

[2] G. K. Batchelor. Note on a class of solutions of the Navier-Stokes equations representing rotationally symmetric flow. *Q. J. Mech. Appl. Maths*, **4**:29, (1951).

[3] H. P. Greenspan and L. N. Howard. On a time dependent motion of a rotating fluid. *J. Fluid Mech.*, (**17**):385, (1963).

[4] J. R. Holton. The influence of viscous boundary layers on transient motions in a stratified rotating fluid. *I. J. Atoms. Sci*, (**22**):402, (1965).

[5] G. Walin. Some aspects of time dependent motion of a stratified rotating fluid. *J. Fluid Mech.*, (**36**):289, (1969).

[6] W. L. Siegmann. The spin-down of rotating stratified fluid. *J. Fluid Mech.*, (**47**):689, (1971).

[7] L. Debnath. On unsteady magnetohydrodynamics boundary layers in a rotating flow. *ZAMM*, (**52**):623, (1972).

[8] R. Berker. A new solution of the Navier-Stokes equation for the motion of a fluid contained between two parallel plates rotating about the same axis. *Arch. Mech. Stos.*, **31**:265, (1979).

[9] R. Berker. An exact solution of the Navier-Stokes equation: The vortex with curvilinear axis. *Int. J. Engg. Sci.*, **20**:217, (1982).

[10] M. E. Erdogan. Unsteady viscous flow between eccentric rotating disks. *Int. J. Non-Linear Mech.*, **30(5)**:711, (1995).

[11] K. R. Rajagopal. On the flow of a simple fluid in an orthogonal rheometer. *Arch. Rat. Mech. Anal*, **79**:39, (1982).

[12] T. N. G. Abbot and K. Waltters. Rheometrical flow systems: Part2. Theory for the orthogonal rheometer, including an exact solution of the Navier-Stokes equations. *J. Fluid. Mech.*, **40**:205, (1970).

[13] K. R. Rajagopal. A class of exact solutions to the Navier-Stokes equations. *Int. J. Engg. Sci.*, **22**:451, (1984).

[14] R. Berker. *Handbook of Fluid Dynamics*, volume **VIII/3**. Springer-Verlag, Berlin, (1963).

[15] M. E. Erdogan. Unsteady flow of a viscous fluid due to noncoaxial rotations of a disk and a fluid at infinity. *Int. J. Non-Linear Mechanics*, **32(2)**:285, (1997).

[16] J. Coirier. Rotations non-coaxiales d'un disque et d'un fluide á l'infini. *J. de Mecanique*, **11(2)**:347, (1972).

[17] A. S. Gupta. Ekman layer on a porous plate. *Phys. Fluids*, **15(5)**:930, (1972).

[18] M. E. Erdogan. Flow due to eccentric rotating a porous disk and a fluid at infinity. *Trans. ASME J. Appl. Mech.*, **43**:203, (1976).

[19] M. E. Erdogan. Flow due to noncoaxial rotations of a porous disk and fluid at infinity. *Rev. Roum., Méc. Appl.*, **22**:171, (1977).

[20] S. H. Smith. Eccentric rotating flows: Exact unsteady solutions of the Navier-Stokes equations. *J. Appl. Math. Phys.(ZAMP)*, **38**:573, (1987).

[21] S. R. Kasiviswanathan and A. R. Rao. An unsteady flow due to eccentrically rotating porous disk and a fluid at infinity. *Int. J. Engg. Sci.*, **25**:1419, (1987).

[22] I Pop. Unsteady flow due to noncoaxially rotating a disk and a fluid at infinity. *Bull. Tech. Uni. Ist.*, **32**:14, (1979).

[23] A. S. Gupta. Magnetohydrodynamic Ekman layer. *Acta Mech.*, **13**:155, (1972).

[24] S. N. Murthy and R. K. P. Ram. MHD flow and heat transfer due to eccentric rotations of a porous disk and a fluid at infinity. *Int. J. Engg. Sci.*, **16**:943, (1978).

[25] H. K. Mohanty. Hydromagnetic flow between two rotating disks with non-coincident parallel axes of rotation. *The Phys. Fluids*, **15**:1456, (1972).

[26] C. S. Ekman. *Lett. Appl. Engg. Sci.*, (**3**):51, (1975).

[27] C. Truesdell and W. Noll. *Handbuch der Physik*, volume **III**, chapter The non-linear field theories of mechanics, page 3. Berlin Heidelberg New York: Springer Verlag, (1965).

[28] A. C. Srivatsava. The effect of magnetic field on the flow between two non-parallel planes. *Quart. J. Math. Appl. Mech.*, **14**:353, (1961).

[29] R. K. Bhatnagar. *Proc. Indian Acad. Sci.*, **58**:279, (1963).

[30] M. E. Erdogan. Non-newtonian flow due to noncoaxial rotations of a disk and a fluid at infinity. *ZAMM*, **56**:141, (1976).

[31] R. K. Bhatnagar and J. V. Zago. Numerical investigations of flow of a viscoelastic fluid between rotating coaxial disks. *Rheol. Acta.*, **17**:557, (1978).

[32] K. R. Rajagopal. Flow of viscoelastic fluids between rotating disks. *Theor. Comput. Fluid Dynamics*, **3**:185, (1992).

[33] B. Maxwell and R. P. Chartoff. Studies of a polymer melt in an orthogonal rheometer. *Trans. Soc. Rheol.*, **9**:41, (1965).

[34] L. L. Blyler and S. J. Kurtz. Analysis of the Maxwell orthogonal rheometer. *J. Appl.Polym. Sci.*, **11**:127, (1967).

[35] R. B. Bird and E. K. Harris. Analysis of steady state shearing and stress relaxation in the Maxwell orthogonal rheometer. *A. I. Ch. E. J.*, **14**:758, (1968).

[36] K. R. Rajagopal. The flow of a second order fluid between rotating parallel plates. *J. Non-Newtonian Fluid. Mech.*, **9**:185, (1981).

[37] K. R. Rajagopal and A. S. Gupta. Flow and stability of a second grade fluid between two parallel plates rotating about noncoincident axes. *Int. J. Engg. Sci.*, **19**:1401, (1981).

[38] K. R. Rajagopal and A. S. Wineman. On the flow of a BKZ fluid in an orthogonal rheometer. *J. Rheol.*, **27**:509, (1983).

[39] R. X. Dai, K. R. Rajagopal and A. Z. Szeri. A numerical study of the flow of a K-BKZ fluid between plates rotating about non-coincident axes. *J. Non-Newtonian Fluid. Mech.*, **38**:289, (1991).

[40] M. S. Göğüs. The steady flow of a binary mixture between two rotating non-coaxial disks. *Int. J. Engg. Sci.*, **30(5)**:665, (1992).

[41] A. R. Rao and S. R. Kasiviswanathan. A class of exact solutions for the flow of a micropolar fluid. *Int. J. Engg. Sci.*, **25**:443, (1987).

[42] K. R. Rajagopal. On an exact solution for the flow of an Oldroyd-B fluid. *Bull. Tech. Uni. Ist.*, **49**:617, (1996).

[43] H. V. Ersoy. MHD flow of an Oldroyd-B fluid between eccentric rotating disks. *Int. J. Engg. Sci.*, **37**:1973, (1999).

[44] D. G. Knight. Flow between eccentric disks rotating at different speeds: Inertia effects. *J. Appl. Math. Phys.(ZAMP)*, **31**:309, (1980).

[45] S. V. Parter and K. R. Rajagopal. Swirling flow between rotating plates. *Arch. Rat. Mech. Anal.*, **86**:305, (1984).

[46] R. S. Rivlin and J. L. Ericksen. Stress- deformation relations for isotropic materials. *Arch. Rat. Mech. Anal.*, **4**:323, (1955).

[47] W. R. Schowalter. *Mechanics of Non-Newtonian fluids.* Pergamon, (1978).

[48] M. J. Crochet A. R. Davies and K. Walters. *Numerical Simulation of Non-Newtonian flow*, volume 1. Elsevier, (1984).

[49] J. E. Dunn and R. L. Fosdick. Thermodynamics, stability and boundedness of fluids of complexity 2 and fluids of second grade. *Arch. Rat. Mech. Anal.*, **56**:191, (1974).

[50] C. G. Speziale. On turbulent secondary flows in pipes of non-circular cross section. *Int. J. Engg. Sci.*, **7**:863, (1982).

[51] B. D. Coleman and W. Noll. An approximation theorem for functionals with applications in continuum mechanics. *Arch. Rat. Mech. Anal.*, **6**:355, (1960).

[52] R. L. Fosdick and K. R. Rajagopal. Thermodynamics and stability of fluids of third grade. *Proc. Roy. Soc. Lond. Ser.*, **A,339**:351, (1980).

[53] J. E. Dunn and K. R. Rajagopal. Fluids of differential type. *Int. J. Engg. Sci.*, **33**:689, (1995).

[54] J. A. Shercliff. *A textbook of Magnetohydrodynamics*. Pergamon Press, Oxford, first edition, (1965).

[55] V. J. Rossow. On flow of electrically conducting fluids over a flat plate in the presence of a transverse magnetic field. *NASA Report No.*, **(1385)**:p 489, (1958).

[56] I. N. Sneddon. *The use of integral transforms*. New York, McGraw-Hill, (1972).

[57] B. M. Abramovitz and I. A. Stegun. *Handbook of Mathematical Functions*. NewYork, Dover, (1965).

[58] M. E. Erdogan. On the flow of a non-Newtonian fluid past a porous flat plate. *ZAMM*, **55**:79, (1975).

[59] N. W. McLachlan. *Complex Variable Theory and Transform Calculus with Technical Applications*. Cambridge University press, second edition, (1963).

[60] G. Pontrelli and R. K. Bhatnagar. Flow of a viscoelastic fluid between two rotating circular cylinders subject to suction or injection. *Int. J. Numerical Methods in Fluids*, **24**:337, (1997).

[61] G. H. Klopfer and D. S. McRae. Non-linear truncation error analysis of FDF for the Euler equations. *AIAA J.*, **21**:487, (1983).

[62] R. D. Richtmyer and K. W. Morton. *Difference Methods for initial-value problems*. Number 4. Interscience, second edition, (1967).

[63] Dr. Hermann Schlichting. *Boundary-Layer Theory*. McGraw-Hill Series in Mechanical Engineering. McGraw-Hill, seventh edition, (1979).

[64] M. J. Lighthill. The response of laminar skin friction and heat transfer to flucations in the stream velocity. *Proc. Roy. Soc.*, **A 224**:1, (1954).

[65] S. Turbatu, K. Buhler and J. Zierep. New solution of II-Stokes problem for an oscillating flat plate. *Acta Mech.*, **129**:25, (1998).

[66] M. E. Erdogan. A note on an unsteady flow of a viscous fluid due to an oscillating plane wall. *Int. J. Non-Linear Mech.*, **35**:1, (2000).

[67] M. E. Erdogan. Flow induced by non-coaxial rotation of a disk executing non-torsional oscillations and a fluid rotating at infinity. *Int. J. Engg. Sci.*, **38**:175, (2000).

Published work from the thesis of the Author

Acta Mechanica 151, 127–134 (2001)

ACTA MECHANICA

Unsteady MHD flow due to non-coaxial rotations of a porous disk and a fluid at infinity

T. Hayat and S. Asghar, Islamabad, Pakistan, A. M. Siddiqui, York, Pennsylvania, and T. Haroon, Islamabad, Pakistan

(Received April 16, 1999; revised September 8, 1999)

Summary. An exact solution of the unsteady three-dimensional Navier-Stokes equations is derived for the case of flow due to non-coaxial rotations of a porous disk and a fluid at infinity in the presence of a uniform transverse magnetic field. An analytical solution of the problem is established by the method of Laplace transform, and the velocity field is presented in terms of the tabulated functions. It is found that the boundary layer thickness in the cases of suction/blowing decreases with the increase in the magnetic parameter.

1 Introduction

An investigation of MHD boundary layers under the influence of viscous forces is of importance in understanding a variety of geophysical, astrophysical and engineering phenomena such as those that occur at the core-mantle interface of the earth. The possibility of an exact solution of the Navier-Stokes equations for the flow due to non-coaxial rotations of a disk and a fluid at infinity has been implied by Berker [1]. He [1] has considered the flow between two disks which are rotating with the same angular velocity. Coirier [2] studied the flow due to a disk and a fluid at infinity which are rotating non-coaxially at a slightly different angular velocity. The work of Coirier [2] for the case of a porous disk assuming that rotations are with the same angular velocity has been discussed by Erdogan [3]. He established, as did Gupta [4], that for uniform suction or uniform blowing at the disk an asymptotic profile exists for the velocity distribution. Murthy and Ram [5] have considered the magnetohydrodynamic flow due to eccentric rotations of a porous disk and a fluid at infinity. Rajagopal [6] has considered the flow of a simple fluid in an orthogonal rheometer. The flows of Newtonian and non-Newtonian fluids between parallel disks rotating about a common axis have been reviewed by Rajagopal [7].

The unsteady flow created by a rotating disk in otherwise quiescent or rotating viscous fluid has been the subject of a large number of investigations. The solutions of many practical rotating flow problems hinge on the understanding of the behavior of the unsteady boundary layers. Mention may be made of the interesting work of Greenspan and Howard [8]. The unsteady flow due to non-coaxial rotations of an oscillating disk and a fluid at infinity has been studied by Kasiviswanathan and Rao [9]. Further, Pop [10] presented the flow due to eccentric rotations of a disk and a fluid at infinity which are impulsively started. He assumes that the flow is two-dimensional, and both the disk and the fluid at infinity are initially at rest and that they are impulsively started at time zero. More recently, it has been pointed out by

Erdogan [11] that if the disk and the fluid at infinity are initially at rest the problem becomes three-dimensional, and the solution cannot be obtained easily. To overcome this difficulty Erdogan [11] suggested a change in the initial condition and proposed that the disk and the fluid at infinity are initially rotating about the z'-axis and suddenly set in motion, the disk rotating about the z-axis and the fluid at infinity about the z'-axis with the same angular velocity. He [11] showed that now the problem is solvable and presents an analytical solution for the velocity field.

The aim of the present paper is to discuss the influence of an externally applied magnetic field on the velocity distribution in both suction and blowing cases. It is assumed that both the porous disk and the fluid at infinity are initially rotating about the z'-axis and suddenly set in motion. We assume that the fluid is electrically conducting but the porous disk is not. In Sections 2 and 3 the formulation and the solution of the problem are given.

The present motivation comes from a desire to understand, at least qualitatively, the effect of porosity and its role on the boundary layer likely to exist at the core-mantle interface to the earth where rotation and magnetic field effects are simultaneously present; in particular, to know how the geophysically important suction velocity is effected by the magnetic field and rotation.

2 The constitutive equations and boundary conditions

We consider a semi-infinite expanse of homogeneous, incompressible, electrically conducting viscous fluid which occupies the space $z > 0$ and is bounded by an infinite non-conducting porous disk at $z = 0$. The axes of rotation, of both the disk and the fluid, are assumed to be in the plane $x = 0$, with the distance between the axes being l. The disk and the fluid at infinity are initially rotating about the z'-axis with the same angular velocity Ω, and at time $t = 0$ the disk starts to rotate suddenly about the z-axis with the same angular velocity Ω, and the fluid at infinity continues to rotate about the z'-axis with the same angular velocity. The fluid is electrically conducting and assumed to be permeated by a magnetic field $\mathbf{B}_0$ having no components in the x- and y-directions. Following Erdogan [11] we take the boundary conditions as

$$\begin{aligned} &u = -\Omega y, \quad v = \Omega x, \quad w = -W_0 \quad \text{at} \quad z = 0 \quad \text{for} \quad t > 0, \\ &u = -\Omega(y - l), \quad v = \Omega x, \quad w = -W_0 \quad \text{as} \quad z \to \infty \quad \text{for all} \quad t, \\ &u = -\Omega(y - l), \quad v = \Omega x, \quad t = 0 \quad \text{for} \quad z > 0, \end{aligned} \tag{2.1}$$

where u, v, w are the components of the velocity. The boundary and initial conditions show that the motion is a summation of the helical and translatory motion with the velocity profiles being

$$u = -\Omega y + f(z,t), \qquad v = \Omega x + g(z,t), \qquad w = -W_0. \tag{2.2}$$

The unsteady motion of the conducting fluid in the Cartesian coordinate system is governed by the conservation laws of momentum and of mass which are

$$\frac{\partial \mathbf{V}}{\partial t} + (\mathbf{V}.\nabla)\,\mathbf{V} = -\frac{1}{\varrho}\nabla p + \nu\nabla^2\mathbf{V} + \frac{1}{\varrho}\mathbf{j} \times \mathbf{B}, \tag{2.3}$$

$$div\,\mathbf{V} = 0, \tag{2.4}$$

where V is the velocity vector, p is the pressure, ϱ is the density, j is the electric current density, B is the total magnetic field so that $\mathbf{B} = \mathbf{B}_0 + \mathbf{b}$, b is the induced magnetic field, and ν is the kinematic viscosity.

Neglecting the displacement currents, the Maxwell equations and the generalized Ohm's law are

$$div\,\mathbf{B} = 0\,, \qquad \mathrm{curl}\mathbf{B} = \mu\mathbf{j}\,, \qquad \mathrm{curl}\mathbf{E} = -\frac{\partial\mathbf{B}}{\partial t}\,, \tag{2.5.1 − 3}$$

$$\mathbf{j} = \sigma(\mathbf{E} + \mathbf{V}\times\mathbf{B})\,, \tag{2.6}$$

where μ is the magnetic permeability, E is the electric field and σ is the electrical conductivity of the fluid.

We make the following assumptions:

(i) The quantities ϱ, ν, μ and σ are all constants throughout the flow field.

(ii) The magnetic field B is perpendicular to the velocity field V, and the induced magnetic field is negligible compared with the imposed field so that the magnetic Reynolds number is small [12].

(iii) The electric field is assumed to be zero.

(iv) The velocity vector V is a function of z and t alone with $w = -W_0$.

In view of these assumptions, the electromagnetic body force involved in (2.3) takes the linearized form [13]

$$\begin{aligned}\frac{1}{\varrho}\mathbf{j}\times\mathbf{B} &= \frac{\sigma}{\varrho}[(\mathbf{V}\times\mathbf{B})\times\mathbf{B}]\\ &= \frac{\sigma}{\varrho}[\mathbf{B}_0(\mathbf{V}\cdot\mathbf{B}_0) - \mathbf{V}(\mathbf{B}_0\cdot\mathbf{B}_0)]\\ &= -\frac{\sigma}{\varrho}B_0^2\mathbf{V}\,,\end{aligned} \tag{2.7}$$

where $\left(\frac{\sigma}{\varrho}B_0^2\right)$ has the same dimension as Ω.

Substituting (2.2) and (2.7) in (2.3) we obtain

$$\frac{1}{\varrho}\frac{\partial p}{\partial x} = \Omega^2 x + \Omega g + W_0\frac{\partial f}{\partial z} - \frac{\partial f}{\partial t} + \nu\frac{\partial^2 f}{\partial z^2} - \frac{\sigma}{\varrho}B_0^2[f(z,t) - \Omega y]\,, \tag{2.8}$$

$$\frac{1}{\varrho}\frac{\partial p}{\partial y} = \Omega^2 y - \Omega f + W_0\frac{\partial g}{\partial z} - \frac{\partial g}{\partial t} + \nu\frac{\partial^2 g}{\partial z^2} - \frac{\sigma}{\varrho}B_0^2[g(z,t) + \Omega x]\,, \tag{2.9}$$

$$\frac{1}{\varrho}\frac{\partial p}{\partial z} = \frac{\sigma}{\varrho}B_0^2 W_0\,. \tag{2.10}$$

Eliminating p from (2.8) and (2.9) by differentiating with respect to z and combining them with (2.10), we get

$$\nu\frac{\partial^3 F}{\partial z^3} + W_0\frac{\partial^2 F}{\partial z^2} - \frac{\partial^2 F}{\partial t\partial z} - \left(i\Omega + \frac{\sigma}{\varrho}B_0^2\right)\frac{\partial F}{\partial z} = 0\,, \tag{2.11}$$

where

$$F = f + ig\,. \tag{2.12}$$

By (2.1), (2.2) and (2.12) we have

$$F(0,t) = 0\,, \qquad F(\infty,t) = \Omega l\,, \qquad F(z,0) = \Omega l\,. \tag{2.13}$$

3 The solution of the problem

The problem given by (2.11) and (2.13) can be solved directly by the use of the Laplace transform pair [14]

$$\psi(z,s)=\int_0^\infty F(z,t)\,e^{-st}\,dt\,, \tag{3.1}$$

$$F(z,t)=\frac{1}{2\pi i}\int_{\lambda-i\infty}^{\lambda+i\infty}\psi(z,s)\,e^{st}\,ds\,,\quad \lambda>0\,. \tag{3.2}$$

In view of the Laplace transform (3.1), the solution of the above differential system is obtained in the form

$$\psi(z,s)=\frac{\Omega l}{s}\left[1-\exp\left\{-\left(\frac{W_0}{2\nu}+\sqrt{\left(\frac{W_0}{2\nu}\right)^2+\left(\frac{N+s}{\nu}\right)}\right)z\right\}\right], \tag{3.3}$$

where

$$N=i\Omega+\frac{\sigma B_0{}^2}{\varrho}\,.$$

Using (3.3) in (3.2) and then making reference to the table of Campbell and Foster [15], the solution for the velocity field can be evaluated exactly and is obtained as

$$\frac{f}{\Omega l}+i\frac{g}{\Omega l}=1-\frac{e^{-\frac{W_0}{2\nu}z}}{2}\left[\begin{array}{l} e^{-z\sqrt{\frac{W_0^2}{4\nu^2}+\frac{\sigma B_0^2}{\varrho\nu}+\frac{i\Omega}{\nu}}}\,\operatorname{erf}c\left(\frac{z}{2\sqrt{\nu t}}-\sqrt{\left(\frac{W_0{}^2}{4\nu}+\frac{\sigma B_0{}^2}{\varrho}+i\Omega\right)t}\right)\\ +e^{z\sqrt{\frac{W_0^2}{4\nu^2}+\frac{\sigma B_0^2}{\varrho\nu}+\frac{i\Omega}{\nu}}}\,\operatorname{erf}c\left(\frac{z}{2\sqrt{\nu t}}+\sqrt{\left(\frac{W_0{}^2}{4\nu}+\frac{\sigma B_0{}^2}{\varrho}+i\Omega\right)t}\right)\end{array}\right], \tag{3.4}$$

where $\operatorname{erf}c(x)$ is the complementary error function defined by

$$\operatorname{erf}c(x)=1-\operatorname{erf}(x)=\int_x^\infty e^{-r^2}\,dr\,. \tag{3.5}$$

We note from (3.4) that $W_0=0$ gives the impermeable case while $W_0=0=B_0$ gives Erdogans problem [11]. The real part gives $\frac{f}{\Omega l}$, and the imaginary part gives $\frac{g}{\Omega l}$. For that it is better to write (3.4) in the following form:

$$\frac{f}{\Omega l}+i\frac{g}{\Omega l}=1-\frac{e^{-\frac{W_0}{2\nu}z}}{2}\left[\begin{array}{l} e^{-\frac{\alpha z}{\sqrt{\nu}}}\left(\cos\frac{\beta z}{\sqrt{\nu}}-i\sin\frac{\beta z}{\sqrt{\nu}}\right)\operatorname{erf}c\left(\frac{z}{2\sqrt{\nu t}}-(\alpha+i\beta)\sqrt{t}\right)\\ +e^{\frac{\alpha z}{\sqrt{\nu}}}\left(\cos\frac{\beta z}{\sqrt{\nu}}+i\sin\frac{\beta z}{\sqrt{\nu}}\right)\operatorname{erf}c\left(\frac{z}{2\sqrt{\nu t}}+(\alpha+i\beta)\sqrt{t}\right)\end{array}\right], \tag{3.6}$$

where

$$\alpha=\left[\frac{1}{2}\left\{\sqrt{\left(\frac{W_0{}^2}{4\nu}+\frac{\sigma B_0{}^2}{\varrho}\right)^2+\Omega^2}+\left(\frac{W_0{}^2}{4\nu}+\frac{\sigma B_0{}^2}{\varrho}\right)\right\}\right]^{\frac{1}{2}},$$

$$\beta=\left[\frac{1}{2}\left\{\sqrt{\left(\frac{W_0{}^2}{4\nu}+\frac{\sigma B_0{}^2}{\varrho}\right)^2+\Omega^2}-\left(\frac{W_0{}^2}{4\nu}+\frac{\sigma B_0{}^2}{\varrho}\right)\right\}\right]^{\frac{1}{2}},$$

and erf $c(x+iy)$ can be calculated in terms of the tabulated functions [16]. The tables given in [16] do not give erf $c(x+iy)$ directly but an auxiliary function $H(x+iy)$, which is defined as

$$\operatorname{erf c}(x+iy) = e^{-(x+iy)^2} H(-y+ix)\,, \tag{3.7}$$

where

$$H(-x+iy) = \overline{H(x+iy)}\,, \qquad H(x-iy) = 2e^{-(x+iy)^2} - \overline{H(x+iy)}\,,$$

and $\overline{H(x+iy)}$ is the complex conjugate of $H(x+iy)$. For large times, we can write (3.6) as

$$\begin{aligned}\frac{f}{\Omega l} + i\frac{g}{\Omega l} = {} & \left[1 - e^{-\frac{W_0}{2\nu}z - \frac{\alpha z}{\sqrt{\nu}}}\left(\cos\frac{\beta z}{\sqrt{\nu}} - i\sin\frac{\beta z}{\sqrt{\nu}}\right)\right] + \frac{e^{-\frac{W_0}{2\nu}z}}{2} \\ & \times \left[\begin{array}{l} e^{-\frac{\alpha z}{\sqrt{\nu}}}\left(\cos\frac{\beta z}{\sqrt{\nu}} - i\sin\frac{\beta z}{\sqrt{\nu}}\right)\operatorname{erf c}\left((\alpha+i\beta)\sqrt{t} - \frac{z}{2\sqrt{\nu t}}\right) \\ -e^{\frac{\alpha z}{\sqrt{\nu}}}\left(\cos\frac{\beta z}{\sqrt{\nu}} + i\sin\frac{\beta z}{\sqrt{\nu}}\right)\operatorname{erf c}\left((\alpha+i\beta)\sqrt{t} + \frac{z}{2\sqrt{\nu t}}\right)\end{array}\right],\end{aligned} \tag{3.8}$$

where the first term of the right-hand side corresponds to the steady state and the second one denotes the deviation from it.

On introducing the nondimensional quantities

$$\zeta = \sqrt{\frac{\Omega}{2\nu}}z, \tau = \Omega t\,, \qquad N_1 = \frac{\sigma B_0{}^2}{\varrho\Omega}\,, \qquad S = \frac{W_0}{2\sqrt{\Omega\nu}}\,, \tag{3.9}$$

Eq. (3.8) becomes

$$\begin{aligned}\frac{f}{\Omega l} + i\frac{g}{\Omega l} = {} & 1 - e^{-\sqrt{2}S\zeta - (\hat\alpha + i\hat\beta)\zeta} + \frac{e^{-\sqrt{2}S\zeta}}{2} \\ & \times \left[\begin{array}{l} e^{-(\hat\alpha+i\hat\beta)\zeta}\operatorname{erf c}\left((\hat\alpha+i\hat\beta)\sqrt{\frac{\tau}{2}} - \frac{\zeta}{\sqrt{2\tau}}\right) \\ -e^{(\hat\alpha+i\hat\beta)\zeta}\operatorname{erf c}\left((\hat\alpha+i\hat\beta)\sqrt{\frac{\tau}{2}} + \frac{\zeta}{\sqrt{2\tau}}\right)\end{array}\right],\end{aligned} \tag{3.10}$$

$$\begin{aligned}\hat\alpha &= \sqrt{\frac{2}{\Omega}}\alpha = \left[\sqrt{(S^2+N_1)^2+1} + (S^2+N_1)\right]^{\frac{1}{2}}, \\ \hat\beta &= \sqrt{\frac{2}{\Omega}}\beta = \left[\sqrt{(S^2+N_1)^2+1} - (S^2+N_1)\right]^{\frac{1}{2}}.\end{aligned} \tag{3.11}$$

For $z \ll 2\sqrt{\nu t}$ and $t \gg 1$ the velocity field (3.8) has the approximate form

$$\begin{aligned}\frac{f}{\Omega l} = {} & 1 - e^{-\frac{W_0}{2\nu}z - \frac{\alpha z}{\sqrt{\nu}}}\cos\frac{\beta z}{\sqrt{\nu}} \\ & - \frac{e^{-\frac{W_0}{2\nu}z + (\beta^2-\alpha^2)t}}{\sqrt{\pi t}(\alpha^2+\beta^2)}\left[\begin{array}{l}(\alpha\cos 2\alpha\beta t - \beta\sin 2\alpha\beta t)\sinh\frac{\alpha z}{\sqrt{\nu}}\cos\frac{\beta z}{\sqrt{\nu}} \\ +(\beta\cos 2\alpha\beta t + \alpha\sin 2\alpha\beta t)\cosh\frac{\alpha z}{\sqrt{\nu}}\sin\frac{\beta z}{\sqrt{\nu}}\end{array}\right],\end{aligned} \tag{3.12}$$

$$\begin{aligned}\frac{g}{\Omega l} = {} & e^{-\frac{W_0}{2\nu}z - \frac{\alpha z}{\sqrt{\nu}}}\sin\frac{\beta z}{\sqrt{\nu}} \\ & - \frac{e^{-\frac{W_0}{2\nu}z + (\beta^2-\alpha^2)t}}{\sqrt{\pi t}(\alpha^2+\beta^2)}\left[\begin{array}{l}(\alpha\cos 2\alpha\beta t - \beta\sin 2\alpha\beta t)\cosh\frac{\alpha z}{\sqrt{\nu}}\sin\frac{\beta z}{\sqrt{\nu}} \\ -(\beta\cos 2\alpha\beta t + \alpha\sin 2\alpha\beta t)\sinh\frac{\alpha z}{\sqrt{\nu}}\cos\frac{\beta z}{\sqrt{\nu}}\end{array}\right].\end{aligned} \tag{3.13}$$

Blowing: In this case $W_0 < 0$, say $W_0 = -\tilde{W}_0$. The solutions of (2.11) satisfying conditions (2.13) are

$$\frac{f}{\Omega l} = 1 - e^{-\frac{\tilde{W}_0}{2\nu}z - \frac{\tilde{\alpha}z}{\sqrt{\nu}}} \cos\frac{\tilde{\beta}z}{\sqrt{\nu}} - \frac{e^{-\frac{\tilde{W}_0}{2\nu}z + (\tilde{\beta}^2 - \tilde{\alpha}^2)t}}{\sqrt{\pi t}(\tilde{\alpha}^2 + \tilde{\beta}^2)} \begin{bmatrix} (\tilde{\alpha}\cos 2\tilde{\alpha}\tilde{\beta}t - \tilde{\beta}\sin 2\tilde{\alpha}\tilde{\beta}t)\sinh\frac{\tilde{\alpha}z}{\sqrt{\nu}}\cos\frac{\tilde{\beta}z}{\sqrt{\nu}} \\ +(\tilde{\beta}\cos 2\tilde{\alpha}\tilde{\beta}t + \tilde{\alpha}\sin 2\tilde{\alpha}\tilde{\beta}t)\cosh\frac{\tilde{\alpha}z}{\sqrt{\nu}}\sin\frac{\tilde{\beta}z}{\sqrt{\nu}} \end{bmatrix}, \tag{3.14}$$

$$\frac{g}{\Omega l} = e^{-\frac{\tilde{W}_0}{2\nu}z - \frac{\tilde{\alpha}z}{\sqrt{\nu}}} \sin\frac{\tilde{\beta}z}{\sqrt{\nu}} - \frac{e^{-\frac{\tilde{W}_0}{2\nu}z + (\tilde{\beta}^2 - \tilde{\alpha}^2)t}}{\sqrt{\pi t}(\tilde{\alpha}^2 + \tilde{\beta}^2)} \begin{bmatrix} (\tilde{\alpha}\cos 2\tilde{\alpha}\tilde{\beta}t - \tilde{\beta}\sin 2\tilde{\alpha}\tilde{\beta}t)\cosh\frac{\tilde{\alpha}z}{\sqrt{\nu}}\sin\frac{\tilde{\beta}z}{\sqrt{\nu}} \\ -(\tilde{\beta}\cos 2\tilde{\alpha}\tilde{\beta}t + \tilde{\alpha}\sin 2\tilde{\alpha}\tilde{\beta}t)\sinh\frac{\tilde{\alpha}z}{\sqrt{\nu}}\cos\frac{\tilde{\beta}z}{\sqrt{\nu}} \end{bmatrix}, \tag{3.15}$$

where

$$\tilde{\alpha} = \left[\frac{1}{2}\left\{\sqrt{\left(\frac{\tilde{W}_0^2}{4\nu} + \frac{\sigma B_0^2}{\varrho}\right)^2 + \Omega^2} + \left(\frac{\tilde{W}_0^2}{4\nu} + \frac{\sigma B_0^2}{\varrho}\right)\right\}\right]^{\frac{1}{2}}, \tag{3.16}$$

$$\tilde{\beta} = \left[\frac{1}{2}\left\{\sqrt{\left(\frac{\tilde{W}_0^2}{4\nu} + \frac{\sigma B_0^2}{\varrho}\right)^2 + \Omega^2} - \left(\frac{\tilde{W}_0^2}{4\nu} + \frac{\sigma B_0^2}{\varrho}\right)\right\}\right]^{\frac{1}{2}}. \tag{3.17}$$

Once again it is found that an asymptotic solution exists for the velocity distribution unlike the case of a porous disk subjected to uniform blowing in the case of a nonrotating frame. The existence of an asymptotic solution is due to the fact that the vorticity layer thickness decreases with an increase in the rotation. It is interesting to note that the velocity boundary layer has a thickness of order $\left(\frac{W_0}{2\nu} + \frac{\alpha}{\sqrt{\nu}}\right)^{-1}$ in the case of suction and of order $\left(\frac{\tilde{W}_0}{2\nu} + \frac{\tilde{\alpha}}{\sqrt{\nu}}\right)^{-1}$ in the case of blowing. It is clear that the layer of thickness of order $\left(\frac{W_0}{2\nu} + \frac{\alpha}{\sqrt{\nu}}\right)^{-1}$ decreases with an increase in W_0 and B_0, and the layer thickness of order $\left(\frac{\tilde{W}_0}{2\nu} + \frac{\tilde{\alpha}}{\sqrt{\nu}}\right)^{-1}$ decreases with an increase in $\tilde{W}_0$ and B_0. The solution with zero magnetic field and a nonporous disk obtained by Erdogan [11] can be recovered directly from (3.12) and (3.13) with $W_0 = B_0 = 0$.

The influence of suction ($S = 0.5$), blowing ($S = -0.5$) and no porosity ($S = 0$) on the boundary layer thickness at $\tau = 12$ and $B_0 = 0$ is shown in Fig. 1. Figures 2 and 3 depict the variations of f and g in the case of a rotating permeable disk and $N_1 = 2$ for different values of τ, i.e. $\tau = .005, .05, .5, 2, 4, 6, 8, 10, 12, 14$. We observe from these figures that the boundary layer thickness steadily increases and then gives the behavior of a steady state after a certain time. In the absence of porosity and a magnetic field, a steady state is achieved at $\tau = 8$. But when there is a magnetic field and no porosity, we get a steady state rather quickly, i.e. after $\tau = .5$. In the case of suction and no magnetic field, a steady state is achieved at $\tau = 2$. Also

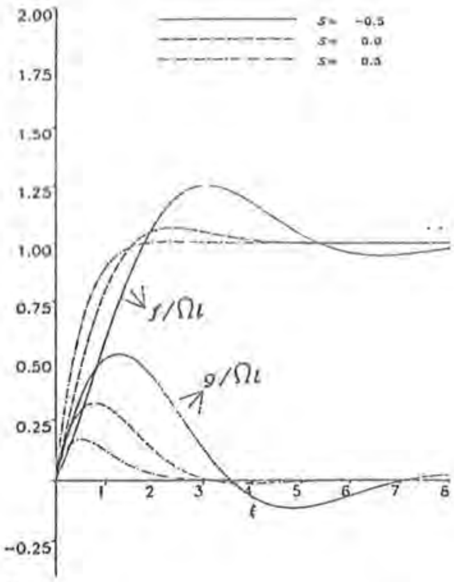

Fig. 1.

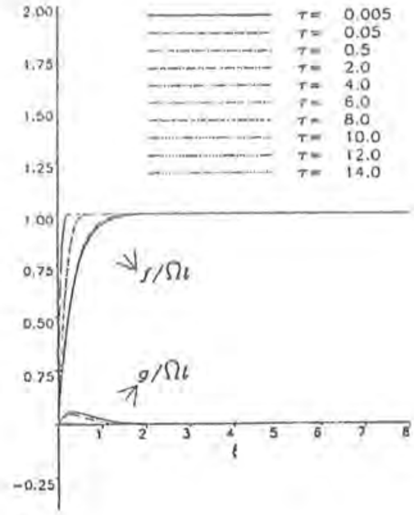

Fig. 2.

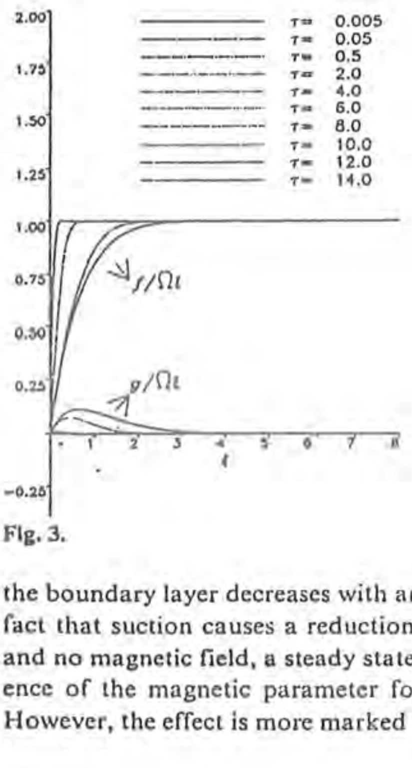

Fig. 3.

Fig. 1. The influence of suction and injection in the absence of a magnetic field ($N = 0.$) on f and g with ξ when $\tau = 12$

Fig. 2. The influence of suction ($S = 0.5$) in the presence of a magnetic field ($N = 2$) on f and g with ξ for different values of τ

Fig. 3. The influence of injection ($S = -0.5$) in the presence of a magnetic field ($N = 2$) on f and g with ξ for different values of τ

the boundary layer decreases with an increase in the suction parameter. This is in line with the fact that suction causes a reduction in the boundary layer thickness. In the case of blowing and no magnetic field, a steady state is obtained after $\tau = 10$. Further, it is seen that the influence of the magnetic parameter for both suction and blowing is to decrease the velocity. However, the effect is more marked in blowing than suction.

Acknowledgements

The comments of Prof. J. Zierep regarding an earlier version of this paper are deeply appreciated. Two of the authors, T. Hayat and S. Asghar, gratefully acknowledge the financial support of Quaid-i-Azam University research fund. Dr. Siddiqui thanks the Pennsylvania State University for the R.D.G.

References

[1] Berker, R.: Handbook of fluid dynamics, vol. VIII/3, p. 87. Berlin: Springer 1963.
[2] Coirier, J.: Rotations non-coaxiales d'un disque et d'un fluide à l'infini. J. de Mecanique 11, 317–340 (1972).
[3] Erdogan, M. E.: Flow due to eccentric rotating a porous disk and a fluid at infinity. Trans. ASME J. Appl. Mech. 43, 203–204 (1976).
[4] Gupta, A. S.: Ekman layer on a porous plate. Phys. Fluids 15(5), 930–931 (1972).
[5] Murthy, S. N., Ram, R. K. P.: Magnetohydrodynamic flow and heat transfer due to eccentric rotations of a porous disk and a fluid at infinity. Int. J. Engng Sci. 16, 943–949 (1978).
[6] Rajagopal, K. R.: On the flow of a simple fluid in an orthogonal rheometer. Arch. Rat. Mech. Anal. 79, 39–47 (1982).
[7] Rajagopal, K. R.: Flow of viscoelastic fluids between rotating disks. Theor. Comput. Fluid Dynamics 3, 185–206 (1992).
[8] Greenspan, H. P., Howard, L. N.: On a time dependent motion of a rotating fluid. J. Fluid Mech. 17, 385–404 (1963).
[9] Kasiviswanathan, S. R., Rao, A. R.: An unsteady flow due to eccentrically rotating porous disk and a fluid at infinity. Int. J. Engng Sci. 25, 1419–1425 (1987).
[10] Pop, I.: Unsteady flow due to noncoaxially rotating a disk and a fluid at infinity. Bull. Techn. Uni. Ist. 32, 14–18 (1979).
[11] Erdogan, M. E.: Unsteady flow of a viscous fluid due to non-coaxial rotations of a disk and a fluid at infinity. Int. J. Non-Linear Mech. 12, 285–290 (1997).
[12] Shercliff, J. A.: A textbook of magnetohydrodynamics. 1st ed. Oxford New York: Pergamon Press 1965.
[13] Rossow, V. J.: On flow of electrically conducting fluids over a flat plate in the presence of a transverse magnetic field. NASA Report No. 1385, p. 489 (1958).
[14] Sneddon, I. N.: The use of integral transform. New York: McGraw-Hill 1972.
[15] Campbell, G. A., Foster, R. M.: Fourier integrals for practical applications. New York: Van Nostrand 1948.
[16] Abramovitz, B. M., Stegun, I. A.: Handbook of mathematical functions, p. 325. New York: Dover 1964.

Authors' addresses: T. Hayat, S. Asghar and T. Haroon, Department of Mathematics, Quaid-i-Azam University, Islamabad, Pakistan; A. M. Siddiqui, Department of Mathematics, Pennsylvania State University, York Campus, York, Pennsylvania, 17403, USA

Verleger: Springer-Verlag KG, Sachsenplatz 4–6, A-1201 Wien. – Herausgeber: Prof. Dipl.-Ing. Dr. Hans Troger und Prof. Dipl.-Ing. Dr. Franz Ziegler, beide Technische Universität, Wiedner Hauptstraße 8–10, A-1040 Wien. – Redaktion: Wiedner Hauptstraße 8–10, A-1040 Wien. – Hersteller: Druckerei zu Altenburg GmbH, D-04600 Altenburg – Verlagsort: Wien. – Herstellungsort: Altenburg. – Printed in Germany.

Acta Mechanica 147, 99 – 109 (2001)

ACTA MECHANICA

Unsteady MHD flow of a non-Newtonian fluid due to eccentric rotations of a porous disk and a fluid at infinity

A. M. Siddiqui, York, Pennsylvania, and **T. Haroon**, **T. Hayat**, and **S. Asghar**, Islamabad, Pakistan

(Received January 18, 2000)

Summary. An exact solution of the unsteady flow of a second-order fluid due to non-coaxial rotations of a porous disk and a fluid at infinity in the presence of a uniform transverse magnetic field is investigated. It is once again shown that for uniform suction or uniform injection at the disk an asymptotic profile exists for the velocity distribution. The effects of the magnetic field, the material parameters of the second-order fluid, suction and injection on the velocity distribution are studied. Further, from the solution of a rigid disk, it is found that for parameter $\beta > .01$, a non-Newtonian effect is present in the velocity field. However, for $\beta < .01$ the velocity field becomes a Newtonian one.

1 Introduction

An investigation of MHD boundary-layers under the influence of viscous forces is of importance in understanding a variety of geophysical, astrophysical and engineering phenomena such as those that occur at the core-mantle interface of the earth. An exact solution for the flow due to non-coaxial rotations of a disk and a fluid at infinity has been implied by Berker [1]. He has considered the flow between two disks which are rotating with the same angular velocity. A general case in which rotations are performed with slightly different angular velocities has been carried out by Coirier [2]. After the initiation by Berker, there have been many works on the flow due to non-coaxial rotations of a disk and a fluid at infinity. Mention may be made of the interesting works of Erdogan [3], [4], Murthy and Ram [5], Kasiviswanathan and Rao [6], Rajagopal [7], [8], and Pop [9]. Recently, Erdogan [10] pointed out that flow due to eccentric rotations of a disk and a fluid at infinity which are impulsively started is three-dimensional and not two-dimensional as assumed by Pop [9]. To make the flow two-dimensional Erdogan [10] suggested a change in the initial condition and proposed that the disk and the fluid are initially rotating about the z'-axis and suddenly set in motion; the disk rotating about z-axis and fluid about z'-axis. He showed that the problem is two-dimensional and presented an analytical solution for the velocity field.

In view of both industrial and technological applications, considerable attention has been paid to the flow of non-Newtonian fluids due to rotating plates and disks. Srivastava [11] studied the flow of a Reiner-Rivlin fluid between rotating parallel plates using a perturbation approach. Bhatnagar [12] studied the flow between two disks of a Reiner-Rivlin fluid in which one disk is stationary and the other rotating. This model was introduced by Reiner [13] to describe the behavior of wet sand but was at one time considered as a possible model for non-Newtonian fluid behavior. The model does not account for the possibility of both normal stress differences or shear-thinning or shear-thickening and is not currently considered as a viable model for viscoelastic fluids. Erdogan [14] seems to have been the first to study the steady flow of a fluid of second order, a model [15] which allows for both the normal stress differences, due to a rotating disk, with the fluid at infinity also rotating with an angular speed. Later, Bhatnagar and Zago [16] studied the flow of a fluid of second order to two rotating disks, about a common axis. The flows of Newtonian and non-Newtonian fluids between parallel disks rotating about a common axis have been reviewed by Rajagopal [17].

The purpose of the present investigation is threefold. Firstly, the flow of a second order fluid produced by a disk which rotates non-coaxially with the fluid at infinity is considered. It is shown that the equations of motion have an exact solution. Since the equations governing the flow of non-Newtonian fluids are more complicated than the Navier-Stokes equations, to solve the equations of motion of a non-Newtonian fluid is important. Secondly, to discuss the influence of an externally applied magnetic field on the velocity distribution. Thirdly, to include the effect of porosity by taking into account the porous disk instead of a rigid disk. The solution of Erdogan [10] can be obtained as a special case of the presented analysis by taking the magnetic parameter, suction/injection velocity and material parameter of the second-order fluid to be zero.

2 The governing equations

We introduce a Cartesian coordinate system with the z-axis normal to the porous disk, which lies in the plane $z = 0$. The axes of rotation, of both the disk and the fluid, are assumed to be in the plane $x = 0$, with the distance between the axes being l. The common angular velocity of the disk and the fluid is taken as Ω. The fluid is electrically conducting and assumed to be permeated by a magnetic field B_o having no components in the x- and y-directions. We seek a solution for the velocity filed which is of the form:

$$u = -\Omega y + f(z,t)\,, \qquad v = \Omega x + g(z,t)\,, \qquad w = -w_o \tag{1}$$

$$\begin{aligned} &u = -\Omega y\,, && v = \Omega x\,, && w = -w_o\,, && \text{at} \quad z = 0\,, \quad t > 0\,, \\ &u = -\Omega(y-l)\,, && v = \Omega x\,, && w = -w_o\,, && \text{as} \quad z \to \infty \quad \text{for all} \quad t\,, \\ &u = -\Omega(y-l)\,, && v = \Omega x\,, && w = -w_o\,, && \text{at} \quad t = 0\,, \quad z > 0\,, \end{aligned} \tag{2}$$

where u, v and w are the components of the velocity. Obviously $w_o > 0$ is the suction velocity and $w_o > 0$ is the injection velocity. The unsteady motion of the electrically conducting, incompressible second order fluid is governed by the conservation laws of momentum and of mass which are

$$\varrho \frac{D\mathbf{V}}{Dt} = \nabla \cdot \mathbf{T} + \mathbf{J} \times \mathbf{B}\,, \tag{3}$$

$$\nabla \cdot \mathbf{V} = 0\,, \tag{4}$$

where $\frac{D}{Dt}$ is the usual material time derivative, ϱ is the density, $\mathbf{V}$ is the velocity vector, $\mathbf{J}$ is the electric current density, $\mathbf{B}$ is the total magnetic field so that $\mathbf{B} = \mathbf{B}_o + \mathbf{b}$, where $\mathbf{b}$ is the induced magnetic field. The magnetic Reynolds number R_m [18] is assumed to be small as is the case with most of the conducting fluids, and hence the induced magnetic field is small in comparison with the applied magnetic field and is therefore not taken into account. The magnetic body force $\mathbf{J} \times \mathbf{B}$ now becomes $\sigma(\mathbf{V} \times \mathbf{B}) \times \mathbf{B}$. Here σ is the electrical conductivity of the fluid. The Cauchy stress $\mathbf{T}$ in an incompressible fluid of second order is given by

$$\mathbf{T} = -p\mathbf{I} + \mu \mathbf{A}_1 + \alpha_1 \mathbf{A}_2 + \alpha_2 \mathbf{A}_1^2 , \tag{5}$$

where the spherical part of the stress $-p\mathbf{I}$ is due to the constraint of incompressibility, $\mu(\geq 0)$ is the viscosity, α_1 and α_2 are the normal stress moduli satisfying $\alpha_1 > 0, \alpha_1 + \alpha_2 = 0$ [19], and $\mathbf{A}_1$ and $\mathbf{A}_2$ are the kinematical tensors [20] given by

$$\mathbf{A}_1 = (\text{grad}\,\mathbf{V}) + (\text{grad}\,\mathbf{V})^T ,$$

$$\mathbf{A}_2 = \frac{D\mathbf{A}_1}{Dt} + \mathbf{A}_1(\text{grad}\,\mathbf{V}) + (\text{grad}\,\mathbf{V})^T \mathbf{A}_1 . \tag{6}$$

In view of the assumption of small R_m, Eqs. (1) and (5), we have from Eq. (3)

$$\varrho\left[\frac{\partial f}{\partial t} - \Omega^2 x - \Omega g - w_o \frac{\partial f}{\partial z}\right] = -\frac{\partial P}{\partial x} + \mu \frac{\partial^2 f}{\partial z^2} - \sigma B_o^2 (f - \Omega y) + \alpha_1 \left[\frac{\partial^3 f}{\partial t \partial z^2} - w_o \frac{\partial^3 f}{\partial z^3} + \Omega \frac{\partial^2 g}{\partial z^2}\right] , \tag{7}$$

$$\varrho\left[\frac{\partial g}{\partial t} - \Omega^2 y + \Omega f - w_o \frac{\partial g}{\partial z}\right] = -\frac{\partial P}{\partial y} + \mu \frac{\partial^2 g}{\partial z^2} - \sigma B_o^2 (g + \Omega x) + \alpha_1 \left[\frac{\partial^3 g}{\partial t \partial z^2} - w_o \frac{\partial^3 g}{\partial z^3} - \Omega \frac{\partial^2 f}{\partial z^2}\right] ; \tag{8}$$

$$\sigma B_o^2 w_o = \frac{\partial P}{\partial z} , \tag{9}$$

together with

$$\begin{aligned} &f(0,t) = 0 , && g(0,t) = 0 , && \text{for } \; t > 0 , \\ &f(\infty,t) = \Omega l , && g(\infty,t) = 0 , && \text{for all } \; t , \\ &f(z,0) = \Omega l , && g(z,0) = 0 , && \text{for } \; z > 0 , \end{aligned} \tag{10}$$

where

$$P = p - (2\alpha_1 + \alpha_2)\left\{\left(\frac{\partial f}{\partial z}\right)^2 + \left(\frac{\partial g}{\partial z}\right)^2\right\} . \tag{11}$$

Eliminating P from (7) to (9) and using boundary condition (10), we get

$$\alpha \frac{\partial^3 F^*}{\partial t \partial z^2} - \alpha w_o \frac{\partial^3 F^*}{\partial z^3} + (\nu - i\alpha\Omega) \frac{\partial^2 F^*}{\partial z^2} + w_o \frac{\partial F^*}{\partial z} - \frac{\partial F^*}{\partial t} - \Omega\left(i + \frac{\sigma}{\varrho\Omega} B_o^2\right) F^* = -\Omega^2 l \left(i + \frac{\sigma}{\varrho\Omega} B_o^2\right) , \tag{12}$$

with the following initial and boundary conditions:

$$F^*(0,t) = 0 , \qquad F^*(\infty,t) = \Omega l , \qquad F^*(z,0) = \Omega l , \tag{13}$$

where

$$\alpha = \frac{\alpha_1}{\varrho}, \qquad \nu = \frac{\mu}{\varrho}, \qquad F^* = f + ig. \tag{14}$$

We note that for $\alpha_1 = B_o = w_o = 0$ Eq. (12) corresponds to the differential equation for classical viscous fluids [10].

Introducing

$$\xi = \sqrt{\frac{\Omega}{2\nu}} z, \qquad \tau = \Omega t, \qquad \beta = \frac{\Omega}{\nu} \alpha, \qquad \varepsilon = \frac{w_o}{\sqrt{2\nu\Omega}}, \qquad N = \frac{\sigma}{\varrho\Omega} B_o^2,$$
$$F(\xi, \tau) = \frac{F^*}{\Omega l} - 1, \qquad H(\xi, \tau) = F(\xi, \tau) e^{i\tau}, \tag{15}$$

Eq. (12) and conditions (13) become

$$\beta \frac{\partial^3 H}{\partial \tau \partial \xi^2} - \beta\varepsilon \frac{\partial^3 H}{\partial \xi^3} + (1 - 2i\beta) \frac{\partial^2 H}{\partial \xi^2} + 2\varepsilon \frac{\partial H}{\partial \xi} - 2 \frac{\partial H}{\partial \tau} - 2NH = 0, \tag{16}$$

$$H(0, \tau) = -e^{i\tau}, \qquad H(\infty, \tau) = 0, \qquad H(\xi, 0) = 0. \tag{17}$$

3 Solution of the problem

Let us suppose that $H(\xi, \tau)$ is an arbitrary function that has a Laplace transform in the variable τ. That is,

$$\bar{H}(\xi, s) = \int_0^\infty H e^{-s\tau} d\tau. \tag{18}$$

Using (18), the initial-boundary value problem in the transformed s-plane can be written as

$$\beta\varepsilon \bar{H}''' - (1 - 2i\beta + \beta s) \bar{H}'' - 2\varepsilon \bar{H}' + 2(s + N) \bar{H} = 0, \tag{19}$$

$$\bar{H}(0, s) = -\frac{1}{s - i}, \qquad \bar{H}(\infty, s) = 0, \tag{20}$$

where primes denote differentiation with respect to ξ.

Before proceeding with the solution of the above problem it would be interesting to remark here that although in the classical viscous case ($\alpha_1 = 0 = \alpha_2$) we encounter a differential equation of order two [10], the presence of material parameters of the second order fluid increases the order to three. It would, therefore, seem that an additional boundary condition must be imposed in order to get a unique solution. The difficulty, in the present case, is however removed by seeking a solution of the form [21]

$$\bar{H} = \bar{H}_1 + \beta \bar{H}_2 + O(\beta^2) \tag{21}$$

which is valid for small values of β only.

Substituting expression (21) into Eq. (19) and boundary conditions (20), and then collecting terms of like powers of β, one obtains the following systems of differential equations along with the appropriate boundary conditions:

3.1 System of order zero

$$\bar{H}_1'' + 2\varepsilon \bar{H}_1' - 2(s + N)\,\bar{H}_1 = 0\,,$$
$$\bar{H}_1(0, s) = -\frac{1}{s-i}\,, \qquad \bar{H}_1(\infty, s) = 0\,. \tag{22}$$

3.2 System of order one

$$\varepsilon \bar{H}_1''' - \bar{H}_2'' - (s - 2i)\,\bar{H}_1'' - 2\varepsilon \bar{H}_2' + 2(s + N)\,\bar{H}_2 = 0\,,$$
$$\bar{H}_2(0, s) = 0\,, \qquad \bar{H}_2(\infty, s) = 0\,. \tag{23}$$

Solving the systems (22) and (23) and then using Eq. (21) we arrive at

$$\bar{H}(\xi, s) = -\frac{1}{s-i}\, e^{-\left(\varepsilon + \sqrt{\varepsilon^2+2s}\right)\xi} - \frac{\beta\xi e^{-\left(\varepsilon+\sqrt{\varepsilon^2+2(s+N)}\right)\xi}}{(s-i)\sqrt{\varepsilon^2+2(s+N)}}\Big[2\varepsilon^4 + 3\varepsilon^2(s+N)$$
$$+ (\varepsilon^2 + s + N)\,(s - 2i) + \varepsilon(2\varepsilon^2 + 2s + N - 2i)\sqrt{\varepsilon^2 + 2(s+N)}\Big]\,. \tag{24}$$

Note that the first term in Eq. (24) corresponds to the zeroth-order solution while all the other terms correspond to the first-order solution. The inverse of $\bar{H}$ is calculated and is given by

$$H(\xi, \tau) = e^{-(\varepsilon+Y)\xi + i\tau} erfc\left(\frac{\xi}{\sqrt{2\tau}} - Y\sqrt{\frac{\tau}{2}}\right)\Big[-\frac{1}{2}\left(1 + \xi\beta\big(2\varepsilon^3 + \varepsilon(N-2i)\big)\right)$$
$$- \frac{\xi\beta}{4Y}\left(2\varepsilon^4 + 3\varepsilon^2 N - 2i(\varepsilon^2+N)\right) - \frac{i\xi\beta}{2Y}\left(4\varepsilon^2 + N - 2i\right) + \frac{\xi\beta}{2Y} - i\xi\beta\varepsilon\Big]$$
$$+ e^{-(\varepsilon-Y)\xi + i\tau} erfc\left(\frac{\xi}{\sqrt{2\tau}} + Y\sqrt{\frac{\tau}{2}}\right)\Big[-\frac{1}{2}\left(1 + \xi\beta\big(2\varepsilon^3 + \varepsilon(N-2i)\big)\right)$$
$$+ \frac{\xi\beta}{4Y}\left(2\varepsilon^4 + 3\varepsilon^3 N - 2i(\varepsilon^2+N)\right) + \frac{i\xi\beta}{2Y}\left(4\varepsilon^2 + N - 2i\right) - \frac{\xi\beta}{2Y} - i\xi\beta\varepsilon\Big]$$
$$- \frac{\xi\beta}{\sqrt{2\pi\tau}}\left(4\varepsilon^2 + N - 2i\right) e^{-\varepsilon\xi - \frac{\xi^2}{2\tau} - (\varepsilon^2+2N)\frac{\tau}{2}} + \frac{\xi\beta}{2\sqrt{2\pi\tau}}\left(\varepsilon^2 + 2N - 2i\right) e^{-\varepsilon\xi - \frac{\xi^2}{2\tau} - (\varepsilon^2+2N)\frac{\tau}{2}}$$
$$- \frac{2\varepsilon\xi^2\beta}{\sqrt{2\pi\tau^3}}\, e^{-\varepsilon\xi - \frac{\xi^2}{2\tau} - (\varepsilon^2+2N)\frac{\tau}{2}}\,, \tag{25}$$

where $Y = \sqrt{\varepsilon^2 + 2(i+N)}$.
With the help of Eqs. (14), (15) and (25) we have:

$$\frac{f}{\Omega l} + i\,\frac{g}{\Omega l} = 1 + e^{-z_1\xi}(\cos b\xi - i\sin b\xi)\, erfc\left(\frac{\xi}{\sqrt{2\tau}} - (a+ib)\sqrt{\frac{\tau}{2}}\right)$$
$$\left[-\frac{1}{2} - \xi\beta\left\{\varepsilon^2 + \frac{\varepsilon N}{2} + \frac{(a-ib)}{2(a^2+b^2)}\left(\varepsilon^4 + \frac{3}{2}\,\varepsilon^2 N + 3i\varepsilon^2 + 1\right)\right\}\right]$$
$$+ e^{-z_2\xi}(\cos b\xi + i\sin b\xi)\, erfc\left(\frac{\xi}{\sqrt{2\tau}} + (a+ib)\sqrt{\frac{\tau}{2}}\right) \tag{26}$$

$$\left[-\frac{1}{2}-\xi\beta\left\{\varepsilon^2+\frac{\varepsilon N}{2}+\frac{(a-ib)}{2(a^2+b^2)}\left(\varepsilon^4+\frac{3}{2}\varepsilon^2 N+3i\varepsilon^2+1\right)\right\}\right]$$
$$+\frac{e^{-\varepsilon\xi-\frac{\xi^2}{2\tau}-(\varepsilon^2+2N)\frac{\tau}{2}}}{\sqrt{2\pi\tau}}\xi\beta(\cos\tau-i\sin\tau)\left[-\frac{7\varepsilon^2}{2}+i-\frac{2\xi\varepsilon}{\tau}\right], \tag{26}$$

where

$$z_1=\varepsilon+a,\qquad z_2=\varepsilon-a,$$

$$a=\left(\frac{\sqrt{(\varepsilon^2+2N)^2+4}+(\varepsilon^2+2N)}{2}\right)^{\frac{1}{2}},$$

$$b=\left(\frac{\sqrt{(\varepsilon^2+2N)^2+4}-(\varepsilon^2+2N)}{2}\right)^{\frac{1}{2}}.$$

For large times, Eq. (26) can be written in the form:

$$\frac{f}{\Omega l}+i\,\frac{g}{\Omega l}=\left[1-e^{-z_1\xi}(\cos b\xi-i\sin b\xi)\left\{1+\xi\beta\left(2\varepsilon^3+\varepsilon N\right.\right.\right.$$
$$\left.\left.\left.+\frac{(a-ib)}{(a^2+b^2)}\left(2\varepsilon^4+3\varepsilon^2 N+1-i(N-2\varepsilon^2)\right)\right)\right\}\right]$$
$$+\left[e^{-z_1\xi}(\cos b\xi-i\sin b\xi)\,erfc\left(\frac{\xi}{\sqrt{2\tau}}-(a+ib)\sqrt{\frac{\tau}{2}}\right)\right.$$
$$\left\{-\frac{1}{2}-\xi\beta\left(\varepsilon^3+\frac{\varepsilon N}{2}+\frac{(a-ib)}{2(a^2+b^2)}\left(\varepsilon^4+\frac{3}{2}\varepsilon^2 N+3i\varepsilon^2+1\right)\right)\right\}$$
$$+e^{-z_2\xi}(\cos b\xi+i\sin b\xi)\,erfc\left(\frac{\xi}{\sqrt{2\tau}}+(a+ib)\sqrt{\frac{\tau}{2}}\right)$$
$$\left\{-\frac{1}{2}-\xi\beta\left(\varepsilon^3+\frac{\varepsilon N}{2}-\frac{(a-ib)}{2(a^2+b^2)}\left(\varepsilon^4+\frac{3}{2}\varepsilon^2 N+3i\varepsilon^2+1\right)\right)\right\}$$
$$\left.+\frac{e^{-\varepsilon\xi-\frac{\xi^2}{2\tau}-(\varepsilon^2+2N)\frac{\tau}{2}}}{\sqrt{2\pi\tau}}\xi\beta(\cos\tau-i\sin\tau)\left\{-\frac{7\varepsilon^2}{2}+i-\frac{2\xi\varepsilon}{\tau}\right\}\right], \tag{27}$$

where the first term in bracket [.] on the right-hand side corresponds to the steady state and the second denotes the deviation from it.

For $\xi \ll \sqrt{2\tau}$ and $\tau \gg 1$ we get the approximate form:

$$\frac{f}{\Omega l}=1-e^{-z_1\xi}\cos b\xi-e^{-z_1\xi}\frac{\xi\beta}{(a^2+b^2)}[\{a(2\varepsilon^4+3\varepsilon^2 N+1)-b(N-2\varepsilon^2)\}\cos b\xi$$
$$-\{b(2\varepsilon^4+3\varepsilon^2 N+1)+a(N-2\varepsilon^2)\}\sin b\xi]-\xi\beta e^{-z_1\xi}(2\varepsilon^3+\varepsilon N)\cos b\xi$$
$$+\frac{e^{-z_1\xi-(a^2-b^2)\frac{\tau}{2}}}{\sqrt{\frac{\pi\tau}{2}}(a^2+b^2)}\left[\left(\frac{a}{2}+a\xi\beta\left(\varepsilon^3+\frac{\varepsilon N}{2}\right)+\frac{(a^2-b^2)}{2(a^2+b^2)}\xi\beta\left(\varepsilon^4+\frac{3}{2}\varepsilon^2 N+1\right)\right.\right.$$
$$\left.+\frac{3ab\xi\beta\varepsilon^2}{(a^2+b^2)}\right)\cos(b\xi+ab\tau)-\left(\frac{b}{2}+b\xi\beta\left(\varepsilon^3+\frac{\varepsilon N}{2}\right)+\frac{ab\xi\beta}{(a^2+b^2)}\left(\varepsilon^4+\frac{3}{2}\varepsilon^2 N+1\right)\right. \tag{28}$$

$$-\frac{3(a^2-b^2)}{2(a^2+b^2)}\xi\beta\varepsilon^2\Big)\sin(b\xi+ab\tau)\Big]-\frac{e^{-z_1\xi-(a^2-b^2)\frac{\tau}{2}}}{\sqrt{\frac{\pi\tau}{2}}(a^2+b^2)}\Big[\Big(\frac{a}{2}+a\xi\beta\Big(\varepsilon^3+\frac{\varepsilon N}{2}\Big)$$

$$-\frac{(a^2-b^2)}{2(a^2+b^2)}\xi\beta\Big(\varepsilon^4+\frac{3}{2}\varepsilon^2N+1\Big)-\frac{3ab\xi\beta\varepsilon^2}{(a^2+b^2)}\Big)\cos(b\xi-ab\tau)+\Big(\frac{b}{2}+b\xi\beta\Big(\varepsilon^3+\frac{\varepsilon N}{2}\Big)$$

$$-\frac{ab\xi\beta}{(a^2+b^2)}\Big(\varepsilon^4+\frac{3}{2}\varepsilon^2N+1\Big)+\frac{3(a^2-b^2)}{2(a^2+b^2)}\xi\beta\varepsilon^2\Big)\sin(b\xi-ab\tau)\Big], \tag{28}$$

$$\frac{g}{\Omega l}=e^{-z_1\xi}\sin b\xi+e^{-z_1\xi}\frac{\xi\beta}{(a^2+b^2)}[\{a(2\varepsilon^4+3\varepsilon^2N+1)-b(N-2\varepsilon^2)\}\sin b\xi$$

$$+\{b(2\varepsilon^4+3\varepsilon^2N+1)+a(N-2\varepsilon^2)\}\cos b\xi]+\xi\beta e^{-z_1\xi}(2\varepsilon^3+\varepsilon N)\sin b\xi$$

$$-\frac{e^{-z_1\xi-(a^2-b^2)\frac{\tau}{2}}}{\sqrt{\frac{\pi\tau}{2}}(a^2+b^2)}\Big[\Big(\frac{a}{2}+a\xi\beta\Big(\varepsilon^3+\frac{\varepsilon N}{2}\Big)+\frac{(a^2-b^2)}{2(a^2+b^2)}\xi\beta\Big(\varepsilon^2+\frac{3}{2}\varepsilon^2N+1\Big)$$

$$+\frac{3ab\xi\beta\varepsilon^2}{(a^2+b^2)}\Big)\sin(b\xi+ab\tau)+\Big(\frac{b}{2}+b\xi\beta\Big(\varepsilon^3+\frac{\varepsilon N}{2}\Big)+\frac{ab\xi\beta}{(a^2+b^2)}\Big(\varepsilon^4+\frac{3}{2}\varepsilon^2N+1\Big)$$

$$-\frac{3(a^2-b^2)}{2(a^2+b^2)}\xi\beta\varepsilon^2\Big)\cos(b\xi+ab\tau)-\Big(\frac{b}{2}+b\xi\beta\Big(\varepsilon^3+\frac{\varepsilon N}{2}\Big)-\frac{ab\xi\beta}{(a^2+b^2)}\Big(\varepsilon^4+\frac{3}{2}\varepsilon^2N+1\Big)$$

$$+\frac{3\xi\beta\varepsilon^2(a^2-b^2)}{2(a^2+b^2)}\Big)\cos(b\xi-ab\tau)+\Big(\frac{a}{2}+a\xi\beta\Big(\varepsilon^3+\frac{\varepsilon N}{2}\Big)$$

$$-\frac{(a^2-b^2)}{2(a^2+b^2)}\xi\beta\Big(\varepsilon^4+\frac{3}{2}\varepsilon^2N+1\Big)-\frac{3ab\xi\beta\varepsilon^2}{(a^2+b^2)}\Big)\sin(b\xi-ab\tau)\Big]. \tag{29}$$

4 Injection

In the case of injection $\varepsilon < 0$, and we take $\varepsilon = -\delta$ so that $\delta > 0$. The asymptotic solution is given by

$$\frac{f}{\Omega l}+\iota\frac{g}{\Omega l}=1+e^{-x_1\xi}(\cos d\xi-i\sin d\xi)\,erfc\Big(\frac{\xi}{\sqrt{2\tau}}-(c+id)\sqrt{\frac{\tau}{2}}\Big)$$

$$\Big[-\frac{1}{2}+\xi\beta\Big\{\delta^3+\frac{\delta N}{2}-\frac{(c-id)}{2(c^2+d^2)}\Big(\delta^4+\frac{3\delta^2N}{2}+3i\delta^2+1\Big)\Big\}\Big]$$

$$+e^{x_2\xi}(\cos d\xi+i\sin d\xi)\,erfc\Big(\frac{\xi}{\sqrt{2\tau}}+(c+id)\sqrt{\frac{\tau}{2}}\Big)$$

$$\Big[-\frac{1}{2}+\beta\xi\Big\{\delta^3+\frac{\delta N}{2}+\frac{(c-id)}{2(c^2+d^2)}\Big(\delta^4+\frac{3\delta^2N}{2}+3i\delta^2+1\Big)\Big\}\Big]$$

$$+\frac{e^{\delta\xi-\frac{\xi^2}{2\tau}-(\delta^2+2N)\frac{\tau}{2}}}{\sqrt{2\pi\tau}}\xi\beta(\cos\tau-i\sin\tau)\Big[-\frac{7\delta^2}{2}+i+\frac{2\xi\delta}{\tau}\Big], \tag{30}$$

where

$x_1 = c-\delta, \qquad x_2 = c+\delta,$

and

$$c=\left\{\frac{\sqrt{(\delta^2+2N)^2+4}+(\delta^2+2N)}{2}\right\}^{\frac{1}{2}},$$

$$d=\left\{\frac{\sqrt{(\delta^2+2N)^2+4}-(\delta^2+2N)}{2}\right\}^{\frac{1}{2}}.$$

For large times, Eq. (30) can be written in the form:

$$\begin{aligned}\frac{f}{\Omega l}+i\,\frac{g}{\Omega l}=&\Bigg[1-e^{-z_1\xi}(\cos d\xi-i\sin d\xi)\left\{1-\xi\beta\Bigg(2\delta^3+\delta N\right.\\&\left.-\frac{(c-id)}{(c^2+d^2)}\left(2\delta^4+3\delta^2N+1-i(N-2\delta^2)\right)\Bigg)\right\}\Bigg]\\&+\Bigg[e^{-z_1\xi}(\cos d\xi-i\sin d\xi)\,erfc\left(\frac{\xi}{\sqrt{2\tau}}-(c-id)\sqrt{\frac{\tau}{2}}\right)\\&\left\{-\frac{1}{2}+\xi\beta\left(\delta^3+\frac{\delta N}{2}-\frac{(c-id)}{(c^2+d^2)}\left\{\delta^4+\frac{3\delta^2N}{2}+3i\delta^2+1\right\}\right)\right\}\\&+e^{z_1\xi}(\cos d\xi+i\sin d\xi)\,erfc\left(\frac{\xi}{\sqrt{2\tau}}+(c+id)\sqrt{\frac{\tau}{2}}\right)\\&\left\{-\frac{1}{2}+\xi\beta\left(\delta^3+\frac{\delta N}{2}+\frac{(c-id)}{(c^2+d^2)}\left\{\delta^4+\frac{3\delta^2N}{2}+3i\delta^2+1\right\}\right)\right\}\\&+\frac{e^{\delta\xi-\frac{\xi^2}{2\tau}-(\delta^2+2N)\frac{\tau}{2}}}{\sqrt{2\pi\tau}}\,\xi\beta(\cos\tau-i\sin\tau)-\frac{7\delta^2}{2}+i+\frac{2\xi\delta}{\tau}\Bigg\}\Bigg].\end{aligned}\tag{31}$$

For $\xi \ll \sqrt{2\tau}$ and $\tau \gg 1$ we get the approximate form:

$$\begin{aligned}\frac{f}{\Omega l}=&1-e^{-z_1\xi}\cos d\xi-e^{-z_1\xi}\frac{\xi\beta}{(c^2+d^2)}\left[\{c(2\delta^4+3\delta^2N+1)\right.\\&\left.-d(N-2\delta^2)\}\cos d\xi-\{d(2\delta^4+3\delta^2N+1)+c(N-2\delta^2)\}\sin d\xi\right]\\&+\xi\beta e^{-z_1\xi}(2\delta^3+\delta N)\cos d\xi+\frac{e^{-z_1\xi-(c^2-d^2)\frac{\tau}{2}}}{\sqrt{\frac{\pi\tau}{2}}(c^2+d^2)}\left[\left(\frac{c}{2}-c\xi\beta\left(\delta^3+\frac{\delta N}{2}\right)\right.\right.\\&\left.+\frac{(c^2-d^2)}{2(c^2+d^2)}\xi\beta\left(\delta^4+\frac{3}{2}\delta^2N+1\right)+\frac{3cd\xi\beta\delta^2}{(c^2+d^2)}\right)\cos(c\xi+cd\tau)\\&-\left(\frac{d}{2}-d\xi\beta\left(\delta^3+\frac{\delta N}{2}\right)+\frac{cd\xi\beta}{(c^2+d^2)}\left(\delta^4+\frac{3}{2}\delta^2N+1\right)\right.\\&\left.\left.-\frac{3(c^2-d^2)}{2(c^2+d^2)}\xi\beta\delta^2\right)\sin(d\xi+cd\tau)\right]-\frac{e^{z_1\xi-(c^2-d^2)\frac{\tau}{2}}}{\sqrt{\frac{\pi\tau}{2}}(c^2+d^2)}\left[\left(\frac{c}{2}-c\xi\beta\left(\delta^3+\frac{\delta N}{2}\right)\right.\right.\\&\left.-\frac{(c^2-d^2)}{2(c^2+d^2)}\xi\beta\left(\delta^4+\frac{3}{2}\delta^2N+1\right)-\frac{3cd\xi\beta\delta^2}{(c^2+d^2)}\right)\cos(d\xi-cd\tau)\end{aligned}\tag{32}$$

$$
+\left(\frac{d}{2}-d\xi\beta\left(\delta^3+\frac{\delta N}{2}\right)-\frac{cd\xi\beta}{(c^2+d^2)}\left(\delta^4+\frac{3}{2}\delta^2 N+1\right)
+\frac{3(c^2-d^2)}{2(c^2+d^2)}\,\xi\beta\delta^2\right)\sin(d\xi-cd\tau)\Bigg], \tag{32}
$$

$$
\begin{aligned}
\frac{g}{\Omega l}={}& e^{-z_1\xi}\sin d\xi+e^{-z_1\xi}\frac{\xi\beta}{(c^2+d^2)}\left[\{c(2\delta^4+3\delta^2N+1)-d(N-2\delta^2)\}\sin d\xi\right.\\
&\left.+\{d(2\delta^4+3\delta^2N+1)+c(N-2\delta^2)\}\cos d\xi\right]-\xi\beta e^{-z_1\xi}(2\delta^3+\delta N)\sin d\xi\\
&-\frac{e^{-z_1\xi-(c^2-d^2)\xi}}{\sqrt{\frac{\pi\tau}{2}}\,(c^2+d^2)}\left[\left(\frac{c}{2}-c\xi\beta\left(\delta^3+\frac{\delta N}{2}\right)+\frac{(c^2-d^2)}{2(c^2+d^2)}\xi\beta\left(\delta^4+\frac{3}{2}\delta^2N+1\right)\right.\right.\\
&+\left.\frac{3cd\xi\beta\delta^2}{(c^2+d^2)}\right)\sin(d\xi+cd\tau)+\left(\frac{d}{2}-d\xi\beta\left(\delta^3+\frac{\delta N}{2}\right)+\frac{cd\xi\beta}{(c^2+d^2)}\left(\delta^4+\frac{3}{2}\delta^2N+1\right)\right.\\
&-\left.\frac{3(c^2-d^2)}{2(c^2+d^2)}\xi\beta\delta^2\right)\cos(d\xi+cd\tau)-\left(\frac{d}{2}-d\xi\beta\left(\delta^3+\frac{\delta N}{2}\right)\right.\\
&-\left.\frac{cd\xi\beta}{(c^2+d^2)}\left(\delta^4+\frac{3}{2}\delta^2N+1\right)+\frac{3\xi\beta\delta^2(c^2-d^2)}{2(c^2+d^2)}\right)\cos(d\xi-cd\tau)\\
&+\left.\left(\frac{c}{2}-c\xi\beta\left(\delta^3+\frac{\delta N}{2}\right)-\frac{(c^2-d^2)}{2(c^2+d^2)}\xi\beta\left(\delta^4+\frac{3}{2}\delta^2N+1\right)-\frac{3cd\xi\beta\delta^2}{(c^2+d^2)}\right)\sin(d\xi-cd\tau)\right].
\end{aligned} \tag{33}
$$

5 Discussion

In order to get the nature of the velocity distribution near the disk the expressions for f and g are plotted.

When suction and a magnetic field are absent, i.e., $\varepsilon=0, N=0$ in Eqs. (28) and (29), the effect of the material constant β is shown in Fig. 1. We note that for small values of β we get the same velocity profile, and the fluid behaves like a Newtonian fluid which is in agreement

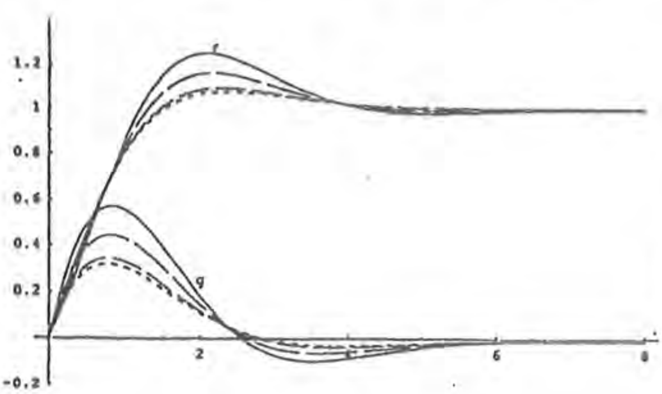

Fig. 1. Variation in f and g with ξ for $\tau=12$ without suction or magnetic field for different values of β;
---- $\beta=0$, – – – – $\beta=.1$, ——— $\beta=.5$, ——— $\beta=1$

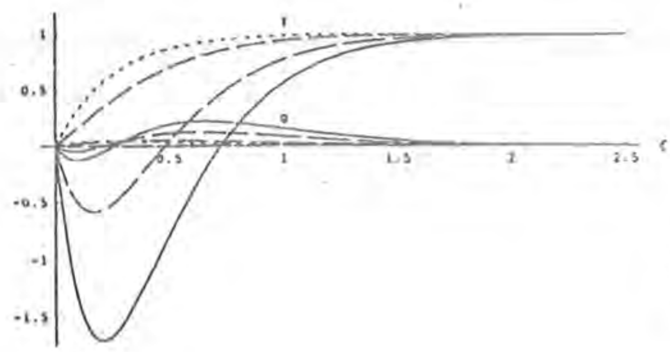

Fig. 2. Variation in f and g with ξ for $\tau = 12$ and $\varepsilon = 2$, $N = 0$; ···· $\beta = 0$, ---- $\beta = .1$, — — — $\beta = .5$, —— $\beta = 1$

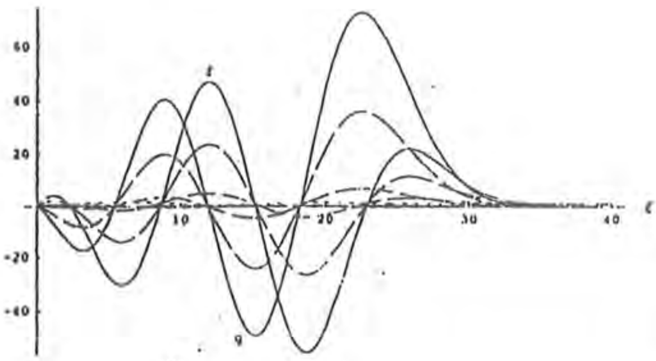

Fig. 3. Variation in f and g with ξ for $\tau = 12$ and $\varepsilon = -2$, $N = 0$; ···· $\beta = 0$, ---- $\beta = .1$, — — — $\beta = .5$, —— $\beta = 1$

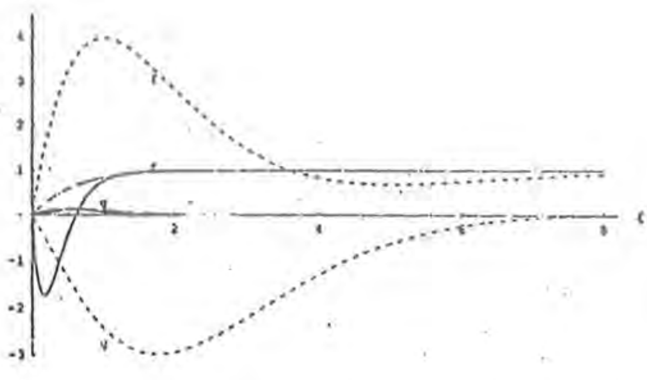

Fig. 4. Variation in f and g with ξ for $\tau = 12$ for different values of ε, $N = 2$, and $\beta = 1$; ---- $\varepsilon = -2$, ---- $\varepsilon = 0$, —— $\varepsilon = 2$

with [22]. However, β starts influencing the flow field for its values near .01. We further observe that the boundary-layer thickness increases with the increase in β.

Figure 2 shows the effect of β in the presence of suction, $\varepsilon = 2$, without magnetic field ($N = 0$). We found that the boundary-layer thickness is controlled by the suction parameter, i.e., it decreases with an increase in the suction parameter.

In the case of injection, $\delta = 2$ and $N = 0$, the boundary-layer thickness becomes very large as is expected physically which is shown in Fig. 3.

Figure 4 gives the variation in f and g for the cases when $\beta = 1, N = 2$ (—— for suction $\varepsilon = 2$, ---- without suction or injection, ····· for injection $\delta = 2$).

Comparing Figs. 3 and 4, we observe that the boundary-layer thickness is drastically decreased by introducing a magnetic field. The magnetic field can control the boundary-layer structure of a fluid which is enhanced by introducing a suction parameter.

References

[1] Berker, R.: Handbook of fluid dynamics, vol. VIII/3. Berlin: Springer 1963.
[2] Coirier, J.: Rotations non-coaxiales d'un disque et d'un fluide l'infini. J. de Mecanique 11, 317–340 (1972).
[3] Erdogan, M. E.: Flow due to eccentric rotating a porous disk and a fluid at infinity. Trans. ASME J. Appl. Mech. 43, 203–204 (1976).
[4] Erdogan, M. E.: Flow due to noncoaxial rotations of a porous disk and fluid at infinity. Rev. Roum. Méc. Appl. 22, 171–178 (1977).
[5] Murthy, S. N., Ram, R. K. P.: MHD flow and heat transfer due to eccentric rotations of a porous disk and a fluid at infinity. Int. J. Engng Sci. 16, 943–949 (1978).
[6] Kasiviswanathan, S. R., Rao, A. R.: An unsteady flow due to eccentrically rotating porous disk and a fluid at infinity. Int. J. Engng Sci. 25, 1419–1425 (1987).
[7] Rajagopal, K. R.: On the flow of a simple fluid in an orthogonal rheometer. Arch. Rat. Mech. Anal 79, 39–47 (1982).
[8] Rajagopal, K. R.: A class of exact solutions to the Navier-Stokes equations. Int. J. Engng Sci. 22, 451–455 (1984).
[9] Pop, I.: Unsteady flow due to noncoaxially rotating a disk and a fluid at infinity. Bull. Tech. Uni. Ist. 32, 14–18 (1979).
[10] Erdogan, M. E.: Unsteady flow of a viscous fluid due to noncoaxial rotations of a disk and a fluid at infinity. Int. J. Non-Linear Mech. 32, 285–290 (1997).
[11] Srivastava, A. C.: The effect of magnetic field on the flow between two non-parallel planes. Quart. J. Math. Mech. 14, 353–359 (1961).
[12] Bhatnagar, R. K.: Proc. Indian Acad. Sci. 58, 279–289 (1963).
[13] Reiner, M.: A mathematical theory of dilatancy. Amer. J. Math. 67, 350–354 (1945).
[14] Erdogan, M. E.: Non-Newtonian flow due to noncoaxial rotations of a disk and a fluid at infinity. ZAMM 56, 141–146 (1976).
[15] Truesdell, C., Noll, W.: Handbuch der Physik, vol. III, Chapter: The nonlinear field theories of mechanics, pp. 3–23. Berlin Heidelberg New York: Springer 1965.
[16] Bhatnagar, R. K., Zago, J. V.: Numerical investigations of flow of a viscoelastic fluid between rotating coaxial disks. Rheol. Acta 17, 557–569 (1978).
[17] Rajagopal, K. R.: Flow of viscoelastic fluids between rotating disks. Theor. Comput. Fluid Dynamics 3, 185–206 (1992).
[18] Shercliff, J. A.: A textbook of magnetohydrodynamics. Ist ed. Oxford New York: Pergamon 1965.
[19] Dunn, J. E., Fosdick, R. L.: Thermodynamics, stability and boundedness of fluids of complexity 2 and fluids of second grade. Arch. Rat. Mech. Anal. 3, 191–252 (1974).
[20] Rivlin, R. S., Ericksen, J. L.: Stress-deformation relations for isotropic materials. Arch. Rat. Mech. Anal. 4, 323–425 (1955).
[21] Erdogan, M. E.: On the flow of a non-Newtonian fluid past a porous flat plate. ZAMM 55, 79–83 (1975).
[22] Pontrelli, G., Bhatnagar, R. K.: Flow of a viscoelastic fluid between two rotating circular cylinders subject to suction or injection. Int. J. Num. Meth. Fluids 24, 337–349 (1997).

Authors' addresses: A. M. Siddiqui, Department of Mathematics, Pennsylvania State University, York Campus, York, Pennsylvania 17403, U.S.A. T. Haroon, T. Hayat, and S. Asghar, Department of Mathematics, Quaid-I-Azam University, Islamabad, Pakistan

NLM779 pp: 1–11 (col.fig.: nil) PROD. TYPE: COM ED: Mamatha PAGN: Anitha – SCAN: Bindu

ARTICLE IN PRESS

INTERNATIONAL JOURNAL OF NON-LINEAR MECHANICS

PERGAMON International Journal of Non-Linear Mechanics ■■ (■■■■) ■■■–■■■

www.elsevier.com/locate/ijnonlinmec

MHD flow of a third-grade fluid due to eccentric rotations of a porous disk and a fluid at infinity

T. Hayat[a], Tahira Haroon[a], S. Asghar[a], A.M. Siddiqui[b,*]

[a] *Department of Mathematics, Quaid-I-Azam University, Islamabad, Pakistan*
[b] *Department of Mathematics, Pennsylvania State University, York Campus, York, PA 17403, USA*

Received 20 November 2000; received in revised form 5 August 2001

Abstract

The problem of magnetohydrodynamics (MHD) flow of a conducting, incompressible third-grade fluid due to non-coaxial rotations of a porous disk and a fluid at infinity in the presence of a uniform transverse magnetic field is considered. An exact analysis is carried out to model the governing non-linear partial differential equation. A numerical solution of the third-order non-linear partial differential equation has been obtained. Several graphs and tables have been drawn to show the influence of porosity ε, magnetic parameter N, material parameters α and β on the velocity distribution. © 2001 Elsevier Science Ltd. All rights reserved.

Keywords: ■; ■; ■

1. Introduction

The flow between eccentric rotating disks has been examined by a number of investigators. Berker [1] first found an exact solution for a Newtonian fluid in this type of flow which he defined as "pseudo plane motions" when the disks rotate with the same angular velocity. However, this study by Berker was omitted in later papers and this mistake was corrected in [2]. Berker [3,4] showed that there is the existence of an infinity of non-trivial solutions to the Navier–Stokes equations between two infinite parallel plates rotating about a common axis or about different axes. He assumed the flow is symmetric with respect to the origin for a single solution. The studies on non-Newtonian fluids for this type of flow have also been investigated. Maxwell and Chartoff [5] pointed out that it is possible to determine the complex dynamic viscosity of an elastico-viscous liquid by using the orthogonal rheometer which is an instrument consisting of two parallel plates which rotate with the same angular velocity about two axes normal to the plates but not coincident. Blyler and Kurtz [6] and Bird and Harris [7] established various studies to obtain the complex viscosity of the fluid. The inertia of the fluid was neglected in Refs. [5–7]. Abbott and Walters [8] both introduced an exact solution for a Newtonian fluid including inertia effects and examined the flow of a viscoelastic fluid assuming that the distance between the axes is small. The same problem was investigated for a second-grade fluid by Rajagopal [9,10], Rajagopal and Gupta [11], for a BKZ fluid by Rajagopal and Wineman [12], for a K-BKZ fluid by Dai et al. [13]. Separately, Göğüs

* Corresponding author. Fax: +1-717-771-8404.
E-mail address: ams5@psu.edu (A.M. Siddiqui).

0020-7462/01/$ - see front matter
PII: S0020-7462(01)00075-0

MHD Flow of a Third-Grade Fluid Due to Eccentric Rotations of a Porous Disk and a Fluid at Infinity

T. Hayat, Tahira Haroon, S. Asghar, and A. M. Siddiqui*

Department of Mathematics, Quaid-I-Azam University, Islamabad, Pakistan.

* *Department of Mathematics, Pennsylvania State University, York Campus, York, Pennsylvania 17403, U. S. A.*

Abstract

The problem of magnetohydrodynamics (MHD) flow of a conducting, incompressible third grade fluid due to non-coaxial rotations of a porous disk and a fluid at infinity in the presence of a uniform transverse magnetic field is considered. An exact analysis is carried out to model the governing non-linear partial differential equation. A numerical solution of the third order non-linear partial differential equation has been obtained. Several graphs and tables have been drawn to show the influence of porosity ϵ, magnetic parameter N, material parameters α and β on the velocity distribution.

1 Introduction

The flow between eccentric rotating disks has been examined by a number of investigators. Berker [1] first found an exact solution for a Newtonian fluid in this type of flow which he defined as "pseudo plane motions " when the disks rotate with the same angular velocity. However, this study by Berker was omitted in later papers and this mistake was corrected in [2]. Berker [3, 4] showed that there is the existence of an infinity of non-trivial solutions to the Navier-Stokes equations between two infinite parallel plates rotating about a common axis or about different axes. He assumed the flow is symmetric with respect to the origin for a single solution. The studies on non-Newtonian fluids for this type of flow have also been investigated.

Maxwell and Chartoff [5] pointed out that it is possible to determine the complex dynamic viscosity of an elastico-viscous liquid by using the orthogonal rheometer which is an instrument consisting of two parallel plates which rotate with the same angular velocity about two axes normal to the plates but not coincident. Blyler and Kurtz [6] and Bird and Harris [7] established various studies to obtain the complex viscosity of the fluid. The inertia of the fluid was neglected in Refs. [5, 6, 7]. Abbott and Walters [8] both introduced an exact solution for a Newtonian fluid including inertia effects and examined the flow of a viscoelastic fluid assuming that the distance between the axes is small. The same problem was investgated for a second grade fluid by Rajagopal [9, 10], Rajagopal and Gupta [11], for a BKZ fluid by Rajagopal and Wineman [12], for a K-BKZ fluid by Dai et al. [13]. Separately, Göğüs [14] obtained an exact solution for a mixture of two incompressible Newtonian fluids. Erdogan [15] found an exact solution of the time-dependent flow between eccentric rotating disks for a Newtonian fluid.

Exact solutions for the flow due to a single disk in a variety of situations have been obtained by a number of workers. The flow due to a disk and a fluid at infinity which are rotating non-coaxially at slightly different angular velocities has been studied by Coirier [16]. Exact solutions of the three dimensional Navier-Stokes equations have been obtained by Erdogan [17, 18] for the flow due to non-coaxial rotation of a porous disk and a fluid at infinity. Erdogan established that for uniform suction or uniform blowing at the disk, asymptotic solutions exist for the velocity distributions. Non-Newtonian flow due to a disk and a fluid at infinity which are rotating non-coaxially at slightly different angular velocity has been investigated by Erdogan [19]. Murthy and Ram [20] have considered the magnetohydrodynamic flow and heat transfer due to eccentric rotations of a porous disk and a fluid at infinity.

The flow of a second order fluid between rotating parallel plates was considered by Rajagopal [21]. The stability of this type of flow was investigated for a Newtonian fluid by using the energy method [3, 4] and for the second order fluid [11]. Magnetohydrodynamic flow between eccentric rotating disks with the same angular velocity was investigated by Mohanty [22], for the symmetric case. Rao and Kasiviswanathan [23] extended this type of flow to a micropolar fluid. Other extensions of this type of flow to an Oldroyd-B fluid and to an electrically conducting Oldroyd-B fluid were given by Rajagopal [24] and Ersoy [25], respectively. Knight [26] investigated the inertia effects of the non-Newtonian flow between eccentric disks rotating at different speeds. Parter and Rajagopal [27] proved that when the disks rotate with different angular velocities about distinct axes or a common axis, there is a one parameter family of solutions.

The unsteady flow of an incompressible viscous fluid between two eccentric rotating disks for which the streamlines at a given instant are concentric circles in planes parallel to a fixed plane and where each point on the plane is performing non-torsional oscillations is considered by Rao and Kasiviswanathan [28]. In another paper, Kasiviswanathan and Rao [29] investigated the unsteady flow due to non-coaxial rotations of a disk, executing non-torsional oscillations in its own plane, and a fluid at infinity. The work of Berker [4] to include time-dependent terms has been extended by Smith [30]. The unsteady flow due to eccentric rotations of a disk and a fluid at infinity which are impulsively started was investigated by Pop [31]. He assumes that the flow is two-dimensional, and both the disk and the fluid at infinity are initially at rest and that they are impulsively stared at time zero. Later, Erdogan [15, 32] pointed out that under the assumed conditions by Pop [31] the flow becomes three dimensional. He suggested a change in the initial conditions which makes the flow two-dimensional.

In the present paper, the MHD flow of a conducting, incompressible third grade fluid due to a disk which rotates non-coaxially with the fluid at infinity is studied and a numerical solution is obtained for this case. Since the equations governing the flow of third grade fluids are more complicated than the Navier-Stokes equations, to solve the equations of a third grade fluid is important. The work is more general and corresponds to the specific cases of practical interest: because of the study of the motion of non-Newtonian fluids in the absence as well as in the presence of a magnetic field. A few examples are the flow of nuclear slurries, flow of liquid metals and alloys such as the flow of gallium at ordinary temperatures ($30°C.$), flow of plasma, flow of mercury amalgams, handling of biological fluids, flow of blood–a Bingham fluid with some thixotropic behavior, coating of paper, plastic extrusion and lubrication with heavy oils and greases.

2 Basic Equations

An incompressible third grade fluid filling the semi-infinite space $z > 0$ in contact with an infinite porous disk at $z = 0$ is considered. The axis of rotations of the disk and that of fluid at infinity are assumed to be in the plane $x = 0$ and distance between the axes is l as shown in Fig. 1. The fluid is electrically conducting and assumed to be permeated by a magnetic field $\mathbf{B}_\circ$ having no components in the x and y directions. The disk and fluid at infinity are initially rotating about the z'-axis with the same angular velocity Ω, and at time $t = 0$, the disk starts to rotate impulsively about the z-axis with the same angular velocity Ω and the fluid at infinity continues to rotate about the z'-axis with the same angular velocity. Therefore, the boundary and initial conditions can be written in the following form

$$\begin{aligned}
u &= -\Omega y, & v &= \Omega x, & w &= -w_\circ, & at \quad z &= 0, & t &> 0, \\
u &= -\Omega(y-l), & v &= \Omega x, & w &= -w_\circ, & as \quad z &\to \infty, & for \quad all \quad t&, \\
u &= -\Omega(y-l), & v &= \Omega x, & w &= -w_\circ, & at \quad t &= 0, & for \quad z &> 0,
\end{aligned} \tag{1}$$

where u, v and w are the components of the velocity. Obviously $w_\circ > 0$ is the suction velocity and $w_\circ < 0$ is the injection velocity. The boundary and the initial conditions given by equation (1) suggest that the components u and v of the velocity can be written in the following form

$$u = -\Omega y + f(z,t), \quad v = \Omega x + g(z,t), \quad w = -w_o. \tag{2}$$

The equations governing the unsteady MHD flow are

$$\rho \frac{D\mathbf{V}}{Dt} = \nabla . \mathbf{T} + \mathbf{J} \times \mathbf{B}, \tag{3}$$
$$\nabla . \mathbf{V} = 0, \tag{4}$$
$$\nabla . \mathbf{B} = 0, \tag{5}$$
$$\nabla \times \mathbf{B} = \mu_m \mathbf{j}, \tag{6}$$
$$\nabla \times \mathbf{E} = -\frac{\partial \mathbf{B}}{\partial t}, \tag{7}$$
$$\mathbf{J} = \sigma(\mathbf{E} + \mathbf{V} \times \mathbf{B}), \tag{8}$$

where ρ is the density, $\frac{D}{Dt}$ the material time derivative, $\mathbf{J}$ the electric current density, μ_m the magnetic permeability, $\mathbf{E}$ the electric field, $\mathbf{B}$ the total magnetic field so that $\mathbf{B} = \mathbf{B}_o + \mathbf{b}$, $\mathbf{b}$ the induced magnetic field, σ the electric conductivity of the fluid, displacement currents are neglected. In equations (5 - 8) the magnetic Reynolds number R_m [33] is assumed to be small as is the case with the most of the conducting fluids and hence the induced magnetic field is small in comparison with the applied magnetic field and is therefore not taken into account. The magnetic body forces $\mathbf{J} \times \mathbf{B}$ now becomes $\sigma(\mathbf{V} \times \mathbf{B}) \times \mathbf{B}$.

The incompressible, homogeneous fluid of third grade is a simple fluid of the differential type whose Cauchy stress tensor $\mathbf{T}$ has the representation [34]:

$$\begin{aligned} \mathbf{T} &= -p\mathbf{I} + \mu \mathbf{A}_1 + \alpha_1 \mathbf{A}_2 + \alpha_2 \mathbf{A}_1^2 \\ &+ \beta_1 \mathbf{A}_3 + \beta_2(\mathbf{A}_1\mathbf{A}_2 + \mathbf{A}_2\mathbf{A}_1) + \beta_3(tr\mathbf{A}_1^2)\mathbf{A}_1, \end{aligned} \tag{9}$$

where $-p\mathbf{I}$ is the indeterminate part of the stress due to the constraint of incompressibility, $\mu, \alpha_1, \alpha_2, \beta_1, \beta_2$ and β_3 are material constants, and the tensors $\mathbf{A}_i$, $i = 1, 2, 3$ are defined through [35]:

$$\begin{aligned} \mathbf{A}_1 &= (\mathbf{grad\ V}) + (\mathbf{grad\ V})^T, \\ \mathbf{A}_i &= \frac{D\mathbf{A}_{i-1}}{Dt} + \mathbf{A}_{i-1}\,(\mathbf{grad\ V}) + (\mathbf{grad\ V})^T\,\mathbf{A}_{i-1},\ i > 1. \end{aligned}$$

We shall not consider the above model as an approximation to a simple fluid [36] in the sense of a retardation, but consider it to be an exact model in the sense described by Fosdick and Rajagopal in [37] (see also [38]). We require that the Clausius-Duhem inequality hold and that the specific Helmholtz free energy be a minimum when the fluid is locally at rest, which leads to the following restrictions on the material coefficients:

$$\begin{gathered}\mu \geq 0, \quad \alpha_1 \geq 0, \quad \beta_1 = \beta_2 = 0, \quad \beta_3 \geq 0, \\ -\sqrt{24\mu\beta_3} \ \leq \alpha_1 + \alpha_2 \ \leq \sqrt{24\mu\beta_3}.\end{gathered} \tag{10}$$

Therefore, the model of equation (9) reduces to

$$\mathrm{T} \;=\; -p\mathrm{I} + \mu\mathrm{A}_1 + \alpha_1\mathrm{A}_2 + \alpha_2\mathrm{A}_1^2 + \beta_3(tr\mathrm{A}_1^2)\mathrm{A}_1. \tag{11}$$

Using equation (2), equation of continuity is identically satisfied. Further in view of small Reynold number, equations (2) and (11) one obtains from equation (3) as

$$\begin{aligned}\rho\left[\frac{\partial f}{\partial t} - \Omega^2 x - \Omega g - w_\circ \frac{\partial f}{\partial z}\right] &= -\frac{\partial P}{\partial x} + \mu\frac{\partial^2 f}{\partial z^2} - \sigma B_\circ^2(f - \Omega y) \\ &+ \alpha_1\left[\frac{\partial^3 f}{\partial t \partial z^2} - w_\circ\frac{\partial^3 f}{\partial z^3} + \Omega\frac{\partial^2 g}{\partial z^2}\right] \\ &+ 2\beta_3\frac{\partial}{\partial z}\left[\frac{\partial f}{\partial z}\left\{\left(\frac{\partial f}{\partial z}\right)^2 + \left(\frac{\partial g}{\partial z}\right)^2\right\}\right],\end{aligned} \tag{12}$$

$$\begin{aligned}\rho\left[\frac{\partial g}{\partial t} - \Omega^2 y + \Omega f - w_\circ \frac{\partial g}{\partial z}\right] &= -\frac{\partial P}{\partial y} + \mu\frac{\partial^2 g}{\partial z^2} - \sigma B_\circ^2(g + \Omega x) \\ &+ \alpha_1\left[\frac{\partial^3 g}{\partial t \partial z^2} - w_\circ\frac{\partial^3 g}{\partial z^3} - \Omega\frac{\partial^2 f}{\partial z^2}\right] \\ &+ 2\beta_3\frac{\partial}{\partial z}\left[\frac{\partial g}{\partial z}\left\{\left(\frac{\partial f}{\partial z}\right)^2 + \left(\frac{\partial g}{\partial z}\right)^2\right\}\right],\end{aligned} \tag{13}$$

$$\sigma B_\circ^2 w_\circ \;=\; \frac{\partial P}{\partial z}, \tag{14}$$

where

$$P \;=\; p - (2\alpha_1 + \alpha_2)\left\{\left(\frac{\partial f}{\partial z}\right)^2 + \left(\frac{\partial g}{\partial z}\right)^2\right\}. \tag{15}$$

Now eliminating P from equations (12) to (13) and then using boundary conditions (1) we obtain

$$\rho\left[\frac{\partial f}{\partial t}-\Omega g-w_{\circ}\frac{\partial f}{\partial z}\right] = \mu\frac{\partial^2 f}{\partial z^2}-\sigma B_{\circ}^2(f-\Omega l) + \alpha_1\left[\frac{\partial^3 f}{\partial t\partial z^2}-w_{\circ}\frac{\partial^3 f}{\partial z^3}+\Omega\frac{\partial^2 g}{\partial z^2}\right] + 2\beta_3\frac{\partial}{\partial z}\left[\frac{\partial f}{\partial z}\left\{\left(\frac{\partial f}{\partial z}\right)^2+\left(\frac{\partial g}{\partial z}\right)^2\right\}\right], \tag{16}$$

$$\rho\left[\frac{\partial g}{\partial t}+\Omega f-w_{\circ}\frac{\partial g}{\partial z}\right] = \mu\frac{\partial^2 g}{\partial z^2}-\sigma B_{\circ}^2 g+\Omega^2 l + \alpha_1\left[\frac{\partial^3 g}{\partial t\partial z^2}-w_{\circ}\frac{\partial^3 g}{\partial z^3}-\Omega\frac{\partial^2 f}{\partial z^2}\right] + 2\beta_3\frac{\partial}{\partial z}\left[\frac{\partial g}{\partial z}\left\{\left(\frac{\partial f}{\partial z}\right)^2+\left(\frac{\partial g}{\partial z}\right)^2\right\}\right]. \tag{17}$$

By (1) and (2) we have

$$\begin{array}{llll} f(0,t)=0, & g(0,t)=0, & for\ \ t>0, \\ f(\infty,t)=\Omega l, & g(\infty,t)=0, & for\ \ all\ \ t, \\ f(z,0)=\Omega l, & g(z,0)=0, & for\ \ z>0. \end{array} \tag{18}$$

Introducing

$$F^* = f + i\,g, \tag{19}$$

equations (16) and (17) can be written in the following form

$$\left[\frac{\partial F^*}{\partial t}+i\,\Omega F^*-w_{\circ}\frac{\partial F^*}{\partial z}\right] = \nu\frac{\partial^2 F^*}{\partial z^2}-\frac{\sigma}{\rho}B_{\circ}^2(F^*-\Omega l)+i\,\Omega^2 l + \frac{\alpha_1}{\rho}\left[\frac{\partial^3 F^*}{\partial t\partial z^2}-w_{\circ}\frac{\partial^3 F^*}{\partial z^3}-i\,\Omega\frac{\partial^2 F^*}{\partial z^2}\right] + 2\beta_3\frac{\partial}{\partial z}\left[\left(\frac{\partial F^*}{\partial z}\right)^2\frac{\partial \bar{F}^*}{\partial z}\right], \tag{20}$$

where $\nu=\frac{\mu}{\rho}$, $\bar{F}^*$ is the complex conjugate of F^* and the initial and boundary conditions (18) become

$$F^*(0,t)=0, \qquad F^*(\infty,t)=\Omega l, \qquad F^*(z,0)=\Omega l. \tag{21}$$

We note that for $\alpha_1 = B_\circ = w_\circ = \beta_3 = 0$, equation (20) correspond to the differential equations for classical viscous and $\alpha_1 = 0$, and second grade fluids, respectively.

Defining

$$\xi = \sqrt{\frac{\Omega}{2\nu}}z, \quad \tau = \Omega t, \quad \alpha = \frac{\Omega\alpha_1}{\rho\nu}, \quad \epsilon = \frac{w_\circ}{\sqrt{2\nu\Omega}}, \quad N = \frac{\sigma}{\rho\Omega}B_\circ^2,$$
$$\beta = \frac{\Omega^3 l^2 \beta_3}{\rho\nu^2}, \quad F(\xi,\tau) = \frac{F^*}{\Omega l} - 1, \quad \bar{F}(\xi,\tau) = \frac{\bar{F}^*}{\Omega l} - 1 \tag{22}$$

equation (20) and conditions (21) become

$$\alpha\frac{\partial^3 F}{\partial\tau\partial\xi^2} - \alpha\epsilon\frac{\partial^3 F}{\partial\xi^3} + (1-i\alpha)\frac{\partial^2 F}{\partial\xi^2} + 2\epsilon\frac{\partial F}{\partial\xi}$$
$$- 2\frac{\partial F}{\partial\tau} - 2(i+N)F + \beta\frac{\partial}{\partial\xi}\left[\left(\frac{\partial F}{\partial\xi}\right)^2\frac{\partial\bar{F}}{\partial\xi}\right] = 0, \tag{23}$$

$$F(0,\tau) = -1, \quad F(\infty,\tau) = 0, \quad F(\xi,0) = 0. \tag{24}$$

We note that the equation (23) is a third order partial differential equation. Moreover, this equation is highly non-linear as compared to case of second order and Newtonian flow equations. As a result, it seems to be impossible to obtain the general solution in closed form for arbitrary values of all parameters arising in this non-linear equation. Further, equation (23) is parabolic with respect to time which allows a time marching solution to the equation. Dealing with parabolic equation, there is only one characteristic direction. The information at one point influences the entire region on one side of the vertical characteristic and contained within the two boundaries. Therefore, lend itself to marching solution. Starting with the initial data, the solution between the two boundaries is obtained by marching in the τ direction. The convective terms are non-linear in the above equation. The convective non-linearity must be supressed in applying the Von Neumann stability analysis. This is done by treating solution-dependent coefficients multiplying derivatives as being tempoarily frozen. The modified equation approach to analyzing non-linear computational algorithm is applicable [39] but the appearance of products of higher-order derivatives makes the construction of more accurate schemes less precise than the case of linear equations.

As this problem is time dependent and has mixed derivative with respect to time and space coordinates so we are forced to use an implicit scheme. Applying implicit scheme to nonlinear equation (23) is not as straight forward as for linear equations. To convert partial differential equation (23) to a system of algebraic equations a number of choices are available. A modified Crank-Nicolson implicit formulation with forward time and central finite difference approximation is used, so equation (23) is transformed into algebraic equation of the form

$$a_j^n F_{j-1}^{n+1} + b_j^n F_j^{n+1} + c_j^n F_{j+1}^{n+1} = d_j^n, \tag{25}$$

where

$$\begin{aligned}
a_j^n &= -\left(\frac{\alpha}{h^2} + \frac{(1-i\alpha)\Delta\tau}{2h^2}\right),\\
b_j^n &= 2\left(\frac{\alpha}{h^2} + \frac{(1-i\alpha)\Delta\tau}{2h^2} + 1\right),\\
c_j^n &= -\left(\frac{\alpha}{h^2} + \frac{(1-i\alpha)\Delta\tau}{2h^2}\right),\\
d_j^n &= -\left(\frac{\alpha}{h^2} + \frac{(1-i\alpha)\Delta\tau}{2h^2}\right)(F_{j+1}^n - 2F_j^n + F_{j-1}^n)\\
&- \frac{\epsilon\alpha\Delta\tau}{2h^3}(F_{j+2}^n - 2F_{j+1}^n + 2F_{j-1}^n - F_{j-2}^n)\\
&+ \frac{\epsilon\Delta\tau}{h}(F_{j+1}^n - F_{j-1}^n) + 2(1 - \Delta\tau(i+N))F_j^n\\
&+ \frac{\beta\Delta\tau}{4h^4}((F_{j+1}^n - F_{j-1}^n)^2(\bar{F}_{j+1}^n - 2\bar{F}_j^n + \bar{F}_{j-1}^n)\\
&+ 2(F_{j+1}^n - F_{j-1}^n)(F_{j+1}^n - 2F_j^n + F_{j-1}^n)(\bar{F}_{j+1}^n - \bar{F}_{j-1}^n)).
\end{aligned} \tag{26}$$

Here $\xi = [\xi_j]_{j=1}^{j=M}$ is taken as strictly increasing sequence of discrete points such that $0 = \xi_1 < \xi_2 < \xi_3 < \cdots < \xi_M$ and $h = \xi_i - \xi_{i-1} = \frac{\xi_M - \xi_1}{M-1}$, where M is the number of grid points in space coordinates and $\Delta\tau = \tau^{n+1} - \tau^n$is time interval. The right hand side of equation (25) is considered in some fashion as known, say from the previous time step and left hand side as the dependent variable in a computational solution of an unsteady flow problem. The steady state approached asymptotically at large times.

The implicit methods are uncoditionally stable unless non-linear effects cause instability, which is controlled by suitable choice of $\Delta\tau$ and h. The equation (25) must be written at all interior grid points resulting in a system of algebraic equations of order M from which the unknowns F_j^{n+1} for all j can be solved simultaneously, which can be solved by using the generalized Thomas algorithm.

For this let us consider system of equations

$$\mathbf{A}\,\mathbf{F} = \mathbf{B}, \tag{27}$$

where $\mathbb{F}$ is a vector of unknown nodal values in equation (25), $\mathbb{A}$ contains the algebraic coefficients arising from discretization and $\mathbb{B}$ is made up of algebraic coefficients associated with discretisation and known values of $\mathbb{F}$ e. g., values of $\mathbb{F}$ on previous time step and given by the boundary conditions.

The matrix $\mathbb{A}$ is typically sparse and the non-zero terms are close to the diagonal. As in our case $\mathbb{A}$ does not depend on $\mathbb{F}$ only one step of outer iteration is required. When the non-zero elements lie close to the main diagonal it is useful to consider variants of Gauss elimination that take advantage of the banded nature of $\mathbb{A}$. Consider equation (25) which when repeated for every node gives

$$\begin{pmatrix} b_1 & c_1 & & & & & & \\ a_2 & b_2 & c_2 & & & & & \\ & a_3 & b_3 & c_3 & & & & \\ & & \cdot & \cdot & \cdot & & & \\ & & & a_j & b_j & c_j & & \\ & & & & \cdot & \cdot & \cdot & \\ & & & & & a_{M-1} & b_{M-1} & c_{M-1} \\ & & & & & & a_M & b_M \end{pmatrix} \begin{bmatrix} F_1 \\ F_2 \\ F_3 \\ \cdot \\ F_j \\ \cdot \\ F_{M-1} \\ F_M \end{bmatrix} = \begin{bmatrix} d_1 \\ d_2 \\ d_3 \\ \cdot \\ d_j \\ \cdot \\ d_{M-1} \\ d_M \end{bmatrix}$$

where a_j, b_j, c_j and d_j are given by equation (26), non-zero values of d_j are associated with source terms or for d_1 and d_M with boundary conditions. All terms in $\mathbb{A}$ other than those shown are zero.

The Thomas algorithm for solving above matrix consists of two parts:

First, the a_j coefficients have been eliminated and b_j coefficients normalized to unity. The equations are modified in a forward sweep.

The second stage consists of a backward-substitution (backward sweep).

The Thomas algorithm is particularly economical; it requires only 5M-4 operations (multiplications and divisions). But to prevent ill-conditioning it is necessary that $|b_j| > |a_j| + |c_j|$.

3 Numerical Discussion

Equation (25) has been solved by using a modified Crank Nicolson implicit formulation with forward time and central difference space approximation using 100 grid points ($\xi = 10$) for sufficient accuracy when the case of suction or no porosity is considered but for the case of injection 1000 grid points ($\xi = 100$) are used. For all computations we have taken $h = .1$. For the case $\alpha = 0, \beta = 0$ we get solution for the Newtonian fluid, and results matched with the analytical solution with very small relative error.

Numerically, we found the behvior of $\frac{f}{\Omega l}$ and $\frac{g}{\Omega l}$ at different values of ξ for varying time corresponding to three types of flows (Newtonian, second grade and third grade), with and without suction and magnetic parameter. Results described below report solutions up to $\xi = 6$, where free stream velocities have not yet been reached in most cases. We observed that; for the Newtonian case boundary layer thickness increases with the increase in time and steady state approaches after $\tau = 10$. Initially fluid moves with the disk, so the magnitude of $\frac{f}{\Omega l}$ is large near the disk. With time the magnitude of $\frac{f}{\Omega l}$ decreases and then increases to become stable, while $\frac{g}{\Omega l}$ keeps on increasing and then becomes stable after $\tau = 10$.

For the second-grade fluid when $(\alpha \neq 0)$ boundary layer thickness increases with the increase in α. Time taken to reach steady-state is also increased. Initially, fluid adjacent to disk moves with the disk and $\frac{f}{\Omega l}$ and $\frac{g}{\Omega l}$ are very high. With time the values of $\frac{f}{\Omega l}$ decreases while the values of $\frac{g}{\Omega l}$ increases and then approaches its steady-state condition. For the steady state case the value of $\frac{f}{\Omega l}$ near the disk are small as compared to the case of Newtonian fluid. Time taken to reach steady state is larger as compared to its time for Newtonian fluid. The values of $\frac{g}{\Omega l}$ are large and they keep on increasing with time untill steady state condition is achieved. For the third grade fluid (when $\alpha \neq 0$, $\beta \neq 0$) the values of $\frac{f}{\Omega l}$ and $\frac{g}{\Omega l}$ near the disk decrease with the increase in time. The values of $\frac{f}{\Omega l}$ decrease near the disk but increase at small distance away from the disk and then decrease to become free stream. Time increases to approach its steady state condition also boundary layer thickness increases with the increase in time in third grade fluid during the transient period and then becomes stable.

By introducing suction $(\epsilon > 0)$ in Newtonian fluid there is a considerable decrease in boundary layer thickness and also in the time to reach steady state condition i. e. just after $\tau = .5$, we get steady-flow. Boundary layer thickness decreases due to suction in second-grade fluid but in comparison with the Newtonian fluid its value is high and the time to achieve steady state is also increased. It means that α increases the boundary layer thickness and also time to approach its steady state while suction decreases the boundary layer thickness and also time to approach its steady state. In third grade fluid i. e., (for $\alpha \neq 0$, $\beta \neq 0$) boundary layer thickness increases further as compared to the results of second grade fluid and also time to reach steady state is increased but these values are small in comparision with the case when suction was not present in the third-grade fluid.

We also considered the effect of suction and magnetic parameter on all these three types of fluids. Boundary layer thickness decreases further due to magnetic parameter also the time to reach steady state is reduced further. It means that magnetic parameter is responsible for further reduction in boundary layer thickness as well as time to reach steady-state in all three cases.

When we proceed from Newtonian fluid to non-Newtonian fluid the effect of α and β can also be observed in steady state condition. We observe that the boundary layer thickness increases with the increase in α as well as in β. The magnitude of $\frac{f}{\Omega l}$ decreases near the disk while its value increases in a considerable amount at some distance away from the disk with the increase in α these effects are enhanced further by the increase in β. The magnitude of $\frac{g}{\Omega l}$ increases near the disk and decreases away from disk with the increase in α but β decreases the magnitude of $\frac{g}{\Omega l}$ near the disk and increases away from the disk.

Suction and magnetic parameter are always responsible for the reduction in the boundary layer thickness and also reduce the magnitudes of $\frac{f}{\Omega l}$ and $\frac{g}{\Omega l}$. The effect of magnetic parameter on $\frac{g}{\Omega l}$ is more prominant as compared to its affect on $\frac{f}{\Omega l}$.

When injection is applied, boundary layer thickness becomes very very large and it approaches to free stream at a very large distance (solution exists), and with the increase in α and β it increases further but by introducing magnetic parameter boundary layer thickness can be reduced drastically.

References

[1] R. Berker. *Handbook of Fluid Dynamics*, volume VIII/3. Springer-Verlag, Berlin, 1963.

[2] T. N. G. Abbot, C. W. Bowen, K. Waltters. Some suggestions for new rheometer designs. I Theory. *J. Phys. D: Appl. Phys.*, 4(1971)190-203.

[3] R. Berker. A new solution of the Navier-Stokes equation for the motion of a fluid contained between two parallel plates rotating about the same axis. *Arch. Mech. Stos.*, 31(1979)265-280.

[4] R. Berker. An exact solution of the Navier-Stokes equation: The vortex with curvilinear axis. *Int. J. Engng. Sci.*, 20(1982)217-230.

[5] B. Maxwell, R. P. Chartoff. Studies of a polymer melt in an orthogonal rheometer. *Trans. Soc. Rheol.*, 9(1965)51.

[6] L. L. Blyler, S. J. Kurtz. Analysis of the Maxwell orthogonal rheometer. *J. Appl.Polym. Sci.*, 11(1967)127.

[7] R. B. Bird, E. K. Harris. Analysis of steady state shearing and stress relaxation in the Maxwell orthogonal rheometer. *A. I. Ch. E. J.*, 14(1968)758.

[8] T. N. G. Abbot, K. Waltters. Rheometrical flow systems: Part2. Theory for the orthogonal rheometer, including an exact solution of the Navier-Stokes equations. *J. Fluid. Mech.*, 40(1970)205-213.

[9] K. R. Rajagopal. The flow of a second order fluid between rotating parallel plates. *J. Non-Newtonian Fluid. Mech.*, 9(1981)185-190.

[10] K. R. Rajagopal. On the flow of a simple fluid in an orthogonal rheometer. *Arch. Rat. Mech. Anal*, 79(1982)39-47.

[11] K. R. Rajagopal, A. S. Gupta. Flow and stability of a second grade fluid between two parallel plates rotating about noncoincident axes. *Int. J. Engng. Sci.*, 19(1981)1401-1409.

[12] K. R. Rajagopal, A. S. Wineman. Flow of a BKZ fluid in an orthogonal rheometer. *J. Rheol.*, 27(1983)509.

[13] R. X. Dai, K. R. Rajagopal, A. Z. Szeri. A numerical study of the flow of a K-BKZ fluid between plates rotating about non-coincident axes. *J. Non-Newtonian Fluid. Mech.*, 38(1991)289.

[14] M. S. Göğüs. The steady flow of a binary mixture between two rotating non-coaxial disks. *Int. J. Engng. Sci.*, 30(5)(1992)665.

[15] M. E. Erdogan. Unsteady viscous flow between eccentric rotating disks. *Int. J. Non-Linear Mech.*, 30(5)(1995)711-717.

[16] J. Coirier. Rotations non-coaxiales d'un disque et d'un fluide á l' infini. *J. de Mécanique*, 11(1972)317-340.

[17] M. E. Erdogan. Flow due to eccentric rotating a porous disk and a fluid at infinity. *Trans. ASME J. Appl. Mech.*, 43(1976)203-204.

[18] M. E. Erdogan. Flow due to non-coaxially rotations of a porous disk and a fluid at infinity. *Rev. Roum., Méc. Appl.*, 22(1977)171-178.

[19] M. E. Erdogan. Non-newtonian flow due to non-coaxially rotations of a disk and a fluid at infinity. *Z. Angew Math. Mech.(ZAMM)*, 56(1976)141-146.

[20] S. N. Murthy, R. K. P. Ram. MHD flow and heat transfer due to eccentric rotations of a porous disk and a fluid at infinity. *Int. J. Engng. Sci.*, 16(1978)943-949.

[21] K. R. Rajagopal. The flow of a second order fluid between rotating parallel plates. *J. Non-Newtonian Fluid Mech.*, 9(1981)185.

[22] H. K. Mohanty. Hydromagnetic flow between two rotating disks with non-coincident parallel axes of rotation. *The Phys. Fluids*, 15(1972)1456-1458.

[23] A. R. Rao, S. R. Kasiviswanathan. A class of exact solutions for the flow of a micropolar fluid. *Int. J. Engng. Sci.*, 25(1987)443-453.

[24] K. R. Rajagopal. On an exact solution for the flow of an Oldroyd-B fluid. *Bull. Tech. Uni. Ist.*, 49(1996)617-623.

[25] H. V. Ersoy. MHD flow of an Oldroyd-B fluid between eccentric rotating disks. *Int. J. Engng. Sci.*, 37(1999)1973-1984.

[26] D. G. Knight. Flow between eccentric disks rotating at different speeds: Inertia effects. *J. Appl. Math. Phys.(ZAMP)*, 31(1980)309-317.

[27] S. V. Parter, K. R. Rajagopal. Swirling flow between rotating plates. *Arch. Rat. Mech. Anal.*, 86(1984)305-315.

[28] A. R. Rao, S. R. Kasiviswanathan. On exact solutions of the unsteady Navier-Stokes equations. The vortex with instantaneous curvilinear axis. *Int. J. Engng. Sci.*, 25(1987)337-349.

[29] S. R. Kasiviswanathan, Rao A. R. An unsteady flow due to eccentrically rotating porous disk and a fluid at infinity. *Int. J. Engng. Sci.*, 25(1987)1419-1425.

[30] S. H. Smith. Eccentric rotating flows: Exact unsteady solutions of the Navier-Stokes equations. *J. Appl. Math. Phys.(ZAMP)*, 38(1987)573-579.

[31] I. Pop. Unsteady flow due to noncoaxially rotating disk and a fluid at infinity. *Bull. Tech. Uni. Ist.*, 32(1979)14.

[32] M. E. Erdogan. Unsteady flow of a viscous fluid due to non-coaxial rotations of a disk and a fluid at infinity. *Int. J. Non-Linear Mechanics*, pages 285–290, 32(1997)285-290.

[33] J. A. Shercliff. *A textbook of Magnetohydrodynamics*. Pergamon, 1965.

[34] C. Truesdell, W. Noll. *Handbuch der Physik*, volume III, chapter The non-linear field theories of mechanics, pages 3–23. Berlin Heidelberg New York: Springer Verlag, (1965).

[35] C. G. Speziale. On turbulent secondary flows in pipes of non-circular cross section. *Int. J. Engng. Sci.*, 7(1982)863.

[36] B. D. Coleman, W. Noll. An approximation theorem for functional with applications in continuum mechanics. *Arch. Rat. Mech. Anal.*, 6(1960)355-370.

[37] R. L. Fosdick, K. R. Rajagopal. Thermodynamics and stability of fluids of third grade. *Proc. Roy. Soc. Lond. Ser.*, A,339(1980)351.

[38] J. E. Dunn, K. R. Rajagopal. Fluids of differential type. *Int. J. Engng. Sci.*, 21(1983)487.

[39] G. H. Klopfer, D. S. McRae. Non-linear truncation error analysis of FDF for the Euler equations. *AIAA J.*, 21(1983)487.

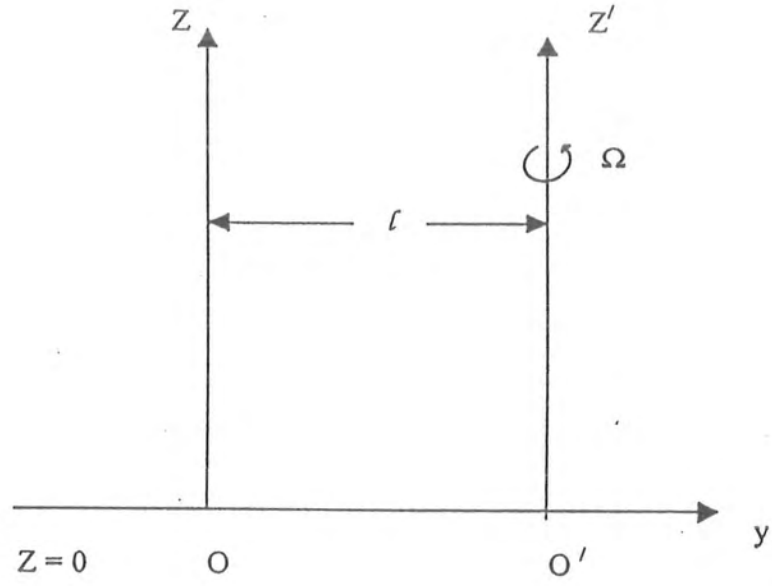

Fig. 1. Flow geometry

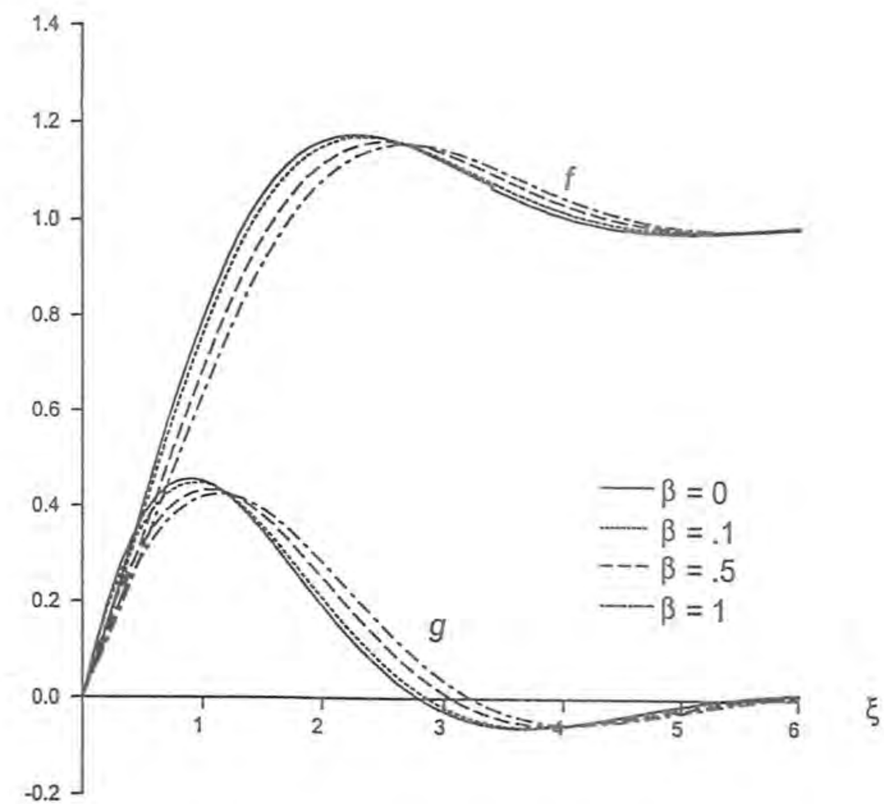

Fig. 1. Variation in f and g with ξ when $\alpha = 1$, $\varepsilon = 0$, $N = 0$, $\tau = 100$ for different β

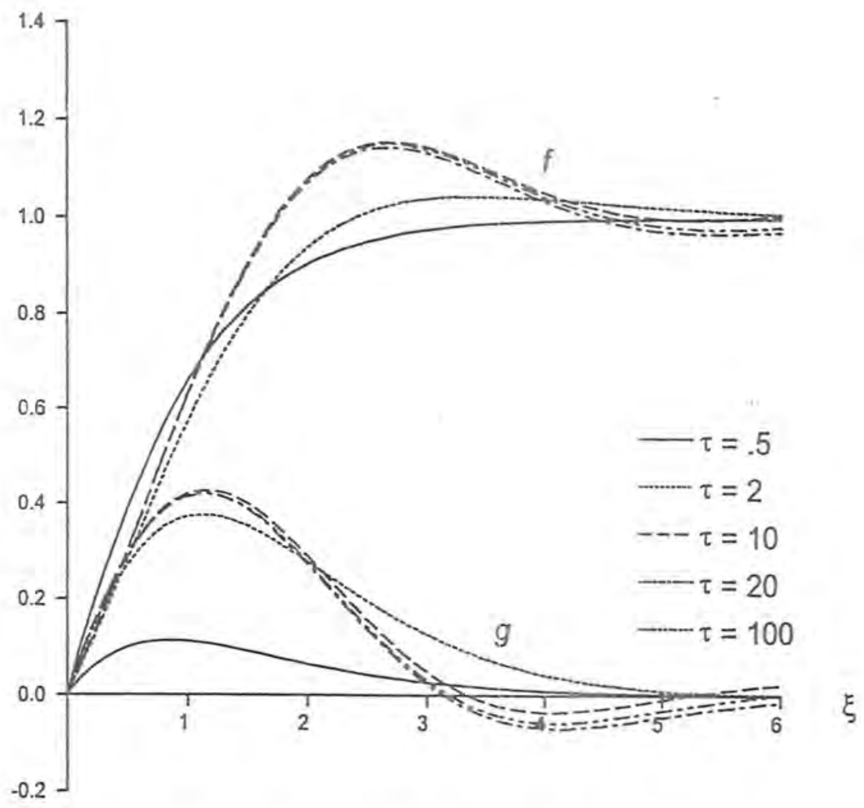

Fig. 2. Variation in f and g with ξ for different values of τ when α = 1, β = 1, ε = 0, N = 0.

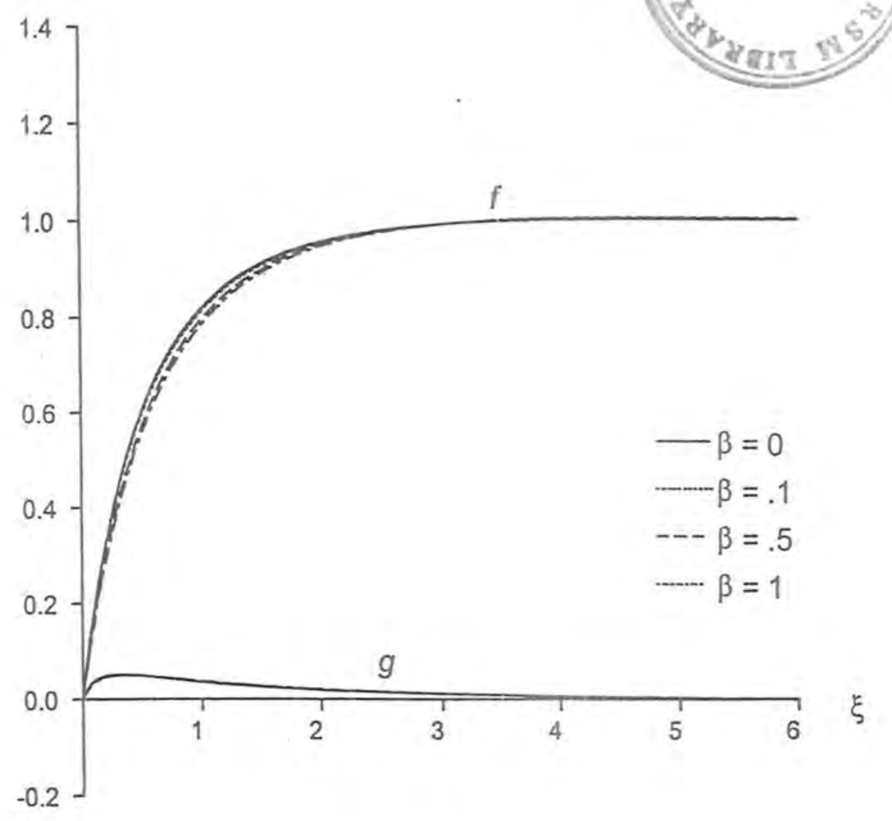

Fig. 3. variation in f and g with ξ for different values of β when
$\alpha = 1$, $\varepsilon = 2$, $N = 2$, $\tau = 100$

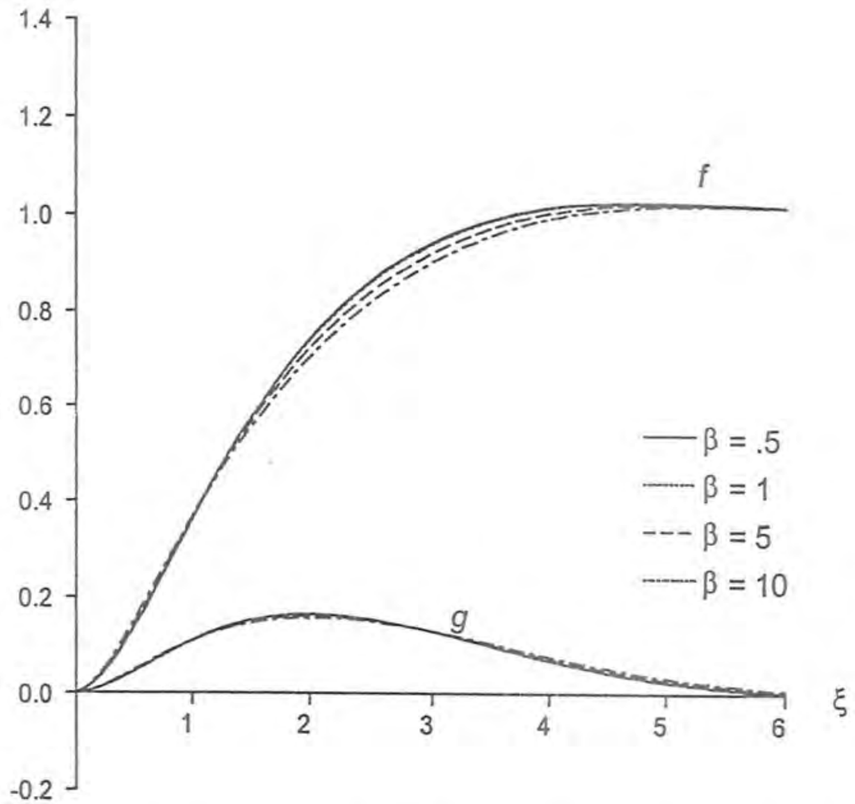

Fig. 4. Variation in f and g with ξ for different values of β when
$\alpha = 1$, $\varepsilon = -2$, $N = 2$, $\tau = 100$.

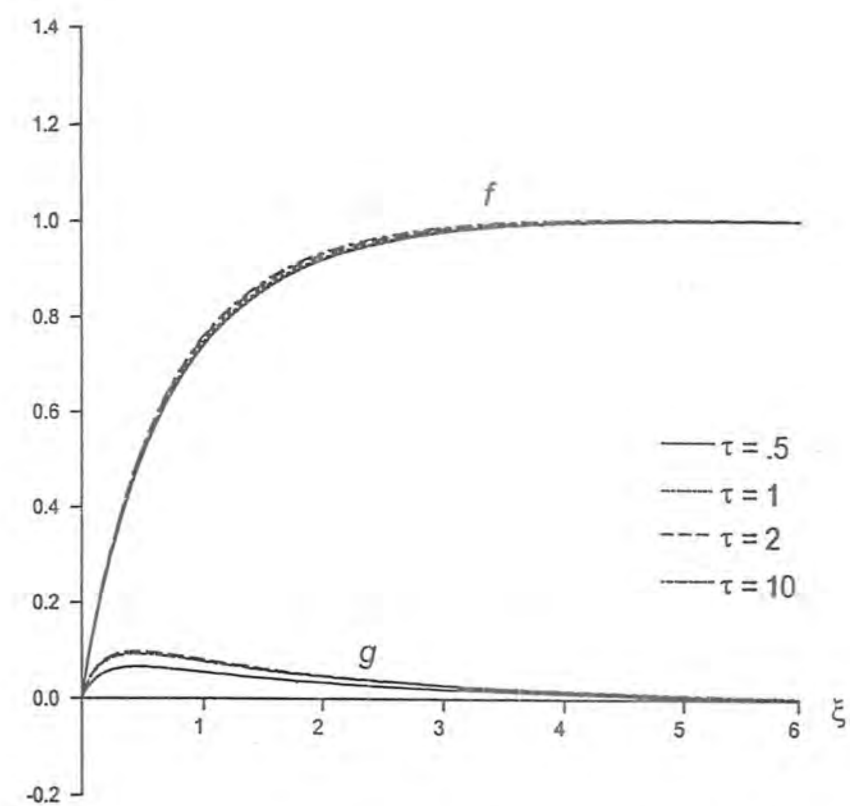

Fig. 5. Variation in f and g with ξ for different values of τ when α = 1, β = 0 ε = 2, N = 0.

Already Submitted to ZAMM.

MHD Flow of a Third-Grade Fluid Induced by Non-Coaxial Rotations of a Porous Disk Executing Non-Torsional Oscillations and a Fluid at Infinity

T. Hayat, Tahira Haroon, S. Asghar, and A. M. Siddiqui*

Department of Mathematics, Quaid-I-Azam University, Islamabad, Pakistan.

* *Department of Mathematics, Pennsylvania State University, York Campus, York, Pennsylvania 17403, U. S. A.*

Summary

The problem of magnetohydrodynamics (MHD) flow of a conducting, incompressible flow due to non-coaxial rotations of a porous disk, executing oscillations in its own plane, and a fluid at infinity is considered in the presence of a uniform transverse magnetic field. The porous character of disk and the non-linearity of the fluid increase the order of the differential equation. The solutions for three cases when the angular velocity is greater than the frequency of oscillation or it is smaller than the frequency or it is equal to the frequency are examined. The structure of the velocity distributions and the associated boundary layers are investigated including the case of blowing and resonant oscillations. It is found that unlike the hydrodynamic situation for the case of blowing and resonance, the hydromagnetic steady state solution satisfies the boundary condition at infinity. The inherent difficulty involved in the purely hydrodynamic problem associated with the case of blowing and the resonant frequency has been resolved in this paper by the addition of the magnetic field.

1 Introduction

Exact solutions for the flow due to a single disk in a variety of situations have been obtained by a number of workers. Berker [1] has considered the flow due to non-coaxial roatations of a disk and a fluid at infinity and implied the possibility of an exact solution of the Navier-Stokes equations. Thornley [2] has studied the flow due to non-torsional oscillations of a single disk in semi-infinite expanse of fluid in a rotating frame of reference. The MHD effect on the Ekman layer over an infinite horizontal plate at rest relative to an electrically conducting liquid which is rotating with uniform angular velocity about a vertical axes has been studied by Gupta [3]. The flow due to rotations of a porous disk and a fluid at infinity rotating about a different axes has been studied by Erdogan [4]. Murthy and Ram [5] have considered the MHD flow and heat transfer due to eccentric rotations of a porous disk and a fluid at infinity. Rajagopal [6] has considered the flow of a simple fluid in an orthogonal rheometer.

In order to generalize the work of Berker [1], Kasiviswanathan and Rao [7] discussed the flow due to non-coaxial rotations of a disk, executing non-torsional oscillations in its own plane and a fluid at infinity. The unsteady flow due to non-coaxial rotations of a disk and a fluid at infinity which are impulsively started was investigated by Pop [8]. Later, it has been pointed out by Erdogan [4] that if the disk and the fluid at infinity are initially at rest the problem becomes three dimensional and the solution cannot be obtained easily. To overcome this difficulty, Erdogan [4] suggested a change in initial condition and proposed that the disk and the fluid are initially rotating about z'-axis and suddenly sets in motion; the disk rotating about z-axis and fluid about z'-axis. He showed that now the problem is solvable and presents an analytic solution for the velocity field. In another paper, Erdogan [9] found an exact solution of the time-dependent Navier-Stokes equations for the flow due to non-coaxial rotations of an oscillating disk and a fluid at infinity.

In this paper, numerical solution of the time-dependent equations is given for the magnetohydrodynamic incompressible flow due to non-coaxial rotations of a porous disk and a third grade fluid at infinity. Additionally, the disk is executing oscillations in its own plane. The porous disk and non-linear fluid behavior considered in this study results in the increase of the order of the non-linear differential equation with constant complex coefficients obtained by inserting the velocity field into the equations of motion. It is apparent from physical considerations that suction and blowing have opposite effects on the boundary layer flows. Indeed, the suction prevents the imposed nontorsional oscillations from spreading far away from the disk by viscous diffusion for all values of the frequency parameter n. On the contrary, the blowing promotes the spreading of the oscillations far away from the disk. In the case of blowing and resonance, the oscillatory boundary layer flows are no longer possible. Thus, it remains to answer the question of finding a meaningful solution for the case of blowing and the resonant frequency. An attempt is made to answer this question by posing a hydromagnetic boundary on initial-boundary value problem. It is shown that unlike the hydrodynamic situation for the case of blowing and resonance, the hydromagnetic steady state solution satisfies the boundary condition at infinity.

2 Basic Equations

We introduce a Cartesian coordinate system with the z-axis normal to the porous disk which lies in the plane $z = 0$. The region $z > 0$ is occupied by an incompressible third-grade fluid. The axis of rotation, of both the disk and the fluid, are assumed to be in the plane $x = 0$, with the distance between the axes being l. The disk and the fluid at infinity are initially rotating about the z'-axis with the same angular velocity $\mathbf{\Omega}$, and at time $t = 0$, the disk starts to oscillate suddenly along the x-axis and to rotate impulsively about the z-axis with the same angular velocity $\mathbf{\Omega}$ and the fluid at infinity continues to rotate about the z'-axis with the same angular velocity. The fluid is electrically conducting and assumed to be permeated by a magnetic field $\mathbf{B}_\circ$ having no components in the x and y directions. The velocity field is chosen as follows:

$$u = -\Omega y + f(z,t), \quad v = \Omega x + g(z,t), \quad w = -w_\circ, \tag{1}$$

where u, v, w are the components of the velocity vector $\mathbf{V}$, in the directions x, y, z respectively. Obviously $w_\circ > 0$ is the suction velocity and $w_\circ < 0$ is the blowing velocity.

As it is seen, the velocity field satisfies $\nabla \, . \, \mathbf{V} = \mathbf{0}$, directly which is nothing else than the incompressibility condition. For the problem under consideration, the boundary and the initial conditions can be written in the following form

$$\begin{aligned}
u &= \left.\begin{matrix} -\Omega y + U cosnt \\ or \\ -\Omega y + U sinnt \end{matrix}\right\}, & v &= \Omega x, & w &= -w_\circ, & at \quad z &= 0, & t &> 0, \\
u &= -\Omega(y-l), & v &= \Omega x, & w &= -w_\circ, & as \quad z &\to \infty, & for \ all \ t&, \\
u &= -\Omega(y-l), & v &= \Omega x, & w &= -w_\circ, & at \quad t &= 0, & for \quad z &> 0,
\end{aligned} \tag{2}$$

where n is the frequency of the non-torsional oscillations and U the velocity.

The hydromagnetic equations of motion for an electrically conducting, incompressible fluid are

$$\rho \frac{D\mathbf{V}}{Dt} = \nabla \, . \, \mathbf{T} + \mathbf{J} \times \mathbf{B}, \tag{3}$$

$$\nabla \, . \, \mathbf{B} = 0, \tag{4}$$

$$\nabla \times \mathbf{B} = \mu_m \, \mathbf{J}, \tag{5}$$

$$\nabla \times \mathbf{E} = -\frac{\partial \mathbf{B}}{\partial t}, \tag{6}$$

and Ohm's law for a moving conductor

$$\mathbf{J} = \sigma(\mathbf{E} + \mathbf{V} \times \mathbf{B}). \tag{7}$$

In above equations, ρ is the density, $\frac{D}{Dt}$ the material time derivative, $\mathbf{J}$ the electric current density, μ_m the magnetic permeability, $\mathbf{E}$ the electric field, $\mathbf{B}$ the total magnetic field so that $\mathbf{B} = \mathbf{B}_o + \mathbf{b}$, $\mathbf{b}$ the induced magnetic field, σ the electric conductivity of the fluid. In equations (4 - 7) the magnetic Reynolds number R_m [10] is assumed to be small as is the case with the most of the conducting fluids and hence the induced magnetic field is small in comparison with the applied magnetic field and is therefore not taken into account. The magnetic body forces $\mathbf{J} \times \mathbf{B}$ now becomes $\sigma(\mathbf{V} \times \mathbf{B}) \times \mathbf{B}$.

The constitutive equation of third-grade fluid is

$$\begin{aligned} \mathbf{T} &= -p\mathbf{I} + \mu\mathbf{A}_1 + \alpha_1\mathbf{A}_2 + \alpha_2\mathbf{A}_1^2 \\ &+ \beta_1\mathbf{A}_3 + \beta_2(\mathbf{A}_1\mathbf{A}_2 + \mathbf{A}_2\mathbf{A}_1) + \beta_3(tr\mathbf{A}_1^2)\mathbf{A}_1, \end{aligned} \quad (8)$$

where $\mathbf{T}$ is the stress tensor, $\mathbf{I}$ is the identity, $\mathbf{A}_1$ the Rivlin-Ericksen tensor of the first order, $\mathbf{A}_2$ and $\mathbf{A}_3$ the Rivlin-Ericksen tensors of the second and third orders, respectively, p the static fluid pressure ($p = p(x, y, z)$), μ the dynamic viscosity coefficient,$\alpha_1, \alpha_2, \beta_1, \beta_2$ and β_3 are material constants. The first, second- and third-order Rivlin-Ericksen tensors are respectively:

$$\begin{aligned} \mathbf{A}_1 &= (\text{grad } \mathbf{V}) + (\text{grad } \mathbf{V})^T, \\ \mathbf{A}_i &= \frac{D\mathbf{A}_{i-1}}{Dt} + \mathbf{A}_{i-1} (\text{grad } \mathbf{V}) + (\text{grad } \mathbf{V})^T \mathbf{A}_{i-1}, \ i > 1. \end{aligned}$$

The thermodynamics of fluid modeled by equation (8) has been object of a detailed study by Fosdick and Rajagopal in [11] and Dunn and Rajagopal [12]. They show that the equation (8) to be compatible with thermodynamics and the free energy to be minimum when the fluid is at rest, the material constants should satisfy the relations

$$\begin{aligned} &\mu \geq 0, \quad \alpha_1 \geq 0, \quad \beta_1 = \beta_2 = 0, \quad \beta_3 \geq 0, \\ &-\sqrt{24\mu\beta_3} \ \leq \alpha_1 + \alpha_2 \ \leq \sqrt{24\mu\beta_3} \end{aligned} \quad (9)$$

and specific Helmholtz free energy Ψ has the form

$$\Psi = \hat{\Psi}(\theta, \mathbf{L}) = \hat{\Psi}(\theta, 0) + \frac{\alpha_1}{4\rho}|\mathbf{L} + \mathbf{L}^T|^2. \quad (10)$$

In above expressions

$$\mathbf{L} = \text{grad } \mathbf{V}. \quad (11)$$

In our analysis we assume that the fluid is thermodynamically compatible; hence the stress constitutive relation (8) reduces to

$$\mathbf{T} \;=\; -p\mathbf{I} + \mu\mathbf{A}_1 + \alpha_1\mathbf{A}_2 + \alpha_2\mathbf{A}_1^2 + \beta_3(tr\mathbf{A}_1^2)\mathbf{A}_1. \tag{12}$$

Substituting equation (12) and $\mathbf{J} \times \mathbf{B} = -\sigma\ \mathbf{B}_\circ^2\mathbf{V}$ into equation (3) and then eliminating the modified pressure one obtains

$$\begin{aligned}\left[\frac{\partial F^*}{\partial t} + i\,\Omega F^* - w_\circ\frac{\partial F^*}{\partial z}\right] &= \nu\frac{\partial^2 F^*}{\partial z^2} - \frac{\sigma}{\rho}B_\circ^2(F^* - \Omega l) + i\,\Omega^2 l \\ &+ \frac{\alpha_1}{\rho}\left[\frac{\partial^3 F^*}{\partial t\partial z^2} - w_\circ\frac{\partial^3 F^*}{\partial z^3} - i\,\Omega\frac{\partial^2 F^*}{\partial z^2}\right] \\ &+ 2\beta_3\frac{\partial}{\partial z}\left[\left(\frac{\partial F^*}{\partial z}\right)^2\frac{\partial \bar{F}^*}{\partial z}\right],\end{aligned} \tag{13}$$

where

$$F^* = f + i\,g, \tag{14}$$

where $\nu = \frac{\mu}{\rho}$, $\bar{F}^*$ is the complex conjugate of F^*.

From equations (1), (14) and conditions (2) we have

$$\begin{aligned} F^*(0,t) &= U\cos nt \quad \text{or} \quad F^*(0,t) = U\sin nt; \\ F^*(\infty,t) &= \Omega l, \qquad\qquad\quad F^*(z,0) = \Omega l. \end{aligned} \tag{15}$$

On introducing non-dimensional parameters

$$\begin{aligned} &\xi = \sqrt{\frac{\Omega}{2\nu}}z, \quad \tau = \Omega t, \quad F(\xi,\tau) = \frac{F^*}{\Omega l} - 1, \quad \bar{F}(\xi,\tau) = \frac{\bar{F}^*}{\Omega l} - 1, \\ &U_\circ = \frac{U}{\Omega l} \quad \beta = \frac{\Omega^3 l^2\beta_3}{\rho\nu^2}, \quad \alpha = \frac{\Omega\alpha_1}{\rho\nu}, \quad \epsilon = \frac{w_\circ}{\sqrt{2\nu\Omega}}, \quad N = \frac{\sigma}{\rho\Omega}B_\circ^2 \end{aligned} \tag{16}$$

equation (13) and conditions (14) becomes

$$\begin{aligned} \alpha\frac{\partial^3 F}{\partial\tau\partial\xi^2} &- \alpha\epsilon\frac{\partial^3 F}{\partial\xi^3} + (1 - i\alpha)\frac{\partial^2 F}{\partial\xi^2} + 2\epsilon\frac{\partial F}{\partial\xi} \\ &- 2\frac{\partial F}{\partial\tau} - 2(i+N)F + \beta\frac{\partial}{\partial\xi}\left[\left(\frac{\partial F}{\partial\xi}\right)^2\frac{\partial\bar{F}}{\partial\xi}\right] = 0, \end{aligned} \tag{17}$$

$$F(0,\tau) = U_\circ \cos nt - 1, \quad F(\infty,\tau) = 0, \quad F(\xi,0) = 0. \tag{18}$$

We note that the equation (17) is a third order partial differential equation. Moreover, this equation is highly non-linear as compared to case of second order and Newtonian flow equations. As a result, it seems to be impossible to obtain the general solution in closed form for arbitrary values of all parameters arising in this non-linear equation. Further, equation (17) is parabolic with respect to time which allows a time marching solution to the equation. Dealing with parabolic equation, there is only one characteristic direction. The information at one point influences the entire region on one side of the vertical characteristic and contained within the two boundaries. Therefore, lend itself to marching solution. Starting with the initial data, the solution between the two boundaries is obtained by marching in the τ direction. The above equation is non-linear. This non-linearity must be supressed in applying the Von Neumann stability analysis. This is done by treating solution-dependent coefficients multiplying derivatives as being tempoarily frozen. The modified equation approach to analyzing non-linear computational algorithm is applicable [13] but the appearance of products of higher-order derivatives makes the construction of more accurate schemes less precise than the case of linear equations.

As this problem is time dependent and has mixed derivative with respect to time and space coordinates so we are forced to use an implicit scheme. Applying implicit scheme to nonlinear equation (17) is not as straight forward as for linear equations. To convert partial differential equation (17) to a system of algebraic equations a number of choices are available. If this parabolic partial differential equation is discretized in space first, it becomes an initial value problem of coupled ordinary differential equations. Therefore, numerical methods for a parabolic partial differential equation include both

1) a boundary value problem and
2) an initial value problem.

For these reasons, numerical methods for a parabolic partial differential equation can be developed by combining the numerical methods for the initial and boundary value problems of ordinary differential equations. Most of the numerical methods for initial value problems may result in very complicated or, at least, inefficient methods e. g. higher order Runge-Kutta methods or predictor-corrector methods [14]. This limitation leads us to consideration of the simplest group of numerical methods for initial value problems. A modified Crank-Nicolson implicit formulation with forward time and central finite difference space approximation is used, so that equation (17) is transformed into algebraic equation of the form

$$a_j^n F_{j-1}^{n+1} + b_j^n F_j^{n+1} + c_j^n F_{j+1}^{n+1} = d_j^n, \tag{19}$$

where

$$\begin{aligned}
a_j^n &= -\left(\frac{\alpha}{h^2} + \frac{(1-i\alpha)\Delta\tau}{2h^2}\right), \\
b_j^n &= 2\left(\frac{\alpha}{h^2} + \frac{(1-i\alpha)\Delta\tau}{2h^2} + 1\right), \\
c_j^n &= -\left(\frac{\alpha}{h^2} + \frac{(1-i\alpha)\Delta\tau}{2h^2}\right), \\
d_j^n &= -\left(\frac{\alpha}{h^2} + \frac{(1-i\alpha)\Delta\tau}{2h^2}\right)(F_{j+1}^n - 2F_j^n + F_{j-1}^n) \\
&- \frac{\epsilon\alpha\Delta\tau}{2h^3}(F_{j+2}^n - 2F_{j+1}^n + 2F_{j-1}^n - F_{j-2}^n) \\
&+ \frac{\epsilon\Delta\tau}{h}(F_{j+1}^n - F_{j-1}^n) + 2(1 - \Delta\tau(i+N))F_j^n \\
&+ \frac{\beta\Delta\tau}{4h^4}((F_{j+1}^n - F_{j-1}^n)^2(\bar{F}_{j+1}^n - 2\bar{F}_j^n + \bar{F}_{j-1}^n) \\
&+ 2(F_{j+1}^n - F_{j-1}^n)(F_{j+1}^n - 2F_j^n + F_{j-1}^n)(\bar{F}_{j+1}^n - \bar{F}_{j-1}^n)).
\end{aligned} \tag{20}$$

Here $\xi = [\xi_j]_{j=1}^{j=M}$ is taken as strictly increasing sequence of discrete points such that $0 = \xi_1 < \xi_2 < \xi_3 < \cdots < \xi_M$ and $h = \xi_i - \xi_{i-1} = \frac{\xi_M - \xi_1}{M-1}$, where M is the number of grid points in space coordinates and $\Delta\tau = \tau^{n+1} - \tau^n$ is time interval. The right hand side of equation (19) is considered in some fashion as known, say from the previous time step and left hand side as the dependent variable in a numerical solution of an unsteady flow problem. The steady state approached asymptotically at large times.

The implicit methods are uncoditionally stable unless non-linear effects cause instability, which is controlled by suitable choice of $\Delta\tau$ and h. The equation (19) must be written at all interior grid points resulting in a system of algebraic equations of order M from which the unknowns F_j^{n+1} for all j can be solved simultaneously, which can be solved by using the generalized Thomas algorithm especially, when a single equation is discretized using an implicit algorithm [15].

Let us consider system of equations of the form

$$\mathbf{A}\,\mathbf{F} = \mathbf{B}. \tag{21}$$

In above equation, $\mathbf{F}$ is a vector of unknown nodal values, $\mathbf{A}$ contains the algebraic coefficients arising from discretization and $\mathbf{B}$ is made up of algebraic coefficients associated with discretisation and known values of $\mathbf{F}$ e. g., values of $\mathbf{F}$ on previous time step and given by the boundary conditions.

The matrix $\mathbf{A}$ is typically sparse and the non-zero terms are close to the diagonal. As in our case $\mathbf{A}$ does not depend on $\mathbf{F}$ only one step of outer iteration is required. When the non-zero elements lie close to the main diagonal it is useful to consider variants of Gauss elimination that take advantage of the banded nature of A. Considering every node, equation (21) yields

$$\begin{pmatrix} b_1 & c_1 & & & & & & \\ a_2 & b_2 & c_2 & & & & & \\ & a_3 & b_3 & c_3 & & & & \\ & & . & . & . & & & \\ & & & a_j & b_j & c_j & & \\ & & & & . & . & . & \\ & & & & & a_{M-1} & b_{M-1} & c_{M-1} \\ & & & & & & a_M & b_M \end{pmatrix} \begin{bmatrix} F_1 \\ F_2 \\ F_3 \\ . \\ F_j \\ . \\ F_{M-1} \\ F_M \end{bmatrix} = \begin{bmatrix} d_1 \\ d_2 \\ d_3 \\ . \\ d_j \\ . \\ d_{M-1} \\ d_M \end{bmatrix},$$

where a_j, b_j, c_j and d_j are given by equation (20), non-zero values of d_j are associated with source terms or for d_1 and d_M with boundary conditions. All terms in **A** other than those shown are zero.

The Thomas algorithm for solving above matrix consists of two parts:

First, the a_j coefficients have been eliminated and b_j coefficients normalized to unity. The equations are modified in a forward sweep.

The second stage consists of a backward-substitution (backward sweep).

The Thomas algorithm is particularly economical; it requires only 5M-4 operations (multiplications and divisions). But to prevent ill-conditioning it is necessary that $|b_j| > |a_j| + |c_j|$.

3 Numerical Discussion

Equation(19) has been solved by using a modified Crank Nicolson implicit formulation with forward time and central difference space approximation using 100 grid points ($\xi = 10$) for sufficient accuracy. For all computations we have taken $h = .1$ and $\Delta\tau = .001$. For the case $\alpha = 0, \beta = 0$ we get solution for the Newtonian fluid, and results matched with the analytical solution [9]. Numerical solutions confirm that for large times the starting solutions tend to the steady-state solutions. For some times after the initiation of motion, the velocity field contain transients then these transients disappear and steady state is achieved.

The time required to attain steady flow for the cosine and sine oscillations is obtained for $n > \Omega$, $n = \Omega$ and $n < \Omega$. The value of this time for cosine oscillation is shorter than that for sine oscillation and it depends on the ratio of the frequency of oscillation to the angular velocity of the disk $\frac{n}{\Omega}$ and the ratio $\frac{U}{\Omega l}$.

In the case of $n > \Omega$, the oscillation of the disk dominates, then the time required to attain steady flow both for the cosine and sine oscillations becomes very short. However, in the case of $n < \Omega$ the time required to attain steady flow for the sine oscillation become large.

Numerically, we have computed the magnitudes of $\frac{f}{\Omega l}$ and $\frac{g}{\Omega l}$ with the distance from the disk for cosine and sine oscillations keeping amplitude constant $\frac{U}{\Omega l} = 4$ at $\frac{n}{\Omega} = .5, 1, 2, 5$ with varying time corresponding to three types of flows (Newtonian, second-grade and third-grade), with and without suction. The full lines denote starting velocities and dotted lines show steady-state velocities. Results described below report solutions up to $\xi = 2$, where free stream velocities have not yet been reached in most cases.

For Newtonian fluids, we observed that without oscillations steady state is achieved after $\tau = 10$. When cosine or sine oscillations are introduced, time to reach steady state is reduced.

With the cosine oscillations, when suction ($\epsilon = 2$) is introduced, its value is reduced further and boundary layer thickness is also reduced due to suction. Magnitudes of $\frac{f}{\Omega l}$ also reduced but the magnitudes of $\frac{g}{\Omega l}$ near the disk are increased due to suction.

When only disk is rotating then time to reach its steady state is $\tau = 10$. Introducing cosine oscillation $\frac{n}{\Omega} = .5 < 1$ this time is reduced to $\tau = 5$, and for sine oscillation its values is 7. For $\frac{n}{\Omega} = 2 > 1$ due to cosine oscillation the value of τ when we get steady-state is 4.5 while for the sine oscillation its value is 5.5. For $\frac{n}{\Omega} = 5 > 1$ system with cosine oscillation approaches to its steady-state at $\tau = 2$ and for system with sine oscillation the value is $\tau = 3$ (By introducing oscillations time to reach steady-state is reduced. This time is shorter for cosine oscillations as compared to sine oscillations). No oscillatory behavior can be observed for the Newtonian fluids with and without suction.

For the second-grade fluid ($\alpha \neq 0$) time to reach steady-state is increased and also oscillatory behavior become visible in fluid velocities ($\frac{f}{\Omega l}$ and $\frac{g}{\Omega l}$). Near the disk the magnitudes of the velocities ($\frac{f}{\Omega l}$ and $\frac{g}{\Omega l}$) is also increased. Boundary layer thickness is also increased due to α.

By introducing suction ($\epsilon = 2$) in the second-grade fluid, time to reach steady-state is decreased but oscillatory behavior becomes very prominent, boundary layer thickness is increased. That is to say, that the oscillatory behavior is due to both non-Newtonian fluids and suction (become visible for non-Newtonian fluid and enhanced by suction, in our case). By increasing the value of α time to reach steady state is also increased. Boundary layer thickness is also increased due to non-Newtonian nature of the fluid and oscillatory behavior.

For the third-grade fluid ($\alpha \neq 0, \beta \neq 0$) time to reach steady state is delayed further but oscillatory behavior diminish when β is introduced. Inclusion of suction increases oscillatory behavior. By increasing oscillation of the disk steady state is achieved much earlier. Increasing oscillations reduces boundary layer thickness. For the third-grade fluid ($\alpha \neq 0, \beta \neq 0$) time to reach steady state is increased further but due to oscillations its value is reduced. When $\frac{n}{\Omega} = .5$ steady-state is achieved at $\tau = 3$, for $\frac{n}{\Omega} = 2$ we get $\tau > .5$ and when $\frac{n}{\Omega} = 5$ its value becomes $= .3$. The time to reach steady state for the third-grade fluid in the presence of cosine oscillations is reduced. In the presence of suction ($\epsilon = 2$) time to reach steady state is increased in considerable amount. When $\frac{n}{\Omega} = .5$ its value is $\tau = 5$, for $\frac{n}{\Omega} = 2$, τ becomes 4 and for $\frac{n}{\Omega} = 5$, $\tau = 1$. i. e. time to reach steady state is further delayed in the third grade fluid (when suction is applied, perhaps this is due to oscillatory behavior).

When we consider the sine oscillations then we note that the time to reach steady-state is again reduced and with the increase in oscillations the time to reach steady-state is decreased further. By introducing suction ($\epsilon = 2$) time to reach steady-state is reduced in a considerable amount. Boundary layer thickness is also reduced. The magnitude of $\frac{f}{\Omega l}$ is reduced by suction while the magnitude of $\frac{g}{\Omega l}$ are increased near the disk.

For the second-grade fluid the time to reach steady-state is increased. Oscillatory behavior can be seen near the disk. The magnitude of $\frac{f}{\Omega l}$ and $\frac{g}{\Omega l}$ near the disk is increased. Boundary layer thickness is also increased for the second grade fluid.

When suction is applied to the second grade fluid oscillatory behavior becomes prominent and can be seen up to considerable distance from the disk. Boundary layer thickness is increased due to this oscillatory behavior. Time to reach steady-state is reduced. For $n > \Omega$ boundary layer thickness is also reduced but oscillatory behavior is prominent and with the increase in frequency the value of boundary layer thickness is reduced further.

For $\frac{n}{\Omega} = 1$ (resonant case) boundary conditions at infinity for the steady case are not met when fluid is Newtonian or non-Newtonian. When suction is applied then condition at infinity is fulfilled but for blowing, the condition at infinity is not satisfied. If we consider electrically conducting fluid then boundary condition at infinity is also satisfied for blowing and resonance. It is likely that the magnetic field provides some mechanism to control the growth of the boundary layer thickness at the resonant frequency.

Concluding Remarks

The most distinctive feature is that unlike the hydrodynamic situation for the case of the resonant oscillations, the solution satisfies the boundary condition at infinity for all values of the frequency parameter n, and the associated boundary layers remain bounded for all values of the frequency including $n = 2$. The physical implication of this conclusion is that for the case of resonance and blowing, the unbounded spreading of the oscillations away from the disk is controlled by the external magnetic field. Consequently, the hydromagnetic oscillations are confined to the ultimate boundary layers.

References

[1] R. Berker. *Handbook of Fluid Dynamics*, volume VIII/3. Springer-Verlag, Berlin, 1963.

[2] Claire Thornley. On Stokes and Rayleigh Layers in a Rotating System. *Quart. Jr. Mech. and Applied Math.*, XXI:451–460, 1968.

[3] A. S. Gupta. Ekman layer on a porous plate. *Phys. Fluids*, **155**:903–931, (1972).

[4] M. E. Erdogan. Unsteady Flow of a Viscous Fluid due to Non-Coaxial Rotations of a Disk and a Fluid at Infinity. *Int. J. Non-Linear Mechanics*, **32(2)**:285–290, (1997).

[5] Murthy S. N. Ram R. K. P. MHD Flow and Heat Transfer due to Eeccentric Rotations of a Porous Disk and a Fluid at Infinity. *Int. J. Engng. Sci.*, **16**:943–949, (1978).

[6] Rajagopal K. R. On the Flow of a Simple Fluid in an Orthogonal Rheometer. *Arch. Rat. Mech. Anal*, **79**:39–47, (1982).

[7] Kasiviswanathan S. R. Rao A. R. An Unsteady Flow due to Eccentrically Rotating Porous Disk and a Fluid at Infinity. *Int. J. Engng. Sci.*, **25**:1419–1425, (1987).

[8] Pop I. Unsteady Flow due to Non-Coaxially Rotating a Disk and a Fluid at Infinity. *Bull. Tech. Uni. Ist.*, **32**:14–18, (1979).

[9] M. E. Erdogan. An Exact Solution of the Time-Dependent Navier-Stokes Equations for the Flow due to Non-Coaxial Rotations of an Oscillating Disk and Fluid at Infinity. *Int. J. Engng Sci.*, 38(2000)175.

[10] Shercliff J. A. *A textbook of Magnetohydrodynamics*. Pergamon, (1965).

[11] R. L. Fosdick, K. R. Rajagopal. Thermodynamics and Stability of Fluids of Third-Grade. *Proc. Roy. Soc. Lond. Ser.*, A,339(1980)351.

[12] J. E. Dunn, K. R. Rajagopal. Fluids of Differential Type. *Int. J. Engng. Sci.*, 21(1983)487.

[13] G. H. Klopfer, D. S. McRae. Non-linear Truncation Error Analysis of FDF for the Euler Equations. *AIAA J.*, 21(1983)487.

[14] R. D. Richtmyer and K. W. Morton. *Difference Methods for Initial-Value Problems*. Number 4 in Interscience Tracts in Pure and Applied Mathematics. Interscience Publishers, second edition edition, 1967.

[15] C. A. J. Fletcher. *Computational Techniques for Fluid Dynamics*, volume I. Springer-Verlag Berlin Heidelberg, 1988.

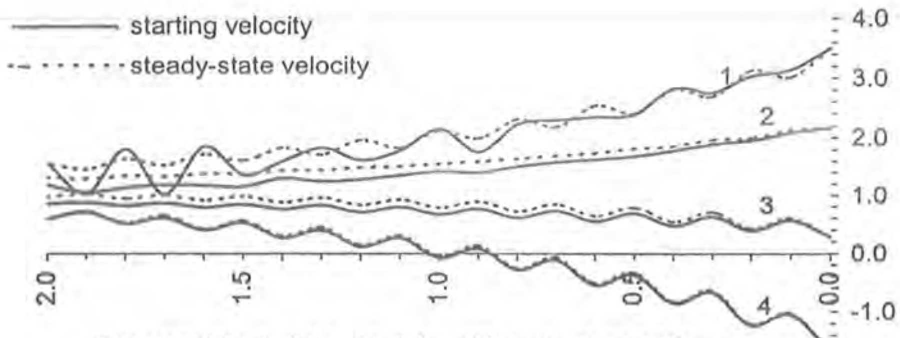

The variation in f/Ωl with ξ for different values of time for cosine oscillation at U/Ωl=4,n/Ω=.5, ε=2, α=2

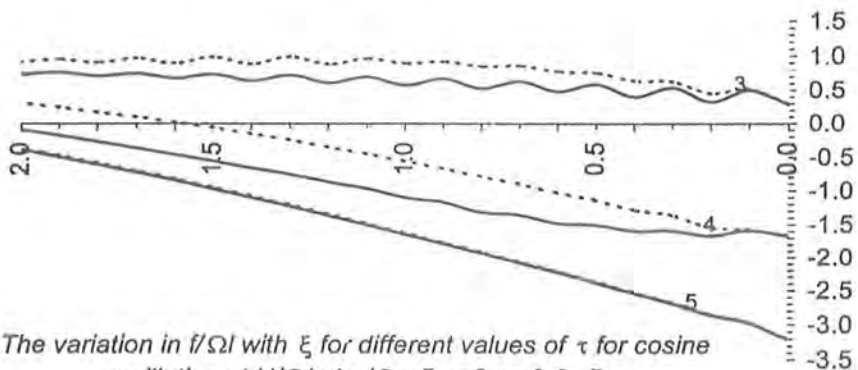

The variation in f/Ωl with ξ for different values of τ for cosine oscillation at U/Ωl=4,n/Ω=.5, ε=2, α=2, β=5.

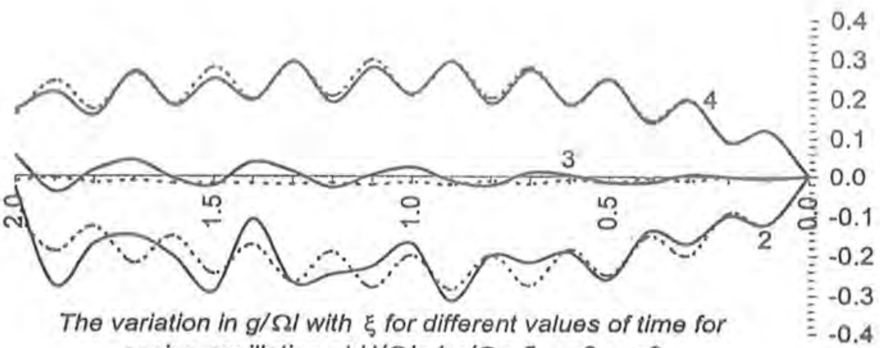

The variation in g/Ωl with ξ for different values of time for cosine oscillation at U/Ωl=4,n/Ω=.5, ε=2, α=2

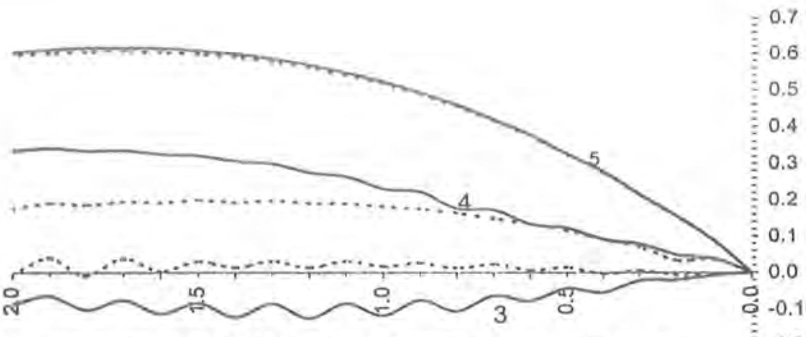

The varition in g/ΩI for ξ at different values τ for cosine oscillation at U/ΩI=4,n/Ω=.5, ε=2, α=2, β=5.

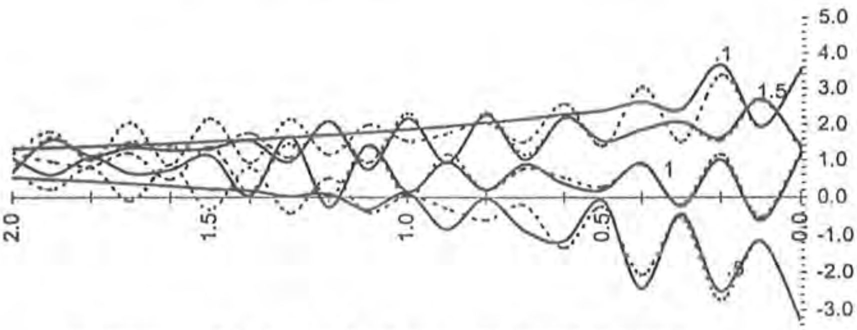

The variation in f/ΩI with ξ for different values of time for cosine oscillation at U/ΩI=4,n/Ω=5, ε=2, α=2.

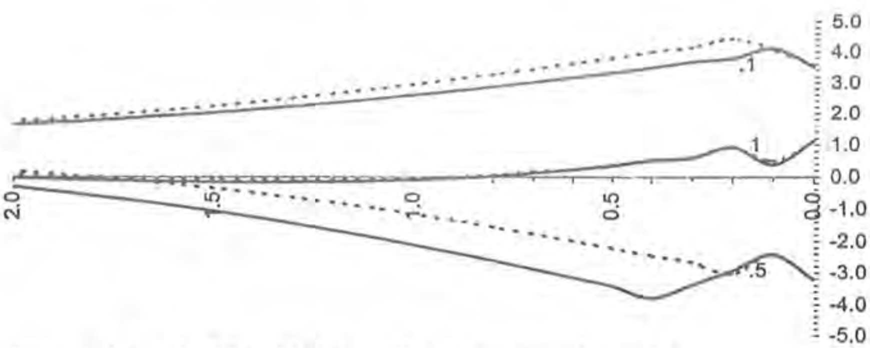

The variation in f/ΩI with ξ for different values of time for cosine oscillation at U/ΩI=4,n/Ω=5, ε=2, α=2, β=5.

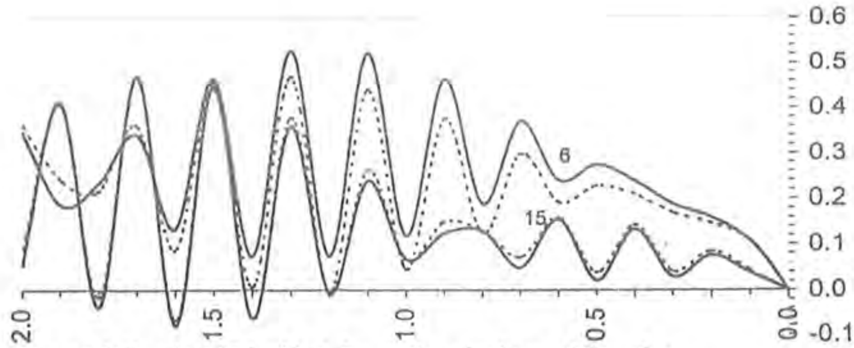

The variation in g/ΩI with ξ for various values of time for cosine oscillation at U/ΩI=4, n/Ω=5, ε=2, α=2

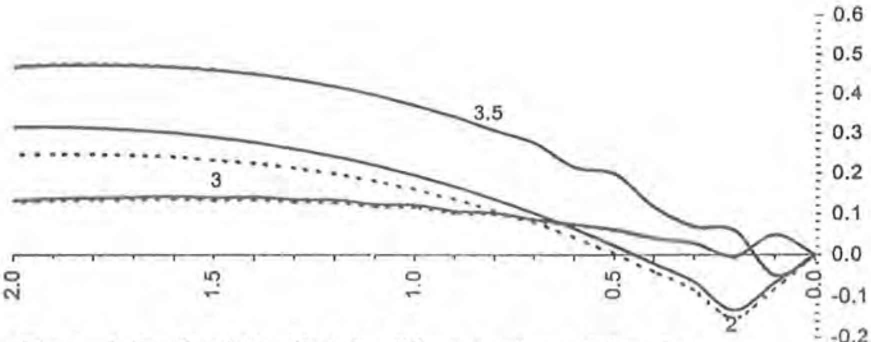

The variation in g/ΩI with ξ for different values of time for cosine oscillation at U/ΩI=4, n/Ω=5, ε=2, α=2, β=5.

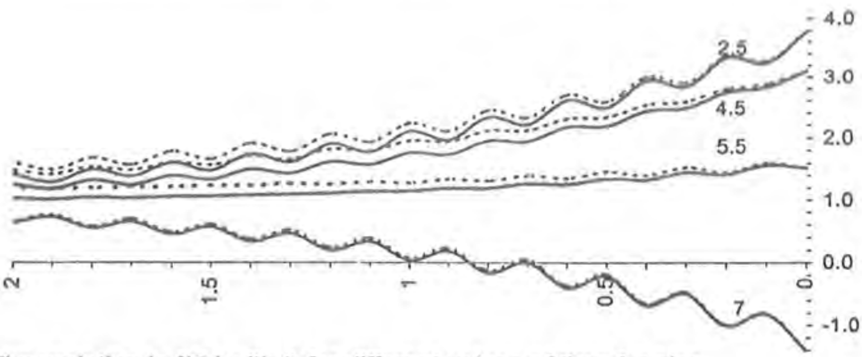

The variation in f/ΩI with ξ for different values of time for sine oscillation at U/ΩI=4, n/Ω=.5, ε=2, α=2

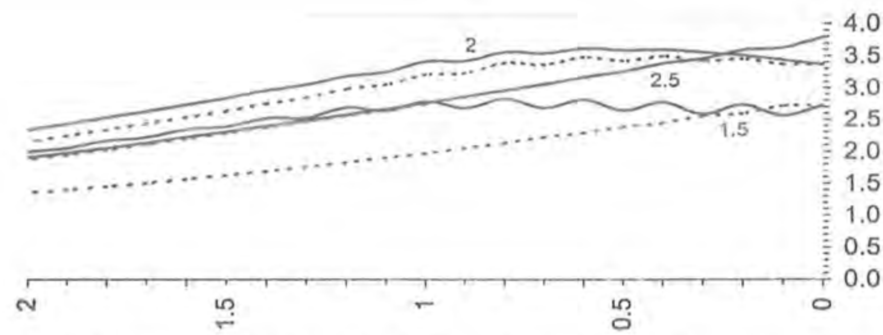

The variation in f/Ωl with ξ for different values of time for sine oscillation at U/Ωl=4,n/Ω=.5, ε=2, α=2, β=5

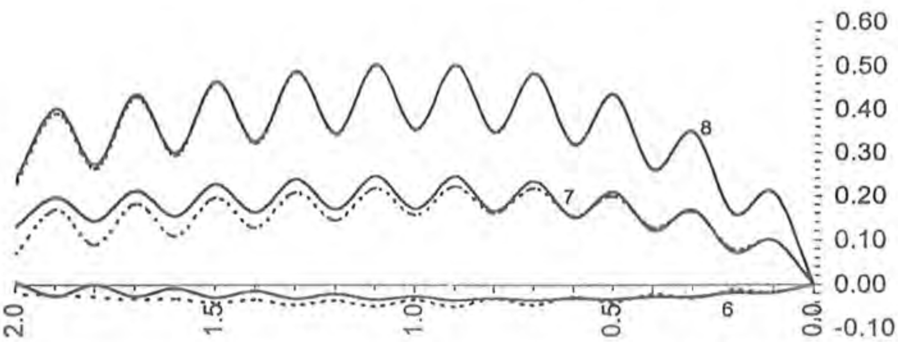

The variation in g/Ωl with ξ for different values of time for sine oscillation at U/Ωl=4,n/Ω=.5, ε=2, α=2

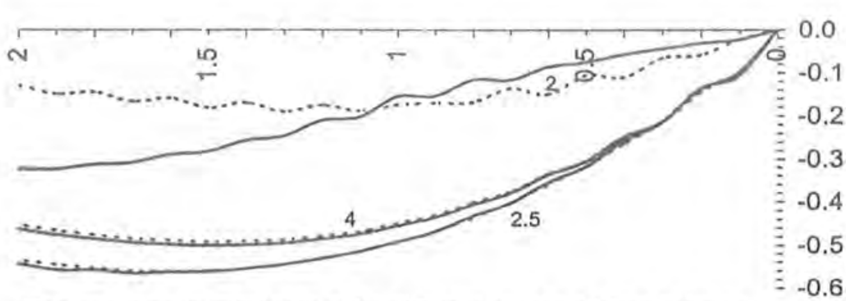

The variation in g/Ωl with ξ for different values of time for sine oscillation at U/Ωl=4,n/Ω=.5, ε=2, α=2, β=5

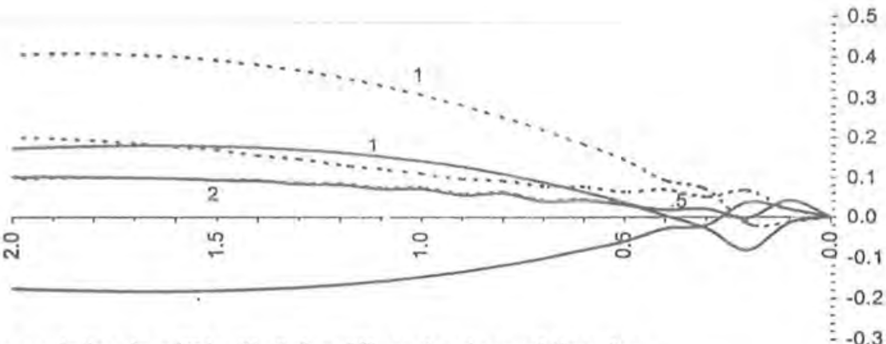

The variation in g/Ωl with ξ for different values of time for sine oscillation at U/Ωl=4, n/Ω=5, ε=2, α=2, β=5.

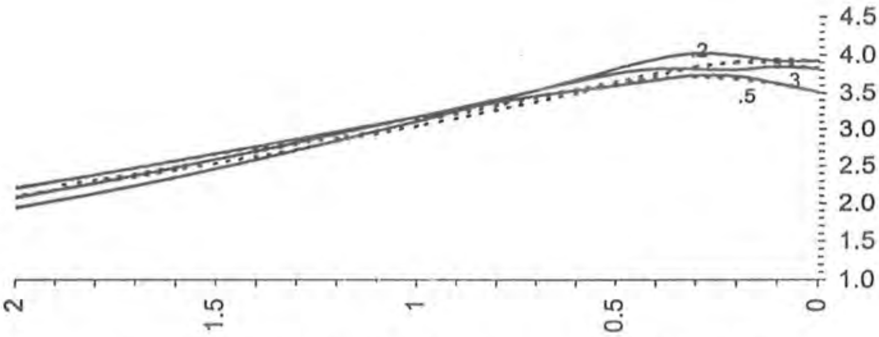

The variation in f/Ωl with ξ for different values of time for cosine oscillation at U/Ωl=4, n/Ω=1, ε=-2, α=2, β=5, N=2

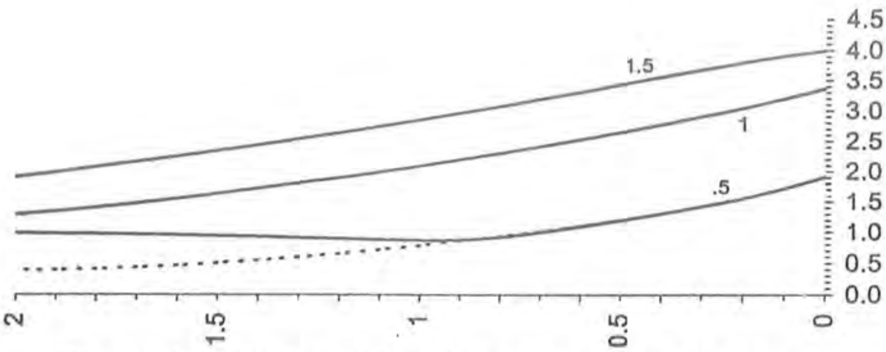

The variation in f/Ωl with ξ for different values of time for sine oscillation at U/Ωl=4, n/Ω=1, ε=-2, α=2, β=5, N=2

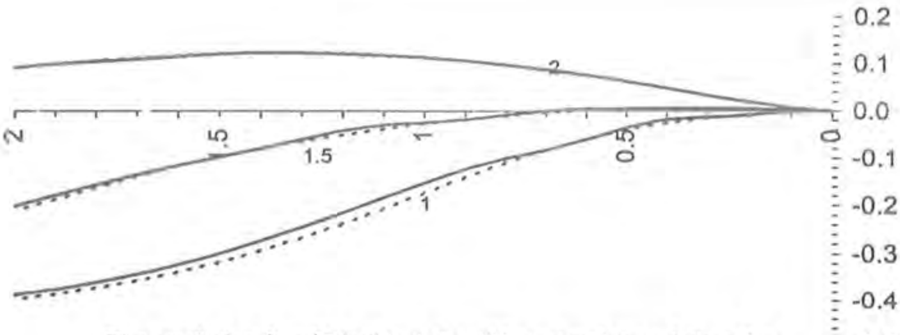

The variation in g/ΩI with ξ for different values of time for cosine oscillation at U/ΩI=4, ε=-2, α=2, β=5, N=2

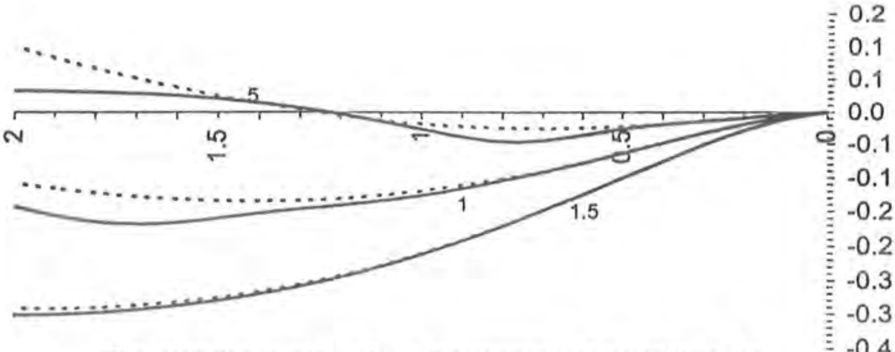

The variation in g/ΩI with ξ for various values of time for sine oscillation at U/ΩI=4,n/Ω=1, ε=-2, α=2, β=5, N=2